DISTINGUISHING BETWEEN NATURAL AND ANTHROPOGENIC SOURCES OF ARSENIC IN SOILS FROM THE GIANT MINE, NORTHWEST TERRITORIES AND THE NORTH BROOKIFIELD MINE, NOVA SCOTIA

By

Lori Ann Wrye

A thesis submitted to the Department of Geological Sciences and Geological Engineering

In conformity with the requirements for

the degree of Master of Science

Queen's University

Kingston, Ontario, Canada

September, 2008

Abstract

Anthropogenic and geogenic sources of arsenic (As) have been identified in mining-impacted soils from the Giant mine (1948-1999), NT and the North Brookfield mine (1886-1906), NS. Both used roasting to extract gold from the arsenopyrite ore, decomposing it to As-bearing iron oxides (roaster oxides or RO) containing As, and releasing As^{3+}-bearing arsenic trioxide (As_2O_3). Arsenic trioxide is considered highly soluble with the dissolved As^{3+} species being more mobile and toxic than other oxidation states.

Soil profiles from the Giant mine show elevated As and antimony (Sb) at the surface (As=140-3300ppm) and decreasing concentrations with depth (As=22-600ppm). Surface soils contain anthropogenically-derived As_2O_3 identified using synchrotron methods (μXRD, μXANES) and environmental SEM. The persistence of As_2O_3 is attributed to Sb in As_2O_3 grains, dry climate and high organics in the soils. Anthropogenically-derived RO of maghemite (containing both As^{3+} and As^{5+}) and natural arsenopyrite were observed. Sequential selective extractions (SSE) from surface soils show between 20% and 75% of As extracted in the crystalline iron-oxide phase is attributed to As_2O_3 and RO, while at depth As is bound by organics in the weaker leaches.

North Brookfield mine soils show lower total As (2ppm to 45ppm) except near the roaster (4300ppm). No As_2O_3 was identified, probably due to the smaller scale and age of the mine, lower organic content and the lack of Sb. As-bearing phases include RO of hematite (As^{5+}), As-rich rims on titanium-oxides, and As associated with clays and goethite. Adjacent to the roaster, SSE show As was also in the amorphous iron-oxide phase, also shown by As in arsenopyrite weathering rims.

There are many differences between the North Brookfield and Giant mine soils including roasting techniques which produced different RO mineralogy, the scale of mining, climate, soil type, and the presence of As_2O_3. Currently, the Giant property is not publically accessible but may become so in the future while the North Brookfield property is accessible. Understanding the form and distribution of As phases is critical because of the potential risk to human and ecosystem health associated with ingestion of soil particles and their control on the total dissolved As in surface and groundwater.

Co-Authorship

Chapters 4 and 5 of this thesis were prepared as separate manuscripts for journal publication as co-authored papers. Both chapters are co-authored with Dr. H.E. Jamieson who conceived the project, contributed to interpretations of the geochemistry and acted in a supervisory and review capacity throughout the entire project. Dr. Jamieson was also involved with field work and synchrotron data collection.

Chapter 4 is prepared to be submitted to *Environmental Science and Technology*, and Chapter 5 is to be submitted to *Applied Geochemistry*.

Acknowledgements

I would first like to thank my supervisor Dr. Heather Jamieson, her guidance was exceptional and her enthusiasm unfaltering throughout the entire thesis. Her curiosity and passion for the environment makes her an inspiration to all.

Everyone in Dr. Jamieson's research group and other students within the department (you know who you are) have been an invaluable resource for me, whether it was through field work, late nights followed by early mornings at the synchrotron, or just by giving me support for the particular task at hand. Thank you- Steve, Steph, Mallory, Karina, Paul and Skya.

Steve Walker and Stephanie DeSisto deserve additional special mention for their indescribable help. Steve, your insightful talks and sharing of ideas on arsenic at the Giant and North Brookfield mines as well as your overall helpfulness for all things synchrotron, helped me more than you know. Steph, all those long days in the office, and sharing of ideas helped to keep me focused for the last year of this thesis, thank you.

I would also like to thank Al Grant, Dave Kempson and Roger Innes from the Department of Geological Sciences for their technical assistance. Dr. Tony Lanzirotti at NSLS, Patricia Hunt and Gwendy Hall from the Geological Survey of Canada-Ottawa, Brenda Coglin from ALS Chemex, Allison Rutter from ASU and Linda Campbell from Dr. Grogan's Lab also deserve a sincere thank you for everything that you have done to help with sample preparation and analysis. Many thanks to Paul Smith and Terry Goodwin from Nova Scotia Department of Natural Resources and Dr. Michael Parsons from the Geological Survey of Canada- Atlantic for their help with sample collection and historical information on the North Brookfield mine. A sincere thank you to Bill Mitchel and the Giant Mine

Remediation Team from Indian and Northern Affairs in Yellowknife for their generous support, without which this project would not have been possible.

Thank you to Kathryn Kitney and Steve Garvin for your hospitality, being amazing friends, great company and awesome chefs! To my parents Janet and Robert Wrye I would like to say thank you for your love and unwavering support, you were always there when I needed you. To my sister Kathy and her husband, thank you for giving me the chance to escape from my work and relax, your home was always inviting. Finally, to my fiancé Adam Best, I dedicate this thesis to you. I cannot begin to describe the sacrifices you have made and patience you have shown me over the past two years, thank you so much.

Table of Contents

List of Figures

List of Tables

List of Equations

List of Abbreviations

As	arsenic
As_2O_3	arsenic trioxide
ASU	analytical services unit
Au	gold
BC	bromocyanidation
BCy	bromine of cyanogen
CCME	Canadian Counsel of Ministers of the Environment
CPHA	Canadian Public Health Authority
DPWM	Department of Public Works and Mines
EIA	environmental impact assessment
EnviroCan	Environment Canada
ESEM	environmental scanning electron microscope
ESG	Environmental Sciences Group
ESP	electrostatic precipitator
Fe	iron
GDZ	giant deformation zones
ICDD	International Centre for Diffraction Data
ICPAES	Inductively Coupled Plasma- Atomic Emission Spectrometer
ICP MS	Inductively Coupled Plasma- Mass Spectrometer
INAC	Indian and Northern Affairs Canada
LCF	linear combination fitting
Mn	manganese
MVLWB	Mackenzie Valley Land and Water Board
NSLS	National Synchrotron Light Source, Brookhaven National Lab, Upton, N.Y.
OC	organic carbon
OM	organic matter
OSS	outcrop soil samples
P	phosphorus
ppm	parts per million
RO	As-bearing roaster-derived iron oxides

RiskLogic	RiskLogic Scientific Services Inc
S	sulphur
Sb	antimony
SCS	soil core samples
SSE	sequential selective extractions
SSP	Slave structural province
Ti	titanium
tpd	tonnes per day
μXANES	micro X-ray adsorption near-edge structure
μXRD	micro X-ray diffraction
μXRF	micro X-ray fluorescence
WHO	World Health Organization
YGB	Yellowknife greenstone belt

Chapter 1: Introduction

1.1 Arsenic in the Environment- The Problem

The element arsenic (As) is a naturally occurring and relatively mobile metalloid that is typically found, in low concentrations, in the environment (waters, rocks, soils and air) as a result of both natural sources and anthropogenic activities (Valberg *et al.*, 1997). The presence of As in surface water, ground water, terrestrial and marine environments has made As an element of concern where detected concentrations are elevated. Above certain levels As may pose a significant ecological and human health risk (e.g., Caussy, 2003; Valberg *et al.*, 1997).

The most common exposure to As is through the ingestion of contaminated groundwater, as seen, for example, in Bangladesh and Taiwan, other methods of As exposure include the ingestion of soil particles, inhalation of windblown soil and dermal adsorption. Since the World Health Organization lowered the As drinking water guideline from 50μg/L to 10 μg/L in 1993, followed by the US in 2001 and Canada in 2006, understanding the cycling of As from solid to aqueous phases has been of international concern in order to meet more strict guidelines (CCME, 2007a; Smedley and Kinniburgh, 2002; US EPA, 2001; WHO, 1993).

Arsenic contamination in soils is of particular importance because of the danger it represents for children as a result of incidental ingestion (Calabrese *et al.*, 1996; Ljung *et al.*, 2006). Young children are more susceptible to the adverse health effects of As because they are in the early stages of development and characteristically have low body weights relative to ingested soil (Calabrese *et al.*, 1996). The complexity and importance of evaluating the risk

associated with soil ingestion stems from the lack of a simple positive correlation between the exposure dose and the associated health risk to humans or animals (Basta *et al.*, 2002; Hughes, 2002; Ruby *et al.*, 1999; Ljung *et al.*, 2006).

The two factors that have the most significant influence on the concentration and nature of As occurrence in soils are the parent rock (natural sources) and human activities (anthropogenic sources) (Bhumbla and Keefer, 1994; Yan-Chu, 1994). The concept of natural background levels of given elements within soils has been widely discussed but can be difficult to determine (Reimann and Garrett, 2005 and references therein). Naturally elevated As concentrations in soils occur in geographical regions that have bedrock containing As-bearing minerals such as arsenopyrite (FeAsS) (e.g., Bhumbla and Keefer, 1994; Cullen and Reimer, 1989; Smedley and Kinniburgh, 2002). Overlying soils are generated by the weathering of these rocks making the soils genetically related as long as mixing or re-distribution (through soil erosion for example) has not occurred (Yan-Chu, 1994).

In Canada, the Canadian Council for the Ministers of the Environment (CCME) has set a guideline of 12 ppm for the As content in soils for the protection of human and ecosystem health based on the average national background As concentration in soils (CCME, 2007b). As part of the Canadian Soil Quality Guidelines, site specific guidelines may be calculated if natural As concentrations in the soils are higher than the national average of 10 ppm (Risklogic, 2002a).

In this thesis the term natural background refers to elemental concentrations that are attributed to natural processes unaffected by anthropogenic activities (Reimann and Garrett, 2005). Values for natural element concentrations vary significantly between and within

regions, making global and even country or province wide average background levels difficult to define. Smedley and Kinniburgh (2002) have examined work by various authors and found that typical soils, in regions where there are no known sulphide deposits, have As concentrations between 0.1 ppm and 55 ppm. Soils near or above sulphide deposits can have natural As concentrations between 2 ppm and 8000 ppm and soils impacted by anthropogenic activities can record even higher As concentrations (Boyle and Jonasson 1973; Smedley and Kinniburgh, 2002).

Anthropogenic activities that cause the release of As vary but are typically related to industrial or manufacturing processes. These include coal combustion, arsenical pesticides and As-treated lumbers. One of the more significant releases of As to the environment is from mining and mining related activities, particularly those such as ore-roasting or smelting (Belluck *et al.*, 2003; Cullen and Reimer, 1989; Valberg *et al.*, 1997). As previously mentioned, arsenopyrite is a common As-bearing mineral that is frequently associated with gold mineralization (Bhumbla and Keefer, 1994). Roasting and smelting activities are used in the production of gold and involve heating the crushed ore to extract the gold by breaking down the host sulphides into porous Fe-oxides more amenable to conventional cyanidation. Breaking down the sulphides releases As-vapour, which combines with oxygen in the atmosphere to form As_2O_3 (i.e., a very mobile form of As) and sulphur dioxide (SO_2) gases (More and Pawson, 1978).

Both roasting and smelting release airborne As-containing particulate matter that can be carried on the wind and eventually find its way into the soil causing As concentrations to be several times higher than natural background concentrations (Yan-Chu, 1994). Removal of ore and subsequent processing, results in the production of significant quantities of

anthropogenic As-bearing waste material such as tailings and aerial dispersed As-bearing particulates (Yan-Chu, 1994). It was approximated by Matschullat (2000) that between 28,400 and 94,000 tonnes of As are released into soils every year with the cumulative global As production estimate at 4.53 million tonnes since the 1930's (Belluck *et al.*, 2003; Han *et al.*, 2003). This As can then be redistributed into soils via agricultural practices, surficial runoff and windblown dust.

To delineate the forms of As in soils influenced by industrial activities, two gold mines known to have used ore-roasting as a method of extracting gold from the host minerals were chosen for this study. The first is the Giant mine in Yellowknife, Northwest Territories. Previous studies at the Giant mine by graduate students at Queen's University (i.e., Andrade, 2006; Fawcett *et al.*, 2006; Fawcett *et al*, 2008; Walker *et al.*, 2005; Walker, 2006) have shown the presence of roaster-derived iron (Fe) oxides (containing As) and natural arsenopyrite, along with other sulphide minerals, in tailings stored on site and in sediments in the adjacent Yellowknife Bay. These graduate studies have focused on understanding the solid phase speciation of As in tailings and mine wastes as well as the anthropogenic input of As to the lake-sediment system. Work at the Giant mine continues with S. Fawcett who is examining the relationship between As and Sb in waste water and sediments. Few studies have examined the soils in detail to characterize the source, form and distribution of As present on the property.

Arsenic concentrations in soil samples were measured from different regions around the mine property by environmental consultants with additional samples from the Giant Townsite were taken by S. Walker (2006) (see section 2.2.2 for a complete description of these studies). The Giant Townsite is a small residential area located on the shores of Yellowknife

Bay that housed miners and their families during the operation of the mine (Figure 1.1). Measured soil As on the property are two to three orders of magnitude higher than the site-specific human health-based soil quality remediation objectives guidelines of 160 ppm set for the region by the Government of the Northwest Territories for

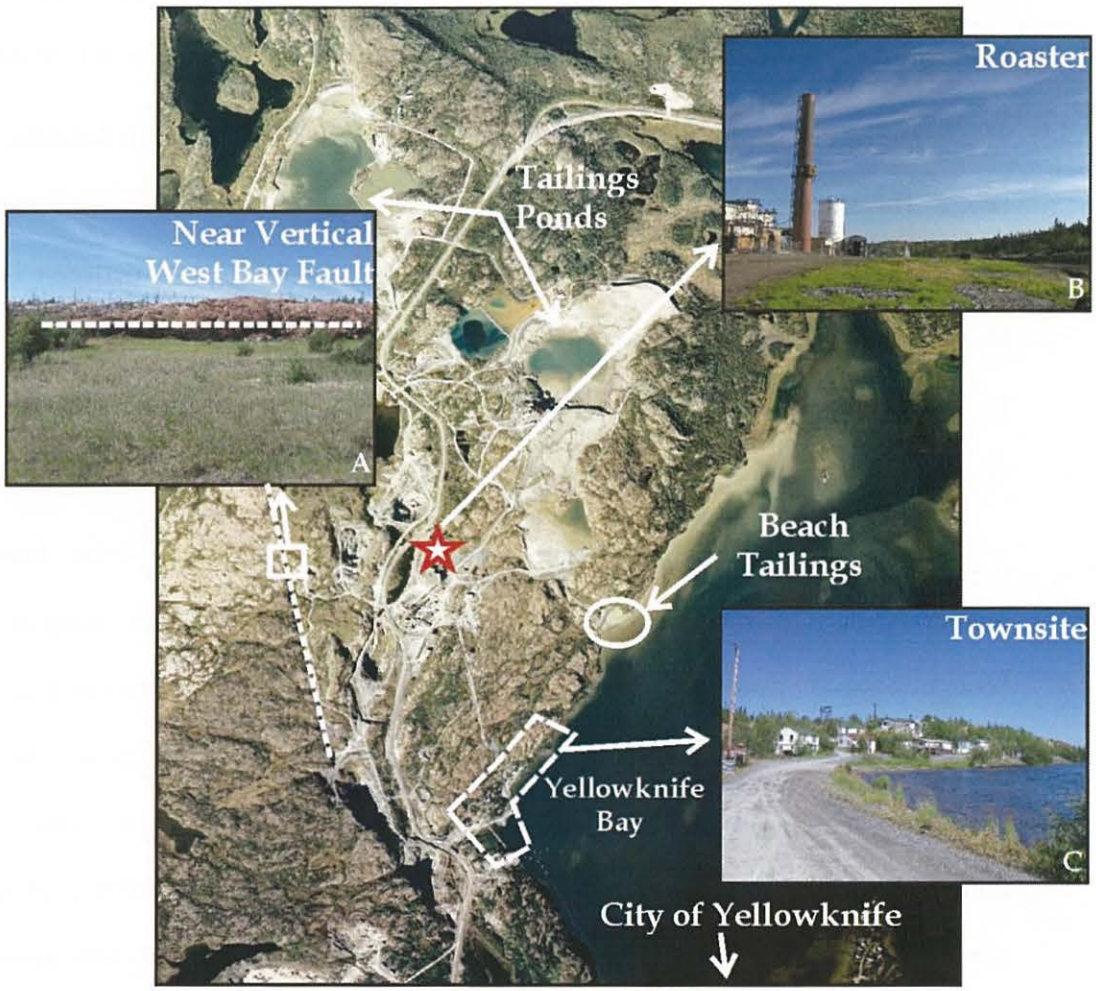

Figure 1.1: Airphoto of the Giant Mine Property, Northwest Territories. Inset **A**: West Bay Fault is on the western edge of the Giant mine property boundary **B**: The Giant mine gold roaster; **C**: When the Giant mine was in operation, the Townsite is where many of the workers and their families were housed. The area leased by the City of Yellowknife and may potentially be the site of new developments in the future.

residential areas (GNWT, 2003; Risklogic, 2002a). The Yellowknife As guidelines were set higher than the CCME standard because of the naturally elevated As concentrations in soils associated with gold mineralization. Also considered was the decreased frequency, duration and intensity of land use due to the snow cover in the winter months. The Giant mine is currently in the remediation process, and future potential development makes it essential to understand the source of As within the soils before the land becomes accessible to the public.

The second study site is the abandoned, historic gold mine in North Brookfield, Nova Scotia. This site is currently publicly accessible and commonly used for dirt bike and All Terrain Vehicle (ATV) racing. There has been very little published work performed on the soils surrounding this site (Golder, 2005; SRK, 2005) so characterizing the form of As at this location was important to understanding the potential health risks that this site could pose to the public.

This thesis was designed to examine the soils surrounding the above two mines. Soils in both regions may have been impacted by the airfall of As from the ore-roasting as well as being influenced by natural As. Understanding and distinguishing between natural and anthropogenic sources of As in soils is important from a remediation perspective, as cleaning a site below natural As concentrations can be difficult and expensive. Also considered is the human health risk assessment perspective as the bioaccessibility, the percentage of As that is released from the ingested soil in the gastrointestinal tract and is available to be absorbed into the bloodstream, is heavily dependent on its mineral form.

The sampling strategy used in this thesis was intended to achieve the goal of differentiating between the two sources by choosing locations where soil profiles appeared to be undisturbed by mining-related activities such as tailings or waste rock deposition, and

potentially impacted by aerial emissions from the ore roaster. Core samples were taken to allow for higher resolution sub-sampling to document the changes in the form of As with depth. Advanced techniques such as synchrotron-based microanalysis, sequential selective extractions (SSE) and the environmental scanning electron microscope (ESEM) made it possible to distinguish the various As-bearing host phases within the soils.

1.2 Site Descriptions

1.2.1 Giant mine, Northwest Territories

Giant mine, located close to the City of Yellowknife on the western side of the Yellowknife Bay, is the site of one of the oldest and most successful gold mining operations in the Slave Province (Figure 1.1) (INAC, 2007). Giant mine operated for more than 50 years from 1948, when the first gold brick was poured, until the ore processing operations ceased in 1999 when the mine went into receivership. Miramar Giant Mine Ltd. purchased the assets of the mine and continued the underground operations at Giant until 2004. During this time the Government of Canada, through Indian and Northern Affairs Canada (INAC), took on the role of caretaker of the pre-existing environmental liabilities on the property (INAC, 2007). Over the lifetime of the mine more than 7 million ounces of gold was produced.

1.2.1.1 *Regional Geology and Mineralization*

In the Yellowknife area, gold was first discovered in the late 1890's by a field party led by the Geological Survey of Canada. The region received little interest from prospectors until the 1920's when better methods of transportation to the north developed. It was not

until July of 1935 that C.J. Baker and H. Muir (on behalf of Burwash Yellowknife Mines Ltd.) staked the first claims that would become the Giant mine (Moir *et al.*, 2006).

Gold in the Yellowknife area is located within the brittle-ductile shear system that transects the Kam Group of the major Archean Yellowknife Greenstone Belt (YGB) in the southwestern portion of the Slave Structural Province (SSP) (Hubbard *et al.*, 2006; Siddorn *et al.*, 2006). The SSP is host to numerous gold mines with the largest and most productive deposits being the Giant and Con mines (Canam, 2006). Both mines are located within the YGB between the Western Plutonic Complex (to the west) and the Duncan Lake Group which conformably overlies it to the east, as seen in Figure 1.2 (Siddorn *et al.*, 2006).

The YGB consists of a succession of tholeiitic massive and pillowed flows, calc-alkaline tuffs and flows, intercalated volcanogenic sediments and sheeted gabbroic dykes (Canam, 2006). It is characterized by three metamorphic facies; the amphibolite facies developed adjacent to the Western Plutonic Complex which then grades through an intermediate epidote amphibolite facies to a poorly defined greenstone facies by the shore of Yellowknife Bay (Boyle, 1979; Siddorn *et al.*, 2006).

There were four superimposed deformational events (D) that led to the structural characteristics of the gold deposits in the Yellowknife area. D_1 was characterized by normal extensional deformation and the stratigraphic tilting and formation of the Giant deformation zones (GDZ). Gold mineralization and alteration was thought to occur during or just after this period of deformation. D_2 is considered the main deformational event where a period of regional E-W compression resulted in the original GDZ and the orebodies becoming flattened, folded and boudinaged. This event marked the formation of the dominant foliation on the Giant property.

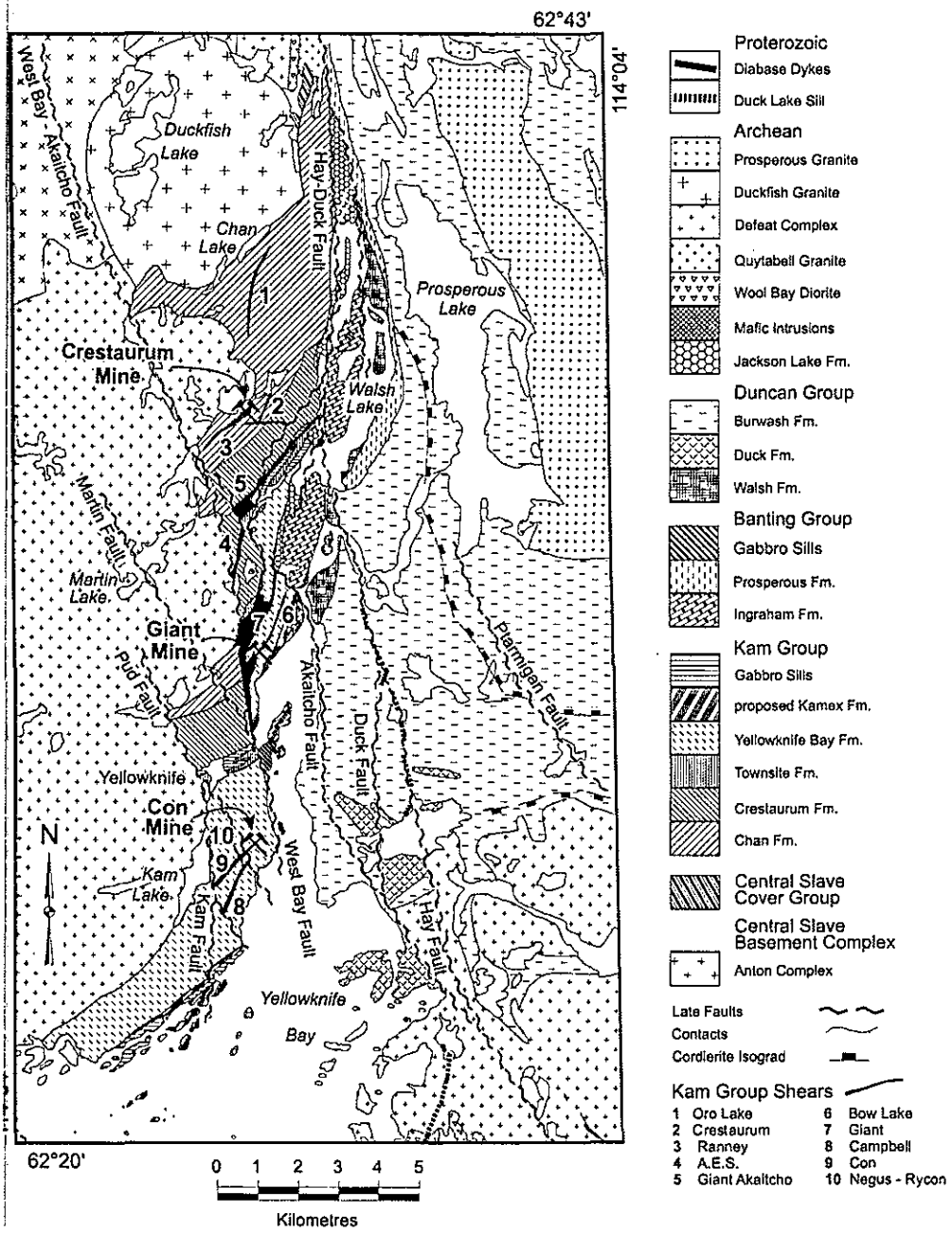

Figure 1.2: Geological and structural map of the Yellowknife greenstone belt. Map shows the location of the City of Yellowknife as well as the Con and Giant gold mines. The bolded numbers represent the various shear zones within the Kam Group. The Giant mine is located within the Giant shear zone in the Kam Group with the West Bay Fault to the West and the Akaitcho Fault to the East (Hubbard *et al.,* 2006).

D_3 represents the late reactivation of the GDZ possibly during the same tectonic regime of D_2 causing the folds to become more angular. Finally, D_4 was the Proterozoic sinistral strike/slip faulting which caused the segmentation and offset of the Giant deposit (via the West Bay Fault) from another gold deposit to the south called the Con deposit (Siddorn *et al.*, 2006). In 1947, Campbell's reconstruction of the movement along the fault systems led to the discovery of a deeper deposit (called the Campbell shear) at the Con mine. It was originally believed that the Giant mine was the eastern faulted portion of the Campbell shear. Recent work on the fault systems suggests that the Giant mine may represent the shallower Con shear and that the lower Campbell shear remains unexplored underground at Giant (Siddorn *et al.*, 2006).

The Giant mine gold deposit comprises gold-quartz veins and silicified zones that are approximately 50 to 500m wide and lie between the West Bay and Akaitcho fault systems (see Figure 1.2) (Boyle, 1979). Mineralization at Giant occurs in a series of quartz and sulphide bands alternating with sericite-carbonate schist. Gold is found as both refractory gold, incorporated within the mineral arsenopyrite, and free gold, with the latter being less common and exploited early in the history of the mine (Hubbard *et al.*, 2006; Siddorn *et al.*, 2006; Tait, 1961). The orientation of the schist zones is thought to be the controlling factor for the shape and orientation of the ore zones. Shallowly dipping schist zones are irregular, roughly ellipsoidal, ore zones whereas more steeply dipping schist zones produce more tabular steeply dipping ore zones (Canam, 2006).

The mineralogy of ore at the Giant mine is variable depending on the ore shoot and the region within the mine making detailed mineralogy dependant on location (Canam, 2006). Based on thorough studies by Coleman (1957) on the orebodies being mined at the

time, sulphides and sulphosalts represent 5% to 15% by volume of the ore, with the average being typically less than 10%. Principle sulphides at Giant include: pyrite, arsenopyrite, sphalerite, chalcopyrite, sulphosalts, pyrrhotite and galena (Canam, 2006; Coleman, 1957).

The relationship between gold mineralization and deformation events has been described by Siddorn *et al.* (2006) and shows mineralization occurring over both the D_1 and D_2 events. D_1 is characterized by refractory mineralization in disseminated arsenopyrite and pyrite, including the formation of other minerals such as galena, sphalerite and lead(Pb)-Sb sulphosalts within schist ore-zones and quartz-veins. D_2 is marked by the formation of free-milling gold in quartz veins containing pyrite, arsenopyrite, chalcopyrite, pyrrhotite, sphalerite, galena, tourmaline and Pb-Sb sulphosalts.

In the Yellowknife area the Late Wisconsin glaciation reached its peak extent 18,000 years ago covering the entire region by ice. Meltwaters from deglaciation formed glacial Lake McConnell that would have inundated the Yellowknife region up to 120 m above the current level of the Great Slave Lake leaving glaciolacustrine tills as the most pervasive sediment in the area (Kerr, 2006). The glaciolacustrine tills consist of poorly to moderately sorted coarse to fine sand, silt and clay with variable amounts of pebbles and cobbles (Kerr, 2006). Organic deposits formed by the accumulation of vegetative matter with shrubs and some smaller trees now cover the tills surrounding the Yellowknife area.

1.2.1.2 Mining and Ore Processing History

Mining first began at the Giant mine in 1948 and the initial capacity of the ore treatment circuit was 250 tonnes per day (tpd). By January of 1949 a flat-hearth roaster was introduced to treat the refractory gold ore. The ore was processed using a series of five

circuits (More and Pawson, 1978). Ore was first crushed, then subjected to a froth flotation to selectively separate the heavier gold hosted sulphides. The concentrate underwent mercury amalgamation (to remove free gold) until 1959 when the nature of the ore changed to be more refractory and this step was eliminated (INAC, 2007). The concentrates were roasted at elevated temperatures breaking down the sulphides into porous Fe-oxides releasing As_2O_3 SO_2 gases (More and Pawson, 1978). Roasting the ore was necessary because the refractory nature of the gold at Giant made it non-amenable to conventional treatment (Tait, 1961). After roasting, cyanide was added to the roaster calcine (oxidized product) to recover the gold.

During the operation of the mine, the majority of changes to the ore treatment systems were directly related to the tailings disposal, ore roasting system, or effluent treatment systems. From 1949 to 1951 the materials that remained after the various processing stages were discharged, without treatment, directly onto the shore of Yellowknife Bay (see Figure 1.1). Additionally, gases and dusts generated by the Edwards type roaster including both As_2O_3 and SO_2 were emitted directly up the stack and dispersed without treatment (More and Pawson, 1978; Tait, 1961). In 1951 the installation of a cold Cottrell Electrostatic Precipitator (Cold ESP) was designed to assist in removing As_2O_3 from the roaster gases.

The Edwards roaster originally built at Giant had a low capacity and at times the temperature at the exit point from the roaster was sufficiently low to cause the As-rich gases to condense (INAC, 2007). To curb these issues a prototype two-stage Dorrco Fluosolids roaster was added to the roasting circuit in 1952, which allowed the milling capacity to be increased (Tait, 1961). This roaster consisted of a single cylindrical reactor, split into two

distinct compartments by an internal dividing wall that allowed separate measured quantities of air into each compartment. Partially roasted calcine under low oxygen conditions from stage 1 would flow through three small transfer ports in the wall, into the second compartment, where the roast continued under oxidizing conditions (More and Pawson, 1978; Tait, 1961).

By 1955 a hot Cottrell Electrostatic Precipitator (hot ESP) was installed to capture gold-bearing As-rich dust that was exiting the roasting stack. In 1958 the two roasters in operation were replaced by one larger capacity two stage Dorrco Fluosolids roaster to deal with an increase in mill tonnage because the ore being mined was more refractory (Figure 1.3) (Tait, 1961). A baghouse was also added in the series with the new roaster and hot ESP

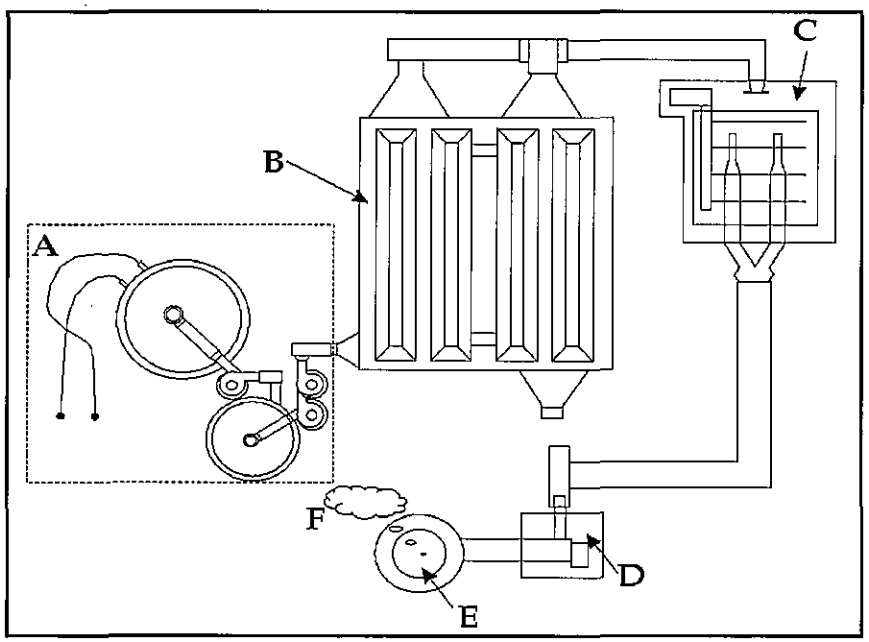

Figure 1.3: Plan view of the 1958 Dorrco no. 2 Fluosolids Roaster and Gas Treatment System at Giant. A Two stage Dorrco fluosolids roaster; B Series of two hot electrostatic precipitators; C Dorrco baghouse; D Stack fan; E Brick Stack; F Emissions from roasting stack. Image modified after Foster, 1963 and Tait; 1961.

for a more efficient removal of As-rich gases and calcine dust. These improvements in the roasting process allowed mill processing rates to increase again to over 1,000 tpd. The new system proved to be very effective in treating the concentrated ore and remained in operation until ore processing ceased in 1999 (INAC, 2007).

In 2007 the Giant Mine Remediation Team submitted the Giant Mine Remediation Plan to the Mackenzie Valley Land and Water Board for review (INAC, 2007). As part of the remediation plan several environmental consulting companies were hired to delineate As contamination around the Giant mine. Supporting documents from the remediation plan show elevated dissolved As in surface water seeps across the mine property that were believed to be attributed to a mobile form of As in the soils (SRK, 2005). The mineralogical source of As in the soils was not determined; however it was speculated that high As in the surface water seeps was the result of atmospheric deposition of As from the roasting operation and wind dispersion of As-rich dust from adjacent to the baghouse. Total As concentrations were also measured in several media (soils and mine wastes) across the property and were found to also have elevated As concentrations (Golder, 2005).

At the time of writing this thesis, the remediation plan for Giant property focused on the long-term containment and storage of the As_2O_3 dust, the demolition and removal of all buildings on the surface, and the remediation of all surface areas including tailings ponds (INAC, 2007). More recently, the City Council in Yellowknife has voted for an Environmental Impact Assessment (EIA) to ensure the current remediation plan will be effective in treating the As-contamination on site with the potential for some regions to become publicly accessible in the future (MVLWB, 2008).

1.2.1.3 Generation and Emission of Arsenic Trioxide from Roasting

At the Giant Mine, roasting of gold ore has generated over 237,000 tonnes of As_2O_3 now stored underground in chambers (mined out stopes) and emitted approximately 20,000 tonnes from the roasting stack over the lifetime of the mine (Table 1.1) (CPHA, 1977; EnviroCan, 2007; GNWT, 1993; INAC, 2007; Tait, 1961). After the installation of the first roaster in January of 1949, numerous worker health problems were reported which prompted the first of many studies into the effects of arsenic pollution in the Yellowknife area. In the first two years of roasting when no emission controls were in place, As_2O_3 emission rates were 7.2 tonnes per day (tpd) - compared to 0.01 tpd at the mines closure in 1999 (CPHA, 1977; EnviroCan, 2007). With the addition of the cold ESP in 1951, the first method of emissions control, As- rich gases and calcine dusts from the roaster were sent to the cold ESP where the inlet gas temperature was low enough that As and Sb-oxides condensed and were recovered by attraction to charged electrodes (Tait, 1961; INAC, 2007)

The addition of the new roaster in 1952 caused a drop in the collection efficiency of the cold ESP as the fumes had a reduced electrostatic charge and much more calcine dust was generated. This overloaded the cold ESP and caused higher As_2O_3 emissions and a loss of gold up the roasting stack (Tait, 1961). The loss of valuable gold spurred the installation of a hot ESP which was used in series with the cold ESP to separate calcine dust containing gold (collected in the hot ESP) from the As_2O_3 (collected in the cold ESP) (INAC, 2007).

The hot ESP was kept at a temperature high enough to prevent As_2O_3 from condensing, while removing the calcine dust. Gases would then pass to the cold ESP where As_2O_3 was condensed and recovered. The increased acidity and reduced electrostatic charge

Table 1.1: Estimates of Aerial Emissions of As_2O_3 dusts from the Giant Mine Roaster between 1949 and 1999.

Year	As_2O_3 Emissions † (tpd)	As_2O_3 Emissions‡ (tonnes)	Year	As_2O_3 Emissions † (tpd)	As_2O_3 Emissions ‡ (tonnes)
1949-1951*	7.3	7963.6	**1968**	0.2	83.0
1952*	5.5	1989.3	**1969**	0.3	109.5
1953*	5.5	1989.3	**1970**	0.2	80.5
1954	5.5	1990.9	**1971**	0.9	320.2
1955	2.9	1061.8	**1972**	0.4	145.2
1956	2.7	995.5	**1973**	0.4	147.7
1957	3.0	1078.4	**1974**	0.2	80.5
1958*	1.5	547.5	**1975-1992***	0.3	1698.9
1959	0.1	19.1	**1991-1993***	0.1	54.8
1960	0.1	27.4	**1994**	0.01	3.6
1961-1963*	0.2	163.3	**1995**	0.01	3.5
1964	0.3	114.5	**1996**	0.01	3.5
1965	0.0	0.0	**1997**	0.02	7.6
1966	0.2	88.8	**1998**	0.015	5.3
1967	0.1	47.3	**1999**	0.01	3.7
		Total As_2O_3 Emissions (tonnes)			**20,824**

† As_2O_3 emissions estimates were measured from the top of the roasting stack and were reported by following sources; CPHA, 1977; EnviroCan, 2007; GNWT, 1993; INAC, 2007; Tait, 1961.

* Emissions for this year or period of years have been estimated based on information from the above sources and known changes to roaster operations.

‡ As_2O_3 emissions for the year or period of years assuming roasting occurred for 365 days. This will be an overestimate of emissions however the dates when the roasted was not in operation are unknown and the majority of As_2O_3 generated was over the first 10 years of roasting.

made removal of As_2O_3 in the cold ESP more difficult so both ESP units were eventually converted to run at the colder temperatures (Foster, 1963; INAC, 2007). From 1952-1958 As_2O_3 emissions varied between 1.5 to 5.5 tpd with the older two roasters (CPHA, 1977).

The second Dorrco roaster, built in 1958, was connected in series with two hot ESP's (added in 1963) and the Dorrco baghouse (1958). It was the most efficient method of

removing As_2O_3 from the roaster gases (INAC, 2007). An image of the 1958 Fluosolids roaster and the gas treatment system can be seen in Figure 1.3. Concentrated ore was brought to the stage 1 reactor (larger reactor) where it was roasted at 496°C under reduced oxygen conditions. It was then transferred to stage 2 (smaller reactor) where oxygen was increased and the temperature was decreased to 468°C to complete the roast (Tait, 1961). Gases and dusts generated during both phases were cleaned in a series of two cyclones, each of which were connected to a separate quench tank. The quench products were then sent, with the roasted material, to be treated by cyanidation (Foster, 1963).

The gases from the cyclones were then sent to the series of two hot ESP's where additional dusts were removed. The final stage of gas treatment was the baghouse where the remaining As_2O_3 was removed and sent to the underground storage facilities (More and Pawson, 1978). The residual "clean" gas was then release up the stack (Figure 1.3) (Foster, 1963; Tait, 1961). With the installation of the newest roaster and baghouse in 1958, emission rates of As_2O_3 decreased to between 0.01 to 0.021 tpd. Rates of As_2O_3 emission remained at approximately this level until the closure of the ore processing plant in 1999 (EnviroCan, 2007).

1.2.2 North Brookfield mine, Nova Scotia

The North Brookfield mine is an abandoned historical underground gold mining operation that is located in southeastern Nova Scotia and produced gold from 1886-1906 (Figure 1.4)(DPWM, 1927; Malcolm, 1976). The mine changed names over the course of its 20 year lifetime which can be a point of confusion in historical documents.

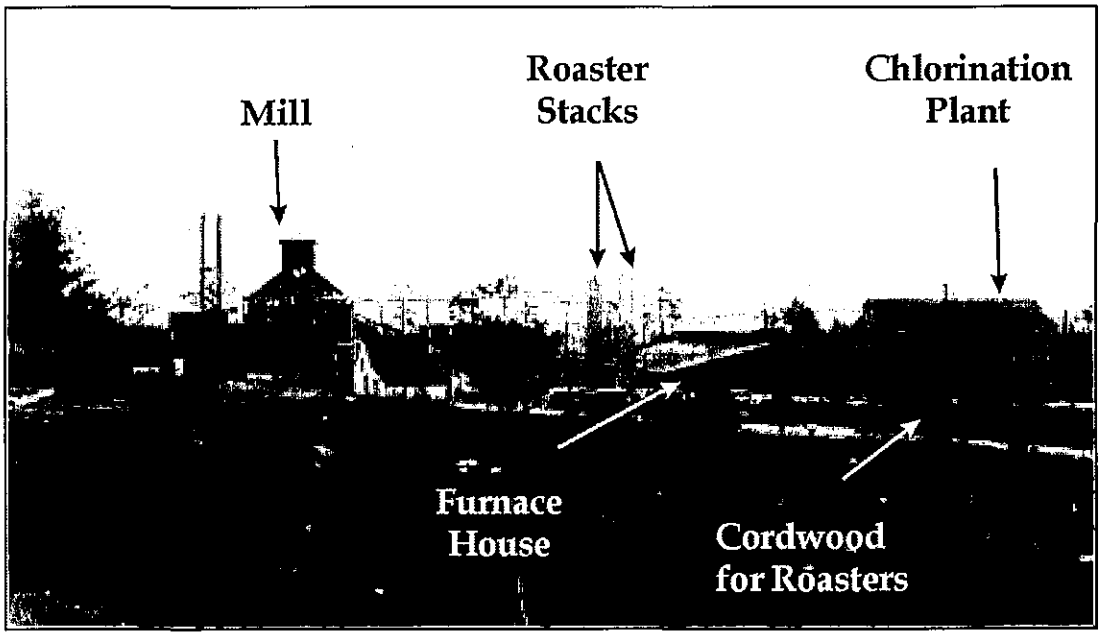

Figure 1.4: North Brookfield mine (ca. 1897). Image from; Men in the Mines- A History of Mining Activity in Nova Scotia, 1720-1992, Nova Scotia Archives and Records Management Photo Collection. <http://www.gov.ns.ca/nsarm/virtual/meninmines/>

Gold was originally discovered at North Brookfield in 1885, with mining initiated on a fissure vein in 1886 by J. McGuire and the Brookfield Mining Company. The mine was shut down from 1888 until 1894 when the property was passed to the Brookfield Mining Associates and was managed by W.L. Libbey, at which point it was commonly known as the Libbey mine until its closure in 1906 (Malcolm, 1927). From this point forward, the term "North Brookfield" or the "North Brookfield mine" refers to the McGuire and Libbey mine and not the mining district unless otherwise stated. Other mines in the North Brookfield district operated from 1886 to 1936 mining a total of 43,000 troy ounces of gold from 105,000 tons of crushed rock (Malcolm, 1929; Malcolm, 1972; Sangster and Smith, 2007).

1.2.2.1 *Regional Geology and Gold Mineralization*

Gold was first discovered in Nova Scotia bedrock in 1858 by Captain C. L'Estrange when he noticed a yellow metal in quartz by the Tangier River. By the 1900's the Provincial Government recognized over 60 gold districts within the province and between 1861 and 1961 over 1.2 million ounces of gold was mined from the 20 largest districts in the province (Sangster and Smith, 2007; Smith *et al.*, 2005).

The majority of the gold in Nova Scotia is hosted in the Cambro-Ordovician Goldenville Formation of the Meguma Group consisting of metamorphosed sandstone, siltstone and shale. The Goldenville Formation is overlain by the slate, shale and siltstones of Halifax Formation that contains minor quantities of gold (Figure 1.5) (Sangster and Smith, 2007; Schenk, 1997; Smith *et al.*, 2005). Structures and bedding seen within the Meguma suggests it was deposited by turbidity currents (Graves and Zentilli, 1982).

The rocks of the Meguma Group have undergone poly-phase deformation in the early Devonian during the Acadian Orogeny and accompanying granitic intrusions. This produced northeasterly-trending, sub-horizontal, broad, open folds that formed domal structures (Sangster, 1992). Gold within the Meguma Group is preferentially found just below the Halifax/Goldenville Formation boundary in bedding-concordant quartz veins that tend to be located either on or near the anticlinal crests (Sangster and Smith, 2007). It is known that these vein structures formed as a result of metamorphic fluids, however, the genesis of the gold veins remains unclear. More recent theories suggest that vein formation may have been episodic and caused by a combination of poly-phase deformation as well as regional and contact metamorphism (Sangster, 1992; Sangster and Smith, 2007; Smith *et al.*, 2005).

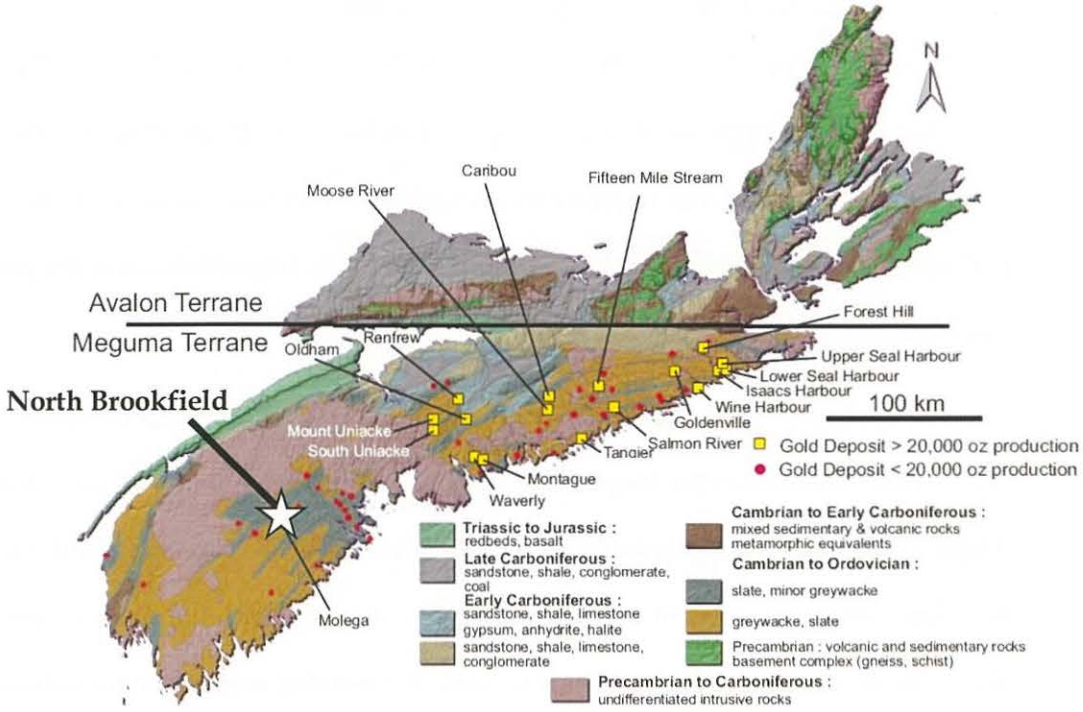

Figure 1.5: Geological map of Nova Scotia showing the many gold mining districts within the province. The map shows the location of the North Brookfield mine within the slates of the Cambro-Ordovician Goldenville Formation of the Meguma Group in the southeastern portion of the province (Sangster and Smith, 2007).

In the North Brookfield Gold District, the main gold producers were the high grade (15g/t Au) Libbey Fissure vein (North Brookfield mine) as well as the King and East Fissures. The Libbey Fissure is a linear discordant quartz vein that cuts the host Goldenville rocks at a very high angle and was approximately 45 cm thick (Ryan and Smith, 1998). Additional local mineralization occurred where the fissure vein intersected bedding concordant veins that were up to 2.5 meters thick. Regional and local alteration resulted in intense silicification, sericitization, sulphidization and chloritization of rock lithologies (Sangster and Smith, 2007).

The North Brookfield mine is one of the deepest mines in the Meguma Terrain, reaching vertical depths of 310m. Its closure in 1906 was a direct result of the high costs of ore production at those depths even though mineralization continued deeper (Malcolm, 1929; Ryan and Smith, 1998). The Libbey Fissure contained free gold as well as gold-bearing arsenopyrite (Forbes, 1904; Ritchie, 1901). Chalcopyrite, also found in the in the area, was generally used as an indicator for mineralized quartz veins as sometimes free gold would be found surrounding these crystals (Ritchie, 1901).

1.2.2.2 Mining and Ore Processing History

At the North Brookfield mine, ore processing methods varied over the period of the operation. Historical records are vague in the method of ore processing prior to 1896 and it is assumed that during this time ore was crushed with mercury amalgamation used to recover the free gold. After acquiring the mine in 1894 the Brookfield Mining Associates sunk an incline on the vein allowing for a large quantity of ore to be stoped and milled. In December of 1896, after successful trials, the Brookfield Mining Associates completed a barrel chlorination plant on-site that was designed to treat between 12 and 16 tons of gold concentrate per day. At this time the ore passed through a circuit of newly built stamp-mills, was then amalgamated, gravity concentrated and roasted prior to being treated by chlorination. Chlorination at North Brookfield proved to be the most effective and economical method of extracting the gold from the ore and by 1898 the mine reported being able to recover 90% of the gold from the roasted concentrates (DPWM, 1899).

An important step in the processing circuit was the roasting of the gold concentrate prior to chlorination to assist in the recovery of the gold from the sulphide-rich ore. As at the Giant mine, roasting was performed by heating the concentrated ore to oxidize the

associated sulphur (S) and As and decompose the arsenopyrite grains into porous iron-oxides. Prior to roasting, the concentrated ore contained approximately 28% S and 16% As by weight. It was necessary to remove the S and As before chlorination as both would be oxidized by the chemical additives used in the process. This would cause a decrease the volume of chlorine available for treatment of the gold and therefore the gold recovery during chlorination (Anonymous, 1897; Forbes, 1904; Ritchie, 1901).

Roasting at the North Brookfield Mine took place in three housed reverbatory furnaces that were located in the northern end of the chlorination house as seen in Figure 1.6 (Forbes, 1904). Each of the three furnaces had a 2 tpd capacity which was divided between

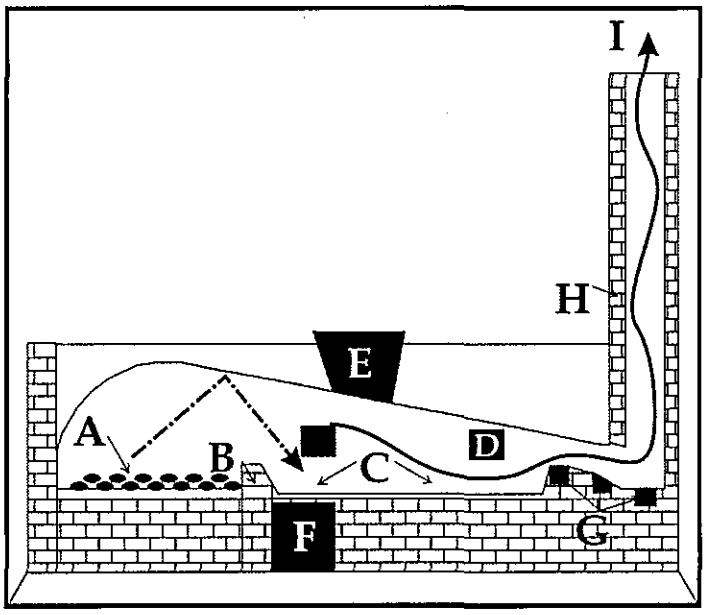

Figure 1.6: Cross section of hand reverbatory furnace from 1897 used at the North Brookfield mine. A is the fire-box where heat for roasting is generated; the flame from the hearth is separated from the ore by a bridge B; Ore is charged through the hopper E to the hearth C; the apertures D are the working doors where the ore is spread and stirred during roasting; F is the discharge pit for the roasted ore; G are the dust chambers where As_2O_3 dust was allowed to collect; H represents the roasting stack and I is the discharge point for heat as well as emissions of As_2O_3 and SO_2. Image modified after Wilson (1897).

four different stages of roasting. *Figure 1.6* is a diagram of a reverbatory roaster common in 1897. The concentrate was first dried closest to the fire box for eight hours then was moved further from the fire to the middle of the roaster where it was burned (Forbes, 1904; Ritchie, 1901; Wilson, 1897). In the final stage of processing, the concentrate was removed from the furnace and allowed to cool prior to chlorination. The remainder roasted concentrate contained approximately 1% *S* suggesting that practically all the *S* and As were driven off during the roast (Forbes, 1904).

Forbes (1904) noted that during the burning phases, after the moisture was expelled, white fumes would rise quickly and persist until the final stage of roasting. He interpreted these fumes as being a combination of SO_2 and As_2O_3 that were released as the ore was oxidized. To release these fumes from the furnace, the hearth was designed to funnel dust towards the chimney when the working doors were kept open. Along the passage to the chimney there were chambers where the fumes were allowed to condense and the dust could be stored. Dust also accumulated at the base of the chimney stacks making it important for both of these areas to be periodically emptied (Forbes, 1904). Historical records do not indicate where this arsenic rich dust would have been stored permanently.

From 1896 to 1904, the concentrate was roasted, cooled, then sent to the chlorination plant where it was treated using the Theies process of barrel chlorination (DPWM, 1899). This process involved the addition of water, sulphuric acid (H_2SO_4), roasted concentrates and bleaching powder ($Ca(OCl)_2$) to lead lined chlorinating barrels with the purpose of using chlorine to liberate the gold (Anonymous, 1897; Ritchie, 1901). The fluid mixture was then filtered into a vat using a series of layers of crushed rock. Once filtered to remove unwanted particulates, $FeSO_4$ was added causing the dissolved gold to precipitate as a

brown solid. The fluids were siphoned off and the precipitates were sent to an additional settling tank for 24 hours. In the final stage of chlorination the precipitates were filtered, air-dried, mixed with reagents and sent for smelting (Ritchie, 1901).

After 1904, the North Brookfield mine switched from chlorination to the Silman and Teed process of bromo-cyanidation (BC) until the mine closed in 1906. Little is known about how this method of gold extraction was used at North Brookfield. Based on Brown (1908), roasted of concentrated ore continued to be a part of the ore treatment to remove arsenic prior to BC, even through it was not a common practice at this time (Clennell, 1915; Nardin, 1910).

In BC the roasted concentrates would have been treated by agitation with cyanide solution where the bromine of cyanogen (BCy) was added. BCy is a volatile crystalline solid that is soluble in water and is the key reagent used in this type of gold extraction (Clennell, 1915). The solution was filtered to remove any sludge that was considered waste and re-filtered through zinc shavings to precipitate gold (Nardin, 1910). Historical reports mention the presence of wastes produced during the chlorination and bromo-cyanidation processes; however, as with wastes from the roasting process, no method or location of waste disposal is discussed. The location of these wastes will have significant implications to the speciation, mineralogy and distribution of arsenic in soils surrounding the mine and potentially the tailings onsite.

Currently the North Brookfield mine remains as one of many publicly-accessible abandoned gold mines in Nova Scotia. Work is ongoing on soils and tailings on the mine property by the Atlantic Division of the Geological Survey of Canada, Queen's University

and the Royal Military College (Meunier *et al*, 2008; Meunier *et al.*, in progress; Walker *et al.*, 2008; Jamieson *et al.*, 2008).

1.2.2.3 Generation and Emission of Arsenic Trioxide from Roasting

Without estimates of emissions released from the roasting stack during mining it is difficult to provide an accurate measurement of aerial emissions at North Brookfield. Unlike the Giant mine, North Brookfield would have had no emission controls in place to prevent the aerial dispersal of SO_2 and As_2O_3 to the surrounding area as environmental controls were not common place in the early 1900's. Using historical reports that recorded the quantity of ore milled over the lifetime of the mine it is possible to provide an estimate of the tonnage of As_2O_3 generated by roasting (Table 1.2).

Based on the assumption that roasting continued when North Brookfield used bromo-cyanidation as well as other assumptions detailed in Table 1.2, it is estimated that 2200 tons of As_2O_3 could have been generated (DPWM, 1899; DPWM, 1927; Forbes, 1904; Malcolm, 1976). However, it is impossible to know the proportion of this dust emitted from the North Brookfield stack since reports mention significant quantities of dust being collected and disposed of from the base of the stack as well as from dust chambers within the hearth. Because it is unlikely that material was transported any distance, it may have been deposited close to the roaster. The total As_2O_3 generated at North Brookfield is approximately 10% of the total As_2O_3 emitted by the roasting stack at the Giant mine.

Table 1.2: Estimates of Aerial Emissions of Arsenic Trioxide from the North Brookfield Mine Roaster between 1986 and 1906.

Year	Total Concentrate roasted (tonnes)	Estimated As in Concentrate † (tonnes)	As released by Roasting‡ (tonnes)
1896[c]	4	1	1
1898	1731	277	274
1899	1740	278	276
1900	1654	265	262
1901	1387	222	220
1902	1558	249	247
1903	1829	293	290
1904	1963	314	311
	Switch to Bromo-Cyanidation (ore still roasted)		
1905	2197	352	348
1906	0	0	0
TOTAL Chlorination and Cyanidation	**25,925**	**2,249**	**2,227**

Estimates of As_2O_3 emissions were made based on the reported volume of material milled from the following reports: DPWM, 1899; DPWM, 1927; Forbes, 1904; Malcolm, 1976.
† Assumed that 16% of the concentrated ore was As;
‡ Assumed 99% removal of As during the roasting of ore-concentrates; [c] - Not included in tpd average

1.3 Research Goals and Thesis Organization

The overall goal of this thesis is to characterize the content, form, speciation and fate of As in soils surrounding the North Brookfield and Giant mines. The North Brookfield mine is currently publicly-accessible and the tailings are known to be used for recreational activities such as dirt biking and all-terrain vehicles. At present the majority of the Giant mine property is not publicly-accessible. However, there are plans for future development in the area once remediation is complete. Understanding the fate of aerial emissions of arsenic

trioxide at both of these mine sites is extremely important to understanding the health risks that they pose.

The following research objectives were set as means of answering the question of aerial emissions of arsenic trioxide;

- To identify and distinguish between natural As and anthropogenic As within the soil horizons
    - Is it possible to identify anthropogenic As within the soil horizons?
    - Is there vertical mobility of As in soil profiles?
    - What effect, if any, does organic matter have on the concentration of As in the soils?
    - If anthropogenic As is present in the soils, is it potentially the source of soluble arsenic measured by SRK Consulting (2005) in surface water seeps at Giant? If so, how long would the loading of soluble arsenic to surface expect to continue?
    - Does the impact of SO_2 deposition, recently discontinued at Giant, effect As speciation and mobility in the soil?
    - Is it possible to identify any geochemical or mineralogical transformations that have occurred in the As-hosting phases since their introduction into the environment?
- To identify roaster derived iron oxides in soils from the North Brookfield and Giant Mines and compare their behaviour in soil environments to roaster

oxides collected by Walker *et al.* (2005) in the sub-aerial and oxidizing environment at Giant mine.

- To compare soils from North Brookfield and Giant mines to better understand the effects of ore-roasting and time on form and speciation of As within soils.

This thesis is organized into six chapters, two of which have been prepared for journal submission. There is some overlap of the introductory material and methods descriptions in the two manuscripts. Chapter 2 is a review of the literature of previous studies performed at Giant mine as well as background information on the As-solid phase interactions in the environment and a short discussion on the toxicity and bioavailability of As. At the time of writing this thesis there have been no published works on As in soils or tailings at the North Brookfield mine. Chapter 3 is a detailed description of the field and analytical methods used in this thesis. The fourth chapter is a manuscript focused on the presence persistence of the anthropogenically derived As_2O_3 in the soils surrounding the Giant Mine, NT using ESEM and synchrotron techniques. Chapter 5 describes the use of sequential selective extractions and synchrotron techniques to understand the form, source and mobility of As in soils from the Giant mine, NT and the North Brookfield mine, NS. Finally, Chapter 6 includes the final conclusions and recommendations for future work at both mine sites. The appendices can be found at the end of the thesis and include full data tables and the remaining data that was not included in the manuscripts prepared for journal submission. Also included are additional site photographs and recorded field information.

Chapter 2: Literature Review

2.1 Arsenic Solid Phases

2.1.1 Arsenic in Soils

The toxicity of As is highly dependent on its form, oxidation state and dosage (Caussy, 2003; Valberg *et al.*, 1997; Walker, 2006). In natural systems, As can exist in a wide range of oxidation states: -3 in arsines (e.g. Arsine gas- AsH_3), -1 for arsenopyrite, 0 for elemental As, 2+ for realgar (As_4S_4), +3 for arsenites (e.g. arsenolite- As_2O_3 and orpiment As_2S_3), and +5 for arsenates (e.g. scorodite $FeAsO_4 \bullet 2H_2O$), with the last two states being the most common in nature (e.g., Harper and Haswell, 1988; Savage *et al*, 2000; Valberg *et al.*, 1997). As^{3+}- bearing minerals are considered to be highly soluble under oxidizing, neutral conditions with the dissolved As^{3+} species being more mobile and toxic in the environment than As^{5+}, which is more common in aerobic or oxygenated soils (DesChamps *et al.*, 2003; Goh and Lim, 2005; Masscheleyn *et al.*, 1991; Walker *et al.*, 2005). The toxicity of As is consequentially related to the mineral form and therefore bioaccessibility of the solid phase in the human body (Bhumbla and Keefer, 1994; DesChamps *et al.*, 2003).

Arsenic can be found in the crystal structure of many sulphide minerals other than arsenopyrite, realgar and orpiment because the chemistry of As closely resembles that of sulphur (S) allowing for substitution. One example of this is As-bearing or arsenian pyrite ($Fe(S,As)_2$) (Smedley and Kinniburgh, 2002). Pyrite, like arsenopyrite, is an important mineral in sulphide ore bodies and forms in high temperature conditions in the earth's crust. Unlike arsenopyrite however, pyrite can also form in low temperature environments under reducing conditions and can sometimes precipitate in a characteristic form called framboidal

pyrite (Smedley and Kinniburgh, 2002). The weathering of arsenopyrite and pyrite follows the *Equations* 2.1 and 2.2 below forming As^{5+}, Fe^{3+}, SO_4 and acid.

$$4FeAsS_{(s)} + 14O_2 + 16H_2O \leftrightarrow 4AsO_4^{3-}{}_{(aq)} + 4Fe(OH)_{3(aq)} + 4SO_4^{2-}{}_{(aq)}\ 20H^{+}{}_{(aq)} \quad \textbf{(Equation 2.1)}$$

$$2FeS_{2(s)} + 7.5O_2 + 7H_2O \rightarrow 2Fe(OH)_{2(s)} + 4SO_4^{2-}{}_{(aq)} + 8H^{+}{}_{(aq)} \quad \textbf{(Equation 2.2)}$$

In light of recent work by Pokrovski *et al.* (2002) that demonstrated a change in the thermodynamic data for arsenopyrite, Craw *et al.* (2003) has found through stability calculations and field observations that arsenopyrite is more chemically sensitive to small changes in the redox potential of the system than previously thought. This work showed that arsenopyrite is extremely soluble in oxidizing conditions while being extremely insoluble or stable in moderately reducing environments (Craw *et al.*, 2003). Arsenopyrite would only become replaced by realgar and orpiment in acidic conditions (pH<4) (Craw *et al.*, 2003). In oxidizing conditions, rims on arsenopyrite are typically composed of Fe-hydroxides, arsenate ($AsO(OH)_3$ or $FeAsO_4$) as well as some arsenite ($As(OH)_3$ and $FeAsO_3$) (Nesbitt and Muir, 1998; Pokrovski *et al.*, 2002).

Arsenic shows evidence of different degrees of attraction to metal oxides in soils and can be found adsorbed to minerals, oxides or hydroxides. These include iron (Fe), aluminum (Al), manganese (Mn) and calcium (Ca) as well as being found sorbed to clays and organic matter (OM) (e.g., Bhumbla and Keefer, 1994; de Mello *et al.*, 2006; Sadiq, 1997; Smedley and Kinniburgh, 2002). Adsorption is a complex process that is important for understanding the attenuation of As within soils as a particular aqueous species can become

sorbed either weakly, though weak electrostatic interactions called physisorption, or through stronger surface complexation reactions called chemisorption (Figure 2.1) (Smedley and Kinniburgh, 2002; Strumm and Morgan, 1996). It should be noted that

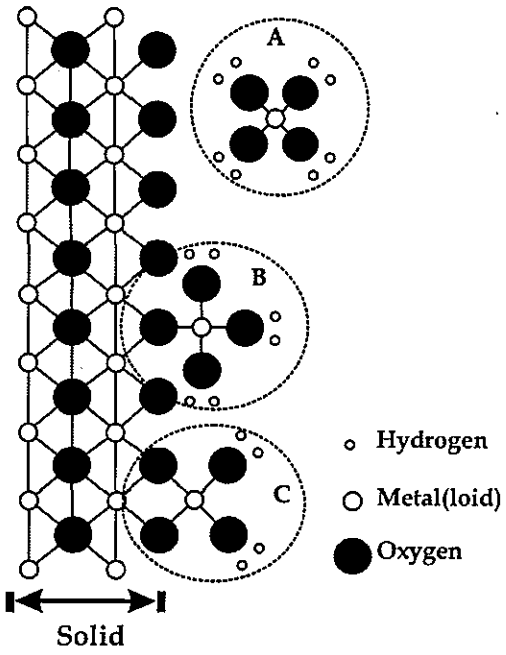

Figure 2.1: Two types of adsorption on oxide mineral surfaces. A Physisorption or outer-sphere weak surface adsorption; B and C are two forms of chemisorption which is stronger inner-sphere surface complexation reaction that is either monodentate (B) or bidentate (C). Modified from Strumm and Morgan, 1996.

while the above mentioned compounds are able to adsorb As, under different environmental conditions the surface of the minerals can become sources of As instead of sinks (de Mello *et al.*, 2006; DesChamps *et al.*, 2003; Scott and Morgan, 1995).

Conditions such as changes in concentrations of species competing for adsorption sites, pH (acidic vs. alkaline), Eh (oxidizing vs. reducing conditions), adsorption/desorption of other metals, biological transformations and properties of the soil such as grain size and organic matter (OM) content, will determine the adsorption of As (e.g., Bhumbla and Keefer,

1994; Goh and Lim, 2005; Sadiq, 1997; Yan-Chu, 1994). It is well documented that As is able to substitute for phosphate because of their similar behaviour in the aqueous state (Sadiq, 1997). In soils, phosphate sorption is generally greater than As sorption because the individual ions are smaller and a larger quantity can adsorb to the surface of the soil particles (Goh and Lim, 2005). From this observation it follows that phosphates compete for adsorption sites and this reduces the ability of As to be bound to the soil particles, thus mobilizing As in the soils (Yan-Chu, 1994).

Sadiq (1997) noted that the adsorption of As to clays can be difficult but has been observed when the soils are particularly acidic. The difficulty in As sorption stems from the fact that clay particles have negatively charged surfaces and would therefore tend to attract positively charged ions (not negative ions such as As-oxyanions). Arsenic will compete or replace phosphate and become sorbed to the surface of the clays either through chemisorption or ligand exchange. In acidic soils the surface charge on the clay becomes more positive, due to protonation, and therefore attracts the negatively charged As-oxyanions (Sadiq, 1997). Figure 2.2 shows the generalized charge distribution on soil colloids depending on pH; more positive charges are more likely to attract the negatively charged As-oxyanions.

Many oxide minerals such as Fe-oxides can incorporate significant amounts of As either within the mineral structure during formation as weathering products of sulphide minerals or as adsorbed species (Smedley and Kinniburgh, 2002). It has also been suggested that when As-oxyanions concentrate on the surface of Fe-oxides, Fe-(oxy)hydroxides or oxides of other elements at high concentrations, an As-bearing solid form may be

precipitated (Sadiq, 1997). The sorption of both As^{3+} and As^{5+} species to Fe-oxides is by far the most common method of As sequestration in soils as the oxides are stable under

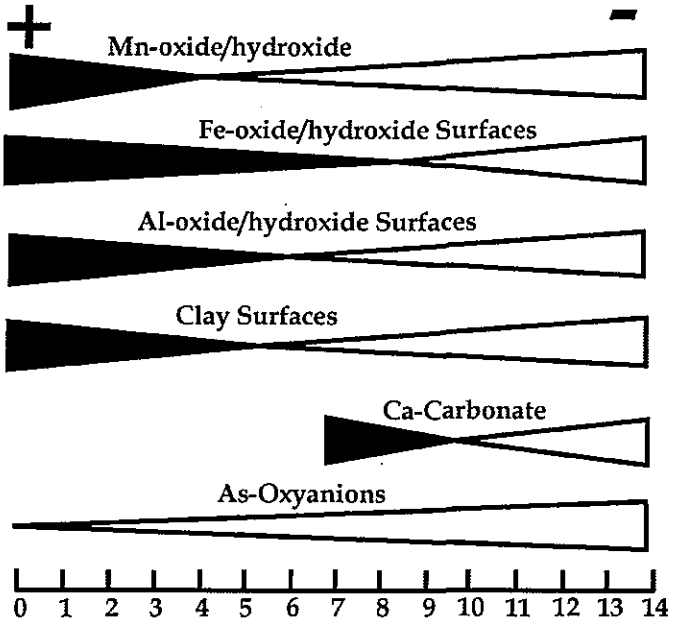

Figure 2.2: Generalized charge and strength distribution of common oxides/hydroxides and As-oxyanions. Surfaces of these oxides/hydroxides appear to play a more significant role in the adsorption of As-oxyanions in acidic soils with the exception of Fe-oxides/hydroxide surfaces which adsorb As-oxyanions up to pH's of 8-9. At the transition between black and white filled triangles the particular mineral surface would have limited adsorption of As. From Sadiq, 1997.

aerobic conditions. These Fe-oxides can preferentially adsorb different As species depending on the conditions within the soil, with arsenite dominating lower pH and arsenate at higher (Deschamps *et al.*, 2003). In oxidizing conditions As is strongly sorbed to Fe-oxides effectively removing As from the pore water. When redox conditions change from aerobic to anerobic, the dissolution of the oxide minerals would cause the strongly sorbed As-oxyanions to be released into the pore water (Smedley and Kinninburgh, 2002).

Experiments by Zobrist *et al.*, (2000) have also shown that desorption of As can occur even before dissolution of oxide minerals if there is a reduction from As^{5+} to As^{3+} on the oxide surface.

Studies have also assessed the effectiveness of natural Mn oxides in immobilizing As by oxidizing As^{3+} to As^{5+} and by directly absorbing As^{3+} into its crystal structure (DesChamps *et al.*, 2003; Sadiq, 1997; Scott and Morgan, 1995). Mn- oxides are important as they lower As^{3+} concentrations, but Fe-oxides are still considered more effective. Work by DesChamps *et al.* (2003) has shown that a natural system composed of Fe and Mn oxides can play a significant role in the oxidation of As from the more toxic to less toxic forms. The forms of Fe and Mn that are stable in reducing conditions are Fe^{2+} and Mn^{2+} both of which exist as soluble species which explains why changing the pH and Eh of soils can cause the desorption of As into the environment from the dissolution of the Fe and Mn oxides (Sadiq, 1997; Scott and Morgan, 1995).

Grain size also plays a role in the absorption of As in soils. The finer soil fractions have the ability to absorb more As than coarser grained soils. Higher surface areas therefore result in more sites of absorption (Yan-Chu, 1994). Studies performed in the 1970's showed a marked increase in As species absorption in soils when there was a fine grain size and Fe, Al and Mn oxides were present (Yan-Chu, 1994).

2.1.2 Stability of Arsenic Trioxide

Examples of mineral polymorphs with the formula of As_2O_3 are arsenolite and claudetite, both of which have nearly identical free energies of formation making it very difficult to determine which would be most stable under standard state conditions

(Nordstrom and Archer, 2003). Arsenolite and claudetite can both form a thin white coating as an uncommon secondary product caused by the oxidation of arsenopyrite and realgar and from native As in reducing conditions, or though the weathering of scorodite (Nordstrom and Archer, 2003 and references therein). Since arsenolite and claudetite form naturally, the release of anthropogenically derived forms of these mineral (for example during ore processing, as discussed in Chapter 1) will be termed As_2O_3 as a method of differentiating the source of As discussed. Understanding the stability of arsenolite, claudetite and As_2O_3 is fundamental to predicting how it will react when released into the environment.

Several authors have examined both minerals to better understand their stability (Nordstrom and Archer, 2003 and references therein). More recent work to decipher the arsenolite-claudetite stability comes from Nordstrom and Archer (2003) who found that claudetite had the greater stability under standard state conditions based on examination of solubility, electrochemical, heat capacity, entropy and enthalpy data. Due to the chemical and optical similarities between these two minerals, small changes in the calculated free energies of formation, temperature, grain size or pressure could cause a change in the stable mineral form (Nordstrom and Archer, 2003).

A stability diagram for the As-O-S-H system can be seen in Figure 2.3 as presented by Nordstrom and Archer (2003) to delineate arsenolite and claudetite stability. Vink (1996) makes no distinction between arsenolite and claudetite and predicts that to be stable, both need to have a high activity ($\sum As=10^{-0.8}\, m$) in a moderately oxidizing to moderately reducing environment. The sulphide minerals orpiment and realgar are stable in acidic to neutral and moderately reducing conditions (Figure 2.3). According to Vink (1996), in this system, at

lower activities, arsenolite and claudetite are not stable and will dissolve according to *Equation 2.3*.

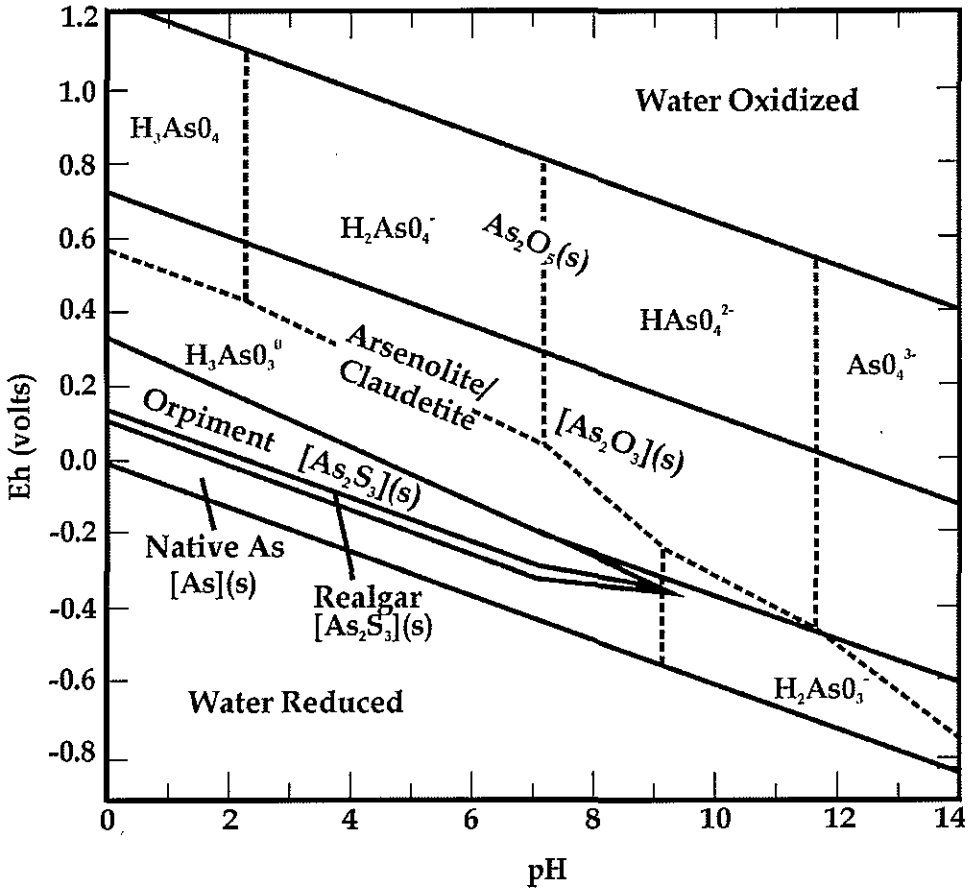

Figure 2.3: Aqueous and solid phase (superimposed) Eh-pH diagram for the As-O-S-H system. System is contoured for the predominant arsenic solid phases (solid black lines) and aqueous phase (dashed dark gray lines) stabilities at standard temperature and pressure. After Nordstrom and Archer, 2003.

$$As_2O_3 + 3H_2O \rightarrow 2H_3AsO^0_{(aq)} \qquad \textbf{(Equation 2.3)}$$

Once dissolved, $H_3AsO^0_{(aq)}$ will oxidize to $H_2AsO_4^-{}_{(aq)}$ (arsenate- As^{5+}) by *Equation 2.4* under oxidizing conditions, or remain as $H_3AsO^0_{(aq)}$ (Appelo and Postma, 1999). Both of the

As-oxyanions could then become sorbed to the surface of oxides, (oxy)hydroxides, clays or OM within the soils or be mobilized in water.

$$2H_3AsO^0_{(aq)} + \tfrac{1}{2} O_2 \rightarrow H_2AsO_4^-{}_{(aq)} + H^+ \qquad \text{(Equation 2.4)}$$

When Fe is added to the system (Figure 2.4A)to allow for the common As mineral

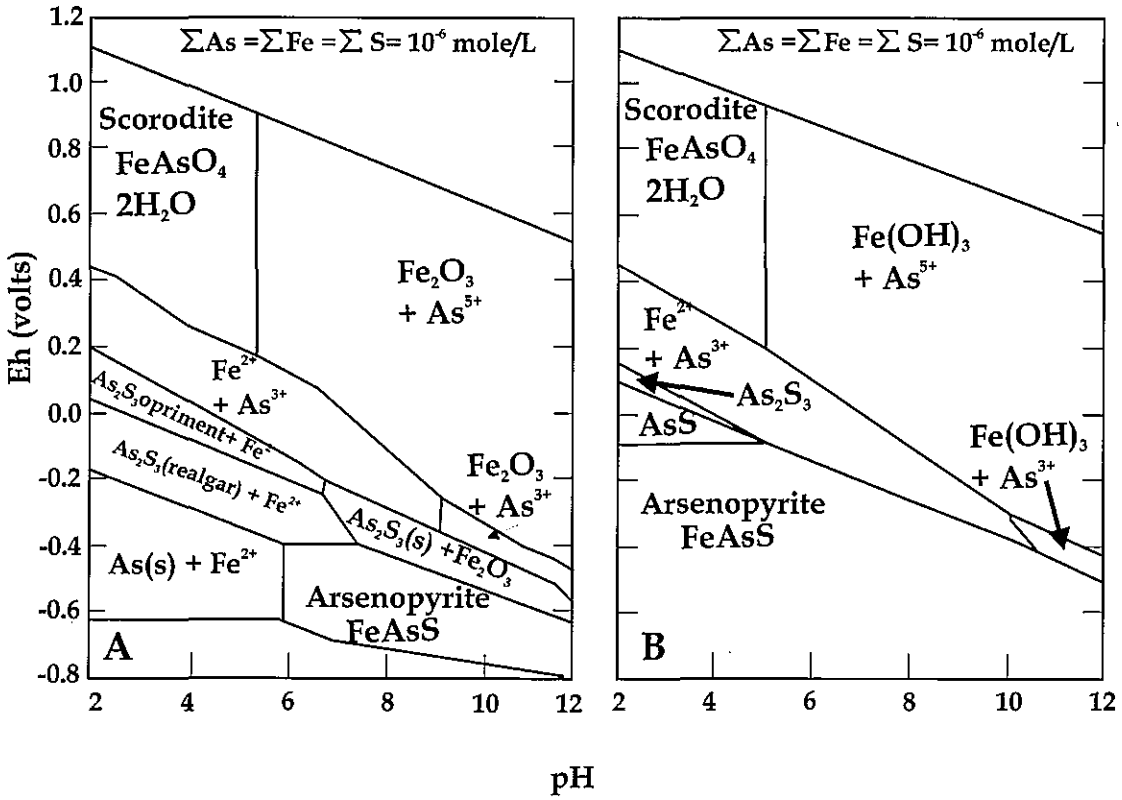

Figure 2.4: Stability diagrams for the As-Fe-O-S-H system at standard state conditions. A is a simplified version of the system from Vink (1996) and B is a simplified version of the system from Craw *et al.*, 2003. The most significant changes between Figures A and B are the arsenopyrite and native As stability field.

arsenopyrite, the arsenolite stability field changes again to accommodate the formation of Fe oxides, e.g. Fe_2O_3 (hematite and magnetite), arsenopyrite as well as other minerals. In more

acidic conditions arsenopyrite would be replaced by realgar and orpiment (As-sulphides). Figure 2.4B is from Craw *et al.* (2003) and is a revised and simplified stability diagram for arsenopyrite stability.

This review of As in the soil environment has shown that this element is particularly sensitive to changes in redox conditions and pH. The release of naturally derived As in the environment can be attributed to the oxidation of As-bearing sulphides along with the desorption from As-bearing Fe, Al, Mn and Ca oxides and from the surfaces of clays and (OM). In reducing environments the mineral claudetite is considered to be more stable than its polymorph arsenolite when it is of natural origin (Nordstrom and Archer, 2003).

2.1.3 Studies of Soils Impacted by Arsenic Trioxide

Anthropogenically derived As_2O_3 is important to consider when examining solid phase interactions in soils as these minerals are highly soluble in the environment and relatively few studies have examined the fate of the As_2O_3 in the environment (Ashley and Lottermoser, 1999; Datta and Sarkar, 2004; Haffert and Craw, 2008; Sarkar et al., 2005; Yang and Donahoe, 2007). Two significant sources of As_2O_3 in soils are from anthropogenic activities such as mineral processing (e.g., ore-roasting and smelting) and the application of arsenical pesticides/herbicides. Soil studies as well as incubation studies that examine the use of arsenical based pesticides/herbicides typically focus on understanding the soil chemistry and bioavailability of As. These studies have found that soil chemistry dictates the geochemical form of As in all of the soils while higher concentrations of OM have the potential to solubilize As, resulting in higher proportions of As taken in by plants and animals (Datta and Sarkar, 2004; Sarkar *et al.*, 2005; Yang and Donahoe, 2007).

Mineralogical studies of the soils contaminated by As_2O_3- based pesticides in the 1950's show that there is no particular mineral form that is host to the As (Yang and Donahoe, 2007). This study took place at two sites in the United States and found a few grains of phaunouxite (a calcium arsenate) using an SEM (Scanning Electron Microscope), but these do not account for the majority of As present within the soil. Leaching experiments from this study showed that As was primarily adsorbed to amorphous Al and Fe-oxyhydroxide surfaces and was no longer present in As_2O_3 (Yang and Donahoe, 2007). Over the span of almost 60 years the original As_2O_3 pesticide would have dissolved in rainwater changing the form and speciation of As within the soils (Yang and Donahoe, 2007).

Studies in Australia and New Zealand have examined the mineralogy and As speciation in mine wastes and soils from abandoned mines where ore-roasting has taken place (Ashley and Lottermoser, 1999; Haffert and Craw, 2008;). The first site was a mine in Mole River, AU where arsenopyrite was mined and processed to produce a pure As oxide. This operation resulted in significant releases of As into the soils, sediments, and vegetation in the region surrounding the mine by atmospheric fallout and later solubilization of As_2O_3 from the flu system and mine wastes (Ashley and Lottermoser, 1999).

Mine wastes at the Mole Rover mine site showed variable As concentrations (between 2.6 and 26.6 wt %) attributed to partial to completely oxidation of mine wastes overtime. This material included the development of scorodite along with the presence of hematite (a roaster-generated iron oxide), clays, gypsum, As_2O_3 and pharmacolite (calcium arsenate-$CaHAsO_4 \cdot 2H_20$). Within the roaster flue system As_2O_3 and pharmacolite were found. In soils, average As concentrations in the highly contaminated soils reach ~ 1wt. % with Sb at

41 ppm. No mineralogical studies of the soils have taken place to determine the form and speciation of As or the effect of Sb in this media (Ashley and Lottermoser, 1999).

The second and more recent study on As_2O_3 in mine wastes was performed at the Blackwater gold mine in NZ (Haffert and Craw, 2008). At this site all processed As was originally present as As_2O_3 at the surface, however arsenolite dissolution in rainwater has led to the precipitation of scorodite as an impermeable surface crust around As_2O_3 grains from the high dissolved As surface waters. In regions where all of the As_2O_3 had dissolved, the dissolution of scorodite, which has lower solubility in water than As_2O_3, now controls the dissolved As concentrations on the property (Haffert and Craw, 2008).

2.2 Arsenic Toxicity and Bioavailability in Soils

Arsenic is considered by International and Governmental Agencies to be a carcinogen and DNA mutagen that has been linked to cardiovascular, respiratory, gastrointestinal and reproductive diseases (e.g., Morton and Dunette, 1994). Chronic and acute exposure to As in soils has not been well documented or researched and most studies refer to the ingestion of contaminated waters. This poses a problem as there are differences in chemical form between water and soil borne As. Table 2.1 is a summary of these differences as presented by Valberg *et al.*, 1997.

Table 2.1: Comparison Between As in Soils and in Waters from a Health Perspective.

	Soil arsenic	Water arsenic
Intake from media	*Low*	*High*
Absorption into the bloodstream	*Low*	*High*
Retention in organs	*Zero - Low*	*Moderate*
Correlation between arsenic concentrations and urinary arsenic concentrations	*Low*	*High*

(Valberg *et al.*, 1997)

Once exposed to As, by soil ingestion or water ingestion, the concentration, form and duration of exposure will dictate the effect on the human body (Jain and Ali, 2000; Hughes, 2002). In short-term high-dose exposures, the common symptoms include fever, projectile vomiting, respiratory tract distress, neuropathy and death. For longer term lower concentration doses or chronic exposure, As can cause many problems the most common of which are skin melanosis (abnormal pigmentation), Blackfoot Disease, brittle nails, and loss of hair (e.g., Jain and Ali, 2000; Hughes, 2002). With chronic exposure As can be stored in organ tissues, bone, skin, nails and hair and can lead to a variety of forms of cancers (Valberg *et al.*, 1997).

In a review paper by Belluck *et al.*, 2003 the authors discussed As induced mortality, and indicated that there was only one possible case of mortality associated with elevated As concentrations in soils. The authors consider that there are two possible reasons for this unusual outcome. Either As in soils simply does not represent a significant human health risk or the current methods of characterizing As toxicity in soils are not adequate and reporting systems do not address As exposure health outcomes (Belluck *et al.*, 2003), the former of which has been supported by other authors (e.g., Freeman *et al.*, 1995; Ruby *et al.*, 1999).

In the body, the percentage of As that is released from the ingested soil in the gastrointestinal tract and is available to be absorbed into the bloodstream is called the bioaccessible As (Valberg *et al.*, 1997; Caussy, 2003). Arsenic that reaches the bloodstream by absorption through the gastrointestinal tract is termed bioavailable As. Many factors control the solubility of As in soils the most important of which is the form of As, either absorbed to minerals or incorporated within the mineral structure. Other factors that can affect solubility

and therefore bioaccessibility and bioavailability include the soil particle size, surface area, mineralogy of the soil matrix, and if As is associated with a rind on a mineral or if it encapsulated by an inert, low solubility mineral (Figure 2.5) (Rudy *et al.*, 1999; Richardson *et al.*, 2006; Valberg *et al.*, 1997). For example from Figure 2.5, the mineral As_2O_3 is highly soluble and will be readily bioaccessible in the human gastrointestinal tract but sulphide minerals, such as arsenopyrite, are significantly less soluble and therefore less bioaccessible (Freeman *et al.*, 1995; Ruby *et al.*, 1999).

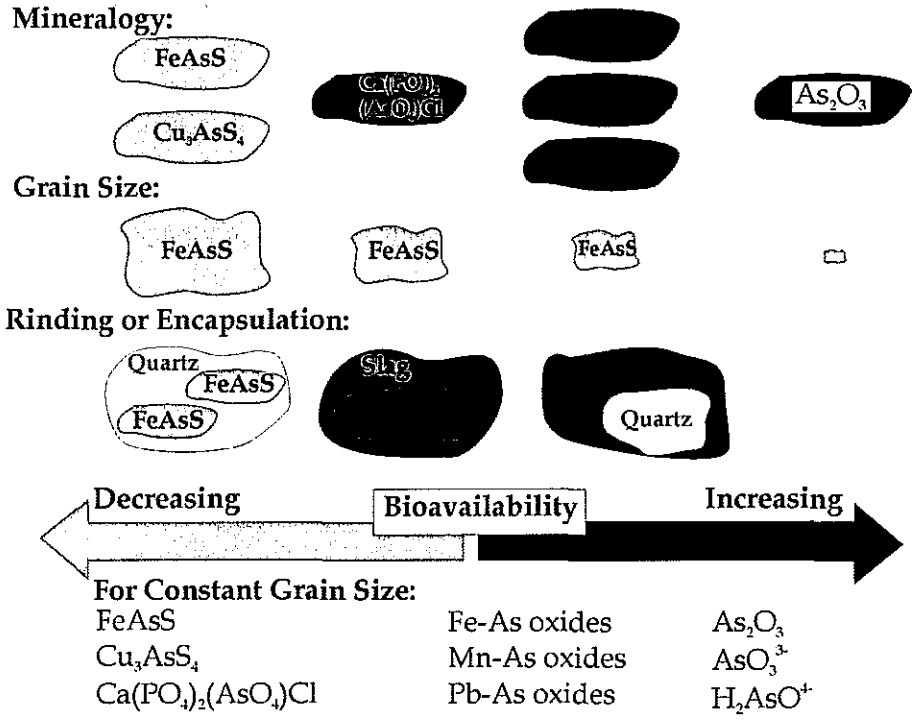

Figure 2.5: Factors affection bioavailability of solid phase As. Bioavailability increases from left to right in this diagram with arsenopyrite (FeAsS) being the least bioavailable and arsenolite/claudetite (As_2O_3) being the most. After Ruby *et al.*, 1999.

Once absorbed into the bloodstream As travels to target organs and the liver where it can be bio-transformed to an organic form of As and is excreted (Caussy, 2003; Rudy *et al.*,

1999; Valberg *et al.*, 1997). Typical estimates of soil As toxicity have not taken into account the characteristics of the metal oxides in soils and the resulting changes in adsorption. Results from both *in vitro* (performed using simulated gastric systems) and *in vivo* (performed using live animals) studies suggests that there are lower risks associated with the ingestion of As from soil or dust when compared to similar quantities of As found in drinking waters (e.g., Freeman *et al.*, 1995; Ruby *et al.*, 1999).

2.3 Background Information

2.3.1 Previous Work at the Giant mine, Northwest Territories

There have been many studies on the environmental and health effects of As related to the Giant mine beginning as early as 1949 and continuing today. The following is a summary of the reports relevant to this thesis.

In 1978 Hocking *et al.* examined the impact of the Giant mine ore-roaster on vegetation and soils within a 40km radius of the mine. Their results showed the highest As concentrations to be in the soils adjacent to the roaster with concentrations decreasing with increasing distance from the source as well as with increasing depth in the soil. Close to the roaster, As concentrations were 21,000 ppm in the surface soils (Hockings *et al.*, 1978), significantly above the current 2002 site-specific human health-based soil quality remediation objectives guidelines of 160 ppm As for Yellowknife soils (GNT, 2003; Risklogic, 2002a). This higher As was the result of rapid condensation and fallout of As_2O_3 from the stack, while increases in As further away would have been due to the dispersion of gaseous As_2O_3 by wind (Hocking *et al.*, 1978). The decline in vegetation noted during this study was not attributed to elevated As, but to the presence of extensive SO_2 damage. The dispersion

of SO_2 over the Yellowknife area ceased with the closure of the roasting operation in 1999 (INAC, 2007).

Human health and ecological risk assessments were performed in 2002 to determine the risk posed by As contamination from the Giant mine (Risklogic, 2002a; Risklogic, 2002b; Risklogic, 2002c). Prior to these assessments Risklogic (2002a), using data collected by the Geological Survey of Canada, the Environmental Sciences Group at the Royal Military College of Canada (RMC) and current mine operators, determined the average natural background concentration of As in the Yellowknife area was 150 ppm. This is significantly higher than the national soil quality guideline proposed by the CCME of 12 ppm, however the CCME recognizes that inorganic elements vary significantly in natural concentration from one region to another (CCME, 2007b). As previously mentioned in Section 1.1, soils that develop over ore-deposits rich in As-bearing minerals will potentially have high As of natural origin. So based on methods described by the CCME a new site-specific human health-based soil quality remediation objective was derived for soil-bore inorganic As in the Yellowknife area. The objectives for the three land uses can be seen in Table 2.2 and take into account the site specific factors that caused the background As concentrations to be different than the national standard.

Table 2.2: Remediation Objectives for As in Yellowknife Area Soils and Sediments

Medium	Land Use	
	Residential (ppm)	Industrial (ppm)
Soil	160	340
Sediment	N/A	N/A

(Risklogic, 2002a; GNT, 2003)

During the same time as the assessment of natural background in the Yellowknife area, studies were also done to assess human and ecological health risks posed by As contamination in soils above natural background (Risklogic, 2002b; Risklogic, 2002c). The ecological risk assessment found that it was not possible to accurately assess the risk posed by the present exposures of wildlife in the Yellowknife area to As in water, soil, sediments and air for several reasons. Most notably because there have been no toxicological studies of oral As exposure to the particular animals present in northern environments and inter-species variability in As toxicity is not well understood (Risklogic, 2002b).

Human health risk assessments in the Yellowknife area have found that the exposure to As through the various media were high compared to non-mineralized regions in Canada especially for toddlers where background As exposure (not including additional exposures from mining in the region) were already equivalent to the tolerable daily intake derived by the US EPA (Risklogic, 2002c). Evaluation of potential skin and lung cancers revealed that the carcinogenic risks were no greater than those posed by background exposures in food or drinking water at the Canadian drinking water guideline level (Risklogic, 2002c). It should be noted that although the risk assessment completed in 2002 showed a low risk to human health, this study took place 3 years after the closure of the Giant mine ore-roaster and more than 40 years after the initiation of stricter emission controls and regulations for the release of As_2O_3 and SO_2 from the Giant mine roaster. It also did not consider the exposure of the public to soils on the mine property, known to have higher total As concentrations than in city soils, or soils downwind (Hockings *et al.*, 1978).

Examination of the As_2O_3 wastes at Giant mine first took place as a study into the potential of creating a purified marketable product of As oxide by leaching the dust with hot

water or acid (Riveros *et al.*, 2001). Using dust samples from As_2O_3 chambers underground at Giant, Riveros *et al.*, (2001) found that the solubility of As_2O_3 was related to the Sb content (ranged between 0-47 wt % Sb) of the dusts. Experiments using water leaches found that temperatures <100°C demonstrates only low-Sb content As_2O_3 grains dissolved, leaving higher Sb- As_2O_3 in the remaining residue, making the final product very pure As_2O_3. It was shown by Riveros *et al.* (2001) that the solubility of these grains increases systematically when heated as well as by the addition of acids. Acid leach tests found that As_2O_3 grains dissolved more rapidly in acid than in water but also dissolved Sb making the final product less pure (both Sb and iron (Fe)).

Small amounts of Sb within the As_2O_3 grains caused a reduction in the As_2O_3 activity coefficient in the water and resulted in lower aqueous solubility. In water the Sb within the As_2O_3 crystals inhibited dissolution, however the acid solution was able to dissolve these crystals more quickly. This was supported by analysis of residues remaining after leaching which contained higher Sb particles, meaning lower Sb- As_2O_3 crystals dissolved first in the leach. Riveros *et al.* (2000) postulated that most of the Sb within As_2O_3 dust was in solid solution within the As_2O_3.

In 2005, as part of the delineation required for the development of the Giant mine remediation plan, SRK Consulting Inc. and Golder Associates Ltd. studied surface water seeps and soils respectively (Golder, 2005; SRK, 2005). Results from dissolved As concentrations in the surface water seeps showed elevated As across the whole property, particularly close to the mill, roaster and baghouse. This region recorded dissolved As concentrations between 0.26 and 24.9 mg/L (current CCME drinking water guidelines = 10 µg/L) and the source was most likely residual As_2O_3 dust from the processing plant.

Speciation of dissolved As in the water showed predominately arsenate (As^{5+}) (SRK, 2005) which is confirmed from Figure 2.3 as the conditions would have been aerobic. Surface material samples taken by Golder Associated Ltd. (2005) in this region have As concentrations between several hundred and a thousand ppm up to 2.3 m depth. Water leach tests showed that between 0.2 and 58% v/v of the As was mobile within the samples which explained the high dissolved As in this region (SRK, 2005; Golder, 2005).

Towards the Giant Townsite, dissolved As concentrations ranged between 0.65 and 2 mg/L potentially due to significant amounts of As from atmospheric dispersion over the lifetime of the mine (SRK, 2005). Surface material samples from the Townsite show between 0.1 and 2.7% water soluble As, significantly lower than close to the mill (Golder, 2005). Mineralogical and morphological examination of these materials revealed that they were composed, at least in part, of crushed mine rock used as fill (Golder, 2005; Walker, 2006). This explains the lower As concentrations in the solids as well as lower dissolved As in the surface water seeps.

Soil profiles were also taken as part of the 2006 EXTECH III Multidisciplinary Project from Yellowknife area. The soil profiles show that close to both the Con and Giant mines, As and Sb are elevated, approximately 900 ppm and 150 ppm respectively, in the leaf litter and humus layer in the soils (Figure 2.6)(Kerr, 2006). Spruce barks as well as Labrador Tea leaves were also found to have both high As and Sb values in their tissues. Till samples from the same area had significantly lower As and Sb, >20 ppm to 200 ppm and >1 ppm to 8 ppm respectively (depending on depth in the profile) (Kerr, 2006). Hocking *et al.* (1978) and Kerr (2006) both found that soils 35km away from the influence of the ore-roasters of both the Con and Giant mines do not show the same enrichment of As and Sb within the organic layers as

the samples close to the mines (Figure 2.7). Elevated As, Sb and other metals in the soils and vegetation close to the two mines was interpreted as being a combination of the high levels

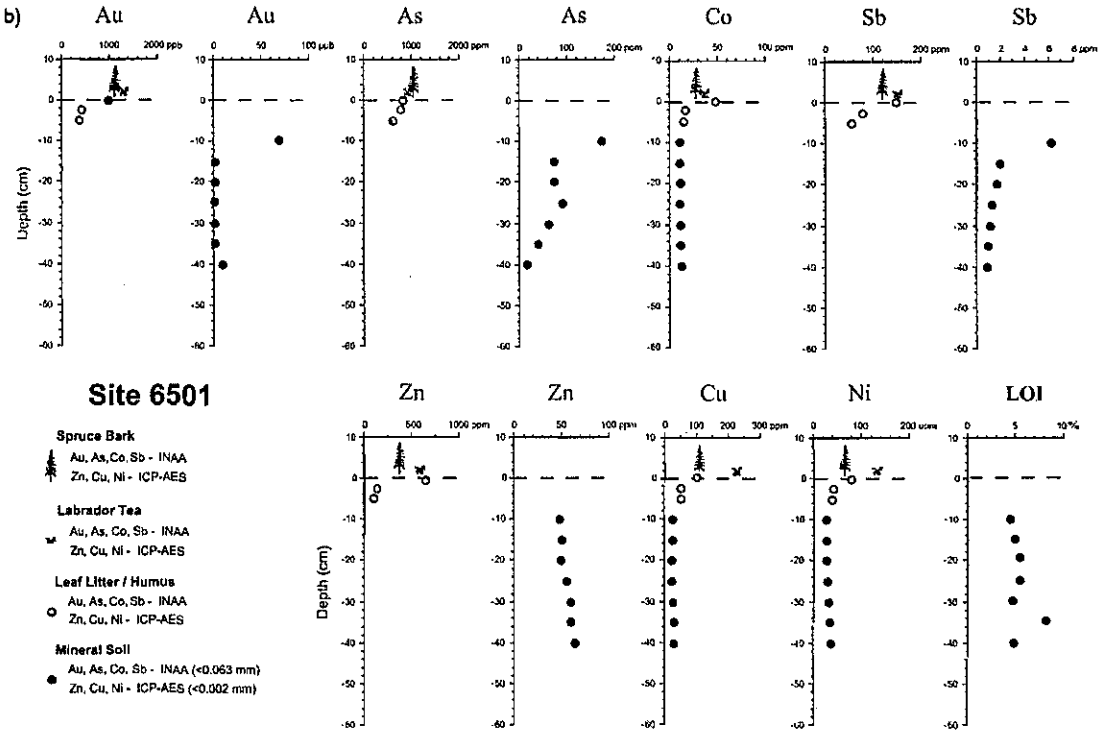

Figure 2.6: Geochemical soil profile from north of the Giant and Con mines. As and Sb concentrations in the surface leaf litter and humus are significantly elevated above the Yellowknife site-specific human health-based soil quality remediation objectives guidelines of 160 pmm for As (Kerr, 2006).

of air-borne material from the roaster and naturally occurring higher values of these element in the till overlying the mineralized zones (Kerr, 2006).

As previously mentioned in Chapter 1, several graduate students at Queen's University have examined the issues associated with As at the Giant mine (Andrade, 2006; Fawcett *et al.*, 2006; Fawcett *et al.*, 2008; Walker *et al.*, 2005; Walker, 2006). In his PhD thesis S. Walker (2006) examined exposed beach tailings, floatation tailings, calcine and electrostatic

precipitator dust from Giant mine as well as several soil samples from the Giant Townsite to better understand the form of As in these materials (ESG and Queen's, 2001; Walker *et al.*, 2005; Walker, 2006).

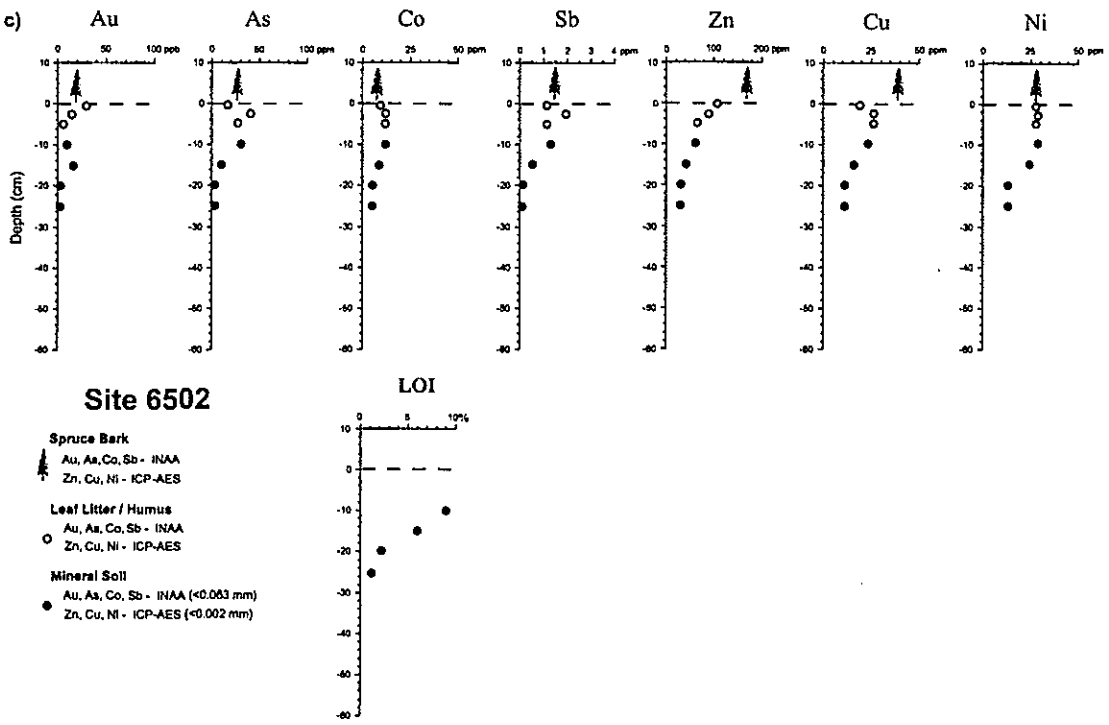

Figure 2.7: Geochemical soil profile from 35km west of the Giant and Con mines. This profile shows significantly lower As and Sb concentrations in comparison to Fig. 2.6. All soils in this profile are below the Yellowknife site-specific human health-based soil quality remediation objectives guidelines of 160 pmm for As (Kerr, 2006).

Using optical microscopy, μXRD, μXANES and leach experiments from his thesis demonstrated that the roaster-derived Fe-oxides were composed of nanocrystalline maghemite or maghemite-hematite mixtures (Fe_2O_3- spinel group) that contained between 0.5 and 7 wt % As. Fe-oxides examined in the mine wastes and beach tailings contained a mixture of As in the 3+ and 5+ oxidation states, with the relative proportions depending on the particular grain analyzed. Even though As^{3+} bearing minerals are typically only stable

under reducing conditions, the presence of an As^{3+} and As^{5+} mixed oxidation state in exposed beach tailings suggests that the As^{3+} was stable within the maghemite in oxidizing conditions. In submerged oxygen-deprived beach tailings the ratio of As^{3+} to As^{5+} changed with As^{3+} being the dominant oxidation state (Andrade, 2006).

Of particular importance for this thesis was the examination by Walker (2006) of the electrostatic precipitator dust (ESP) as this material represents what would have been released from the stack to the environment in the early years of roasting. The only As mineral identified in the ESP dust by conventional XRD was arsenolite (As_2O_3) (Walker, 2006). Sequential selective extractions (SSE), a method of subjecting a solid sample to increasingly stronger chemical reagents designed to release As bound in the soil matrix, was used to characterize the As in the dust. Results from this portion of the study found that in the ESP dust, 25% of the As was in the adsorbed/exchangeable and carbonate extractions, of the least aggressive leaches. This was attributed by Walker (2006) to be due to the high proportion of the As_2O_3 in the soil that is considered to be very soluble in water.

Assessment of soils and crushed rock fill from the Giant Townsite showed elevated As concentrations upwards of 2000 ppm in bulk un-sieved samples (ESG and Queen's, 2001; Walker, 2006). Examination of the materials using XRD and optical microscopy show crushed rock fill contain sulphides such as pyrite and arsenopyrite associated with weathering rims of As-bearing Fe-oxyhydroxides. The presence of a roaster-derived Fe-oxide in the soils taken from the surface of outcrops was significant as it provided evidence that there was an additional source of As from the roasting stack that is considered to be less soluble than the emissions of As_2O_3 (Walker, 2006).

2.3.2 Previous Work at the North Brookfield Mine, Nova Scotia

As mentioned in Chapter 1 of this thesis, work is ongoing on tailings and soil samples from the North Brookfield mine and has yet to be published (Meunier *et al*, 2008; Meunier *et al.*, in progress; Walker *et al.*, 2008; Jamieson *et al.*, 2008). This site shares similar ore-processing techniques with the Giant mine as the ore was roasted after being crushed. The use of chlorination and bromo-cyanidation at North Brookfield for gold extraction, compared to more conventional cyanidation at Giant, could potentially cause a different As signature within the soils especially if wastes from the extraction plant were mixed with roaster wastes prior to disposal onsite.

There are two main factors that differ between the Giant mine and the North Brookfield mine, North Brookfield was a much smaller mine and operated for a short period of time during the turn of the 20th century. This combined with the overwhelming number of small historic gold mines within the province of Nova Scotia, many of which are the subject of current research and risk assessment (DeSisto, *et al.*, 2008; Jamieson *et al.*, 2008, Meunier *et al.*, 2008; Meunier *et al.*, in progress; Walker *et al.*, 2008) may provide an explanation as to why there has been little work performed to characterize As at this site.

Chapter 3: Field and Analytical Methods

3.1 Sampling Design

Soils surrounding the Giant and North Brookfield Mines have been potentially impacted by historic gold roasting operations that aerially dispersed As_2O_3 and SO_2 over the surrounding area. Sampling at these two mine sites was designed to select locations with minimal disturbance of soil horizons and no addition of mine wastes (including mine tailings or liquid effluents) while still targeting areas that would have been impacted by the atmospheric dispersion of roaster stack emissions. This was done to prevent confusion regarding the source of particles when examining soils in detail.

3.1.1 Sample Locations

On the Giant Mine property twenty-three soil core samples (SCS) and ten outcrop soil samples (OSS) were taken (Figure 3.1). Preliminary sample locations were chosen based on vegetated areas in a series of air photos as well as previous soil, tailings and surface water seep studies on the mine property to identify regions with organic soil development over the glacial lacustrine tills (Golder, 2005; Kerr, 2006; SRK, 2005; Walker, 2006). Also considered was the pre-dominant wind direction and historical movement of the stack plume. Soil sample locations were later refined and locations were deleted if there was possible soil horizon disturbance or minimal soil cover as determined during site surveys. Four of the twenty-three SCS were taken from across the Giant mine Townsite based on results from Golder Associated Ltd. (2005) and a joint study through the Environmental Sciences Group (ESG) and Dr. H. Jamieson's Research Group at Queen's University in 2001 and

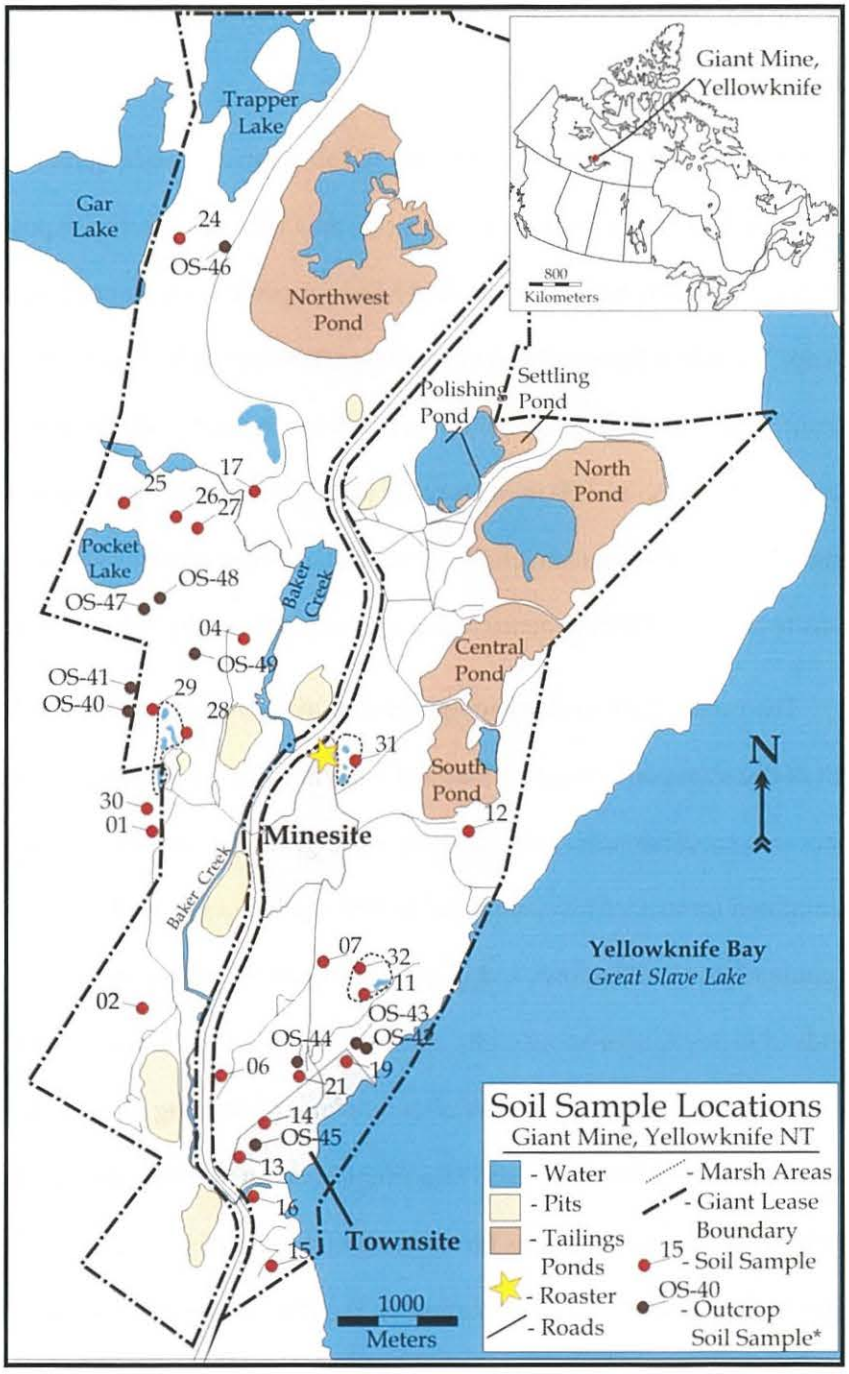

Figure 3.1: Map of sampling locations from the Giant Mine, Yellowknife, Northwest Territories. Red dots represent the soil core samples (SCS) and brown dots represent the outcrop soil samples (OSS). The predominant winds are from the east except in the summer months when it is from the south (GNWT, 1993). Map designed after supporting documents in INAC, 2007.

supplemental work by S. Walker (2006) in his PhD thesis (see Section 2.3.1) (see Appendix A for photographs of site locations).

Outcrop soil samples (OSS) are small soil samples weighing more than 50g that were collected by hand from shallow soil zones located between outcrop exposures. This type of soil sample was only taken on the Giant Mine property where more than 30% of the land is outcrop. Sampling these outcrop soils is important from a human health perspective as these are areas where children would be likely to play and could potentially contain high concentrations of As and Sb in the form of the highly soluble As_2O_3 as emitted from the roaster. In 2006, Walker characterized one such outcrop sample taken from the Giant Townsite and noted the existence of fine grained, potentially roaster-derived iron oxides.

The presence of As-bearing roaster-derived iron oxides (RO) was believed to be a result of the transport of As-rich material via wind and precipitation from the outcrop surface into crevasse soils. During active mining, As-rich roaster particles would have accumulated on surface exposures and eventually be transported into soils that had accumulated in small hallows and crevasses (Figure 3.2) (Hockings *et al.*, 1978; Walker, 2006). Periods of heavy rain or snow melt could have resulted in the wash down of soils from the outcrop surfaces and the small crevasses into larger low lying regions close to the exposures making soils close to outcrops also important in understanding the transport of As-rich material from exposed outcrops (Walker, 2006). For this reason, OSS site locations were chosen based primarily on the proximity of the site to other soil core samples as well as the proximity to the location of the roaster.

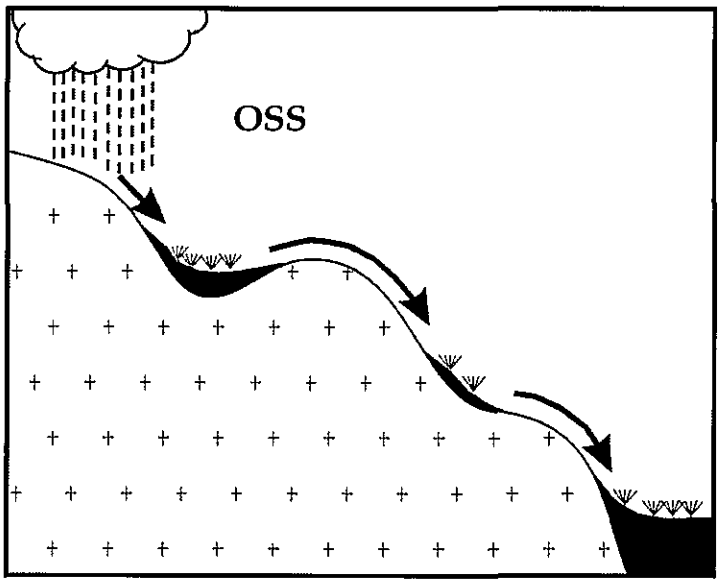

Figure 3.2: Diagram of the accumulation of soil and potentially roaster- derived material in outcrop hallows.

From the North Brookfield Mine Property, eleven soil core samples were taken (Figure 3.3). Minimal published work (Meunier *et al*, 2008; Meunier *et al.*, in progress; Walker *et al.*, 2008; Jamieson *et al.*, 2008) has been performed on the soils surrounding the North Brookfield Mine, so sample sites were chosen based on the known pre-dominant wind direction (to the NE) and the proximity to the footings of the historic roaster. Two samples taken from close to the roaster footings were taken based on work performed by M. Parsons at the Geological Survey of Canada (Atlantic Division) (Parsons, 2007 personal comm). Outcrop soil samples were not taken at North Brookfield as soil cover was more extensive.

Not all of the 33 samples from the two mine properties were examined in this thesis. Sub-samples from soil cores were chosen for bulk analysis based on locations where the profiles appeared to be less disturbed by mining related activities while still having been

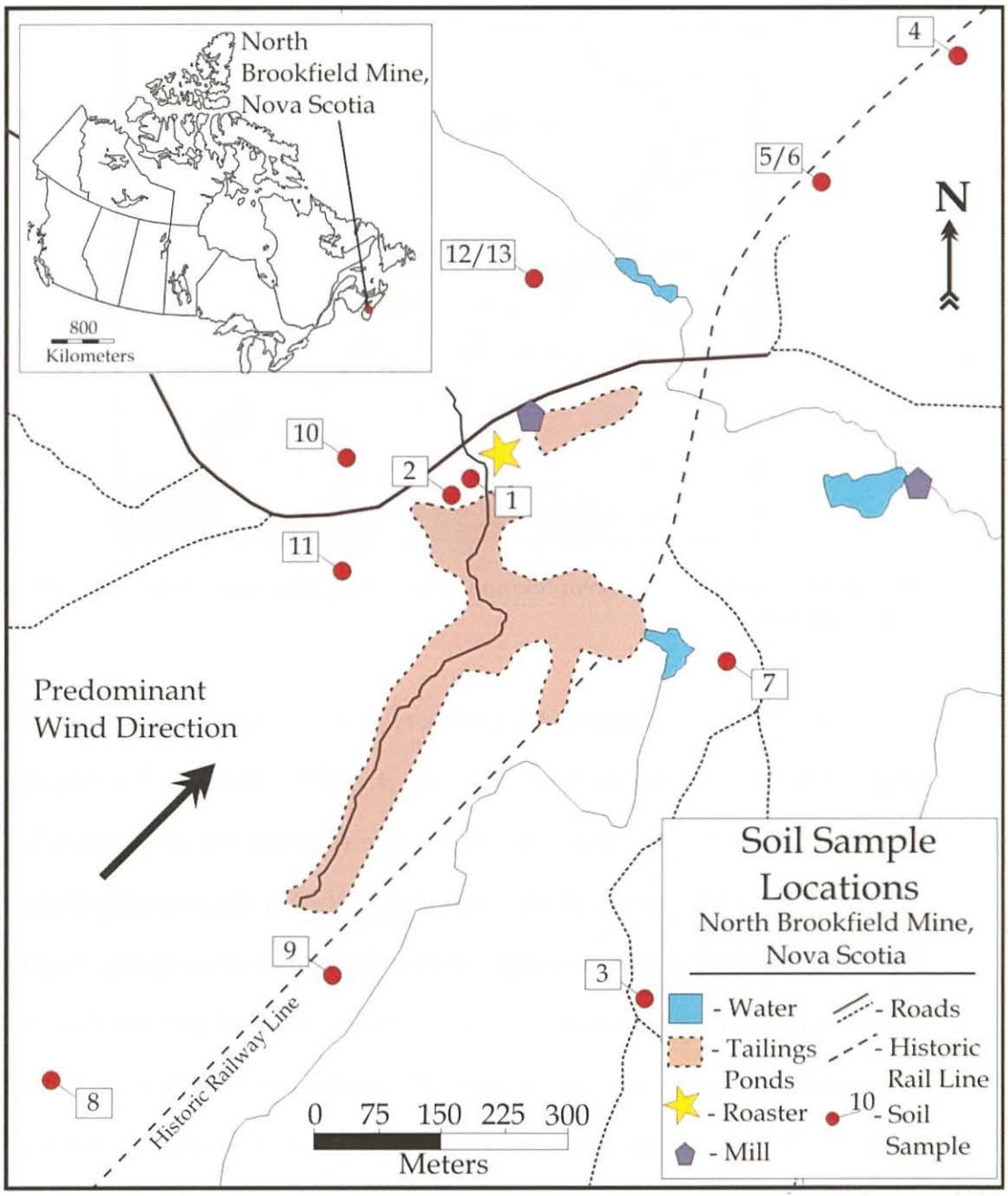

Figure 3.3: Map of sampling locations from the North Brookfield Mine, Nova Scotia. Red dots represent the locations of soil core samples (SCS). The prevailind wind direction at this site is from the southwest. Maps is designed after Parsons, 2008.

potentially influenced by aerial emissions of As from roasting. Disturbed soil horizons were eliminated if mine tailings, waste rock, or fill were found within the organic horizon as could influence the proportion of anthropogenic verses natural As identified in the soils. Also considered was the pre-dominant wind direction (EnviroCan, 2008). Based on bulk sub-sample analysis results (mainly As, Sb and S concentrations), 30 sub-samples were chosen for additional analytical work.

3.1.2 Sample Collection

Unconsolidated soil core samples were taken in the summer of 2007 from the Giant and North Brookfield Mines using 1/16'' walled, 2'' outside diameter aluminum tubing. The tubes were cut to between 50 and 60 cm in length and were driven into the ground using a drivehead, which covered the top of the tube, and a sledge hammer (Figure 3.4).

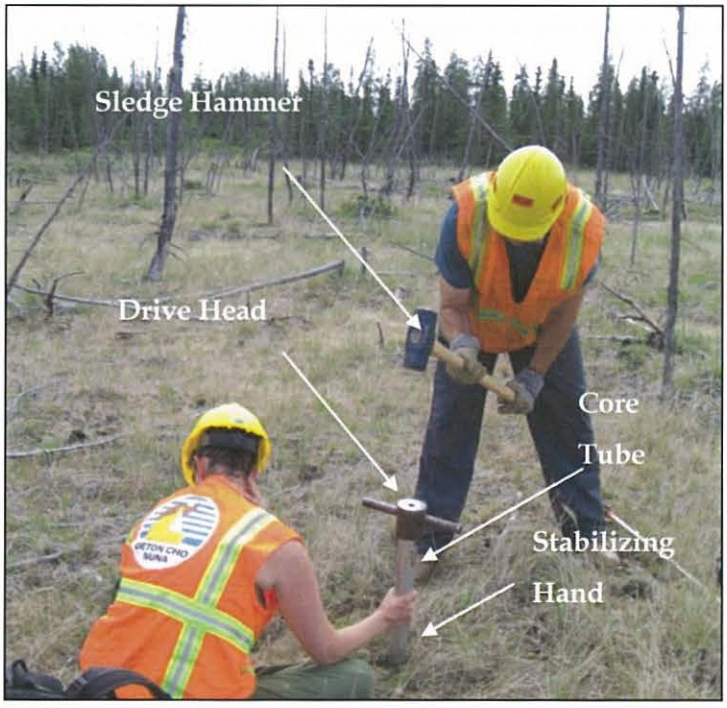

Figure 3.4: Photograph of soil core sampling technique. Image is taken from SCS Site 27, Giant Mine, Yellowknife, Northwest Territories.

Vegetation and dried organic material was removed prior to stabilizing the core tube and driving it into the soil to ensure that all measurements of soil depth began at a consistent horizon within the soil.

In regions where the soils were very dry the tube was held loosely while it was driven into the ground and it was necessary to loosen the soil surrounding the sample prior to removal, without lifting or twisting (Figure 3.4). Once removed, parafilm and duct tape were placed over the bottom opening while the core tube was kept as vertical as possible to prevent sample shifting. The core tube length, soil hole depth, the depth to the soil within the core, and GPS locations were recorded to be used for mapping and determining percent compression within each core. The excess empty tube was cut and the top of the core was covered with parafilm.

Outcrop soil samples were taken from small vertical crevasses between outcrop exposures (Figure 3.5) using a small trowel and were stored in Ziploc® bags. Vegetation and dried leaves were removed prior to collecting the samples. Both SCS and OSS were placed in a cooler with ice packs immediately following collection, and then frozen in preparation for shipment and to preserve solid phases from reacting. Samples were frozen at Taiga Environmental Laboratory- Yellowknife, Northwest Territories (Giant Mine samples) and the Bedford Institute of Oceanography, Halifax, NS (North Brookfield Mine samples). Once returned to the laboratory, the SCS were split in half longitudinally, re-covered with parafilm and kept frozen until preparation for analysis.

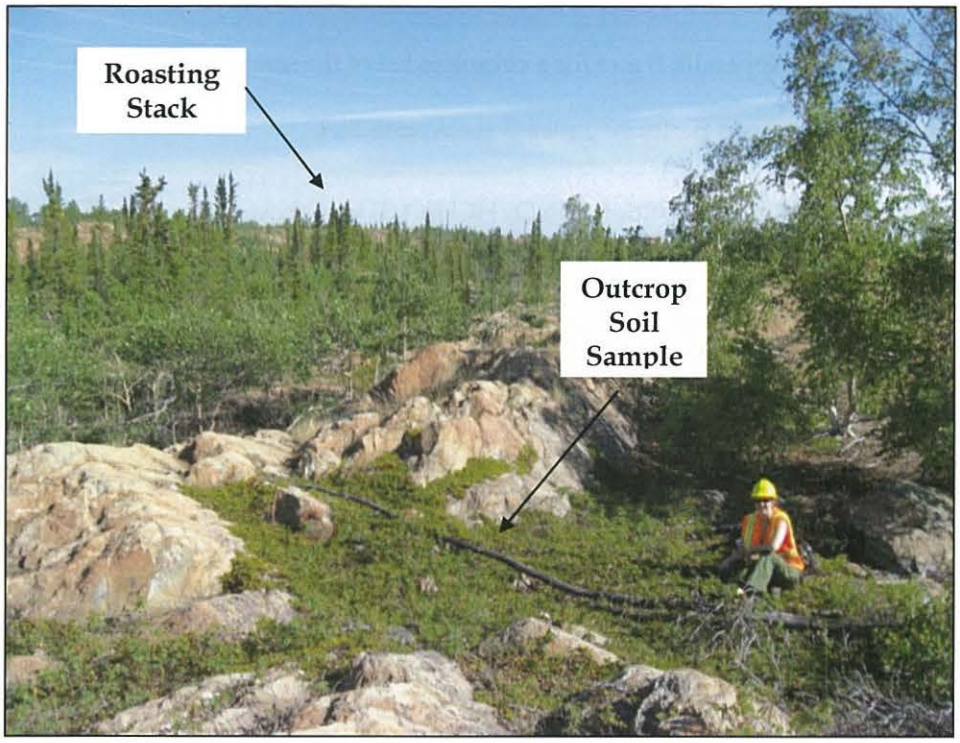

Figure 3.5: Photograph of an outcrop soil sample (OSS) taken near the Townsite, Yellowknife, Northwest Territories. Image is taken from OSS Site 43 looking NW toward the roasting stack. The stack is obscured by taller trees in the centre of the photo.

3.2 Analytical Methods

3.2.1 Elemental and Organic Carbon (OC) Analysis

Core and hand samples were thawed, air dried, described and sub-sectioned, based on soil horizons, prior to being sent to the Analytical Services Unit (ASU) at Queen's University for bulk aqua-regia soil digestion and elemental analysis. Samples were described based on standard soil description methods set by the North American Soil Geochemical Landscape Project (Appendix B). Sub-samples of the SCS were collected based on soil descriptions with samples taken from the surface of the soil profile, as this is a region important when looking at exposure, as well as from transition zones between organic horizons and the underlying glacial-lacustrine tills. Full SCS and sub-sample descriptions

can be seen in Appendix B and for a complete list of the samples analyzed in this thesis and the types of analyses performed please see Appendix C.

The *aqua-regia* digestion (HNO_3:HCl in 1:3) was chosen over a full hot acid soil digestion as the full digestion allows for metals encapsulated by silicates to be reported in the totals where as aqua-regia does not. Total metal concentrations, not including silicate encapsulated metals, is considered to be of greater use in environmental studies as a more accurate representation of available metals in the environment. Furthermore, Parsons (2007, personal comm.) has found evidence for As loss during the full digestion of tailings and soil samples.

At ASU, the samples were ground to a fine powder using a mortar and pestle allowing for the removal of large stones prior to analysis. Approximately 0.5 g of the ground sample was weighed into a test tube where 2mL of nitric acid and 6 mL of hydrochloric acid were added. Samples were then heated overnight (>50°C) to reduce the sample volume to 1-2 mL and cooled prior to adding distilled deionized water to make the solution up to 25 mL. The samples were then filtered through Whatman No. 40 filter papers into plastic vials before a 32 element analysis by a Varian Vista AX simultaneous Inductively Coupled Plasma- Atomic Emission Spectrometer (ICP-AES). The following elements were of particular interest in this thesis: silver (Ag), arsenic (As), gold (Au), calcium (Ca), iron (Fe), manganese (Mn), sulphur (S) and antimony (Sb). Detection limits for the above elements were 2 ppm for Ag, 1 ppm for As, 100 ppm for Ca, 50 ppm for Fe, 1.0 ppm for Mn, 25 ppm for S and 10 ppm for Sb. Full soil digestion data can be seen in Appendix D (Giant) and E (North Brookfield).

Samples were analyzed in groups of up to 36 that included 2 blanks, 2 certified reference materials (NRC Canadian Marine Reference Sediment Mess-3 and the reference standard SS-2) as well as 4 sample replicates. Each standard and blank was run a total of 10 times and accuracies were monitored by ASU to ensure the results were within the control limits determined by in house repeat analyses (Appendix D, Tables D-2, D-3 and D-4). Results from the blanks shows all elements below detection limits. Precision was measured through a series of 23 replicates by ASU and three blind duplicates. Additional blind duplicates were not performed as there was limited sample volume if additional analyses were required. Table 3.1 is a summary of the average relative standard deviations for the six major elements of concern. Two standard deviations for the blind duplicate samples were slightly higher than for replicate samples because of sample preparation. Blind duplicates were separated prior to grinding and therefore were not homogenized together before analysis. The variability in the blind duplicate results would therefore stem from the inhomogeneity within the soils.

Organic Carbon (OC) analysis was performed on 39 selected soil sub-samples at the Grogan Lab at Queen's University using a LECO® CNS-2000 Organic Carbon and Nitrogen analyzer. Samples were chosen for OC analysis based on supplementary thin-section, ESEM and synchrotron work as well as total As and Sb concentrations measured in the soil digestions. For OC analysis, soils were weighed into sample boats in two different volumes depending on the anticipated organic carbon content. For soils with potentially high OC, only 0.300g was added to the sample boat, while soils with lower carbon content required between 1.100g and 1.200g of material in the boat for an accurate OC reading.

Table 3.1: Summary of the average relative standard deviations for house standard, replicate and blind duplicate samples analyzed at ASU, Queen's University.

	Mess-3 Standard	SS-2 Standard	Giant Replicates	North Brookfield Replicates	Ave of all Replicates	Ave of Blind Duplicates
As	3.4	19.1	3.1	10.0	6.5	14.1
Ca	7.82	*22.2	5.0	5.6	5.3	4.3
Fe	12.3	11.7	3.7	2.9	3.3	12.9
Mn	11	6.9	2.9	4.5	3.7	19.4
S	10.1	15.7	2.3	8.1	5.2	10.6
Sb	**BD**	**BD**	0.9	**BD**	0.9	16.7

BD= below detection.
* SS-2 Standard value for Ca had higher average relative standard deviation due to a low Ca analysis. This analysis exceeded the normal range for this standard but was still within control limits.

Samples were combusted at 1050 °C converting carbon into carbon dioxide gas which is measured by the instrument using an infrared detector. A series of three lab standards were run between each set of 10 samples. The standards used were sulfamethazine ($C_{12}H_{14}N_4O_2S$) which was high in carbon and nitrogen, an in-house organic soil which was high in carbon and low in nitrogen as well as an in-house mineral soil which was low in both carbon and nitrogen. Based on repeated analyses of these standards the lab was able to determine an acceptable range of standard values. If the standards' measurement were within the acceptable range of two standard deviations from the accepted mean, the values for the ten samples analyzed between the standards was accepted. OC results are shown in Appendix F.

3.2.2 Thin Section Preparation and Petrography

Based on concentrations of the above elements of interest from the bulk soil digestion, 26 sub-samples from the Giant Mine and 10 sub-samples from the North Brookfield Mine were made into doubly-polished 'liftable' thin sections as described in Walker *et al.*, 2005. The thin sections were made to be liftable for synchrotron-based μXRD analysis which required the removal of the glass slide prior to analysis under the X-ray beam. Of the 36 samples, four from Giant and three from North Brookfield were magnetically separated by hand using a Sepor Automagnet with the magnetic and non-magnetic material being made into separate thin sections. Thin sections of these materials were prepared as grain mounts using room-temperature set epoxy which once set, were sectioned into thin slices. To make the thin sections liftable, one side of the thin slice was polished and mounted onto a glass slide using Krazy Glue®. The sample was then ground and polished to approximately 50 μm which was slightly thicker than normal thin section preparation (30 μm) to prevent the loss of grains when the section was lifted from the glass. The entire procedure required no addition of water or heat beyond the heat generated during the grinding and polishing processes.

Prior to synchrotron analysis, petrography was performed to identify and target potential As-bearing phases. Co-ordinates for the targets were logged using a scanned image of the thin section and multiple images were taken at different magnifications using a combination of transmitted and reflected light to help with locating the targets at the micro-scale. Once targets were identified and the samples were ready for synchrotron analysis, they were lifted from the glass slide as glass diffracts under the x-ray beam and also contains As which was a specific element of interest. To lift the sample, the glass slide was immersed

in ACS-grade acetone until the sample was completely detached from the slide. This took between 1 and 5h depending on the grain size, organic matter content and the quantity of grains in the sample. In more organic- rich samples epoxy would not fill all of the pores within the grains resulting in loss of potential targets during this process. Once removed the sample was allowed to dry before being re-oriented and carefully pressed onto Kapton® tape in a 35mm cardboard slide holder.

3.2.3 Synchrotron-based Analyses

Bulk and micro X-ray Absorption Near Edge Structure (XANES), micro X-ray Diffraction (μXRD) and micro X-ray Radiation Fluorescence mapping (μXRF) were used to characterize the As within these samples. XANES analyses, when used in combination with the relevant standards, can be employed to examine small energy shifts in the position of the As absorption edge in order to determine the specific As oxidation state (Fendorf and Sparks, 1996; Manceau *et al.*, 2002). It is crucial to be able to differentiate between species of As as the presence of As^{3+} in the soils could potentially be linked to anthropogenic inputs because roaster emissions often contain As^{3+}. Micro XRD is a similar technique to the more conventional powder diffraction however it is performed at the micron scale allowing for the identification of individual target grains. Finally, μ-XRF mapping was used to locate, document and correlate elemental associations within the thin sections which provided specific coordinates for μ-XANES and μ-XRD analyses (Manceau *et al.*, 2002, Walker *et al.*, 2005).

Samples were analyzed at two beamlines which are part of the National Synchrotron Light Source (NSLS) at the Brookhaven National Laboratory (BNL) on Long Island, NY. The majority of the analyses were performed at the X26A hard X-ray microprobe beamline, with

additional bulk analyses performed at the adjacent beamline, X27A. X26A uses a series of Rh coated 100mm Si mirrors, arranged in a Kirkpatrick-Baez geometry, to focus the collimated monochromatic beam from 400μm (horizontal) by 400μm (vertical) to a spot size diameter of 10μm (horizontal) by 6μm (vertical) for work at the micron scale. Bulk work performed at this beamline required the beam to be focused to a 1mm x 0.349mm spot size.

The X26A beamline uses a channel-cut Si(111) crystal to achieve a monochromatic beam for XANES experiments, with the Si(Li) detector being placed 90° to the incident beam. The 35mm cardboard sample mounts were placed in a vertical plastic sample holder that is on a 45° angle to the incident beam. This offset is required to allow the user to view the sample using an optical microscope however the angle results in the beam having an elliptical shape when it hits the sample (Walker *et al.*, 2005).

At X27A bulk analyses were performed using a Si(111) channel-cut monochromator with an unfocused beam that had a spot size of 600μm by 600μm. The spot size differed from bulk work at X26A as the flux at this beamline was higher allowing for more X-rays to be generated. The sample holder design was identical to that of X26A.

The extra thickness of the thin sections, while important during the lifting of the section from the glass, can also cause issues during analysis of the samples. In sections where the grains are smaller than the full thickness of the thin section it is possible that several grains, stacked on top of one another, can be simultaneously under the beam (Walker *et al.*, 2005). This would cause multiple phases to be identified in μXRD and unexplained mixed oxidation states in μXANES analyses. Care was taken to avoid areas where material could be buried in the section by carefully examining μXRF maps and target grain photographs prior to analysis.

3.2.3.1 X-Ray Adsorption Near Edge Structure (XANES) Spectra and Analyses

XANES experiments were performed on a bulk and micron-scale by scanning across the As Kα absorption edge (11800 to 11970 eV) in fluorescence mode using a Si(Li) detector. Scans across the edge were broken into three sections each with different step sizes and dwell times. Micro-XANES was performed on lifted thin sections where specific grains of interest were targeted. The relatively small size of the beam (10 μm by 6 μm) allowed for speciation analysis on the rims and cores of individual grains. For μ-XANES the pre-edge (11800.0 to 11850.0eV) had a step size of 5eV with a 2 second dwell time, across the edge (11850.4 to 11880.0eV) the step size was decreased to 0.4eV with a 4 second dwell time providing the maximum detail in the edge region. In the post edge (11881.0 to 11970.0eV) the step size was 1eV, with 3 seconds counting per step.

Bulk XANES analyses were performed on 24 sub-samples from 10 locations at the Giant Mine and 2 sub-samples from 1 location at the North Brookfield Mine. Samples were mounted on Kapton® tape by scooping and flattening a small amount of ground sample onto the tape and placing Kapton® film over the sample to ensure that there was no movement. Sub-samples for analysis were typically chosen from the top 5 cm, an intermediate depth and/or the bottom of the core (between 25 and 40cm depth) to determine if there was any overall shift in As speciation with depth through the soil profile. Between two and four scans were taken per sub-sample to eliminate issues arising from inhomogeneity. At X26A analytical conditions were similar to those used for μXANES, however, the beam spot size was enlarged to 1mm by 0.349mm and the dwell times in the pre-edge, edge and post edge were reduced to 2 seconds per step. Dwell times for bulk XANES at X27A were kept the same and the beam spot size was 600μm by 600μm.

During XANES experiments three As standards were routinely run to document any shift in the edge position that occurred so it could be used in the analysis of the unknown spectra. The three standards chosen were: scorodite ($FeAsO_4 \cdot 2H_2O$) to represent the As^{5+} species, arsenic trioxide (As_2O_3) to represent the As^{3+} species and arsenopyrite (FeAsS) to represent the As^{-1} species (Figure 3.6). Table 3.2 summarizes the standard sources and edge

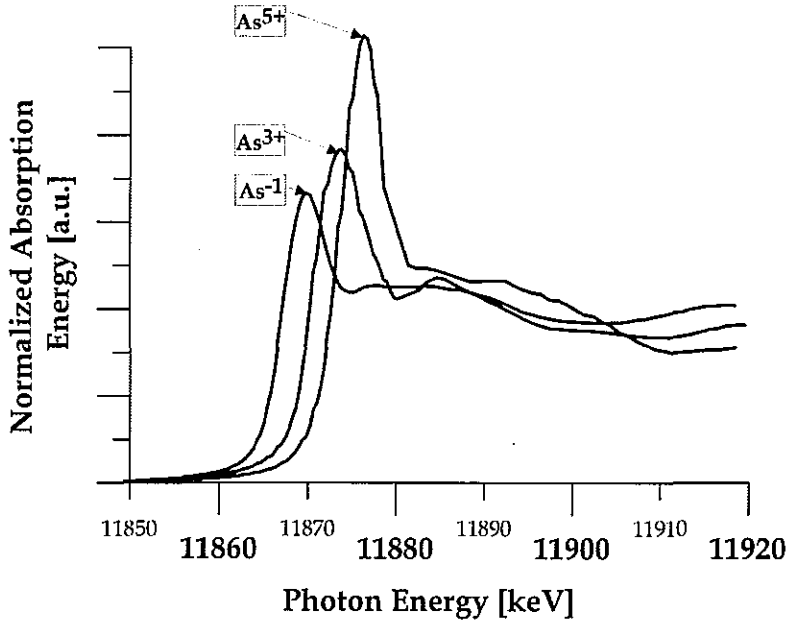

Figure 3.6: Standard μXANES spectra for arsenopyrite (As^{-1}), arsenic trioxide (As^{3+}) and scorodite (As^{5+}) as collected from X26A at NSLS.

positions. For these experiments both diluted and undiluted standards were used. Diluted standards were prepared and mounted by S. Walker in 2002 and used only the finest fraction of the ground standard mixed with boron nitride to obtain a final concentration of 4% As by weight. The standard mixtures were then spread in a thin layer onto the Kapton® tape (see Walker *et al.*, 2005 for full standard preparation description). Additional material had been stored in plastic vials was remounted in 2008 in an attempt to get better standard spectra.

Undiluted standards were prepared by S. Fawcett in 2007 and 2008 by dry-grinding the sample in an agate mortar and pestle and spreading it in a thin layer between two layers of Kapton® tape.

Table 3.2: Standards For μ-XANES Analyses

Standard	Formula	As-Oxidation State	Source	Position of Derivative*
Arsenopyrite	FeAsS	As^{-1}	Mina La Bufa, Mexico [M5579]	11867
Arsenolite	As_2O_3	As^{3+}	J.T. Baker Reagent	11870.2
Scorodite	$FeAsO_4 \cdot 2H_2O$	As^{5+}	Laurium, Greece [M6303]	11874.2

[MXXXX]: Miller Museum Reference, Queen's University Department of Geological Sciences and Geological Engineering.
* Edge positions are in eV at the first maximum in the derivative. Standards were set relative to the arsenopyrite edge at 11867.

Raw bulk and μ-XANES spectra were analyzed using the program ATHENA™ which allowed the standards to be calibrated to the known As edge position and the unknown spectra shifted based on the known energy shifts of the As standards over time. Spectra were normalized using an upstream ion-chamber that measured the incident beam flux as well as pre-edge and post-edge corrected to remove background from the spectra. Once the unknown spectra were calibrated and corrected, the absorption edges were determined using the highest peak(s) in the derivative of the normalized absorption energy and compared to the As standard edge positions.

The ATHENA™ program is also capable of performing Linear Combination Fitting (LCF) that fits the unknown spectra to the white line position of the standards. This program was used to determine relative percentages of the three As species within each

grain (or bulk sample) allowing comparison of grains within a section and between sections. LCF is a powerful technique it requires an excellent series of standards to help reduce error and provide the best fitting results. For bulk XANES where several spectra were taken on each sample, the spectra were merged into one file using ATHENA™ prior to LCF. In samples with low As concentrations, XANES spectra tended to be more noisy so to facilitate fitting, spectra were smoothed using the lowest smoothing function in ATHENA™.

3.2.3.2 Micro-X-Ray Diffraction (μXRD) Analyses

Identification of As-bearing grains was performed using two-dimensional μXRD images. Data was collected for 60 or 300s in transmission mode at high energy (17.347keV and λ=0.7147) using a Bruker SMART 1500 CCD diffractometer at 1024 x 1024 pixel resolution. Raw data were calibrated using the standard reference material 647a (αAl_2O_3) and silver behenate ($AgC_{22}H_{43}O_2$) in the software program Fit2D™ (Hammersley, 1998). The 2-D patterns displayed in Fit2D™ were in the form of diffraction features which were then integrated and brought into the peak-match program X-Pert High Score Plus® to identify the unknown phases using International Centre for Diffraction Data reference powder diffraction patterns (ICDD, 2003). The diffraction features can range from sharp spots that represent micron to sub-micron crystallites to spotty or constant intensity Debye-Scherrer rings that represent randomly oriented nanometer sized crystallites (Manceau, 2002; Walker *et al.*, 2005).

3.2.4 Conventional X-Ray Diffraction (XRD)

Conventional XRD was performed on three sub-samples, two OSS from Giant (Townsite and fault areas) as well as the highest total As sub-sample from Site 2 at North

Brookfield using a Phillips PW3020/00 X'Pert MPD/MRD Rontgen Diffractometer System. Samples were dry ground, mounted in metals disks and scanned from 6° to 80° 2theta. Samples were corrected by shifting the most prominent quartz peak to match the line of synthetic quartz (ICDD, 2003).

3.2.5 Sequential Selective Extraction (SSE) Analyses

Sequential selective extractions were performed at ALS Chemex on 10 sub-samples from the Giant Mine and 7 sub-samples from the North Brookfield Mine (Table 3.3). Sub-samples were chosen based on the following criteria; soil type (organic versus till), soil chemistry (high vs low As and Sb), synchrotron μ-XANES and μ-XRD identification of arsenolite and finally, surface samples were chosen as a proxy for understanding the potential bioaccessibility of the sample locations. Samples were sieved to -80 mesh size (<180 μm) and analyzed using a new eight step method developed by G.E. Hall that was modified from Hall *et al.*, (1996b). The most significant change in the method was the addition of a step to extract the mineral scorodite between the crystalline iron oxide and the sulphide leaches. In the selective extraction, 3 g of sample subjected to increasingly stronger chemical reagents designed to release As bound in the soil matrix in one of 8 forms; adsorbed/exchangeable, organics, carbonates, amorphous iron oxides, crystalline iron oxides, scorodite, sulphides and residuals (Table 3.4). For each extraction supernatant fluid was decanted and analyzed using Inductively Coupled Plasma- Mass Spectrometer (ICP-MS) for a suite of 63 elements including; As, Ca, Fe, Mn, P, Sb and Ti.

Table 3.3: Soil samples chosen for selective extraction

Depth (cm) ↓	Giant Mine- Yellowknife, NT					
	Site 19	Site 28	Site 29	Site 31	OSS-41	OSS-43
	5.0	2.5	8.0	2.0	< 5.0	< 5.0
	26.0	30.0	33.0	32.0		
Depth (cm) ↓	North Brookfield Mine- NS					
	Site 2	Site 4	Site 8			
	< 1.0	4.5	14.5			
	15	29	34.5			
	47					

Table 3.4: Sequential Selective Extractions (SSE) Leaches

	Selective Extraction Steps	Reagents
1	Adsorbed/exchangeable	1M NH_4OAc
2	Organics	0.1M $Na_4P_2O_7$
3	Carbonates	1M NH_4OAc
4	Amorphous Iron Oxides	0.25M NH_2OH
5	Crystalline Iron Oxides	1M NH_2OH
6	Scorodite	4M HCl
7	Sulphides	*Aqua Regia*
8	Residual	HF-$HClO_4$-HNO_3

Included in the 17 SSE tests was one duplicate sample, one standard and a series of test blanks. Comparison of the NIST-2711 Montana soil standard to the same standard run using the same extraction scheme the GSC-Ottawa in G. Hall's laboratory reveals that with the exception of As, the average relative standard deviation is 10% or less. Arsenic average relative standard deviation was higher due to the organic extraction step which was not used in the NIST-2411 GSC extraction. The average relative standard deviation for the duplicate sample was below 10% for all elements of interest (Table 3.5). Complete SSE results as well as results for the NIST-2711 standard and duplicate sample can be seen if Appendix G.

3.2.6 Environmental Scanning Electron Microscopy (ESEM)

Specific thin sections and grains were chosen for Scanning Electron Microscopy (SEM) to determine the source of As in the soils and to image As-bearing grains at high magnification. Environmental Scanning Electron Microscopy (ESEM) was performed on the Zeiss Evo 50 Environmental Scanning Electron Microscope at the Geological Survey of Canada in Ottawa

Table 3.5: Summary of percent differences between ALS and GSC run Montana Soil (NIST-2711) and a duplicate sample run at ALS-Chemex.

	NIST-2711 Montana Soil	Duplicate Sample
As	17.7	9.0
Ca	10.5	3.7
Fe	4.7	8.5
Mn	1.2	6.2
Sb	2.2	9.9
Ti	0.4	8.9

on 23 thin sections. The ESEM was also equipped with an Oxford Inca Energy 450 X-ray micro-analysis system for elemental and phase analysis. The ESEM permits a high degree of magnification as well as qualitative EDS spectra without the need for coating the samples. The operating conditions of the ESEM can be seen in Table 3.6.

Two types of samples were chosen for ESEM work. First, samples with grains containing a high proportion of As^{3+} that did not diffract using synchrotron techniques were chosen to identify the source of As. The ESEM proved to be a very powerful technique in identifying As-oxide grains in these targeted samples and this technique was then applied to

a second set of samples to identify As-bearing minerals. The ESEM was used to scan through samples in an attempt to find As-oxides within the soil sub-samples. Oxfords Inca "feature" software allowed for automated scans through an entire thin-section to find particles and classify them based on chemistry and/or morphology. The software counted each grain within the optimized weight range (calibrated for each sample) for 1s and was able to identify grains larger than 5µm x 5µm. This automated method proved to be helpful in identification of As-oxide grains, however manual inspection of grains also took place to ensure correct automatic identification. Thin sections chosen for the non-targeted ESEM approach were selected based on As, Sb and OC content, as well on synchrotron bulk XANES analyses (Section 3.2.3). Targeted As-oxides grains within the thin-sections were then taken back to the synchrotron for µXRD and µXANES analysis to confirm their identification.

Table 3.6: GSC-Ottawa ESEM standard operating conditions

Zeiss Evo 50 Environmental Scanning Electron Microscope	
EHT	20kV
Probe Current	500pA
Spot Size	480 (no units)
Vaccuum Pressure	50pA
Working Distance	9.0mm
Analysis Time	60s

Chapter 4: The Presence and Persistence of As_2O_3 in Soils from the Giant Mine, Northwest Territories

4.1 Introduction

The arsenic (As) 3+-bearing minerals arsenolite and claudetite (As_2O_3 polymorphs) are important to consider when examining As solid phase interactions in soils as mineral form and oxidation state dictate both mobility and toxicity (Caussy, 2003; Smedley and Kinniburgh, 2002; Valberg *et al.*, 1997). These minerals are highly soluble under oxidizing, neutral conditions and the dissolved As^{3+} species considered more mobile and toxic (Masscheleyn *et al.*, 1991; Walker *et al.*, 2005) especially when directly ingested (Ruby *et al.*, 1999). Understanding the stability of As_2O_3 is fundamental to predicting how it will react in the environment. Works by several authors have determined that arsenolite and claudetite are stable between pe values of 6 to 12 over a wide range of pH conditions (Brookins, 1986; Nordstrom and Archer, 2003) and require high As activity (Vink, 1996).

As_2O_3 in soils can form naturally by the oxidation of arsenopyrite, realgar and native As in reducing conditions (Nordstrom and Archer, 2003) or be introduced through anthropogenic activities such as ore-roasting and smelting (Hocking *et al.*, 1978). Roasting techniques are used in gold (Au) mining when Au is refractory and bound within the host mineral arsenopyrite (FeAsS). Heating the ore converts the host sulphides into porous Fe-oxides more amenable to conventional cyanidation. This process releases As and sulphur (S) vapours, which combine with oxygen in the atmosphere to form As_2O_3 and sulphur dioxide (SO_2) gases that can be carried on the wind. The method of attaining As_2O_3 grains within the soils is not completely known. It is most likely a combination of As_2O_3 condensing in the atmosphere and falling out of the air as solid particles into the soil and solid particles

forming within the soil as a result of if As_2O_3 dissolution in the atmosphere. Studies of anthropogenically-derived As_2O_3 have examined mine wastes and soils surrounding historic gold mines (Ashley and Lottermoser, 1999; Haffert and Craw, 2008) as well as soils impacted by the application of arsenical pesticides (Datta and Sarkar, 2004; Sarkar *et al.*, 2005; Yang and Donahoe, 2007),

The present study focuses on soils from the Giant mine near Yellowknife, Northwest Territories, Canada where As is naturally abundant in association with gold mineralization, and has also been introduced through more than 50 years of mineral processing. The Giant mine generated more than 7 million ounces of gold that was incorporated sub-microscopically in arsenopyrite, necessitating roasting. Based on thorough studies by Coleman (1957) on the orebodies mined at the time, sulphides (pyrite, arsenopyrite etc.) and sulphosalts (containing antimony) represent 5% to 15% by volume of the ore (Canam, 2006; Coleman, 1957).

Over the lifetime of the mine, Giant has generated more than 237,000 tonnes of As_2O_3 dust currently sealed in underground stopes (INAC, 2007) and emitted approximately 20,000 tonnes of As_2O_3 dust from the stack (CPHA, 1977; EnviroCan, 2008; GNWT, 1993; INAC, 2007; Tait, 1961). An estimated 80% of these emissions occurred in the first ten years of operation when few environmental controls were in place. In addition to the releasing As_2O_3 and SO_2, roasting generated fine-grained roaster-derived iron oxides (roaster oxides-RO) some of which were released from the stack and contain upwards of 7 wt. % As (Walker *et al.*, 2005). Currently, the mine is planning to remediate surface materials and waters, tailings, sediments, waste waters and infrastructure. Several studies regarding As and antimony (Sb) mobility at Giant have been completed (Andrade, 2006, Fawcett *et al.*, 2006;

Fawcett *et al.*, 2008, Riveros *et al.*, 2000; Walker *et al.*, 2005, Walker, 2006; INAC, 2007). Supporting documents from the remediation plan show elevated dissolved As in surface water seeps across the mine property (0.13 ppm to 1.1 ppm) that were believed to be attributed to a mobile but unidentified form of As in the soils, possibly from the legacy of the aerial emissions of particulate As_2O_3 (SRK, 2005).

The objectives of this study were to identify the form, distribution and stability of As in soils surrounding the Giant gold mine in the Northwest Territories. Giant is currently in the remediation process with the potential to develop portions of the site in the future making it essential to understand the source of As within the soils before the land becomes accessible to the public. The high solubility of As_2O_3 makes understanding the fate of aerially dispersed As in these soils critical for predicting the flux of soluble As to surface water and the potential bioaccessibility of As within the soils should they be ingested.

4.2 Methods

4.2.1 Sample Collection

To characterize As within the soils at Giant, 23 soil core samples (SCS) and 10 outcrop soil samples (OSS) were taken from across the mine property (Appendix C) of which six SCS and two OSS are discussed here (Appendix A) (Figure 4.1). Outcrop exposures represent more than 30% of the land in the Yellowknife area (Hockings *et al.*, 1978). During active mining, roaster-derived particles would have accumulated on surface exposures and been transported by wind and water to soils in small rock hollows or crevasses (Walker, 2006). For this reason, OSS are important to examine as they could represent a continued source of

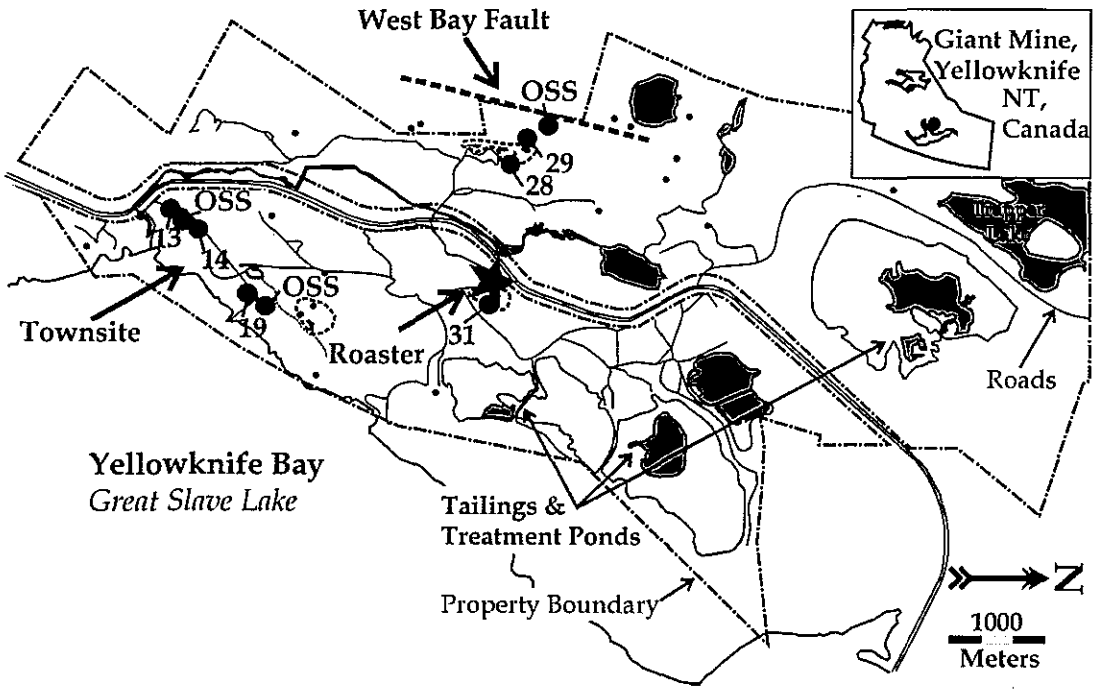

Figure 4.1: Location of soil samples from Giant Mine, Northwest Territories. Samples were taken from three localities (1) The Townsite- a small residential area located on the shores of Yellowknife Bay that housed miners and their families during the operation of the mine, (2) West Bay Fault- a marshy meadow locater beside outcrop that marks the fault, (3) Roaster- a marshy area beside the roaster. Black dots represent outcrop soil samples (OSS) and grey are soil core samples (SCS).

As to surface waters after remediation of the mine. From a human health perspective, these areas are essential to consider as they potentially represent a human health risk because of the potential for high total As and the high solubility of As_2O_3.

Sampling was designed to target areas impacted by atmospheric dispersion of roaster stack emissions based on air photos, wind direction, previous studies on the mine property (ESG and Queen's, 2001; GNWT, 1993; Golder, 2005; Hockings *et al.*, 1978; Kerr, 2006; SRK, 2005; Walker *et al.*, 2005; Walker, 2006) and an initial site survey. Samples were taken away from any regions with obvious As-rich solid waste. SCS were 30 to 60cm deep samples

taken using 1/16" walled, 2" outside diameter aluminum tubing. The tubes were driven into the ground using a drive head and sledge hammer. OSS were <50g samples taken using a small trowel and were stored in Ziploc® bags. Both SCS and OSS were frozen to preserve solid phases.

4.2.2 Elemental and Organic Carbon (OC) Analysis

Core and hand samples were thawed, air dried, and sub-sectioned based on soil horizons prior to being sent for elemental analysis at the Analytical Services Unit (ASU) - Queen's University. Samples were dissolved in *aqua-regia* and analyzed by a Varian Vista AX Simultaneous Inductively Coupled Plasma-Atomic Emission Spectrometer for a suite of elements including arsenic (As), calcium (Ca), iron (Fe), manganese (Mn), sulphur (S) and antimony (Sb). Detection limits for these elements were 1 ppm, 100 ppm, 50 ppm, 1.0 ppm, 25 ppm and 10 ppm respectively. Analyses performed on sample blanks were below detection limits and while certified reference materials and house standards were within the control limits determined by repeat analyses at ASU. Average relative standard deviations (2-sigma) of sample duplicates was <5% for the six elements of concern. Blind duplicate samples submitted to the lab had a higher average relative standard deviation, 14% for As, 13% for Fe 11% for S and 13% for Sb, and as samples were separated prior to grinding and variability this probably represents the inhomogeneity within the soils. Organic Carbon (OC) analysis was performed on sub-samples using a LECO® CNS-2000 Organic Carbon and Nitrogen analyzer in the Biology Department at Queen's University. A series of three standards were run between each set of 10 samples which had well constrained OC content. The standards were within the acceptable range of two standard deviations from the mean, so the values for the unknowns were accepted.

4.2.3 Petrography and Synchrotron Analyses

Bulk and micro X-Ray Absorption Near Edge Structure (bulk XANES and μXANES), micro X-Ray Diffraction (μXRD) and micro X-Ray Fluorescence mapping (μXRF) were performed at X26A and X27A at the National Synchrotron Light Source (NSLS) on Long Island, NY, USA. XANES analyses, when used in combination with the relevant standards, can examine small energy shifts in the position of the As absorption edge to determine the specific As oxidation state at the grain scale or within a bulk material (Fendorf and Sparks, 1996; Manceau *et al.*, 2002). The ability to differentiate between As species was integral in this study as the presence of As^{3+} bearing phases can potentially be linked to lower stability and higher toxicity, and anthropogenic inputs of As as roaster emissions contained As^{3+}.

X26A uses a series of Rh coated 100mm Si mirrors, arranged in a Kirkpatrick-Baez geometry, to focus the collimated monochromatic beam from 400μm by 400μm to a spot size diameter of 10μm by 6μm for work at the micron scale (Eng *et al.*, 1995). A channel-cut Si(111) crystal was used to achieve a monochromatic beam for XANES experiments, with the Si(Li) detector being placed 90° to the incident beam. Bulk work performed at X26A required the beam to be focused to a 1mm x 0.349mm spot size. Only bulk XANES were analyzed at X27A which uses a similar experimental set-up and a 600μm by 600μm unfocused beam.

Samples from SCS were made into doubly-polished thin sections for μ XANES and μXRD analyses. Thin sections were prepared, as described by Walker *et al* (2005), to be 'liftable' as removal of the glass slide was required before analysis. Prior to synchrotron analysis, petrography was performed to identify and target potential As-bearing phases. Techniques for removal of the glass slide are described in Walker *et al.* (2005). Detachment

time and quality varied depending on grain size, organic matter content and the quantity of grains in the sample. Issues arose in the lifting process for organic- rich samples as the epoxy would not fill all of the pores within the grains. During lifting this resulted in loss of potential targets. Samples for bulk XANES were mounted on Kapton® tape by flattening <0.5g of ground sample onto the tape and placing Kapton® film over the sample to prevent movement. Between two and four scans were taken per sub-sample to decrease problems arising from inhomogeneity.

XANES experiments were performed on a bulk and micron-scale by scanning across the As Kα absorption edge (11800 to 11970 eV) in fluorescence mode using a Si(Li) detector. Scans across the edge were broken into three sections, for μXANES analyses in the pre-edge (11800.0 to 11850.0eV), edge (11850.4 to 11880.0eV) and post edge (11881.0 to 11970.0eV) each with 2s, 4s, and 3s dwell times respectively, and varying step sizes. Analytical conditions at X26A and X27A for bulk XANES were the same as those used for μXANES but dwell times in the pre-edge, edge and post edge were reduced to 2s per step.

The As standards scorodite ($FeAsO_4 \cdot 2H_2O$), arsenic trioxide (As_2O_3) and arsenopyrite (FeAsS), were prepared by Walker *et al.* (2005) and routinely run to document shifts in the As edge position (Figure 4.2). Raw bulk and μXANES spectra were analyzed using the program ATHENA™ which allowed the standards to be calibrated to the known As^{-1} edge position of 11867. Unknown spectra were shifted based on the measured shifts of the As standards (Ravel and Newville, 2005, Walker *et al.*, 2005). Spectra were normalized and absorption edge positions were determined using the highest peak in the derivative and compared to the As standard edge positions. Linear Combination Fitting (LCF) was performed using ATHENA™ to fit the unknown spectra to the position of the standards and

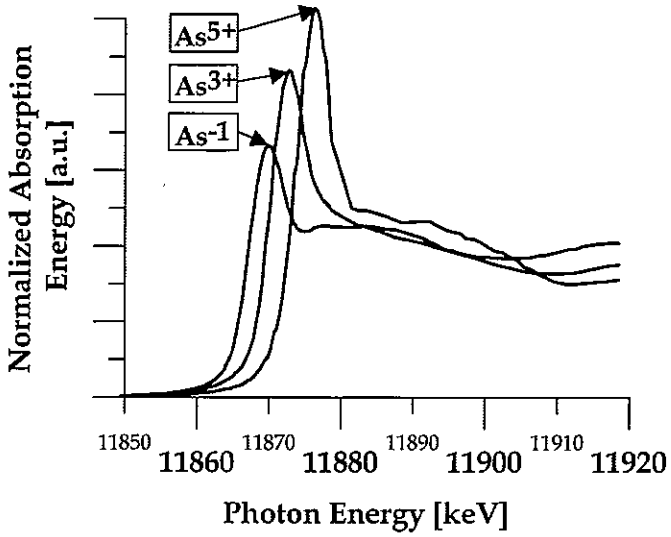

Figure 4.2: Standard μXANES spectra for arsenopyrite (As^{-1}), arsenic trioxide (As^{3+}) and scorodite (As^{5+}) as collected from X26A at NSLS.

determine relative percentages of the three As species within each sample (Ravel and Newville, 2005). For bulk XANES where several spectra were taken on each sample, the spectra were merged prior to LCF.

Micro XRD experiments on As-bearing grains were performed following XANES analyses using a Bruker SMART 1500 CCD diffractometer at 1024 x 1024 pixel resolution, collecting for 60s at high energy (17.347keV and λ=0.7147). Raw data were calibrated using the standard reference material 647a (αAl_2O_3) and silver behenate ($AgC_{22}H_{43}O_2$) in the software program Fit2D™ (Hammersley, 1998). Diffraction features ranged from sharp spots that represent micron to sub-micron crystallites to spotty or constant intensity Debye-Scherrer rings that represent randomly oriented nanometer sized crystallites (Manceau, 2002; Walker *et al.*, 2005).

4.2.4 Environmental Scanning Electron Microscopy (ESEM)

Thin-sections were analyzed directly, without coating, using the Zeiss Evo 50 Environmental Scanning Electron Microscope at the Geological Survey of Canada (Ottawa). The ESEM was operated at a probe current of 500 pA, 50pA vacuum pressure, 9.0 mm working distance, 60s analysis time, and was equipped with an Oxford Inca Energy 450 X-ray μ-analysis system for elemental analysis. Oxfords Inca "feature" software allowed for automated scans through an entire thin-section to find and classify particles based on chemistry and/or morphology. The software counted each grain within the optimized weight range (calibrated for each sample) for 1s and was able to identify grains larger than 5μm x 5μm. This automated method proved helpful in the identification of As-rich phases. Sections were chosen for the non-targeted ESEM approach based on As, Sb, OC and synchrotron bulk XANES.

4.3 Results

The eight selected samples have been grouped into three locations as indicated on Figure 4.1. Three SCS and one OSS were taken from forested areas on the Townsite, a small community that housed mine workers on the property. From the western portion of the property (West Bay fault), Site 28 was from an open meadow, Site 29 was directly beside the near vertical fault and an OSS from the outcrop adjacent to Site 29. Finally, a SCS was taken from a marshy area close to the Giant roaster.

Naturally elevated concentrations of As associated with gold mineralization in the Yellowknife area allowed for the determination of natural background, set at 150 ppm (Risklogic, 2002a). Remediation objectives were determined to be 160 ppm and 340 ppm for residential and industrial soils respectively (GWNT, 2003; Risklogic, 2002a; Risklogic, 2002b;

Risklogic, 2002c). Yellowknife As guidelines were set higher than the national standard of 12 ppm (CCME, 2007b) because of the naturally elevated As as well as the decreased frequency, duration and intensity of land use due to the snow cover in the winter months (Risklogic, 2002a).

4.3.1 Soil Profiles

4.3.1.1 The Townsite- Sites 19, 13 and 14

Site 19 is a wooded area in the eastern portion of the Townsite. The surface soil is organic-rich, containing partially decomposed plant material. Below the organic horizon is a 22cm thick layer of sandy loam followed by a pale yellow till with a silty matrix and 20% to 30% clasts. Total OC, As, and Sb values for this site are presented in Figure 4.3A. Bulk soil

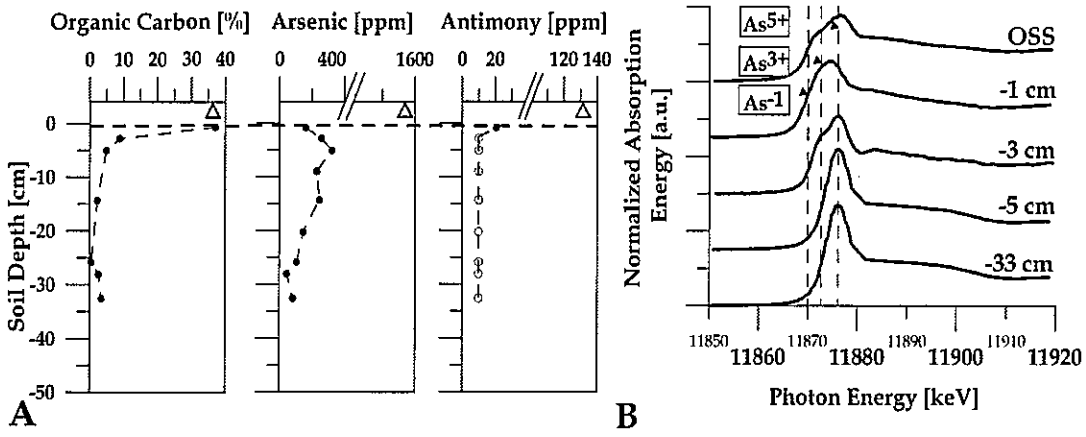

Figure 4.3: Soil profile (A) and bulk XANES (B) for Site 19 and OSS in the Townsite. In A triangles represent measured concentrations in the OSS sample, closed circles are the measured bulk concentrations and open circles in the Sb profile indicates that concentrations are below the detection limit of 10 ppm. In B, -1cm means 1cm depth.

digestions show that As concentrations are low in the surface horizon, increasing to a maximum of 320 ppm at the transition to the sandy loam (5cm depth), decreasing through

this horizon and are below natural background within the till. Sb and S concentrations do not follow As as the highest Sb is in the surface horizon and are below detection after 1cm, corresponding to the decreasing S values (Table 4.1). The OSS taken from this area is also organic rich (OC>35%) has significantly higher total As and Sb concentrations (1590 ppm and 131 ppm respectively). Sb is important to consider in soils at Giant because its presence is an indicator of anthropogenic As based on the work of Riveros *et al.* (2000) on As_2O_3 dust stored underground as well as work by Kerr (2006) who showed elevated Sb concentrations on the mine property compared to samples taken away from the influence of roasting. Riveros *et al.* (2000) found As_2O_3 grains with between 0% and 47% Sb that possibly incorporated in roaster gases when sulphosalts were roasted.

Spectra collected from the ESEM reveal the presence of a particulate phase containing only As and oxygen (termed As-oxides) dispersed in all samples containing As^{3+} bulk XANES signatures. Figure 4.3 B is a bulk XANES profile through the soil profile from Site 19. LCF proportions for all reported bulk XANES can be seen in Table 4.1. At the surface of the SCS no arsenopyrite (As^{-1}) is observed and 66% of the As is present as As^{3+} from 1cm to 3cm depth (Table 4.1). Below 3cm the As signature switches to As^{5+} only. At this site four samples were examined for As-oxides, the OSS, SCS from 1cm, 5cm and 28cm depths. As-oxides were identified in the OSS and SCS from 1cm depth where As^{3+} signatures were detected (Figure 4.4). Samples of surface water seeps south of the Giant Mill by SRK (2005)

Table 4.1
As, Sb, S and LCF Results for Selected Samples

Sample Location	Depth [cm]	Bulk Chemistry [ppm]			Presence of As-oxides	LCF Results (%)		
		As	Sb	S		As^{5+}	As^{3+}	As^{-1}
Site 13	-2	139	14.6	2500	None	14	0	86
	5.3	21.3	<10	2260	None	TL	TL	TL
Site 14	OSS	709	52.9	1600	Yes	67	13	20
	-2	163	13.7	2280	-	42	0	59
	-5	187	33.5	1620	Yes	25	64	11
Site 19	OSS	1589	131	1170	Yes	43	37	20
	-1	161	20.7	2250	Yes	34	66	0
	-3	258.25	<10	591.5	-	36	64	0
	-5	322	<10	326	None	100	0	0
	-33	82.7	<10	89.1	-	100	0	0
Site 28	-2	321	47.85	2170	Yes	39	61	0
	-24	245	<10	1590	-	76	24	0
	-34	607	<10	1455	None	100	0	0
	-38	302	<10	1920	-	100	0	0
Site 29	OSS	3280	506	982	Yes	22	55	23
	-2	936	101	2970	Yes	78	17	5
	-16	1434	92.3	1760	Yes	94	7	0
	-33†	374	<10	264	Yes	62	39	0
Site 31	-2	1423	210	1390	Yes	3	80	18
	-6	333.5	<10	454	-	100	0	0
	-11	270	<10	181	None	100	0	0
	-27	209	<10	85.3	-	100	0	0

† Sample contains Sb below detection and As-oxides. SSE results from Chapter 5 for this sample show significantly higher As and Sb results. Low values in unsieved digestions may be the result of inhomogeniety within the sample.

showed dissolved As concentrations between 0.65 mg/L and 2 mg/L, higher than the 10 µg/L national guideline (CCME, 2007a), showing the presence of a labile source of As within the soils.

No As-oxides were found at 5cm depth even though total As concentrations are the highest from this site. At 28cm depth, as anticipated by the lack of As^{3+} in the bulk XANES analysis, no As-oxides were present. As-oxides identified at this site are of similar size and morphology with grains varying between >2 µm and 15 µm in diameter. Unlike Haffert and

Craw (2008) where As-oxides in Au mine wastes in New Zealand were smooth and showed an oxidation rim of scorodite surrounding the grains, As-oxides at Giant have a mottled texture that may be attributed to dissolution. Based on observations from this site, the total As concentrations in the soils alone are not sufficient to predict the presence of As-oxides.

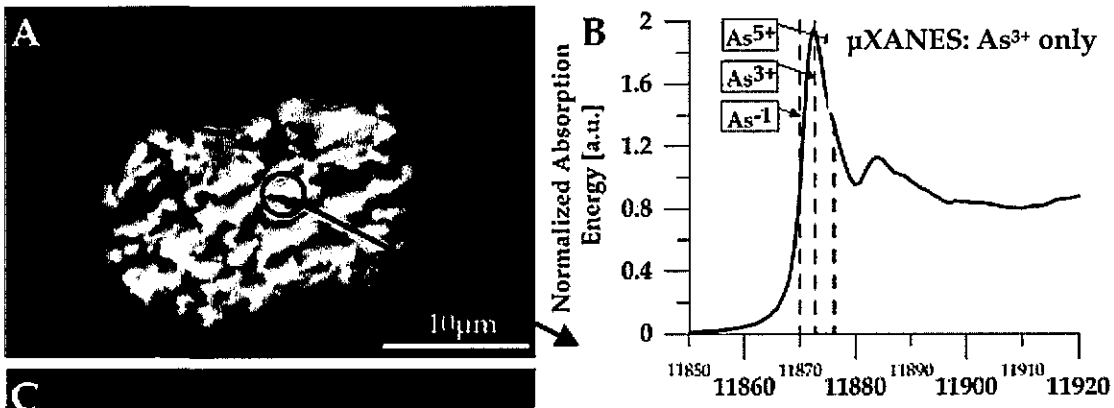

Figure 4.4: Back scatter electron (BSE) images (A,C) and μXANES (B) of As_2O_3 grains from Site 19. A is from the OSS showing the common mottled texture attributed to dissolution and **B** is a μXANES spectra of grain A, dashed lines represent the location of the white line peak for all three As oxidation states. Micro-XRD on this grain show the particle is arsenolite (As_2O_3) **C** is a cluster of grains including some that are in the respirable (<10μm) fraction.

Surface soil samples were also taken from the western portion of the Townsite at sites 13 and 14 to a depth of 5 cm (Figure 4.1). Soils at both sites are organic rich (OC >20%) with As concentrations just below (Site 13) and just above (Site 14) natural background for the Yellowknife area. Sb was above detection limits in the top 2.5 cm at both locations but below detection at 5cm depth in Site 13. Bulk XANES from these two locations shows that As^{3+} was not present in the surface soils and no As-oxides were identified at depth. The presence

of As^{-1} in surface soils at Site 14 suggests that this material might be fill composed of crushed waste rock containing arsenopyrite as seen by a study by ESG and Queen's (2001) and Walker (2006) using conventional XRD. At 5cm depth Site 14 recorded more than 60% As^{3+} in the bulk soil which is consistent with the presence of As-oxides as demonstrated by ESEM results. These have similar size and texture to those found at Site 19.

4.3.1.2 The Fault- Site 28 and 29

A SCS pair and corresponding OSS were taken from a grassy meadow and marsh located beside the almost vertical West Bay fault (Figure 4.1). On the western side of the fault is exposed outcrop as high as 10m above the surface of the meadow. To test the hypothesis of Walker (2006) that roaster derived particles accumulated on outcrop exposures and were washed into outcrop crevasses, a SCS was taken from the meadow directly (<5m) beside the West Bay fault (Site 29) to determine if roaster-derived particles could also be transported into the soils adjacent to outcrop exposures. An OSS to the west of the fault and an additional SCS from the middle of the meadow (Site 28) to the east were taken to compare total As and Sb concentrations and As speciation. Soil cores from these sites are dominated by organic horizons in varying states of decomposition. A disturbed horizon occurs at both Sites 28 and 29, indicated on Figure 4.5A and 4.6A. The horizon is a grayish brown silty loam with low OC at both sites. Unfortunately, the history of this location, and therefore the origin of this disturbed horizon is unknown.

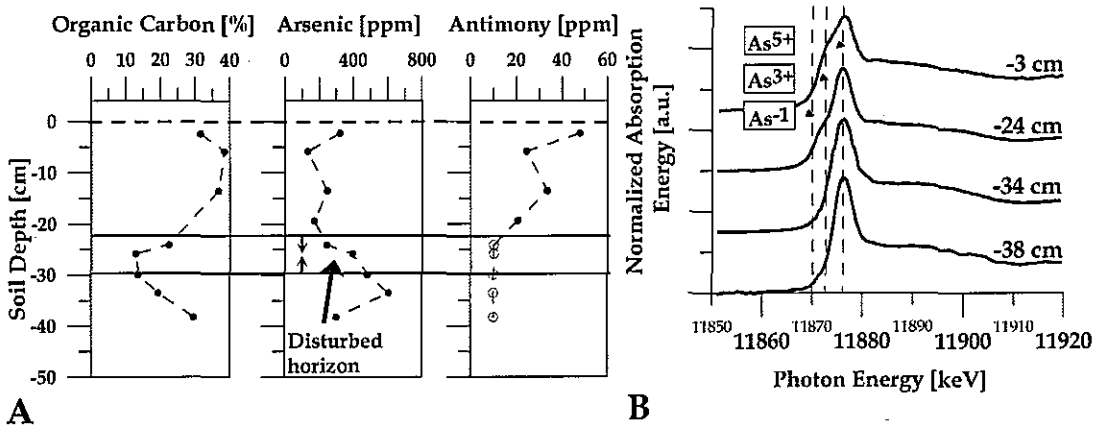

Figure 4.5: Soil profile (A) and bulk XANES (B) for Site 28 by the West Bay Fault. In **A**, closed circles are the measured bulk concentrations open circles and in the Sb profile indicates that concentrations are below the detection limit of 10 ppm. The disturbed horizon is marked by two solid lines. In **B**, -3cm means 3cm depth.

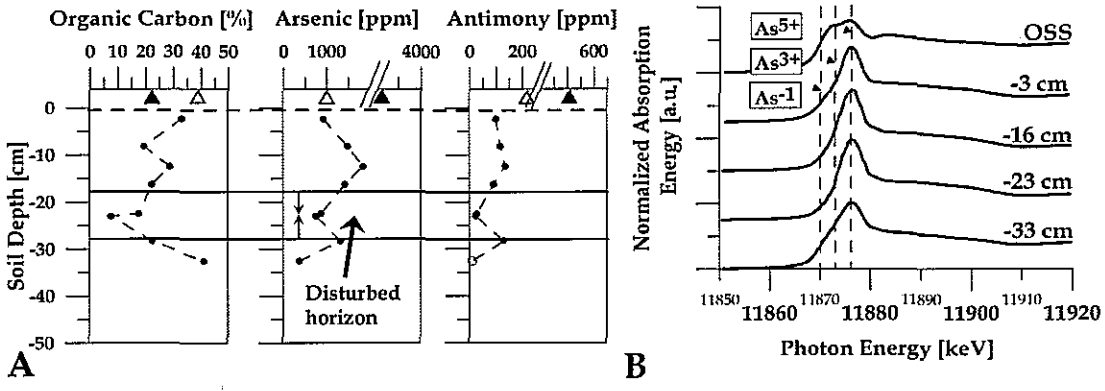

Figure 4.6: Soil profile (A) and bulk XANES (B) for Site 29 and OSS by the West Bay Fault. In **A**, , closed circles are the measured bulk concentrations , triangles represent measured concentrations in the OSS sample and open circles in the Sb profile indicates that concentrations are below the detection limit of 10 ppm. The disturbed horizon is marked by two solid lines. In **B**, -3cm means 3cm depth.

Even though these sites have very similar soil types and are located less than 25m apart, the elemental concentrations within soil profiles are very different (Figures 4.5A and 4.6A). Unlike the clear trend of elevated elements at the surface of Site 19, the sites near the fault have more complicated soil profiles. From the surface soil to the top of the disturbed

horizon at Site 28, As concentrations fluctuate between 340 ppm and 130 ppm, and Sb ranges from 50 ppm to 20 ppm. Bulk XANES from the surface material shows more than 60% of the As in the 3+ oxidation state (Figure 4.5B). Through the disturbed horizon As is higher than samples above, Sb is below detection while S and OC concentrations decrease with depth. Bulk XANES shows a clear As^{3+} signature at the top of this horizon which contains As-oxides. Another spike in total As occurs at 34 cm depth within organic-rich material with no corresponding increase in Sb. Bulk XANES and ESEM from two samples at this depth shows that the increase in As was not related to increasing quantities of As-oxides as none were observed and As was present only as As^{5+}.

Like Site 28, Site 29 near the outcrop shows variability within the soil profile with respect to the major elements. From Figure 4.6A, two distinct peaks in As and Sb concentrations were observed with increasing depth while S decreased (Table 4.1). At the surface As concentrations are almost twice the values recorded at Site 28. The first peak in As concentration occurs at 13cm depth (As=1850 ppm), just above the transition into the disturbed horizon while Sb remains constant at approximately 110 ppm to 17 cm depth. From the surface to 17 cm bulk XANES results show a low presence of As^{3+} (<20%) (Figure 4.6B). Through the disturbed horizon, As, Sb, S and OC all decrease and bulk XANES shows an As^{5+} signature. Just below this disturbance is the second peak in As and Sb corresponding to an increase in OC and As^{3+} to between 20% and 40%. Again OSS is organic rich and contains the highest As and Sb concentrations observed, 3280 ppm and 506 ppm respectively. OSS from this site contains an average of 64% As^{3+}.

As-oxides are found in all samples taken from Sites 28 and 29, including from the disturbed horizon with no As^{3+} signature, and have similar mottled textures as described in

the Townsite (Figure 4.7). The presence of As-oxides in the disturbed horizon was expected as sub-samples of the soil profile were taken across the horizon boundary, meaning half the sub-sample was above the disturbed horizon and half was within it, and As-oxides were identified in sub-samples above.

4.3.1.3 The Roaster- Site 31

A SCS was taken in a small marshy area located beside the roaster, which is still standing although it has not operated since 1999 (Figure 4.1). The soils are unsaturated and in the top 6cm of the profile are partially decomposed organic rich (>20% OC) material, followed by a 2cm transition zone and 33cm of pale brown to dark gray silty-clay. Arsenic, Sb and S concentrations at this site are highest in the surficial organic material (Figure 4.8A), 1423 ppm, 210 ppm and 1390 ppm respectively, an order of magnitude higher than the

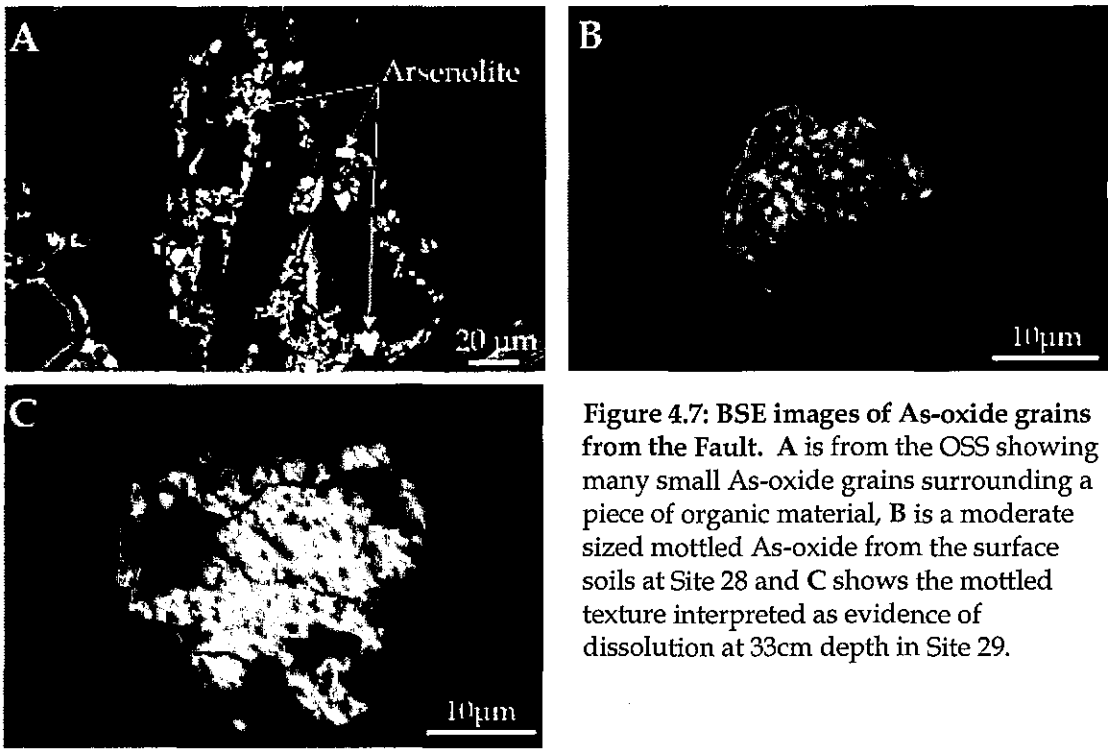

Figure 4.7: BSE images of As-oxide grains from the Fault. A is from the OSS showing many small As-oxide grains surrounding a piece of organic material, B is a moderate sized mottled As-oxide from the surface soils at Site 28 and C shows the mottled texture interpreted as evidence of dissolution at 33cm depth in Site 29.

remaining samples from this core (330 ppm As and Sb below detection). OC, Sb and S show a similar profile to Site 19 with highest concentrations at the surface and decreasing with depth (Figure 4.3).

Bulk XANES from four samples within the core show the proportion of As^{3+} in the organic materials was 80%, the highest recorded at the site (Figure 4.8B) that is consist with the highest recorded dissolved As concentrations between 0.26 mg/L and 24.9 mg/L in surface water seeps in the mill area (SRK, 2005). At 6 cm, 11 cm and 27 cm depth within the silty-clay, only an As^{5+} signature is present. The higher proportion of As^{3+} within the surface soil can be explained by the proximity of the roaster and dust collection systems. Fugitive dusts generated in the use of these facilities could have accumulated in soils within the immediate area.

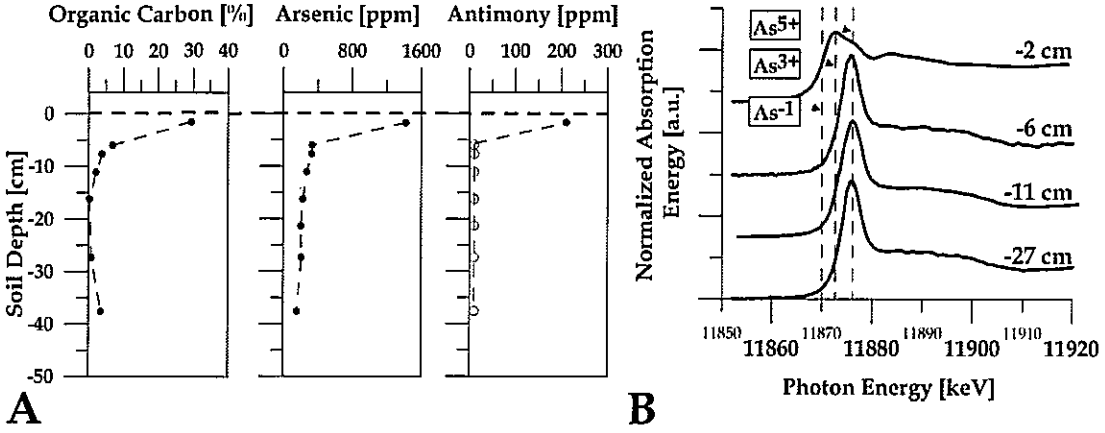

Figure 4.8: Soil profile (A) and bulk XANES (B) for Site 31 beside the roaster.
In **A**, closed circles are bulk concentrations and open circles in the Sb profile indicates that concentrations are below the detection limit of 10 ppm. In **B**, -2cm means 2cm depth.

Examining the soils at this site using the ESEM reveals As-oxides present only in the organic-rich surface materials (Figure 4.9). The texture and size of the As-oxides at this site differ from the other locations. The grains are typically larger (10μm to 300μm) and many

had a smoother texture, while others are mottled similar to As-oxides at other sites. Work by Knight and Henderson (2006) on smelter dusts from the Horne smelter in Rouyn-Noranda, Quebec showed that smelter dust grain size increased to *c.* 17 km away from the source at which point they began to decrease in size. The variety of textures and sizes of the As-oxides at Giant may be the result of slower dissolution rates at this site and not necessarily the proximity to the roaster (Knight and Henderson (2006).

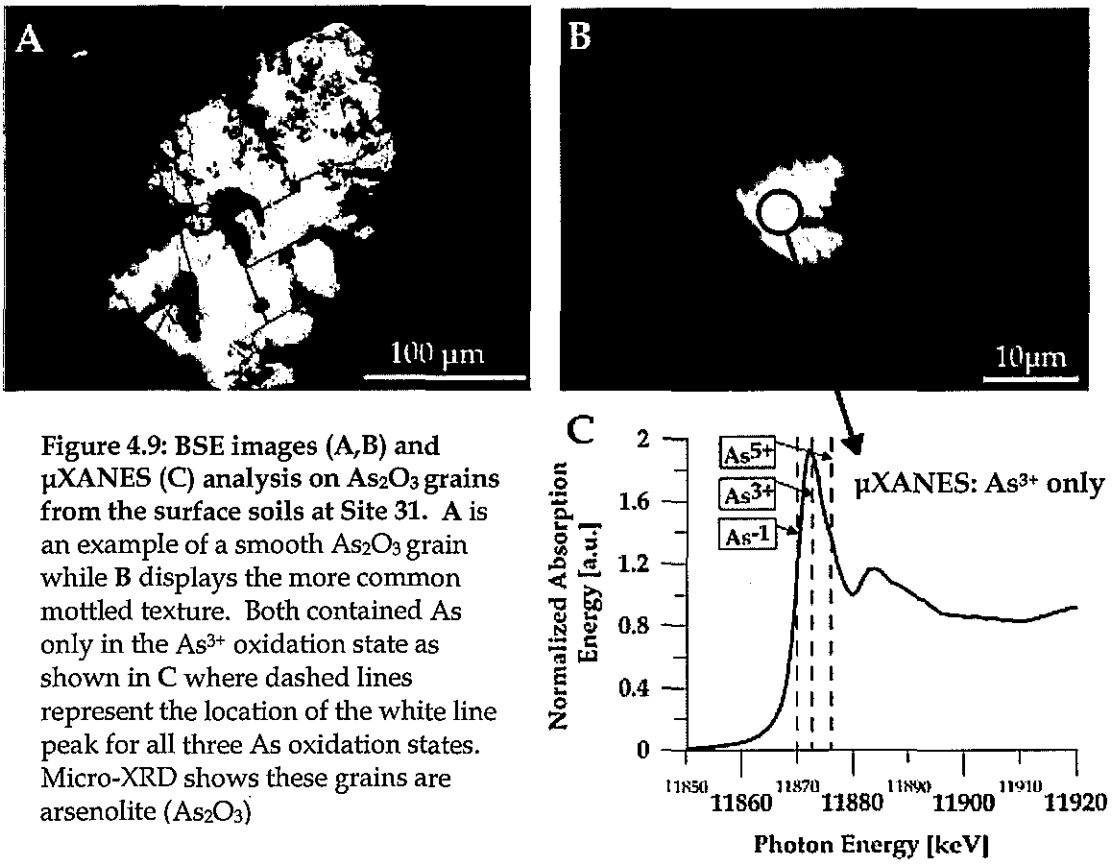

Figure 4.9: BSE images (A,B) and µXANES (C) analysis on As_2O_3 grains from the surface soils at Site 31. A is an example of a smooth As_2O_3 grain while B displays the more common mottled texture. Both contained As only in the As^{3+} oxidation state as shown in C where dashed lines represent the location of the white line peak for all three As oxidation states. Micro-XRD shows these grains are arsenolite (As_2O_3)

4.3.2 Characterization of As-oxides

4.3.2.1 µXRD and µXANES Analyses

Synchrotron µXRD and µXANES analyses were performed on a number of grains identified from the OSS and SCS using the ESEM. All As-oxide grains examined at the

synchrotron were identified as arsenolite, As_2O_3, with the exception of four grains where the 2-dimensional μXRD diffraction patterns contained only one bright spot. This indicates that the average size of the mineral crystallites was large relative to the diameter of the incident synchrotron beam or the orientation of the crystallites was not sufficiently random to produce smooth diffraction rings (Manceau, 2002; Walker *et al.*, 2005). Mineral identification is consistent with work by Walker (2006) who examined As-rich dusts from the dust collection system at Giant using conventional XRD and found As present in the form of arsenolite. Despite the fact that arsenolite is the identified phase, this is formed naturally by the oxidation of arsenopyrite, realgar and native As in reducing conditions (Nordstrom and Archer, 2003) and the identified arsenolite from Giant is formed through anthropogenic activities, and is therefore termed As_2O_3 to distinguish its origin.

Three types of diffraction patters were seen from the As_2O_3 grains from the Giant property. The weakest diffraction pattern came from smoother textured As-oxide grains from Site 31 which had a pattern of spots or points, which could not be easily matched with a diffraction pattern from the ICDD. When diffraction patterns were poor, μXANES spectra were collected on these types of grains to confirm that As^{3+} was the dominant oxidation state within the grain (Figures 4.4B, 4.9C). An intermediate form of diffraction came from smaller grains (20 μm to <2 μm) that had the mottled textures. In these cases the Debye-Scherrer rings were either spotty or in the form of small arcs. Identification of the mineral form in these cases was possible, confirming the mineral was As_2O_3, and μXANES analysis confirmed only As^{3+} was present.

The best diffraction, shown by continuous, smooth Debye-Scherrer rings, occurred on samples where 60s spectra had been collected using the ESEM, prior to μXRD analysis. In

some cases the ESEM beam caused visible damage to the sample. This may have caused grains to melt and re-crystallize reducing the average size of the particle crystallites compared to the incident synchrotron beam, producing a more smooth diffraction pattern. Micro XRD and μXANES on one grain before and after spectra were collected at the ESEM shows that the As oxidation state and crystallography of the re-crystallized portions of the grains did not change.

4.3.2.2 *Relationship between Organic Carbon (OC) and As_2O_3*

Figure 4.10 shows that tills typically have lower OC content (<10%) and lower As (<300 ppm), whereas the organic-rich soils and OSS have a wider range of both As concentration (20 ppm to 3280 ppm) and OC content (15% to 41%). Soils with higher OC

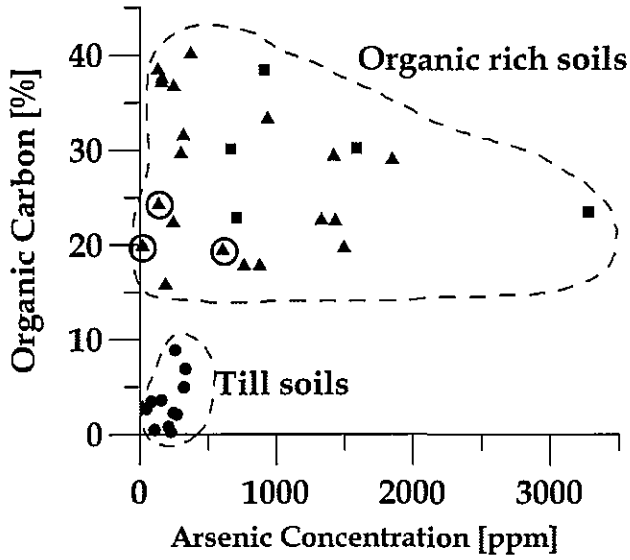

Figure 4.10: Organic Carbon (OC) versus Arsenic concentration. Filled circles represent tills with low OC, low As and no As_2O_3. Filled triangles indicate organic rich soils, most of which contain As_2O_3 and squares are OSS. Circled triangles indicate that no As_2O_3 grains were found.

also have As_2O_3 grains present, verified using a combination of ESEM, bulk and μXANES, and μXRD. There are three exceptions to this pattern: the two samples from Site 13 and one from 34cm depth at Site 28. Unlike the samples containing As_2O_3 particles, all of which have significant concentrations of Sb as measures in the soil digestions, these three contain very low or undetectable concentrations of Sb (Table 4.1). This suggests that the presence of significant Sb in soil may be an indicator of As_2O_3. Bulk XANES from Site 13 shows the presence of As^{-1}, likely in the form of arsenopyrite and because sulfides are not commonly found in other soils not from the Townsite, it is indicative of a form of waste rock fill described by Walker (2006) and Golder (2005) in this area. The lack of an As^{3+} signature at these sites suggests this fill must postdate the more significant As_2O_3 emissions during the 1950's.

4.3.2.3 Calculation of As_2O_3 in Soils

Assuming that the only sources of As^{3+} were in RO and As_2O_3, the bulk XANES proportions of As^{3+} in soils can be used to provide a qualitative estimate of the percentage of total As attributed to As_2O_3 (termed "total As_2O_3"). The percentage of As^{3+} in exposed beach tailings RO's at Giant was demonstrated by Walker *et al.* (2005) as being between 11% and 40% which was found to be consistent with measured values for RO's in these soils. A sensitivity analysis was performed to calculate changes in the calculated percentage of total As_2O_3 in the soils by incrementally changing the percentage of As^{3+} in RO's and the ratio of As_2O_3 to RO grains.

When the ratio of As_2O_3 to RO grains is lowered to 1:1 (As_2O_3: RO) there is a 5% to 15% difference in total As_2O_3 present depending on the percentages of As^{3+} in RO. Only at ratios of 2:1 or greater does the effect of changes in RO As^{3+} percentages become apparent. A

value of 25% As^{3+} in RO with a ratio of 50:1 to 5:1 (As_2O_3: RO) was appropriate for the organic rich soils at Giant and in this range there is little variability between different As^{3+} percentages in RO and ratios of As_2O_3 to RO (Table 4.2). The results from SCS (excluding Site 31 by the roaster) show an average of 28% to 33% of the total As in organic rich soils was attributed to As_2O_3, while in OSS this value was between 38% and 44%. Close to the roaster it was expected that the majority of As was attributed to As_2O_3 and estimates at this site are the highest on the property (69% to 79% of total As).

Table 4.2
Percentage of Total Arsenic as As_2O_3†

Location	Ave As (ppm) in Organic Soils	As_2O_3: RO 50:1	As_2O_3: RO 10:1	As_2O_3: RO 5:1	As_2O_3: RO 1:1
Site 14 (5cm)	175	31	31	30	27
Site 19 (1 to 3cm)	209	55	54	52	47
OSS Townsite	1149	25	24	24	22
Site 28	292	25	20	20	18
Site 29 (2 to 33cm)	1132	20	20	19	18
OSS By Fault	2095	63	63	61	55
Site 31‡ (2cm)	*1423*	*79*	*78*	*76*	*69*
Ave As_2O_3in SCS		**33**	**31**	**30**	**28**
Ave As_2O_3in OSS		**44**	**43**	**42**	**38**

†- Assuming 25% As^{3+} in RO based on Walker *et al* ., 2005
‡- Not included in average because concentrations were high due to proximity to the roaster

The values quoted above may be an overestimate of total As_2O_3 in the soil because of the simplifying assumptions made. Assuming As^{3+} could only be hosted in As_2O_3 and RO may be problematic as As^{3+} could also be adsorbed to the surface of Fe and Mn-oxides or bound by OM. Similar grain sizes were assumed when calculating the proportion of As attributed to each grain type but with the exception of the site closest to the roaster, As_2O_3 grains were on average between 5μm and 20μm in size whereas RO were between 20μm and 30μm. Repeat μXANES analyses are also required on RO in soils to provide a more accurate and better constrained estimate of the proportion of As^{3+} in the soil RO.

4.4 Discussion

4.4.1 Predictions of As_2O_3 Based on As, Sb, and OC at Giant

In soils surrounding the Giant mine, soil digestions, OC analysis, ESEM and synchrotron work were all methods used to characterize and explain the source of As^{3+} in As_2O_3. Common petrographic techniques and the total As concentration in soils are not able to accurately predict the presence of As_2O_3 grains. Using a combination of total As, Sb and OC concentrations, more accurate predictions of the presence of As_2O_3 can be made for these soils. At Giant, soils with OC values greater than 15% tend to contain As_2O_3. OC analyses are not an exact method of predicting As_2O_3, but when used in combination with Sb concentrations, both can help understand the presence of As_2O_3. Sb has a positive correlation with As_2O_3 in As_2O_3 dusts stored underground (Riveros *et al.*, 2000). In these samples, arsenic liberated during digestion was related to the Sb content of the individual grains. Water leach experiments showed that As_2O_3 crystals with low Sb, dissolved readily, leaving higher Sb-rich As_2O_3 in the remaining residue. This suggests that small amounts of Sb within the As_2O_3 grains caused a reduction in the As_2O_3, lowering its aqueous solubility (Riveros *et al.*, 2000). It was postulated that the Sb within As_2O_3 dust was in solid solution within the As_2O_3 crystals (Riveros *et al.*, 2000).

All samples that do not follow the OC and Sb predictions for the presence of As_2O_3 can be explained by either at the horizon boundary (so the sub-sample contains material from both horizons) or sample digestion issues arising from the nature of the soil. In cases where low Sb suggests that no As_2O_3 will be present, but high OC indicates the opposite, it can be difficult to predict the outcome.

4.4.2 The Wash Down Effect

The distinct geochemical differences between the three sites beside the fault (Sites 28, 29 and OSS) and the other sample sites on the property, warrants further discussion. In the Townsite and beside the roaster there is clear evidence of higher As concentrations in the top 5 cm of the soils which can be attributed to the accumulation of condensed gaseous As_2O_3 from the roaster. High As concentrations at Sites 28 and 29 are not limited to the surface horizons but extend through the entire profile. OSS taken from the outcrop surface adjacent to Site 29 has high As and Sb concentrations as well as high proportions of As^{3+} and the visible presence of As_2O_3 solids.

The presence of As_2O_3 to depths of 33 cm in the soil profile adjacent to the outcrop exposure and the agreement of bulk XANES showing high proportions of As^{3+} suggests that there was and still may be transport of As-rich roaster derived solids from the surface of the outcrop or from soils in small rock crevasses to the meadow beside the fault. This wash down theory was first discussed by Walker (2006) to explain the presence of roaster oxides in OSS from the Townsite. Lower total As and Sb concentrations, and the absence of As-oxides at depth in Site 28 may be due to an atmospheric source of As only. Outcrop wash down is unlikely due to the distance (approximately 25m) from the outcrop. This is confirmed by the presence of only As^{5+} at depth at Site 28.

4.4.3 Long-term Stability and Persistence of As_2O_3

In comparison to As_2O_3 grains imaged by Haffert and Craw (2008) that showed distinct oxidation rims, the mottled and smooth textures and lack of reaction rims observed on As_2O_3 grains at Giant suggest current environmental conditions are causing the dissolution of these grains rather than their oxidation. The dissolution of As_2O_3 in soil

samples far away from any obvious As-rich solid waste is consistent with measurement of high dissolved As (on average 1 mg/L) in surface water seeps and soils across the property (Golder, 2005; SRK, 2005), confirming that the soluble source of As in the soils is derived from ore-roasting on site. The highest proportion of As^{3+} in bulk XANES from Site 31 surface soils as well as higher dissolved As in surface water seeps around the mill (SRK, 2005) shows this area is heavily impacted by roasting activities. The presence of smoother textured As_2O_3 along with more weakly mottled grains adjacent to the roaster suggests grains at this site may be dissolving more slowly, shown by larger grain sizes.

In 2005, as part of the remediation plan for Giant, Golder Associates measured paste pH in soils from 20cm depth at various locations on the property, finding a range of pH around neutral conditions between 6 and 8. Sulphur concentrations (Table 4.1) in the soils measured in the present study demonstrates that at this depth S is below the zone of greatest impact. Sulphur can be used as an indicator of more acidic environments as SO_2 emissions from the roaster reacts with water in the atmosphere and eventually forms H+ (acid) and SO_3^{2-} entering the soil via precipitation (Langmuir, 1997). Higher S concentrations at the surface that cannot be attributed to FeAsS (using bulk XANES) and can be an indicator of a more acidic soil environment caused by acid rain. It is expected that currently, and in the future, soil chemistry will be changing on the property as a result of the closure of the roaster and cessation of SO_2 emissions.

More than 80% of the estimated 20,000 tonnes of As_2O_3 emitted from the roaster over the lifetime of the mine occurred between 1949 and 1958, therefore the As_2O_3 grains identified in this study suggest that they have remained in the environment for more than 50 years. There are several potential reasons why As_2O_3 has persisted in the soils around the

mine despite our evidence of dissolution. First, detectable levels of Sb from qualitative ESEM spectra in some of the As_2O_3 grains is in agreement with Riveros *et al.* (2000) who suggested that the presence of Sb in As_2O_3 grains in makes it more stable.

Secondly, climate may play an important role slowing down dissolution reactions as Yellowknife has low precipitation rates (EnviroCan, 2008). This, combined with the higher observed porosity and permeability of the organic soils, means even though rainwater will be undersaturated with respect to As, As_2O_3 grains may not have prolonged contact with it during the summer months. In addition, since the closure of the mine and termination of roasting and SO_2 emissions, the pH of rainwater and soil solution should be increasing. Riveros *et al.* (2000) found that roaster derived dusts dissolved more rapidly in acidic conditions because Sb no longer acted as an inhibitor to dissolution. If this is the case, increasing the pH of rainwater will further slow the rate of dissolution causing As_2O_3 to persist longer in the environment. During the spring months when snow melt could cause soils in low lying areas to be saturated, dissolution rates may change. As stated by Vink (1996), high dissolved As concentrations are needed for As_2O_3 to be stable under moderately oxidizing to moderately reducing conditions. If melt water remains in contact with the soils the amount of As in the aqueous phase will determine if further dissolution will occur.

Finally, in high OC samples, smaller As_2O_3 grains have been found associated with plant material whereas larger grains have been found in the absence of organic matter (OM). Grains found not associated with organic material may preferentially dislodged during grinding or thin section preparation. Smedley and Kinniburgh (2002) discuss the idea of an intense zone of reduction surrounding buried plant or decaying plant material. Based on pe and pH diagrams, As_2O_3 is stable in more reducing conditions at pH's higher than 4. While

pH and pe are unknown at this site, the lack of oxidation rims surrounding the As_2O_3 grains suggest a reducing environment.

Further work is needed to characterize the distribution of As_2O_3 in other soils on the mine property however the presence, persistence and solubility of these grains makes them important to consider during remediation efforts. Measurements of soil pH and redox conditions in the soils surrounding the Giant mine are important to the understanding the environmental conditions on the site and predicting the future of As in the soils and surface waters. Estimates of how long these grains will persist in the environment are difficult without knowing the quantity of As_2O_3 that was added to the soils after 1959 when emission rates dropped significantly.

Chapter 5: Characterizing the Source of Arsenic in Soils from the Giant Mine, Northwest Territories and the North Brookfield Mine, Nova Scotia

5.1 Introduction

In natural systems, arsenic (As) can exist in a wide range of oxidation states in solid species: -3 in arsines, -1 in arsenopyrite, 0 for elemental As, 2+ in realgar (As_4S_4), +3 in arsenites (e.g. arsenolite and claudetite- As_2O_3), and +5 in arsenates (e.g. scorodite- $FeAsO_4 \bullet 2H_2O$), with the last two states being the most common (e.g., Harper and Haswell, 1988; Savage *et al*, 2000; Valberg *et al.*, 1997). As^{3+}, in the dissolved form $H_3ASO_3^0$, is considered to be more toxic, soluble and mobile in the environment than dissolved As^{5+} (DesChamps *et al.*, 2003; Goh and Lim, 2005). The toxicity of As^{3+} and As^{5+} bearing minerals is not well known and is in part dependent on the bioaccessibility, the percentage of As that is released from the ingested soil in the gastrointestinal tract and is available to be absorbed into the bloodstream (Bhumbla and Keefer, 1994; DesChamps *et al.*, 2003).

Arsenic can occur naturally in soils due to the presence of As-bearing minerals in parent rock, or be introduced through anthropogenic activities such as mining and the use of arsenical pesticides (Belluck *et al.*, 2003; Bhumbla and Keefer, 1994; Cullen and Reimer, 1989; Smedley and Kinniburgh, 2002; Yang and Donahoe, 2007). Arsenopyrite (FeAsS) is a common naturally occurring As-bearing mineral frequently associated with gold (Au) mineralization. Mining methods used in processing the Au ore, such as roasting and smelting, involve the production of As-rich vapours, which condense in the atmosphere to form As_2O_3 (More and Pawson, 1978). Soils surrounding mines can therefore have both a natural and anthropogenic component to the total As concentrations.

Arsenic shows evidence of varying degrees of attraction to metal oxides in soils either through weaker electrostatic bonds or stronger surface complexation, and can be found adsorbed to oxides of several different elements under varying environmental conditions (de Mello *et al.*, 2006; DesChamps *et al.*, 2003; Scott and Morgan, 1995; Smedley and Kinniburgh, 2002; Strumm and Morgan, 1996). These elements include iron (Fe), aluminum (Al), manganese (Mn) and calcium (Ca), as well as As sorbed to clays and organic matter (OM) (e.g., Bhumbla and Keefer, 1994; de Mello *et al.*, 2006; Sadiq, 1997; Smedley and Kinniburgh, 2002). Conditions such as changes in concentrations of species competing for adsorption sites (e.g., phosphate (P^{5+}) which has similar aqueous behaviour to dissolved As^{5+}), pH, Eh, adsorption or desorption of other metals, biological transformations and soil properties such as grain size and OM content, will determine the adsorption of As (Bhumbla and Keefer, 1994; Goh and Lim, 2005; Sadiq, 1997; Yan-Chu, 1994). The mobility, solubility and eventual toxicity of As-bearing soils is consequentially related to the solid form or the adsorbed As species on soils particle and is less dependant of the total concentration in the environment (Bhumbla and Keefer, 1994; DesChamps *et al.*, 2003).

Sequential selective extractions (SSE) are becoming a more common method of understanding elemental relationships within industrially contaminated soils (e.g., Datta and Sarkar, 2004; Van Herreweghe *et al.*, 2003; Yang and Donahoe, 2007). Some SSE have been specifically designed to target As in the following fractions; non-specifically adsorbed or exchangeable, organics, carbonates, amorphous and crystalline iron oxides, sulphides, silicates and residuals (Hall *et al.*, 1996a; Hall *et al.*, 1996b; Hall *et al.*, 1996c). This can be a very powerful tool especially when combined with direct methods of assessing As solid phases such as scanning electron microscopy (SEM), micro X-ray adsorption near edge

structure (μXANES) as well as micro and bulk X-ray diffraction (micro and conventional XRD) (Keon *et al.*, 2001).

The purpose of this study is to understand and compare the mineral form and speciation of As in soils surrounding the Giant mine in the Northwest Territories and the North Brookfield mine in Nova Scotia. The soils on both properties are enriched in As as a result of natural mineralization and have potentially been impacted by aerial emissions of particulate As_2O_3 from ore roasting. The historic nature of the North Brookfield mine (ceased operation in 1906) provides an example for roaster-impacted soils left relatively undisturbed in the environment for 100 years. At the Giant mine, operations ceased 10 years ago after onsite roasting for the better part of 50 years. The differences in age of these two locations allows for a better understanding of the effects of time on roasting and aerial dispersal of As-rich particles can be obtained.

5.2 Site Descriptions

5.2.1 Giant Mine, Northwest Territories

The Giant mine is located on the western side of Yellowknife Bay on the Great Slave Lake in the Northwest Territories. It is one of the oldest and most productive gold mines in Canadian history, producing more than 7 million ounces of gold from 1948 when the first gold brick was poured, to 1999 when ore processing operations ceased (Figure 5.1) (INAC, 2007). Mineralization at Giant occurs in a series of gold-quartz veins and silicified zones (Boyle, 1979) and is found as both refractory gold, incorporated within the mineral arsenopyrite, and free gold, with the later being less common and exploited early in the history of the mine (Hubbard *et al.*, 2006; Siddorn *et al.*, 2006; Tait, 1961). Based on thorough

studies by Coleman (1957) on the orebodies mined at the time, sulphides (pyrite, arsenopyrite, sphalerite, chalcopyrite, pyrrhotite and galena) and sulphosalts represent 5% to 15% by volume of the ore, with the average being typically less than 10% (Canam, 2006; Coleman, 1957).

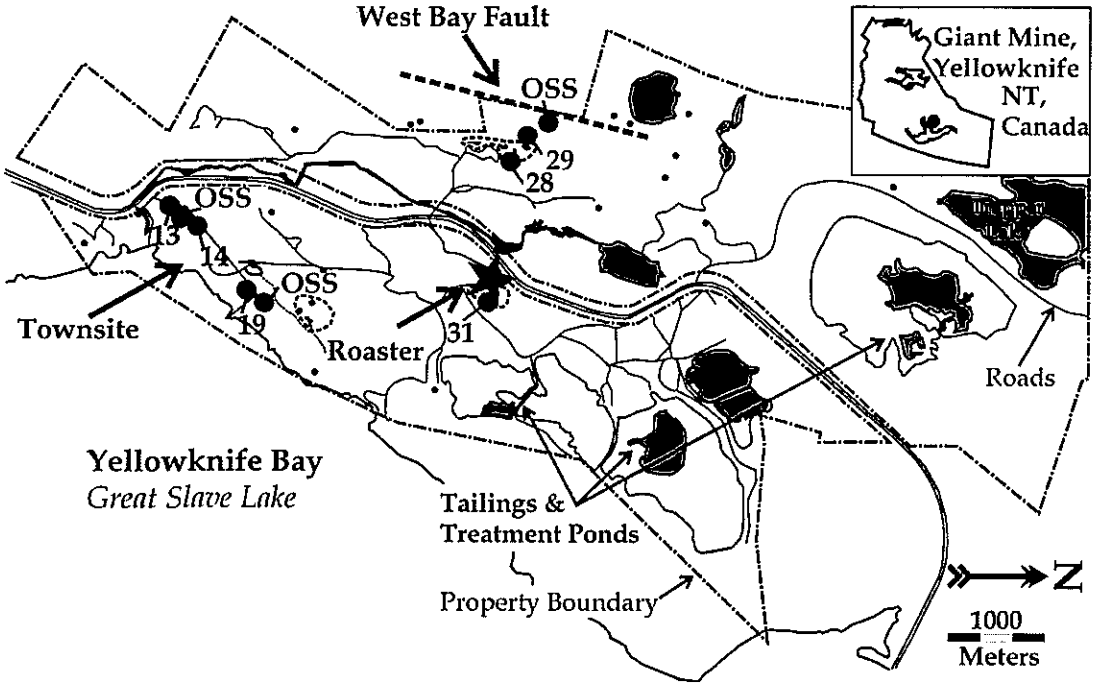

Figure 5.1: Location of soil samples from Giant Mine, Northwest Territories. Samples were taken from three localities (1) The Townsite- a small residential area located on the shores of Yellowknife Bay that housed miners and their families during the operation of the mine, (2) West Bay Fault- a marshy meadow locater beside outcrop that marks the fault, (3) Roaster- a marshy area beside the roaster. Black dots represent outcrop soil samples (OSS) and grey are soil core samples (SCS).

The refractory nature of the gold at Giant made it unavailable to conventional cyanide extraction. Roasting was added to ore processing as a method of breaking down the host sulphides into porous Fe-oxides more amenable to cyanidation and releasing As-rich particles and gases as well as $SO_{2(g)}$ (Davis *et al.*, 1996; More and Pawson, 1978). These

roaster-derived Fe-oxides (or RO) have been found to contain several weight percent As, up to 40% of which is in the As^{3+} oxidation state (Walker *et al.*, 2005). In the first two years of roasting, when no emission controls were in place, As_2O_3 emission rates from the stack were 7.2 tonnes per day (tpd), 720 times higher than emission rates at the mines' closure in 1999 (CPHA, 1977; EnviroCan, 2007; GNWT, 1993; INAC, 2007; More and Pawson, 1978; Tait, 1961). Treatment methods were refined in the mid to late 1950's, with gaseous and particulate As_2O_3 collected using an electrostatic precipitator (ESP) and baghouse. This resulted in significant decreases in As_2O_3 emissions by the 1960's. It has been estimated that during the lifetime of roasting, Giant has generated over 237,000 tonnes of As_2O_3, now stored underground in mined out stopes (INAC, 2007) and emitted approximately 20,000 tonnes (CPHA, 1977; EnviroCan, 2007; GNWT, 1993; INAC, 2007; More and Pawson, 1978; Tait, 1961) from the 45m high stack (Dillion, 1995).

Samples were taken from three sites at the Giant mine (Figure 5.1). The first, Site 19, is located in the Townsite (a small community that housed mine workers on the property) and consists of an OSS and SCS sample, with the latter from a forested area adjacent to the outcrop exposure. By the West Bay fault, a near vertical sinistral strike-slip fault that offsets the Giant mine from another gold deposit to the south, three samples were taken: Site 28 (from the open meadow), Site 29 (directly beside the near vertical fault) and an OSS from the outcrop adjacent to Site 29, are from western portion of the mine property. Finally, a SCS was taken from a marshy area close to the Giant roaster.

5.2.2 North Brookfield Mine, Nova Scotia

The North Brookfield mine is one of many publicly-accessible abandoned gold mines in Nova Scotia (Figure 5.2) and the tailings are known to be currently used for recreational

activities involving dirt bikes and all-terrain vehicles. In 1900's the Provincial Government recognized more than 60 gold districts, with the largest 20 producing over 1.2 million ounces of gold (Sangster and Smith, 2007). The North Brookfield mine produced gold from 1886-1906, with the North Brookfield Gold District mining a total of 43,000 troy ounces of gold from 105,000 tons of crushed rock (DPWM, 1927; Malcolm, 1929; Malcolm, 1976; Ryan and Smith, 1998; Sangster and Smith, 2007). Similar naming of the gold district and the changing name of the North Brookfield mine can be a point of confusion in historical documents so the term "North Brookfield" refers to the individual mine and not the district unless otherwise stated.

The majority of the gold in Nova Scotia is hosted in the Cambro-Ordovician Goldenville Formation of the Meguma Group consisting of metamorphosed sandstone, siltstone and shale (Sangster and Smith, 2007; Schenk, 1997). It was necessary to roast ore at North Brookfield because gold was extracted in a process called barrel chlorination. Sulphur and As were removed (as As_2O_3 and SO_2) by roasting the ore as both would become oxidized by the chemical additives used in the gold extraction process of chlorination (Anonymous, 1897; Forbes, 1904; Ritchie, 1901). Roasting at North Brookfield was different than Giant where the duration of the roast as well as temperature and oxygen levels were more controlled (Carter and Samis, 1952; Tait, 1961). After 1904, the Silman and Teed process of bromo-cyanidation was used at North Brookfield until closure in 1906 and it is believed that roasting continued until closure (Brown, 1908; Clennell, 1915; Nardin, 1910).

As_2O_3 emissions are difficult to estimate as no formal measurements were taken during the mines operation. Unlike the Giant mine (at least in the later years), North Brookfield would have had no emission controls in place to prevent the aerial dispersal of

SO_2 and As_2O_3 to the surrounding area as environmental controls were not common in the early 1900's. It is estimated, based on historical records, that 2200 tons of As_2O_3 could have been generated but it is impossible to know the proportion of this dust emitted from the stack since reports mention significant quantities of dust being collected and "disposed of" from the base of the stack (Forbes, 1904; Ritchie, 1901). As it is unlikely that material was transported any distance, it has been speculated that it may have been dumped, along with chlorination and bromo-cyanidation wastes, close to the roaster. The total As_2O_3 generated at North Brookfield is approximately 10% of the total As_2O_3 emitted by the roasting stack at the Giant mine.

Samples were taken from three areas at North Brookfield (Figure 5.2). Site 2 is the

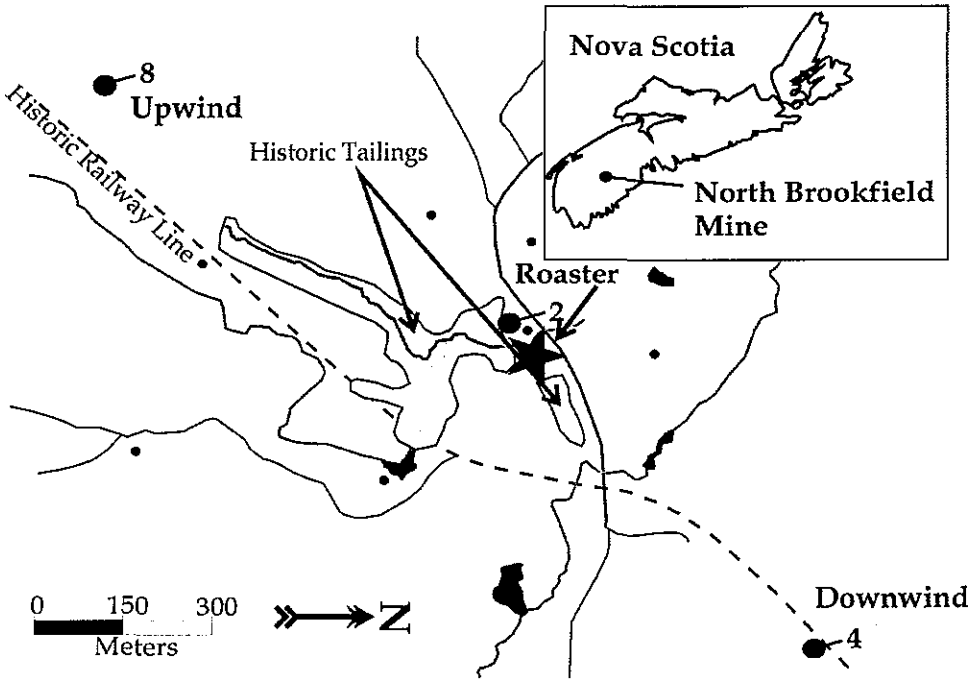

Figure 5.2: Location of soil samples from the North Brookfield mine, Nova Scotia. Samples were taken from three localities (1) The Roaster- near the historic footings of the roaster and chlorination house (2) Downwind- north east of the roaster and (3) Upwind- southwest of the roaster in a forested area. Black dots represent soil core samples (SCS).

closest to the footings of the roaster and was chosen based on unpublished work by M. Parsons of the Geological Survey of Canada-Atlantic (personal comm., 2007) that reported high As concentrations in this area. Site 4 was chosen to be downwind of the roaster based on a predominant northeasterly wind direction, whereas site 8 was taken upwind in an attempt to assess natural As concentrations in soils from the area.

5.3 Methods

5.3.1 Sample Collection and Preparation

Unconsolidated soil core samples (SCS) were taken in 2007 from the Giant and North Brookfield Mines using 1/16" walled, 2" outside diameter aluminum tubing. The tubes 50cm to 60 cm long and driven into the ground using a drivehead and a sledge hammer. As described in Chapter 4, outcrop soil samples (OSS) were taken from the Giant mine from small crevasses between outcrop exposures. These soils were of particular interest as roaster-derived particles would have accumulated on surface exposures and been transported by wind and water to soils in small rock hollows or crevasses. Outcrop exposures surrounding the North Brookfield mine are rare and soils from these areas not considered a significant source of As. Both SCS and OSS were placed in a cooler with ice packs immediately following collection, and then frozen in preparation for shipment and to preserve solid phases from reacting.

Core and hand samples were thawed, air dried, described and sub-sectioned based on soil horizons, prior to being sent to the Analytical Services Unit (ASU) at Queen's University for bulk *aqua-regia* soil digestion (unsieved) and elemental analysis as presented

in Appendix D (Giant) and E (North Brookfield). Elemental concentrations were used as a guideline to choose samples for thin section and sequential selective extraction analysis.

5.3.2 μXANES, μXRD and Bulk XRD Analysis

Prior to synchrotron analysis, petrography was required to identify and target potential As-bearing phases using reflected and transmitted light microscopy. Sub-samples were made into doubly-polished 'liftable' thin sections as described in Walker *et al.*, 2005. The thin sections were made to be liftable for synchrotron-based μXRD analysis which required the removal of the glass slide prior to analysis under the X-ray beam. Full descriptions of thin section preparation and the thin section lifting process are in Chapter 3 and Walker *et al.*, 2006. Once removed from the glass slide, sections were dried, re-oriented and pressed onto Kapton® tape.

Micro X-ray Absorption Near Edge Structure (μXANES), micro X-ray Diffraction (μXRD) and micro X-ray Radiation Fluorescence mapping (μXRF) were used to characterize the As within these samples (Manceau *et al.*, 2002; Walker *et al.*, 2005). XANES analyses can be used to examine small energy shifts in the position of the As absorption edge to determine the specific As oxidation state with a grain (Fendorf and Sparks, 1996; Manceau *et al.*, 2002). In Giant and North Brookfield soils it is critical to differentiate between As oxidation states as the presence of As^{3+} in the soils could be linked to anthropogenic As as roaster emissions contained As^{3+} bearing particulates.

Samples were analyzed at the X26A hard X-ray microprobe beamline at the National Synchrotron Light Source (NSLS) at the Brookhaven National Laboratory (BNL) on Long Island, NY. X26A uses a series of Rh coated 100mm Si mirrors, arranged in a Kirkpatrick-

Baez geometry, to focus the collimated monochromatic beam from 400μm (horizontal) by 400μm (vertical) to a spot size diameter of 10μm (horizontal) by 6μm (vertical) for work at the micron scale. A channel-cut Si(111) crystal is used to achieve a monochromatic beam for XANES experiments, with the Si(Li) detector being placed 90° to the incident beam.

Micro XANES experiments were performed on targeted grains by scanning across the As Kα absorption edge (11800 to 11970 eV) in fluorescence mode using a Si(Li) detector. Three As standards were routinely run to document shifts in the edge position with time so that corrections could be applied to unknown spectra (Walker *et al.*, 2005). The three standards chosen were: scorodite ($FeAsO_4 \cdot 2H_2O$) to represent the As^{5+} species, arsenic trioxide (As_2O_3) to represent the As^{3+} species and arsenopyrite (FeAsS) to represent the As^{-1} species (Table 5.1). Standards were prepared by S. Walker in 2002, and were remounted in

Table 5.1: Standards For μXANES Analyses

Standard	Formula	As-Oxidation State	Source	Position of Derivative*
Arsenopyrite	FeAsS	As^{-1}	Mina La Bufa, Mexico [M5579]	11867
Arsenolite	As_2O_3	As^{3+}	J.T. Baker Reagent	11870.2
Scorodite	$FeAsO_4 \cdot 2H_2O$	As^{5+}	Laurium, Greece [M6303]	11874.2

[MXXXX]: Miller Museum Reference, Queen's University Department of Geological Sciences and Geological Engineering.
* Edge positions are in eV at the first maximum in the derivative. Standards were set relative to the arsenopyrite edge at 11867.

2008 using the finely ground standard mixed with boron nitride to obtain a final concentration of 4% As by weight (see Walker *et al.*, 2005 for full standard preparation description). Raw μXANES spectra were calibrated and analyzed using the program

ATHENA™ to normalize unknown spectra based on shifts in standards. Linear combination fitting (LCF) was performed to determine the relative proportions of the three As oxidation states within the unknowns (Ravel and Newville, 2005).

Conventional XRD was performed on the two outcrop soil samples from the Giant mine, and the top sample from Site 2 at the North Brookfield mine using a Philips X'Pert MPD fitted with a Co tube. Micro-XRD is a similar technique to the conventional powder diffraction except it is performed at the micron scale using a focused synchrotron generated X-ray beam allowing for the identification of individual target grains. Two-dimensional μXRD patterns were collected for 60s in transmission mode, 17.347keV and λ=0.7147, using a Bruker SMART 1500 CCD diffractometer at X26A. The standard reference materials 647a (αAl_2O_3) and silver behenate ($AgC_{22}H_{43}O_2$) were used to calibrate the raw 2-D data in the software program Fit2D™ (Hammersley, 1998). Patterns were integrated and brought into the peak-match program X-Pert High Score Plus® to identify the unknown phases. Diffraction features ranged from sharp spots that represented micron to sub-micron crystallites to spotty or constant intensity Debye-Scherrer rings that represented randomly oriented nanometer sized crystallites (Manceau, 2002; Walker *et al.*, 2005).

5.3.3 Environmental Scanning Electron Microscopy (ESEM)

Several thin sections were examined using the Zeiss Evo 50 Environmental Scanning Electron Microscope (ESEM) at the Geological Survey of Canada in Ottawa to determine the source of As in the soils and to generate images of As-bearing grains at high magnification. The ESEM operated at a probe current of 500 pA, 50pA vacuum pressure, 9.0 mm working distance, 60s analysis time, and was equipped with an Oxford Inca Energy 450 X-ray μ-

analysis system for elemental and phase analysis. The ESEM was mainly used to identify and target As-oxide grains prior to synchrotron work as described in Chapter 4.

5.3.4 Sequential Selective Extraction (SSE) Analysis

Sequential selective extractions (SSE) were performed at ALS Chemex on 10 sub-samples from the Giant Mine and seven sub-samples from the North Brookfield Mine that were sieved to <180μm (Table 5.2). Sub-samples were chosen based soil type, chemistry, and

Table 5.2: Soil samples chosen for SSE.
Negative values indicate depth within the soil.

Depth (cm) ↓	Giant Mine- Yellowknife, NT			
	Site 19	**Site 28**	**Site 29**	**Site 31**
	OSS	-	OSS	-
	-5.0	-2.5	-8.0	-2.0
	-26.0	-30.0	-33.0	-32.0
Depth (cm) ↓	**North Brookfield Mine- NS**			
	Site 2	**Site 4**	**Site 8**	
	< 1.0	-4.5	-14.5	
	-15	-29	-34.5	
	-47	-	-	

mineralogy. To be consistent with other leaches used on soils from both Giant and North Brookfield tailings, a new eight step method developed by G.E. Hall (modified from Hall *et al.*, (1996a, 1996b, 1996c)) was used. A variation of this method was compared to other extractions in Mihaljevič *et al.* (2003), where the Hall method was found to be a better fit between the observed and expected As extractions from spiked samples.

The most significant change in the Hall method was the addition of a step to extract the mineral scorodite ($FeAsO_4 \cdot 2H_2O$) between the crystalline Fe-oxide and the sulphide extraction steps (Table 5.3). In the extraction, 3g of sample was subjected to increasingly

stronger chemical reagents designed to release As bound in the soil matrix in one of eight forms. For each extraction supernatant fluid was decanted and analyzed using ICP-MS for a suite of 63 elements including: arsenic (As), calcium (Ca), iron (Fe), magnesium (Mg), manganese (Mn), phosphorus (P), antimony (Sb) and titanium (Ti). Included in the SSE tests was one duplicate sample, one standard (NIST-2711) and a series of test blanks.

Table 5.3: SSE Steps

	Selective Extraction Step	Reagents
1	Adsorbed exchangeable	1M NH_4OAc
2	Organics	0.1M $Na_4P_2O_7$
3	Carbonates	1M NH_4OAc
4	Amorphous Iron Oxides	0.25M NH_2OH
5	Crystalline Iron Oxides	1M NH_2OH
6	Scorodite	4M HCl
7	Sulphides	*Aqua Regia*
8	Residual	HF-$HClO_4$-HNO_3

Comparison of the NIST-2711 Montana standard to the same standard run using the extraction scheme the GSC-Ottawa (Parsons, personal comm.2007) revealed that, with the exception of As, average relative standard deviations are 10% or less. Arsenic average relative standard deviation was higher due to the organic step which was not used in the GSC extraction. The average relative standard deviation for the duplicate sample was below 10% for all elements of interest. A full set of data and standard deviations are included in Appendix G.

5.4 Results and Discussion

5.4.1 Soil Descriptions and Selected Bulk XRD

Soils in the Yellowknife area consist of organic deposits formed by the accumulation and decay of vegetative matter overlying glaciolacustine tills formed during the Late Wisconsin glaciation (Kerr, 2006). There has been little to no soil development from the tills on the mine property beyond the presence of an organic rich layer at the surface as a result of low precipitation rates, cool temperatures and an average of only four frost free months within a year (EnviroCan, 2008; Pienizt, 1997). The tills are the most pervasive surficial material in the area consisting of poorly to moderately sorted coarse to fine sand, silt and clay with variable amounts of pebbles and cobbles (Kerr, 2006).

All OSS taken were organic-rich and also contain the minerals quartz, clinochlore, rutile (in the Townsite) and quartz, clinochlore, montmorillonite-chlorite, albite and microcline (by the West Bay Fault) (Appendix I). The presence of rutile in the Townsite and feldspar by the West Bay Fault are consistent with the outcrop over which they formed, basalt and granite respectively (Hubbard *et al.*, 2006). Arsenolite was the only identified As-bearing phase within both of these samples, confirmed by the presence of As-oxides as presented in Chapter 4. Walker (2006) also observed the presence of arsenolite in the conventional XRD analysis of ESP dust, showing the source of arsenolite was from the roasting process. Despite the fact that arsenolite is the identified phase, mineral forms naturally by the oxidation of arsenopyrite, realgar and native As in reducing conditions (Nordstrom and Archer, 2003) and the identified arsenolite from Giant is formed through anthropogenic activities, and is therefore termed As_2O_3 to distinguish its origin. The lack of other As-bearing minerals such as arsenopyrite, pyrite and roaster derived Fe-oxides, even

though identified in thin section, reflects their relatively low overall abundance within these soil samples.

North Brookfield soils, unlike Giant, showed well-developed A and B horizons overtop of the C horizon glacial tills that cover the area. At the location upwind from the roaster a thin organic horizon as well as a white leached albic (Ae) horizon was observed, but not at the other locations. Results from conventional X-ray diffraction at North Brookfield Site 2 show the presence of quartz, clinochlore, muscovite, albite and titanite (Appendix I). No As-bearing phases were identified using this technique, even though arsenopyrite was observed in thin section. Low total As concentrations made examination for As-bearing phases in other soil samples from North Brookfield impractical using conventional XRD, μXRD, μXANES and ESEM.

5.4.2 μXANES, μXRD and ESEM Analyses of As-rich particles

A combination of ESEM and synchrotron analyses were performed on the ten sub-sample locations from the Giant mine and the Site 2 surface soil sub-sample from North Brookfield (Table 5.2).

5.4.2.1 Giant Mine

In OSS samples from the Townsite and the Fault, three As-bearing phases are identified. In order of abundance, these particles are As_2O_3 (predominately containing As but some with trace Sb, Figure 5.3), RO (Fe_2O_3) consisting predominately of maghemite (Figure 5.4) and arsenopyrite. As_2O_3 grains contain As in the 3+ oxidation state only, while roaster oxides have a mixture of As^{5+} and As^{3+} oxidation states in the rims and As^{-1} in the core if relic arsenopyrite remains. RO contain either a porous or concentric texture also

shown by Walker *et al.* (2005) in tailings samples. Analyses of several RO at these two sites shows between 20% and 30% of the As is in the 3+ oxidation state (Appendix J).

Surface soil samples (0cm to 10cm) from the Fault area and beside the roaster contain the same three As-bearing phases, As_2O_3, RO and arsenopyrite (only beside the roaster) as

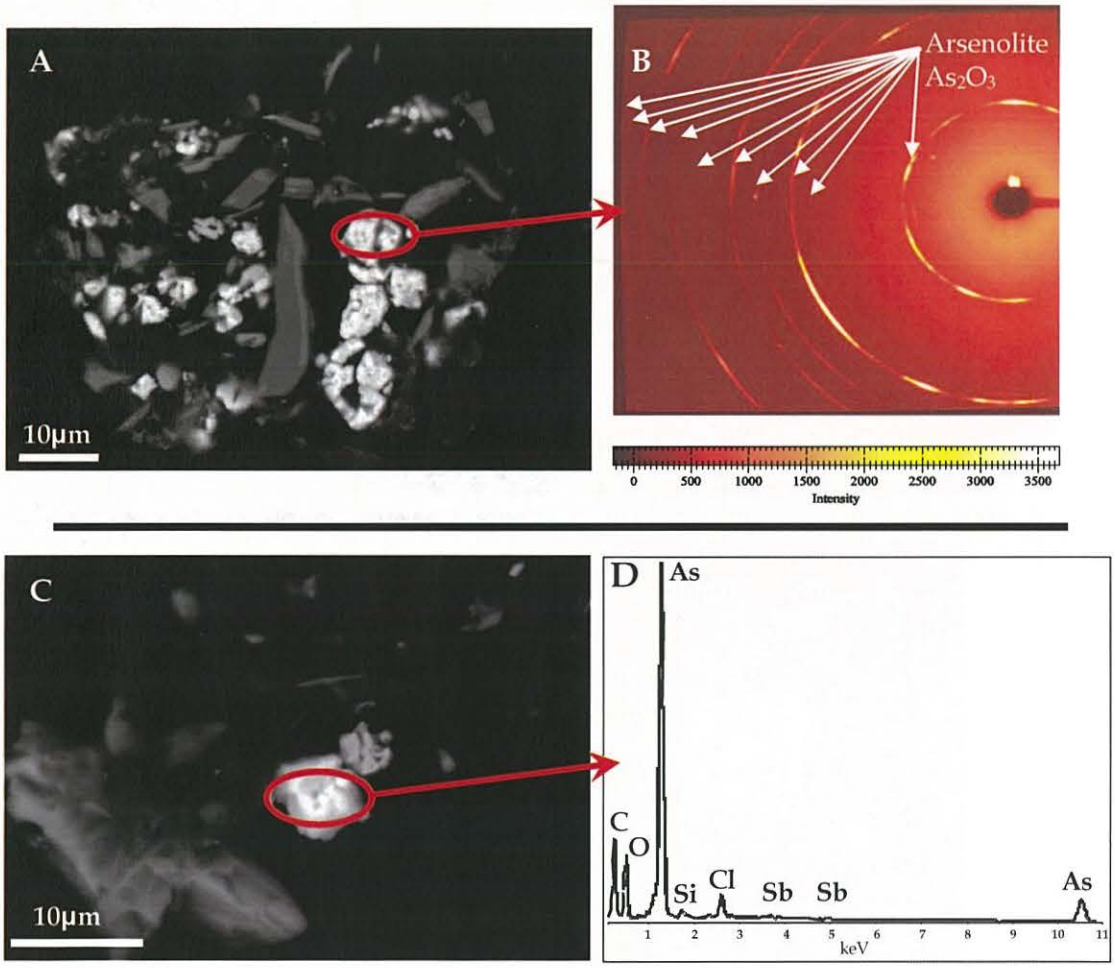

Figure 5.3: Identification of As_2O_3 grains from soils at the Giant mine. **A** is an backscatter electron (BSE) image of several smaller As only grains and B is the corresponding µXRD 2-dimensional pattern. **C** is a BSE image of a small Sb-bearing As-oxide based on **D**, a qualitative EDS spectra from the ESEM.

well as As associated with muscovite and clinochlore. The abundance of arsenopyrite beside the roaster (Site 31) was expected as the transportation of ore around this area would have released sulphide-rich fugitive dusts accumulating in the soil.

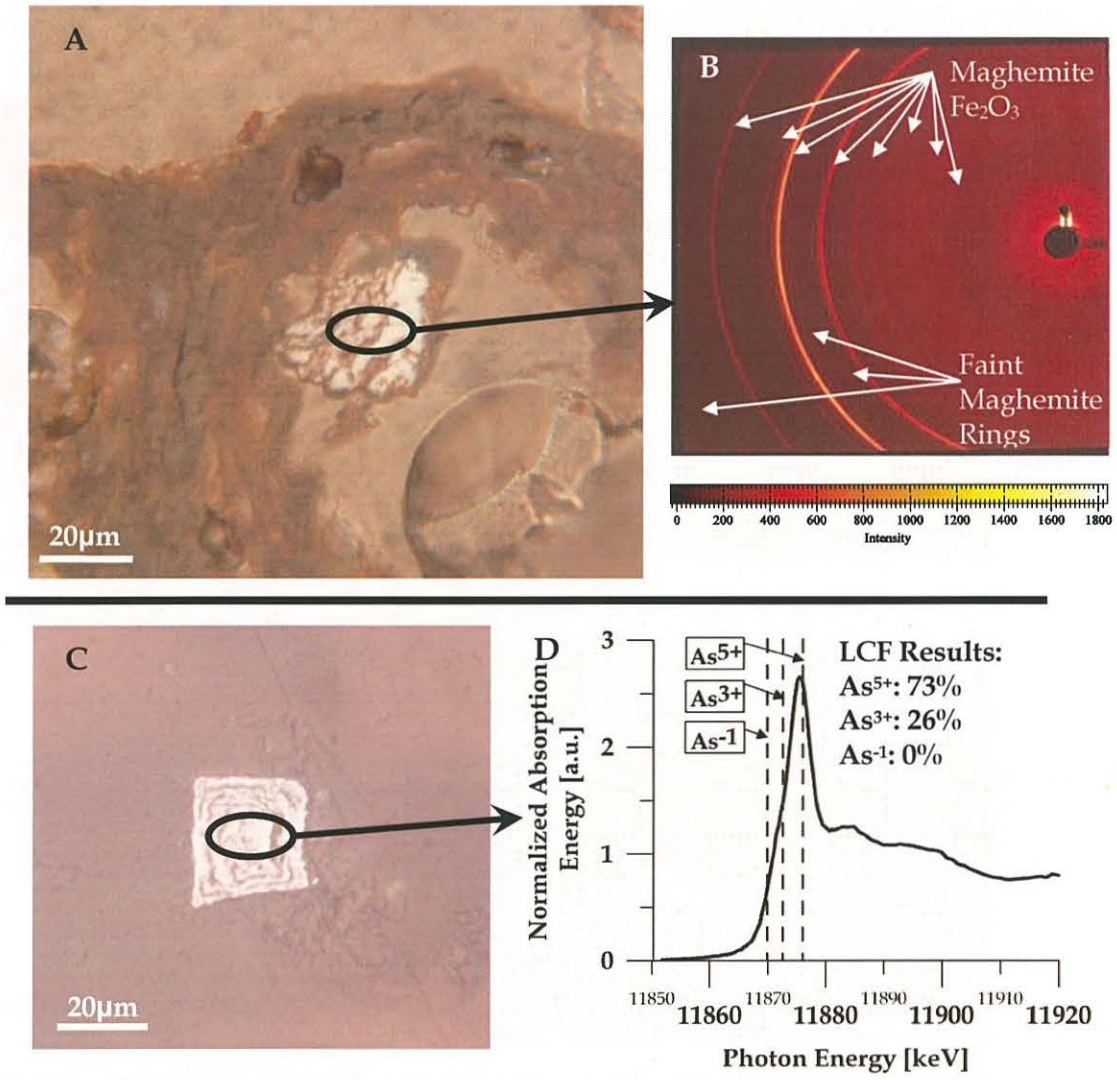

Figure 5.4: Identification of roaster derived Fe-oxides from soils at the Giant mine. A and **C** are reflected and transmitted light photographs of As-bearing roaster oxides. B is the µXRD 2-dimensional pattern (of **A**) and **D** is an example of µXANES and LCF results (from **C**) dashed lines represent the location of the white line peak for all three As oxidation states.

Surface soil samples from the Fault area were studied for the presence of As_2O_3 only, which was confirmed through ESEM and synchrotron analyses. Organic-rich soils from deeper sites near the Fault, despite being less than 25m apart, have different As signatures. Site 28 soils show no As-bearing phases, although the total As concentration of over 400 ppm (Table 5.4) is evidence that As is present. This can be explained by As being sorbed to the surface of Fe-Mn minerals and organic matter and therefore not detectable by ESEM, or As-bearing grains <5um in size and therefore missed by ESEM analysis. Deeper soils from Site 29, which had lower total As concentrations (Table 5.4), contained As_2O_3 grains. No As-bearing phases were identified in the two till soil samples (Site 19: -32 cm and Site 31: -38cm), but the presence of Fe-oxides and Fe-Ti oxides suggests that surface complexation reactions may be binding the As (Smedley and Kinniburgh, 2002; Strumm and Morgan, 1996).

5.4.2.2 North Brookfield Mine

Mineralogical examination of the -1cm soil sample from Site 2 at North Brookfield reveals that As is present in two As-bearing phases, arsenopyrite (plus associated weathering rims) and as a minor component of RO. Arsenic was also found associated with rims on Ti-oxides and Fe-oxyhydroxides, as well as being related to clay minerals. It should be noted that only one grain of each of the above three phases were identified and thorough ESEM examination revealed no As_2O_3 in these soils.

Roaster oxides at North Brookfield all have a porous texture with no relic sulphide cores (Figure 5.5). Repeated μXRD and μXANES on several grains shows RO are composed of only hematite and contain As^{5+} only. Micro XANES spectra on the rim and core of arsenopyrite grains (Figure 5.6) confirm that As is present in the 5+ and -1 states respectively. Micro XRD analysis of the rim shows a wide diffuse ring and combined with

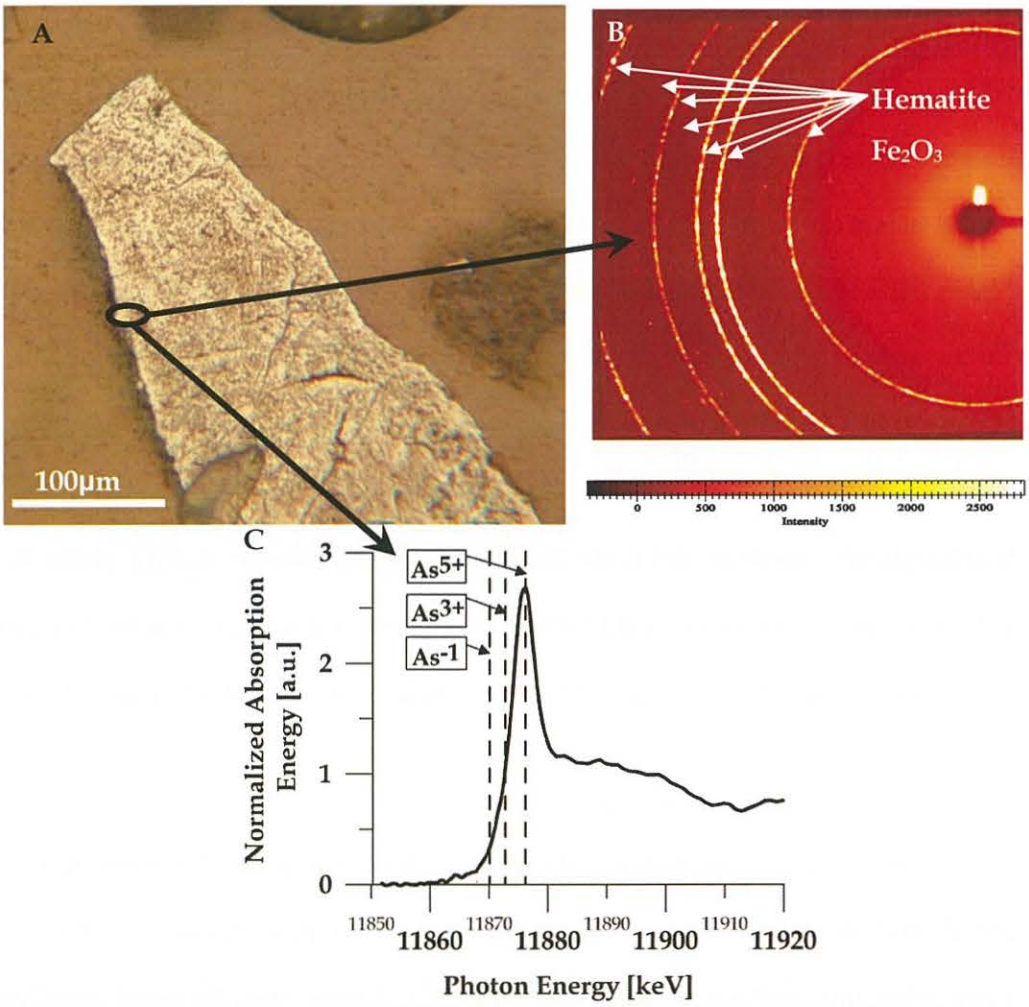

Figure 5.5: Identification of roaster derived Fe-oxide from surface soils at the North Brookfield mine. A is a reflected and transmitted light photographs of an As-bearing RO. **B** and **C** are the corresponding 2-dimensional µXRD pattern and µXANES results respectively. Dashed lines in **C** represent the location of the white line peak for all three As oxidation states

Table 5.4: Normalized arsenic proportions for all eight SSE extraction steps in Giant and North Brookfield soils.

Giant	Depth [cm]	Sieved Sample (<180µm) [% of Total As]									Unsieved Sample	
		Adsorbed/ exchangable	Organics	Carbonates	Amorphous Fe-Oxides	Crystalline Fe-Oxides	Scorodite	Sulphides	Residuals and Silicates	Total As <180µm	Total Bulk As [ppm]	OC [%]
Site 19	OSS	2.8	11.6	11.1	13.1	56.1	3.6	1.1	0.5	**2137.3**	1589	30.2
	-5.1	5.8	34.9	17.3	23.8	15.0	2.5	0.3	0.4	**281.3**	322	5.0
	-32.6	2.1	31.4	15.0	23.9	22.4	4.7	0.1	0.3	**107.8**	83	3.5
Site 28	-2.4	4.7	6.5	3.4	5.3	75.8	3.1	0.9	0.2	**861.8**	321	31.5
	-30.0	7.1	70.7	9.8	9.0	2.9	0.4	0.0	0.1	**655.3**	484	13.7
Site 29	OSS	2.4	26.3	10.0	11.3	45.8	3.5	0.5	0.2	**4541.1**	3280	23.5
	-8.1	1.7	31.7	17.0	16.6	31.2	1.4	0.2	0.1	**2780**	1495	19.7
	-32.6	8.3	12.1	4.7	7.1	62.9	4.3	0.6	0.1	**3276.1**	374	41.1
Site 31	-1.7	8.8	10.6	7.2	5.7	60.1	5.0	2.3	0.3	**1664.7**	1423	29.4
	-37.6	4.3	58.1	17.6	12.5	6.2	1.0	0.1	0.2	**286.4**	158	3.6
North Brookfield												
Site 2	-0.6	0.8	29.1	8.7	29.3	22.5	6.2	3.2	0.2	**3954.5**	4303	3.2
	-15.2	0.3	34.5	5.9	20.5	26.4	9.7	2.1	0.4	**686.5**	418	1.4
	-47.1	0.2	36.9	0.8	8.6	32.0	18.9	1.0	1.6	**61.5**	36	0.5
Site 4	-4.4	2.9	21.5	14.4	17.5	29.9	6.3	2.9	4.7	**62.3**	46	11.1
	-24.4	0.4	36.7	1.1	7.5	22.4	24.2	2.5	5.3	**28.1**	27	1.5
Site 8	-14.3	1.2	36.0	1.4	7.0	18.3	31.4	1.6	3.2	**50.3**	36	5.5
	-39.9	0.2	29.8	1.6	7.7	45.2	12.8	0.8	2.0	**50.7**	36	0.1

μXRF mapping shows the presence of As, Fe and Ca suggesting this may be an amorphous Fe-arsenate formed by the weathering of the associated arsenopyrite grain. The absence of hematite in the rim of the arsenopyrite grains indicates that these have not been roasted and represents the natural weathering of this mineral.

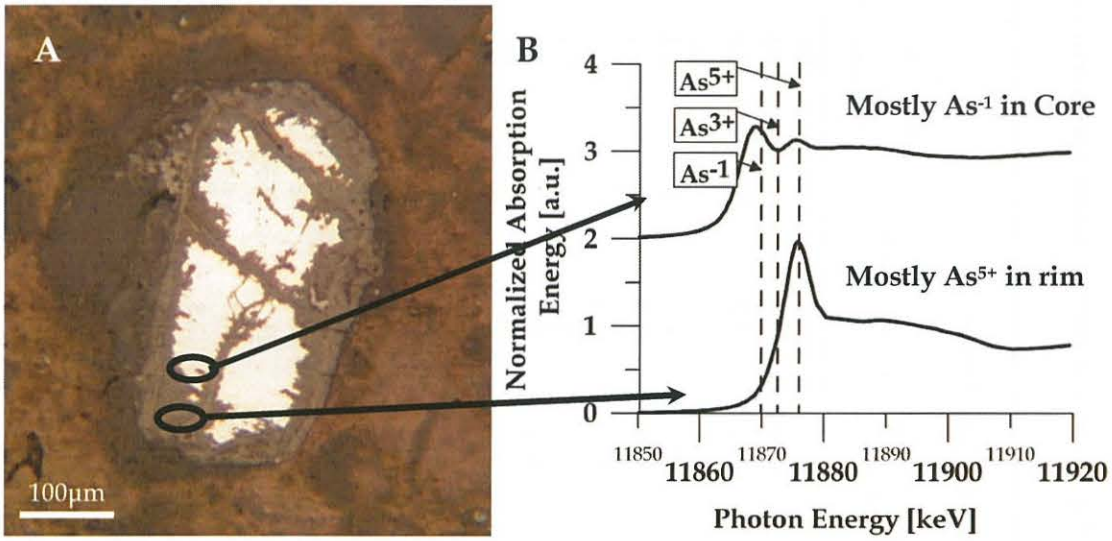

Figure 5.6: Identification of natural arsenopyrite grain and associated weathering rim from surface soils at the North Brookfield mine. **A** is a reflected and transmitted light photographs of the arsenopyrite grain and **B** is the corresponding μXANES results from the core and rim of the grain, dashed lines represent the location of the white line peak for all three As oxidation states.

Arsenic was found in the 3+ oxidation state associated with a chlorite and muscovite mass (Figure 5.7A, B) and in lesser quantities within the core of a goethite grain (Figure 5.7 C,D), with the former containing between 60% and 70% As^{3+}. LCF on the As-rich rim on both the goethite and rutile (TiO_2) grains showed As predominately in the 5+ oxidation state.

5.4.3 Mineralogical Interpretation of Sequential Selective Extractions

5.4.3.1 Giant Mine

Arsenic concentrations for the eight leach steps at the Giant mine can be seen in Figure 5.8. Total As concentrations differ from Chapter 4 where an *aqua regia* digestion was performed on the unsieved soils as this multistep extraction includes the residual (HF acid)

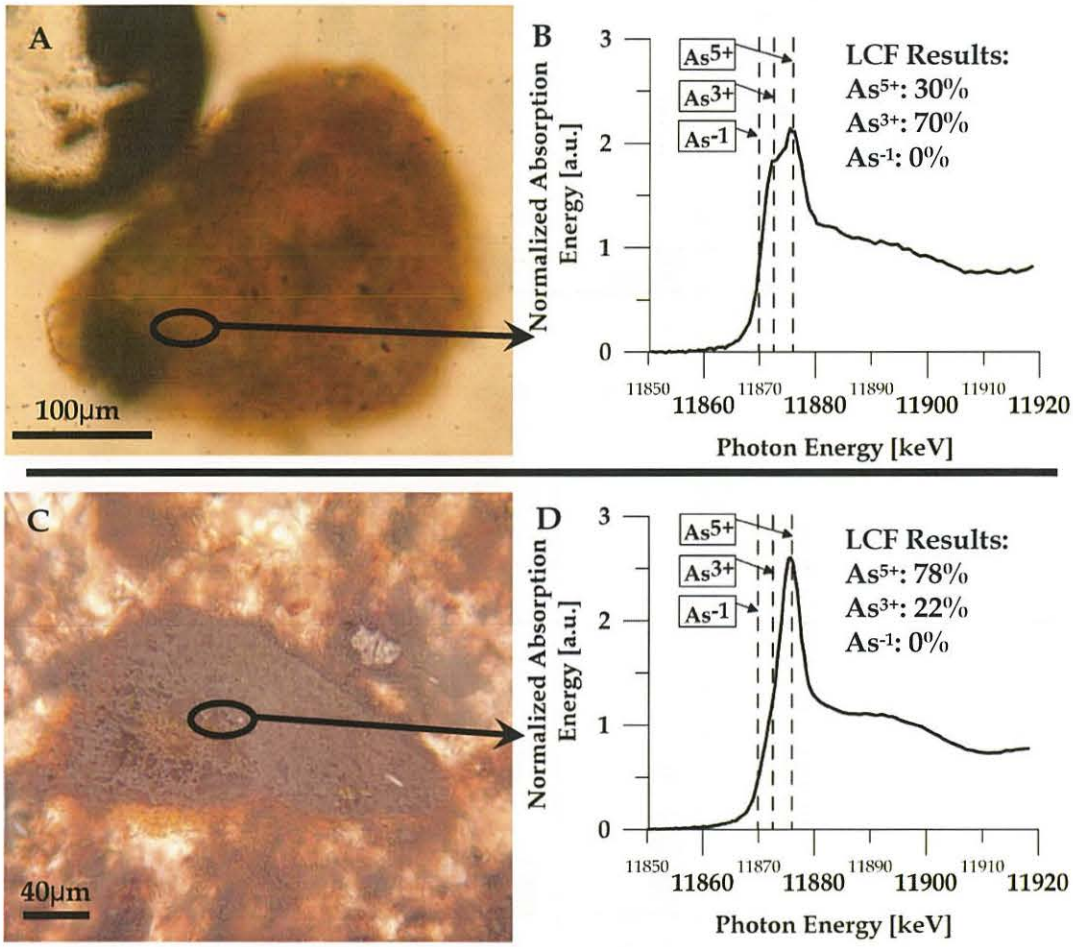

Figure 5.7: Identification of two As^{3+} bearing phases from surface soils at the North Brookfield mine. A is a reflected and transmitted light photograph of a chlorite and muscovite mass (determined by µXRD) and **B** is the corresponding µXANES results showing the presence of approximately 70% As^{3+}. Image **C** is of a goethite grain (determined by µXRD) in the same sample with corresponding µXANES results, **D**, indicating 22% As^{3+}. Dashed lines in **B** and **D** represent the location of the white line peak for all three As oxidation states.

step and that sieving of the soil samples was done for SSE (Table 5.4). Table 5.4 also contains the relative proportions of As for each extraction step. From Figure 5.8A, three of four samples locations show high As concentrations at the surface, including OSS, and decreasing

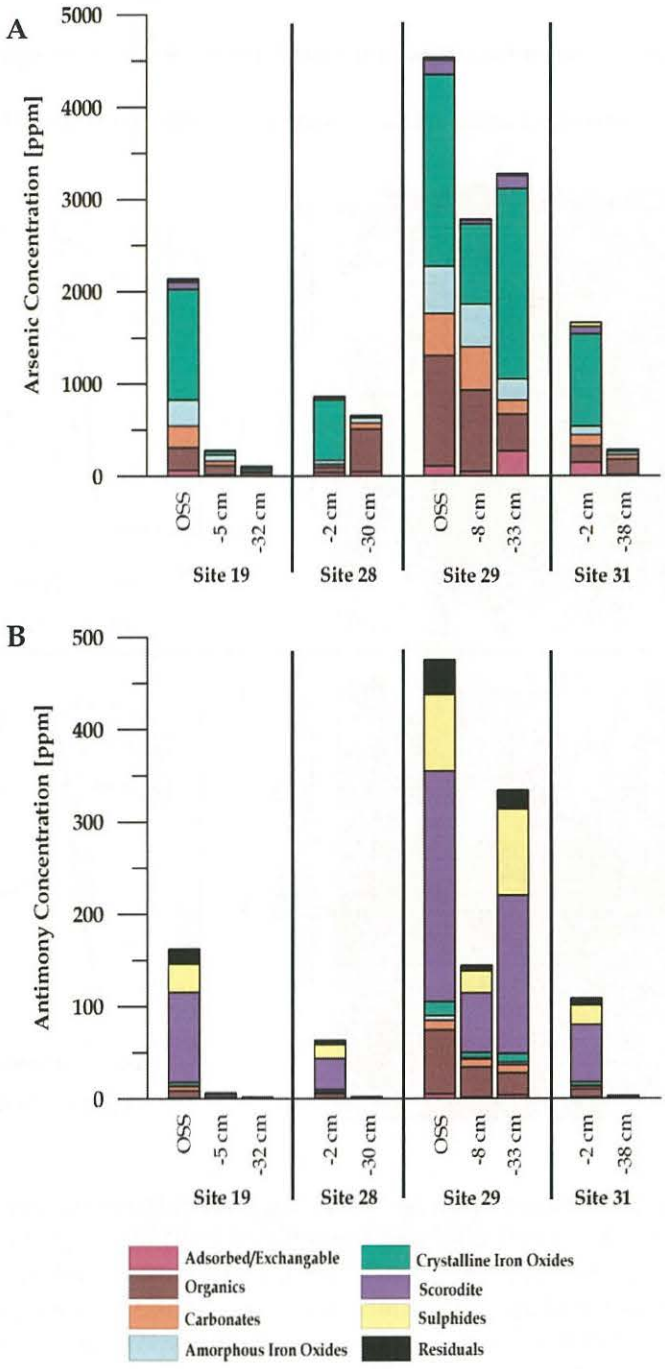

Figure 5.8: Sequential selective extraction results for arsenic (A) and antimony (B) at the Giant mine. Samples are organized by location and depth in the soil profile.

concentrations with depth. Site 29 is an exception with may be explained by the wash down of As-rich material from the outcrop exposure adjacent to this site.

Of the 10 sub-samples analyzed using SSE, the six with the highest As and Sb concentrations show a similar pattern across the eight extraction steps (Figure 5.8). These are Site 19: OSS, Site 28: -2cm, Site 29: OSS, -8cm, -33cm and Site 31: -2cm. Sb is important to consider at the Giant mine as it is present in the ore in the form of sulphosalts (Canam, 2006; Coleman, 1957) and during roasting can become incorporated within the As_2O_3 either in low concentrations or as $(Sb,As)_2O_3$ (Riveros *et al.*, 2000). The most noticeable difference between these six samples and the remaining four is the presence of between 20% and 75% of the total As within the crystalline Fe-oxide leach (Table 5.4). Sb is another indicator that these six soils are different as total Sb in the remaining four samples is considerably lower (Figure 5.8B). Work described above shows that Sb is found in As_2O_3 and it is known that this type of particle is present in all of these six soils.

In Riveros's (2000) work using acid leaches, the 3.0 M HCl leached the most Sb from the As_2O_3 grains in ESP dust. Because the scorodite leach uses 4.0 M HCl, it follows that the most Sb in this step may be from the dissolution of Sb-rich As_2O_3. Arsenic from the Sb-poor and Sb-rich As_2O_3 grains likely dissolves (possibly an incongruent dissolution) in the solution designed to dissolve crystalline Fe-oxides. In the stronger scorodite leach, the remaining more stable Sb-rich As_2O_3 likely dissolves, as shown by the highest Sb in this fraction. Molar ratios of As to Sb in this leach are slightly higher than 1:1 (except site 31 which is 2:1), whereas in other leaches As clearly dominates. This suggests that there may be another source of As extracted in the scorodite leach.

The other anthropogenic form of As observed directly within the soils is As-bearing RO. Knowing that As_2O_3 is present in the six As-rich soils and that RO have also been

identified, examination of Fe extractions should help to confirm the steps where both RO and As_2O_3 dissolve. Unfortunately, Fe is difficult to interpret as there is the potential for more sources and they are well dispersed across the eight extraction steps (Figure 5.9). The higher proportion of Fe in the scorodite extraction step of the six high As samples could be described by the dissolution of RO as As within the leach is not fully explained by the dissolution of Sb-rich As_2O_3. Because As represents up to 7 wt. % of RO (Walker *et al.*, 2005), the dissolution of RO in the scorodite leach could result in the additional As observed in this extraction.

The higher As to Sb molar ratio in surface soils at Site 31 is consistent with the presence of more RO observed in thin section here compared to other locations. This site also contains the highest proportion of As extracted in the sulphide step, consistent with arsenopyrite recognized in thin section, whereas low As in the sulphide extractions from the remaining samples are confirmed by the observation of little arsenopyrite in these soils. In general, Fe extractions show a higher proportion of this element in the sulphide extraction, and low As to Fe molar ratios demonstrates the source of sulphide is not arsenopyrite, but potentially pyrite. Sb is also detected within the sulphide fraction (17% to 27%) and may represent the presence of sulphosalts which are observed within the ore (Canam, 2006; Coleman, 1957) and as one grain in an OSS.

In the four soil samples containing lower total As concentrations (Figure 5.8A) and less than 10 ppm Sb, the organic fraction represents a significant proportion (30% to 70%) of As even though the organic carbon content is lower than the organic-rich samples higher in

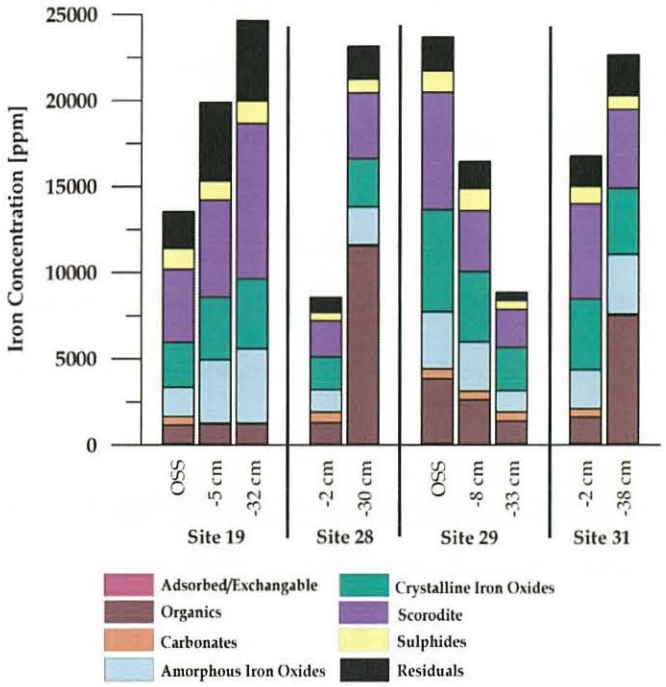

Figure 5.9: Sequential selective extraction results iron at the Giant mine. Samples are organized by location and depth in the soil profile.

the soil profile (Table 5.4). If infiltrating rainwater is dissolving As-bearing particles from the soils above, then it follows that this As could be sequestered by organic material at depth within the soil profile. Organic leaches release As that is strongly adsorbed, bound to or scavenged by humic and fulvic acids (Hall *et al.*, 1995). Even though the pyrophosphate step was not originally designed for As, it has been used by others to liberate strongly adsorbed As while not attacking sulphides as seen with other organic leaches (Mihaljevič, 2003).

There is no clear trend in As or Sb in the adsorbed exchangeable fraction, with both representing <10% of the total of each element within all 10 samples. The highest adsorbed exchangeable As within the soils is from Site 29 at 33cm depth where this fraction contains 270 ppm As, higher than total As in most of the low As soils. The source of this As has not

been explained, but could be the result of the adsorption of As from dissolved As_2O_3 identified in the soils closer to the surface. Between 15% and 85% of the total As within the samples is contained within the first three extractions (adsorbed exchangeable, organics and carbonates) which are potentially the most important from a human health perspective.

5.4.3.2 North Brookfield Mine

Total As concentrations for the eight leach steps at the North Brookfield mine can be seen in Figure 5.10. The total As at North Brookfield is variable with depth in the soil and between sample locations. At the surface, Site 2 has extremely high As compared to the other samples (3900 ppm) with more As extracted in organic fraction then in the remaining samples combined. Downwind (Site 4) As is higher at the surface and decreases with depth into the tills while upwind (Site 8) shows no variation with depth.

There are three major observations that can be made from the North Brookfield SSE data. First, based on total As concentrations (Figure 5.10A), the three sub-samples with the highest total As (Site 2: -1cm, -15cm and Site 4:-5cm) show a significant portion of As, Fe (Figure 5.10B) and Ca (Figure 5.11) as well as Mn and Mg in the amorphous Fe-oxide extraction. Elevated Mn, Mg and some of the Ca and Fe can be explained by the dissolution of minerals in the dolomite ($CaMg(CO_2)_2$) ankerite ($Ca(Fe, Mg, Mn)(CO_3)_2$) series which are known to be present (P. Smith per- comm., 2007) even though they were not identified by conventional XRD. Remaining As, Fe and Ca is most likely explained by the presence of amorphous Fe-arsenates that contain Ca in the weathering rims of arsenopyrite (Corriveau, 2006). Another possible explanation is the potential presence of yukonite

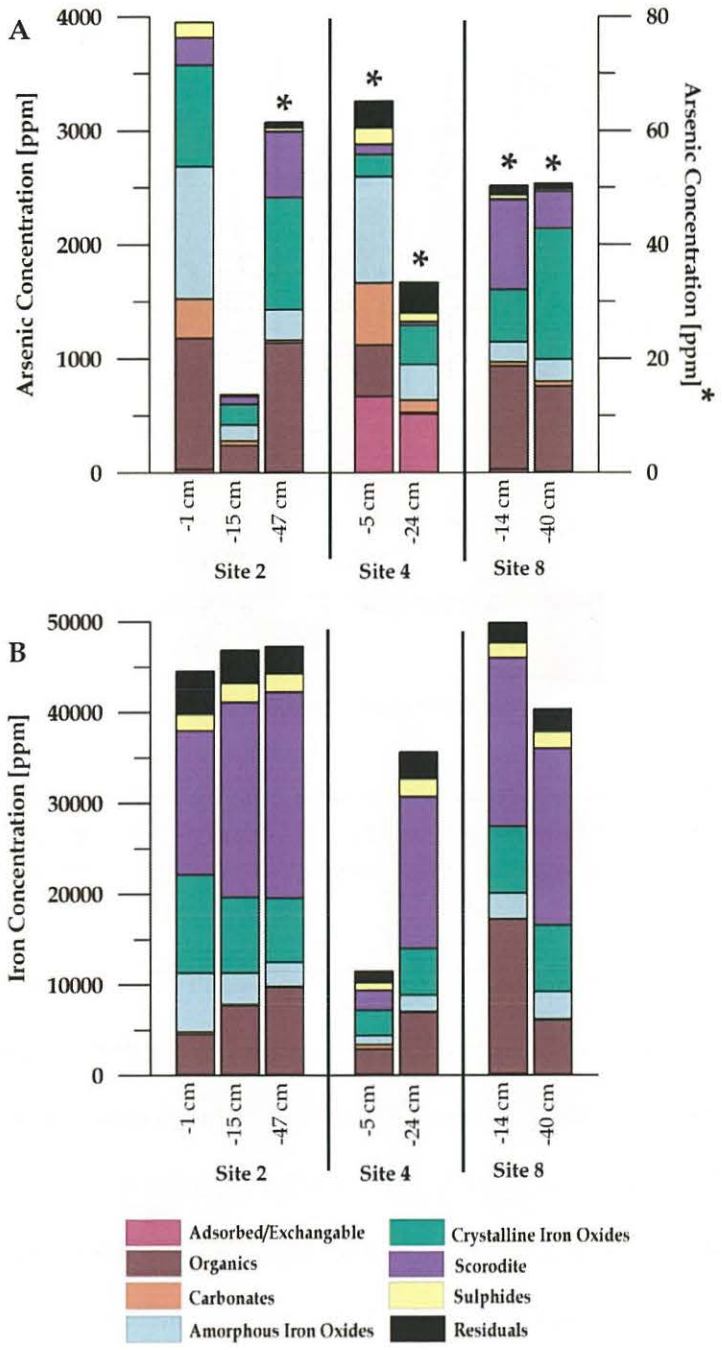

Figure 5.10: Sequential selective extraction results for arsenic (A) and iron (B) at the North Brookfield mine. Samples with asterisks (*) indicate the right hand y-axis was used due to significant differences in scale. Samples are organized by location and depth in the soil profile.

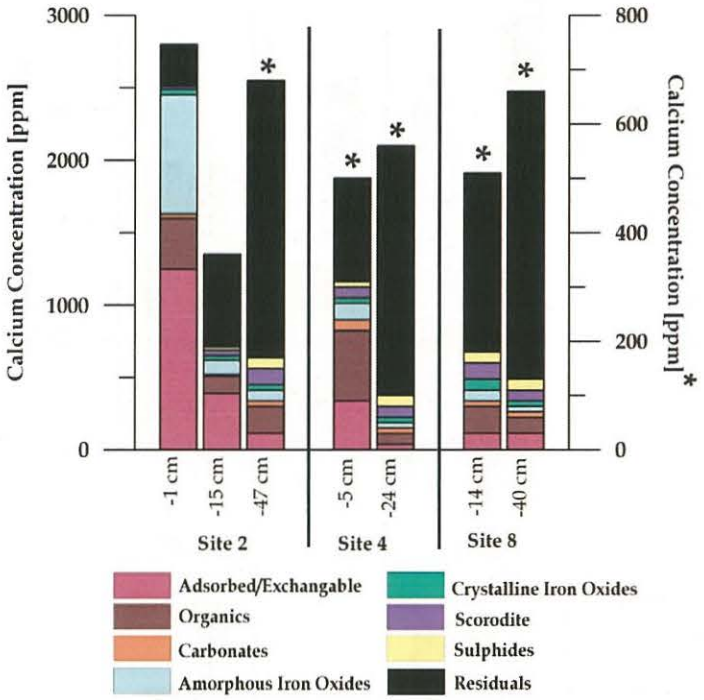

Figure 5.11: Sequential selective extraction results for calcium at the North Brookfield mine. Samples with asterisks indicate the right hand y-axis was used due to significant differences in scale. Samples are organized by location and depth in the soil profile.

($Ca_3Fe_7^{3+}(AsO_4)_6(OH)_9 \bullet 18H_2O$) that has been observed in other historic mining districts in Nova Scotia on arsenopyrite and pyrite rims (Jamieson *et al.*, 2008). Even though no yukonite was observed using μXRD analyses, very few sulphide rims were targeted. Molar ratios of As to Ca and As to Fe do not provide further insight into the As-bearing mineral form as Ca and Fe both dominate As in this step. Further work will be needed to fully identify the source of these elements in the amorphous step as this could represent a combination of amorphous Fe-arsenates and yukonite or another As-bearing phase altogether.

At Giant, the distinctly higher As and Sb in the crystalline Fe-oxide and scorodite leaches of impacted soils is attributed to the presence of As_2O_3 and As-bearing RO observed in thin section. The lack of As_2O_3 in North Brookfield soils and the low As concentrations

observed in RO means it is not possible to confirm the interpretations of mineralogical hosts. It is known that As_2O_3 was generated at North Brookfield, based on historical records, and was most likely present in the soils surrounding the mine during the time of roasting. The absence of this As-bearing phase suggests that over the more than 100 years since the mines closure, As_2O_3 has either oxidized of dissolved over time.

Using the normalized proportions from the Giant and North Brookfield mines there appears to be no difference in the proportion of As in the crystalline Fe-oxide or scorodite extractions, despite the variable total As concentrations. As with Giant, scorodite was not observed in North Brookfield soils by either bulk or μXRD As and Fe, Mn, Mg and Ti are also extracted in this step (see Appendix H for Mn and Ti extraction plots). The presence of the other elements in the scorodite leach at all samples sites suggests that As may be the attributed to a combination of the dissolution of RO and either individual or mixtures of Fe, Mg, Mn, and Ti oxides that are resistant to the crystalline Fe-oxide leach.

Finally, the proportion of As associated with the organic fraction is relatively constant across the sample site even with changing organic carbon content. In the first three extractions between 35% and 40% of the total As is extracted. Even though the proportions of As in each leach step are very similar between the seven North Brookfield samples, the total As in the first three fractions are between 1500 ppm at Site 2 (-1 cm) and 15 ppm at Site 4 (-24 cm), two orders of magnitude difference. This is significant when examining the human and environmental health implications of As at North Brookfield, as the soils closest to the roaster will represent a greater risk.

5.4.4 Differences in Mineralogy and SSE Between Giant and North Brookfield Mines

The only similarity between the Giant and North Brookfield mines is that both used roasting as part of their method of extracting gold from arsenopyrite ore, and in the process generated As_2O_3 and roaster derived Fe-oxides (Forbes, 1904; Tait, 1961). The total As concentrations, soil types, morphology and mineralogy of RO, presence of As_2O_3 and the dominant As containing leach in SSE, all differ between these two sites.

At Giant, As concentrations in all of the organic-rich soils and most of the till soils are elevated above 150 ppm, which is the calculated natural background for Yellowknife based on a site specific assessment performed by Risklogic (2002a). While Giant has high As recorded across the whole property, soils surrounding the North Brookfield mine, sampled for this study, overall have significantly lower total As with the exception of Site 2. Surface soils at Site 2 are more than 300 times the 12 ppm National Soil Quality Guideline and are approximately equal to the highest values recorded in a OSS from Giant (CCME, 2007b). Upwind and downwind sites are both within an order of magnitude of the CCME guideline.

Differences in RO composition, morphology, As speciation and relative As concentrations were also observed between the two sites and can be attributed to different roasting techniques. The North Brookfield roast was less controlled because its purpose was to remove as much As and S as possible prior to chlorination (Anonymous, 1897; Forbes, 1904; Ritchie, 1901). Because of this, RO from North Brookfield contained lower As counts than at Giant, as observed through μXRF mapping. The Giant roast was designed to make the arsenopyrite porous and more amenable to cyanidation to extract the refractory ore, so control of temperature and oxygen content were important to keep the grains porous (Tait, 1961). Examination of As speciation in RO from aerially exposed beach tailings at Giant showed that As^{3+} within the RO has remained stable despite the presence of oxygen for more

than 50 years (Walker *et al.*, 2005; Walker, 2006). The ratios of As^{3+} to As^{5+} in the soils is consistent with values calculated in the beach tailings (Walker, 2006).

The dominant As-bearing phase identified using SSE in the highest total As samples is the most significant difference between these two sample locations. At Giant, the crystalline Fe-oxide and scorodite leaches contain the highest As in roaster impacted soils. At North Brookfield relative proportions of As between the various extraction steps were similar between impacted and non-impacted soils with the exception of the amorphous Fe-oxide step. The lower proportion of As in the RO and the lack of As_2O_3 remaining in the soils explains the lower amount of As extracted in the crystalline Fe-oxide and scorodite extractions at North Brookfield. The lower quantity of natural arsenopyrite and associated weathering rims are a potential explanation for the lower As contents of the amorphous Fe-oxide leach from Giant soils.

As described in Chapter 4, the presence and persistence of As_2O_3 at Giant can be attributed to several factors including climate, duration of mine operation, acidity of the soils and the nature of the ore mined. The colder climate, lower precipitation rates and the fact that there are only four frost free months a year (EnviroCan, 2008; Pienizt, 1997) has resulted in organic-rich soils overlying glaciolacustrine tills in the Yellowknife area. This is a very different soil type compared to the developed A, B and C (till) horizons at North Brookfield. In organic-rich materials at Giant the high porosity allows for rain water to channel through the soils, meaning contact between As_2O_3 grains and rain water is of a very short duration and dissolution reactions are likely to be slowed.

The duration and intensity of mining has also played a significant role in the anthropogenic signature of As in the soils, as Giant was a much larger and longer operation than North Brookfield, and released more As_2O_3 into the environment. The presence of Sb in

the ore roasted at Giant is also important as it can become incorporated in the As_2O_3 either as trace amounts or as a $(As, Sb)_2O_3$. Work by Riveros (2000) shows that the presence of even small quantities of Sb within the As_2O_3 can stabilize the grains by lowering its solubility. This is consistent with the release of Sb from As_2O_3 in the scorodite leach at Giant. The absence of Sb in the ore at North Brookfield could be another explanation for faster As_2O_3 dissolution.

It is known that As_2O_3 was emitted from the roaster at North Brookfield, based on historical reports (Anonymous, 1897; Forbes, 1904; Ritchie, 1901), the lack of As_2O_3 in the soils (by ESEM, and synchrotron techniques) shows that aerial deposition at this site may not have been the main mechanism of As dispersion. Instead of being aerially dispersed through the stack it is possible that condensation of As_2O_3 gases occurred in the roaster and caused the majority of particulate As_2O_3 to accumulate within the roaster dust chambers and at the base of the stack. The very high As concentrations observed at Site 2 could be indicative of a As_2O_3 waste disposal site since As concentrations at other sites surrounding the mine are significantly lower. Some aerial dispersal would explain slightly elevated total As downwind of the historic roaster. This is speculation however, as in the past 100 years since the mine closure any As_2O_3 in the soils has dissolved or oxidized.

5.4.5 Differentiating the Sources of Arsenic in Soils

Distinguishing the mineral form and source of As in soils is vital as both will have an effect on the overall availability of As and consequently the human and ecological risks posed (Bhumbla and Keefer, 1994; DesChamps *et al.*, 2003). The three As-bearing phases observed in surface and outcrop soils at the Giant mine are As_2O_3, roaster derived Fe-oxides and arsenopyrite. Both As_2O_3 and RO are known to be generated during the roasting process (More and Pawson, 1978; Tait, 1961; Walker *et al.*, 2005) and their presence in the

soils is considered to be of anthropogenic origin. Arsenopyrite on the other hand occurs naturally in the ore (Hubbard *et al.*, 2006; Siddorn *et al.*, 2006; Tait, 1961) and is therefore a natural source of As as long as it is not encapsulated by a roaster-derived rim of maghemite or hematite.

The majority of As in deeper organic soils from Site 28 and tills from Sites 19 and 31 was released in the weaker leaches and the source has yet to be identified. The presence of As_2O_3, arsenopyrite and RO in soils above these samples may be a cause for elevated total As at depth. Since As in RO is known to be stable in exposed beach tailings from Giant (Walker *et al.*, 2005) the dissolution of As_2O_3 and weathering products of arsenopyrite (which has been observed in tailings by Walker (2006) but not identified here) may be the source of As in deeper soils. Without further information it is difficult to provide a definitive answer to the source of As with depth, as the dissolution of RO under reducing conditions may also be the cause for elevated As that has become weakly bound by OM at depth.

Understanding the source of As in North Brookfield soils is a more difficult task as a roaster-derived form of As, beyond the As in RO, has not been identified. The abundance of As in the amorphous Fe-oxide step, as either an amorphous Fe-arsenate or potentially as yukonite, could be attributed to the natural weathering of arsenopyrite observed in thin section (Jamieson *et al.*, 2008). The source of As associated with Ti-oxides, Fe-oxyhydroxides, and clay minerals observed in surface soils at Site 2 is almost impossible to pinpoint as it could be associated with the oxidation of sulphides or be the remnants of roaster-derived wastes that have dissolved or oxidized over time. The weathering arsenopyrite observed in thin section could only be partly responsible for observed As given the low abundance of arsenopyrite and the total As concentrations of almost 4000 ppm, similar to an OSS from Giant.

The presence of natural As^{3+} in aerobic surface soils is not common (Sadiq, 1997) and because of this it can be used as a method of distinguishing between anthropogenic and naturally derived As in well oxygenated soils. The mineral tooeleite (a ferric-arsenite) has however been identified in tailings at the Montague Gold mine in Nova Scotia (Jamieson *et al.*, 2008), and is known to exist in waste materials from pyrite and arsenopyrite gold ores (Cesbron and Williams, 1992; Jambor, 1992). The lack of another As-bearing phase at North Brookfield suggests that As_2O_3, if present in the soils during mining, has dissolved and oxidized over time to become bound in the soils by OM, clays and metal oxides. The presence of As^{3+} associated with clay minerals and goethite substantiates the hypothesis of the dissolution of As_2O_3 as no other source of As has been identified at either Giant or North Brookfield. Arsenic in the 5+ oxidation state, found associated with rims on Ti-oxides, may be of natural or anthropogenic origin.

5.5 Conclusions

Using analytical techniques, such as ESEM and synchrotron analyses, and combining them with sequential selective extractions is a powerful method of determining the form and speciation of As within soils. Two gold mines were examined during this study. The first is the Giant mine which is in the beginning stages of remediation and may become more publically accessible in the future and the second is the historic North Brookfield mine which is currently publically accessible. For this reason, understanding the form, distribution and potential mobility of As-bearing phases at these two sites is crucial as there may be potential health implications.

At Giant the presence of the anthropogenically derived As_2O_3 and RO as well as natural arsenopyrite was observed in OSS and surface soil samples from four sites on the property. SSE results on these samples show between 20% and 75% of the total As is

extracted in the crystalline Fe-oxide step that can be explained by the incongruent dissolution of As from As_2O_3 and Sb-rich As_2O_3. The remaining Sb-rich As_2O_3 is probably removed in the scorodite extraction shown by the highest Sb extracted in this step, despite the lack of scorodite in these samples. At depth in the organic rich soils of Site 28 and tills from Sites 19 and 31, more As removed in the weaker As extractions which may be the result of As_2O_3 dissolution from samples higher in the profile and subsequent adsorption and binding by OM. Site 29 has a different SSE profile as OSS, surface and deeper soil samples all show high proportions of As extracted in the crystalline Fe-oxide leach. This is confirmed by the presence of As_2O_3 in all three samples and results from Chapter 4, substantiate the theory that material from outcrops can wash down into low lying soils.

The lack of As_2O_3 at North Brookfield and low As concentrations downwind of the roaster are attributed to the different climate, the smaller scale and age of the mine operation. The total As concentrations at this site in combination with historical records suggests that the area close to the roaster may have been a waste dump where As-rich materials that condensed within the roaster were disposed. This suggests that the aerial dispersal of As_2O_3 at North Brookfield may not have been extensive as seen at Giant. The higher total As concentrations as well as the higher proportion As in the amorphous Fe-oxide SSE extraction are the main differences observed between impacted and non-impacted soils. Synchrotron based μXRD and μXANES analyses showed the presence of an amorphous Fe-arsenate in natural weathering rims of arsenopyrite which could explain the presence of As in the amorphous extraction. Other soils from North Brookfield contained lower total As concentrations and similar As distribution across the various SSE phases. Roaster oxides were also present at North Brookfield but had a different morphology, relative proportions of As, as well as, As speciation and crystallography than Giant. This is potentially explained by the use of different roasting techniques and the difference in age between the two mines.

Chapter 6: Conclusions and Future Work

6.1 Conclusions

Soils in the vicinity of the Giant roaster and the historic North Brookfield roaster have been impacted by aerial emissions of particulate As as well as by naturally derived As-bearing minerals. At both mines Au was extracted from the host arsenopyrite, generating As-bearing RO, As_2O_3 particles and SO_2 (g). At Giant, which operated from 1948 to 1999, more than 20,000 tonnes of As-rich particles were emitted from the stack and 237,000 tonnes are currently stored underground (CPHA, 1977; EnviroCan, 2007; GNWT, 1993; INAC, 2007; Tait, 1961). North Brookfield was a significantly smaller mine that operated from 1886-1906 and generated approximately 4,000 tonnes of As_2O_3 (DPWM, 1899; DPWM, 1927; Forbes, 1904; Malcolm, 1976).

Soil profiles from Giant showed a clear trend of elevated As and Sb concentrations in surface soils and decreased concentrations with depth, except for Site 29 where both elements were high through the profile, likely because of the wash down of As-rich material from the adjacent outcrop surface. The majority of surface soils studied exceeded the 340 ppm As industrial guideline (GNWT, 2003) but total As in the Townsite was close to the background value of 150 ppm and residential guideline of 160 ppm (Risklogic, 2002a; GNWT, 2003). Bulk XANES spectra showed a variable portion of As^{3+} in surface soils and predominately As^{5+} with depth. At North Brookfield soil profiles showed significantly lower total As concentrations upwind (35 ppm) and downwind (45 ppm) of the roaster compared to samples adjacent to the roaster (4300 ppm). Site 2, adjacent to the roaster, was interpreted, based on historical reports, as being close to the location of a waste pile where As_2O_3 dusts that condensed within the stack and chlorination wastes were deposited. This indicates that

aerially dispersed As_2O_3 from this site may not have had as significant an impact on soils surrounding the mine as anticipated.

Five main conclusions can be drawn from this study. First, aerial emissions of As-rich particles from the Giant mine roaster have persisted in the soil environment for almost 50 years. This was confirmed by μXRD with the presence of As_2O_3 and μXANES which showed As in the 3+ oxidation state only.

The long-term persistence and stability of As_2O_3 was attributed to several factors. Riveros *et al.* (2000) has shown that small amounts of Sb within the As_2O_3 crystals can cause a reduction in the thermodynamic activity of As_2O_3, lowering its aqueous solubility. The detectable levels of Sb observed in some As_2O_3 grains from soils, the high total Sb extracted in scorodite SSE leach, and the observed As concentrations in this leach, are consistent with this theory. The cool, dry climate of Yellowknife area as well as the high OC content and the cessation of SO_2 emissions from roasting (in 1999) may also be a cause for slower As_2O_3 dissolution. In organic rich soils and OSS from the mine property it has been calculated, based on total As^{3+} XANES percentages, that between 28% and 45% of the total As was attributed to As_2O_3 grains.

Estimates of how long these grains will persist in the environment are difficult without a better understanding of the distribution of As_2O_3 emissions over the Yellowknife area and the quantity of As_2O_3 in the soils post 1959, when emission rates dropped significantly. Recommendations for how this may be accomplished are discussed in Section 6.2. Unlike Giant, no As_2O_3 was identified within the North Brookfield soils which may be the result of limited sampling but also a warmer, wetter climate, lower OC content and the lack of Sb in the ore to stabilize As_2O_3 grains, may have contributed to faster dissolution. North Brookfield was also a much smaller operation, generating less As_2O_3 over more than 100 years ago.

Secondly, it is possible to distinguish the form of As within the soils and differentiate between anthropogenic and geogenic sources, with a few exceptions, using advanced synchrotron, SSE and ESEM techniques. At Giant three As-bearing phases were observed in the surface and outcrop soils; As_2O_3 (As^{3+}), RO composed of maghemite with As in the 5+ and 3+ oxidation states, as well as arsenopyrite(As^{-1}) and associated As-bearing weathering rims. Both As_2O_3 and RO are known to be of anthropogenic origin as they would have formed during roasting (More and Pawson, 1978; Tait, 1961; Walker *et al.*, 2005) and have been deposited in the soils through airfall, whereas arsenopyrite occurred naturally in the ore (Hubbard *et al.*, 2006; Siddorn *et al.*, 2006; Tait, 1961).

SSE results have shown that the surface soils at Giant were impacted by aerial emissions of particulate As_2O_3 as they contained higher total As concentrations than samples lower in the soil profiles. As well they had a significant portion of As in the crystalline Fe-oxide SSE extraction, believed to be attributed to As_2O_3. The vertical mobility of As was difficult to predict but, the relative abundance of As_2O_3, lower quantities of arsenopyrite and the higher proportion of As bound in the weaker SSE extractions at depth, suggests As at depth may be the result of dissolved As_2O_3 from samples above being bound by organic matter. It is unlikely that As at depth is associated with RO higher in the soil profile as proportionately fewer grains were observed compared to As_2O_3 and RO were shown to be relatively stable in oxidizing conditions by Walker *et al* (2005) in aerially exposed beach tailings.

Five As-bearing phases were identified in surface soils from Site 2 at North Brookfield. These were; arsenopyrite: RO composed of hematite, As-rich rim on Ti-oxide, As in the 3+ oxidation state associated with chlorite and muscovite, and As^{3+} associated with goethite. Like Giant, arsenopyrite is considered to be of natural origin and RO are anthropogenically derived. It was difficult in the case of the remaining three phases to

identify the source of As. The presence of As^{3+} in the clays and goethite grains may be attributed to the dissolution of As_2O_3, known to have been generated at the mine, and subsequent As adsorption, as no other As^{3+}-bearing phase was indentified here or at Giant. Comparing SSE results between sample locations, those close to the roaster contained the highest total As and a noticeable portion of As, Fe and Ca in the amorphous Fe-oxide extraction step. This could be attributed to amorphous Fe-arsenates that contained some Ca and were associated with weathering rims of arsenopyrite, as observed at other sites in Nova Scotia (Corriveau, 2006; Walker, 2008).

The third conclusion is that As-bearing roaster derived Fe-oxides were identified at both minesites, however they had differentcrystallography, As content, As speciation and overall morphology. This could be the result of different roasting technique, as the North Brookfield roast was less controlled and designed to remove as much As and S from the arsenopyrite prior to chlorination (Anonymous, 1897; Forbes, 1904; Ritchie, 1901). At Giant the purpose was to make the arsenopyrite porous for cyanidation so therefore lower temperatures did not remove as much As from the ore (Tait, 1961). Consequently, North Brookfield RO contained lower As counts and As only in the 5+ oxidation state while Giant RO had higher As contents and an As^{3+}-As^{5+} mixture (also observed by Walker *et al.* (2005)).

Based on examination of OSS and SCS, the fourth conclusion is that adjacent to outcrop exposures (<5m) at the Giant mine, the wash down of As rich material from the outcrop surface to lower lying soils explained the higher total As and Sb concentrations as well as the presence of As_2O_3 to depths of 33cm. A SCS taken from less than 25m away from the outcrop shows lower total As and Sb and no As_2O_3 or As^{3+} in bulk XANES after 24cm depth. This supports the hypothesis of Walker (2006) who postulated that roaster derived materials were washed from exposed outcrop surfaces and eventually deposited in low lying areas.

Finally, using ESEM, synchrotron based bulk and micro analyses combined with petrology and SSE were powerful and effective methods of identifying the mineral form and speciation of As in soils. These techniques allowed for the identification of As_2O_3 in the form of arsenolite at Giant that were unidentifiable using petrographic analysis. Once As_2O_3 grains were found in particular sub-samples, it was possible to predict the presence of As_2O_3 in other soils from the property based on total As, Sb and OC content. Soils containing As_2O_3 were typically organic rich (OC content >15%) and had an Sb content above the 10 ppm detection limit of the ICP-AES at ASU.

There are more differences than similarities between the North Brookfield and Giant mines. Ore at both mines consisted of Au-bearing arsenopyrite which led to roasting at these locations. The roasting process generated As-bearing RO, As_2O_3 dusts and SO_2 emissions. Differences in the roasting technique, scale and age of the mines and their dissimilar climates has led to variations in total As concentrations, soil types, as well as the morphology, mineralogy and speciation of RO, and the presence and persistence of As_2O_3 grains.

Currently, the North Brookfield mine is publicly accessible and the tailings are known to be used for recreational activities. At Giant, the majority of the property is not publicly accessible, but may become so in the future as remediation is ongoing. Each site has different associated health risks because of the mineral form and distribution of As. North Brookfield soils have lower total As (with exception of close to the roaster). Overall, downwind and upwind samples show very little difference in total As and represent less of a human health risk than those closer to the roaster. Soils adjacent to roaster have total As as high as observed at Giant, and a significant portion of As is in the weakly extractable leaches. At Giant the presence of low Sb-bearing As_2O_3 in soils, which is known to be soluble in water (Riveros *et al.*, 2000) and is widely distributed across surface and outcrop soils, is important when considering the ingestion of contaminated materials. If remediation of these soils does

not occur, especially outcrop soils without high total As and Sb as well as a significant proportion of As_2O_3, they will continue to be a major source of As to surface waters and surface seeps on the property.

6.2 Future Work

The following are recommendations for future work, based on the results of this research, to further explain the form, distribution, mobility of natural and anthropogenic sources of As in soils from the Giant mine, NT and North Brookfield mine, NS.

- Determine the persistence of As_2O_3 grains in the soil environment at Giant. The link between As in surface water seeps and soils can be confirmed by conducting a sampling program where water seeps and corresponding soil samples are taken. Further delineation of the presence of As_2O_3 grains on the Giant mine property as well as soils further away from the roaster to determine the impact downwind is needed. More sample pairs and OSS samples are required to determine if the wash down effect occurs in other areas across the property and downwind of the roaster.
- Measure soil pH to determine if the source of S in surface soils at the examined sites is attributed to SO_2 emissions. Soil pH will help to understand the rapidly changing geochemical conditions in the soil that would be the result of the closure of the Giant roaster and cessation of SO_2 emissions. Stopping the SO_2 emissions, and as a result increasing soil pH, could cause As_2O_3 grains to be more stable in more reducing environments as shown in the Eh-pH diagram in Chapter 2.

- Soils at site 28 and site 29 show different soil profiles than other sites on the property. Further examination of soils from deeper within the site 28 profile is necessary to identify the source of elevated As at these depths.
- It has been shown that the presence of Sb in soils at the Giant mine is a useful indicator for the presence of As_2O_3. It would therefore be beneficial to perform soil digestion analyses using lower Sb detection limits (e.g. ICP-MS rather than ICP-AES) to identify the Sb threshold value, below which As_2O_3 is unlikely to be present. This may provide a less expensive and faster means of identifying roaster impacted soils at this site than using ESEM or synchrotron work.
- Conduct Electron Probe Micro Analyses (EMPA) on roaster oxides from Giant to determine if the wt. percent As is consistent with observations made by Walker *et al.* (2005) and Walker (2006) as well as on roaster oxides from North Brookfield to compare between the two mines. This would help determine whether As is being leached from RO in soils. Also EMPA could be performed on As_2O_3 grains to provide a quantitative, rather than qualitative, measurement of the Sb content in these grains.
- Bioaccessibility testing on outcrop soils as well as surface soils from areas that will become publically accessible at Giant should be performed to provide insight into the risk they pose to human health. Also an investigation into the most appropriate method of remediating soils contaminated with As_2O_3 from Giant would be valuable.
- Supplementary evaluation of arsenopyrite oxidation rims at both Giant and North Brookfield mines is needed to further understand SSE data and identify the source of As in the amorphous Fe-oxide step.

- In organic-rich samples, the loss of grains targeted for synchrotron analyses during the lifting process may be prevented or at least decreased by sieving the soil samples to remove larger organic pieces that are not completely filled by epoxy.
- In future sequential selective extractions performed at the Giant mine, an As_2O_3 standard should be run to determine which fraction the majority of As is removed in. For most accurate results a sample of As_2O_3 dusts from Giant would be most relevant as it will also evaluate the effectiveness of Sb in stabilizing As_2O_3 grains.
- To substantiate the theory that Site 2 at North Brookfield may be the location of a roaster waste disposal area, more samples should be taken and analyzed from this region to determine if As concentrations are consistently high, or if there are As "hotspots" around the roaster. Also additional samples would assist in identifying any additional As^{3+} bearing phases or their sources within the soils.
- A hydrogeological study should be performed of the area surrounding the North Brookfield mine. As there is no remaining As_2O_3 in the soils, North Brookfield ground and surface waters may contain high concentrations of As.

References

Andrade, C.F. 2006. Arsenic Cycling and Speciation in Mining-Impacted Sediments and pore-waters from Yellowknife Bay, Great Slave Lake, NWT. MSc Thesis Queen's University, Kingston, Ontario, Canada, January 2006; 284pp.

Anonymous. 1897. Free milling and chlorination of gold ores at North Brookfield, Queen's County, N.S. *The Canadian Mining Review*, **16(5)**; 179-180.

Ashley, P.M., and Lottermoser, B.G. 1999. Arsenic contamination at the Mole River mine, northern New South Wales. *Australian Journal of Earth Sciences* **46**; 861-874.

Appelo, C.A.J., Postma, D. 1999. Geochemistry, Groundwater and Pollution. Balkema, Rotterdam.

Basta, N.T., Rodriguez, R.R., and Casteel, S.W. 2002. Chapter 5: Bioavailability and risk of arsenic exposure by the soil ingestion pathway, ***In:*** *Environmental Chemistry of Arsenic.* Marcel Dekker, Inc., New York: 117-141; 391 pp.

Belluck, D.A., Benjamin, S.L., Baveye, P., Sampson, J., and Johnson, B. 2003. Widespread arsenic contamination of soils in residential areas and public spaces: an emerging regulatory or medical crisis? *International Journal of Toxicology* **22**; 109-128.

Bhumbla, D.K., and Keefer, R.F. 1994. Chapter 3: Arsenic Mobilization and Bioavailability in Soils ***In***: Advances in Environmental Science and Technology **v. 26**: Arsenic in the Environment, Part 1: Cycling and Characterization. Edited by: Nriagu, J.O. John iley and Sons, Inc., New York; 51-82.

Boyle, R.W., and Jonasson and I.R., 1973. The geochemistry of As and its use as an indicator element in geochemical prospecting. *Journal of Geochemical Exploration* **2**; 251–296.

Boyle, R.W. 1979. The geochemistry of gold and its deposits. *Geological Survey of Canada, Bulletin*, **280**.

Brookins, D.G. 1986. Geochemical behaviour of antimony, arsenic, cadmium and thallium. *Chemical Geology* **54**; 271-278.

Brown, E.P. 1908. The treatment of stamp mill tailings at the Richardson Mine, Goldboro, N.S. *The Canadian Mining Journal* **29**; 400-401.

Calabrese, E.J., Stanek, E.J., and Barnes, R. 1996. Methodology to estimate the amount and particle size of soil ingested by children: implications for exposure assessment at waste sites. *Regulatory Toxicology and Pharmacology* **24**; 264-268.

Canadian Council for the Ministers of the Environment (CCME). 2007a. [Online Source] Canadian Environmental Quality Guidelines: Guidelines for Canadian Drinking Water Quality- A Summary Table. Canadian Council of Ministers of the Environment. Winnipeg, Manitoba. <http://www.hc-sc.gc.ca/ewh-semt/pubs/water-eau/sum_guides-res_recom/index-eng.php >. Date Accessed: July 27th, 2008.

Canadian Council of Ministers of the Environment (CCME). 2007b. [Online Source] Canadian Environmental Quality Guidelines: Canadian Soil Quality Guidelines for the Protection of Environmental and Human Health. Canadian Council of Ministers of the Environment, Winnipeg, Manitoba. <http://documents.ccme.ca/>. Date Accessed: July 27th, 2008.

Canadian Public Health Association (CPHA). 1977. Final Report- Canadian Public Health Association Task Force of Arsenic, Yellowknife, Northwest Territories. Candia Public Heath Association, Ottawa, December 1977.

Canam, T.W. 2006. Discover, mine production and geology of the Giant mine: Chapter 13 in Gold in the Yellowknife greenstone belt, Northwest Territories: Results of the EXTEXH III Multidisciplinary Research Project (ed.) C.D. Anglin, H. Falck, D.F.

Wright and E.J. Ambrose; Geological Association of Canada, Mineral Deposits Division, Special Publication No 3; 188-196.

Carter, R and Samis, C.S. 1952. The influence of roasting temperature upon gold extraction by cyanidation from refractory gold ores. *Canadian Institute of Mining and Metallurgy, Transactions*, 55; 120-126.

Caussy, D. 2003. Case studies of the impact of understanding bioavailability: arsenic. *Ecotoxicology and Environmental Safety* **56**; 164-173.

Cesbron. F.P. and Williams, S.A. 1992. Tooeleite, a new mineral from the U.S. Mine, Tooele County, Utah. Mineralogy. Magazine, 56, 71–73.

Clennell, J.E. 1915. Special Modifications of the Cyanide Process *In*: The Cyanide Handbook. McGraw-Hill Book Company Inc, New York, New York; 339-380.

Coleman, L.C. 1957. Mineralogy of the Giant Yellowknife Gold mine, Yellowknife, NWT. *Economic Geology*, **52**; 400-425.

Corriveau, M. C. 2006. Characterization of arsenic-bearing near surface airborne particulates from gold mine tailings in Nova Scotia. MSc Thesis Queen's University, Kingston, Ontario, Canada, February 2006; 124pp.

Craw, D., Falconer, D., and Youngson, J.H. 2003. Environmental arsenopyrite stability and dissolution: theory, experiment and field observations. *Chemical Geology*, **199**; 71-82.

Cullen, W.R. and Reimer, K.J. 1989. Arsenic speciation in the environment. *Chemical Reviews* **89**; 713-764.

Datta, R., and Sarkar, D. 2004. Arsenic geochemistry in three soils contaminated with sodium arsenite pesticide: an incubation study. *Environmental Geosciences* 11 (2); 87-97.

de Mello, J.W.V., Roy, W.R., Talbott, J.L., and Stucki, J.W. 2006. Mineralogy and arsenic mobility in arsenic-rich brazilian soils and sediments. *Journal of Soil and Sediments* 6(1); 9-19.

Davis, A., Ruby, M.V., Bloom, M., Schoof, R., Freeman, G., and Vergstrom, P.D. 1996. Mineralogic constraints on the bioavailability of arsenic in smelter-impacted soils. *Environmental Sciences and Technology* **30**; 392-399.

Department of Public Works and Mines (DPWM). 1899. Report on the Mines of Nova Scotia- for the Year of 1890-1899. Halifax, Nova Scotia, Commissioner of Public Works and Mines; Queen's Printer.

Department of Public Works and Mines (DPWM). 1927. Annual Report on the Mines- 1927. Halifax, Nova Scotia, Minister of Public Works and Mines; King's Printer.

DeSisto, S.L., Jamieson, H.E., Parsons, M.B., and Walker, S.R. 2008. Determining arsenic re-mobilization potential from scorodite-bearing hardpan. Montague Gold mines, Nova Scotia (*Poster Abstract*). Metals in the Human Environment Strategic Network (*MITHE-SN*) Symposium, Gatineau Quebec January 28th-29th, 2008.

DesChamps, E., Ciminelli, V.S.T., Weidler, P.G., and Ramos, A.Y. 2003. Arsenic sorption onto soils enriched in Mn and Fe minerals. *Clay and Clay Minerals*, **15** (2); 197-204.

Dillion Consulting (Dillion). 1995. Air dispersion modeling of roaster stack emissions from Royal Oak Giant Yellowknife Mine. Unpublished report to Indian and Northern Affairs Canada. 30pp.

Eng, P.J., Rivers, M., Yang, B.X. and Schildkamp, W. 1995. Micro-focusing 4eV to 65eV x-rays with bent Kirkpatrick-Baez mirrors. *In*: X-ray microbeam technology and applications (W. Yun, ed.) *Proceedings of SP,E* **2516**; 41-51.

Environment Canada (EnviroCan). 2007. [Online Reference] National Pollutant Release Inventory (NPRI)- Online data search 1994-1999 Facility on-site releases, Royal Oak Mines Inc., Giant Mine, < http://www.ec.gc.ca/pdb/querysite/query_e.cfm>. Date Accessed: May, 24th, 2008.

Environment Canada (EnviroCan). 2008. [Online Reference] Canadian climate data online. <http://www.climate.weatheroffice.ec.gc.ca/climateData/canada_e.html>. Date Accessed: August 6th, 2008.

Environmental Sciences Group (ESG) and Queen's University. 2001. Characterization of arsenic in solid phase samples collected on the Giant mine townsite, Yellowknife, NWT. Unpublished report to Indian and Northern Affairs Canada.

Fawcett, S.E., Andrade, C.F., Walker, S.R., and Jamieson, H.E. 2006. Understanding the Environmental Legacy of the Giant Gold Mine, Yellowknife, NWT: Lessons From Recent Research. *In*: Proceeding of the CLRA/ACRSD 2006 Annual Meeting, Reclamation and Remediation: Policy to Practice, August 20-23, 2006, Ottawa, Ontario.

Fawcett, S.E., Jamieson, H.E., and Walker, S.R. 2008. Solid-state speciation of As and Sb associated with mine waste and downstream sediment at the Giant Mine, Yellowknife, Canada *(Presentation Abstract Goldschmit Conference July 2008). Geochimica et Cosmochimica Acta*, 72(12); A259.

Fendorf, S.E. and Sparks, D.L. 1996. X-Ray adsorption fins structure spectroscopy. *In:* Methods of soil analysis 3- Chemical Methods (J.M. Bartels, ed.). Soil Science Society of America Inc. and America Society of Agronomy Inc., Madison, Wisconsin, USA; 377-416.

Forbes, H.L. 1904. The chlorination of gold ore of the North Brookfield Mine, Nova Scotia. *Journal of the Canadian Mining Institute*, 7; 308-318.

Foster, E.O. 1963. The collection and recovery of golf from roaster exit gases at Giant Yellowknife Mines Limited, *Canadian Institute of Mining and Metallurgy, Transactions* **66**; 245-251.

Foster, A.L., Brown, G.E Jr., Tingle, T.N., and Parks, G.A. 1998. Quantitative arsenic speciation in mine tailings using X-ray adsorption spectroscopy. *American Mineralogist* **83**; 553-568.

Freeman, G.B., Schoof, R.A., Ruby, M.V., Davis, A.O., Dill, J.A., Liao, S.C., Lapin, C.A., and Bergstrom, P.D. 1995. Bioavailability of arsenic in soil and house dust impacted by smelter activities following oral administration in *Cynomolgus* monkeys. *Fundamental and Applied Toxicology* **28**: 215-222.

Goh, K.-H. and Lim, T.-T. 2005. Arsenic fractionation in a fine soil fraction and influence of various anions on its mobility in the subsurface environment. *Applied Geochemistry* **20**; 229-239.

Golder Associates. 2005. Distribution of arsenic in surficial materials: Giant mine, *In:* Supporting document I1- Giant mine remediation plan (Indian and Northern Affairs Canada-2007). 184pp.

Government of Northwest Territories (GNWT). 1993. An investigation of atmospheric emissions for the Royal Oak Giant Yellowknife mine. Environmental Protection Division, Department of Renewable Resources, Government of Northwest Territories, Yellowknife, NWT, June 1993.

Government of Northwest Territories (GNWT). 2003. [Online Source] Remediation criteria for arsenic in the Yellowknife area soils and sediment *In*: Environmental guidelines for contaminated site remediation. <http://www.mveirb.nt.ca/upload/project_document/1209683061_GNWT%20Environmental%20Guideline%20for%20Remediation%20of%20Contaminated.pdf>. Date Accessed: July 20th, 2008.

Graves, M.C. and Zentilli, M. 1982. A review of the geology of gold in Nova Scotia. In Geology of Canadian Gold Deposits (R.W. Hodder and W. Petruk eds.) *Canadian Institute of Mining and Metallurgy, Special Volume* **24**; 233-242.

Haffert, L. and Craw, D. 2008. Mineralogical controls on environmental mobility of arsenic from historic mine processing residues. *Applied Geochemistry* **23**; 1467-1483.

Hall, G.E.M., MacLaurin, A.L., Vaive, J.E. 1995. Readsorption of gold during the selective extraction of "soluble organic" phase of humus, soil and sediment samples. *Journal of Geochemical Exploration*, **54**; 27-38.

Hall, G.E.M., Gauthier, G., Pelchat, P. And Vaive, J.E. 1996a. Application of a sequential extraction scheme to ten geological certified reference materials for the determination of 20 elements. *Journal of Analytical Atomic Spectrometry* **11**; 87-96.

Hall, G.E.M., Vaive, J.E., Beer, R., and Hoashi, M. 1996b. Selective leaches revisited with emphasis on the amorphous Fe-oxyhydroxide phase extraction. *Journal of Geochemical Exploration*, **56**; 59-78.

Hall, G.E.M., Vaive, J.E., and MacLaurin, A.I. 1996c. Analytical aspects of the application of sodium pyrophosphate reagent in the specific extraction of the labile organic component of humus and soils. *Journal of Geochemical Exploration*, **56**; 23-36.

Hammersley, A.P. 1998. Fit2D V10.3 Reference Manual V4.0, European Synchrotron Research Facility, Paper ESRF98-HA01T (program and manual available at <http:www.esrf.fr/computing/expg/subgroups/data_analysis/FIT2D/).

Han, F.X., Su, Y., Monts, L., Plodinec, M.J., Namim, A. and Triplett, G.E. 2003. Assessment of global industrial-age anthropogenic arsenic contamination. *Naturwissenschaften* **90** (9); 395-401.

Harper, M. and Haswell, S.J. 1988. A comparison of copper, lead, and arsenic extraction from polluted and unpolluted soils. *Environmental Technology Letter*. 9; 1271-1280.

Hocking, D., Kuchar, P., Plambeck, J.A., and Smith, R.A. 1978. The impact of gold smelter emissions on vegetation and soils of a sub-arctic forest tundra transition ecosystem. *Journal of Air Pollution Control Association*, **28**; 133-137

Hubbard, L., Marshall, D., Anglin, C.D., Thorkelson, D., and Robinson, M.H. 2006. Giant mine: Alteration, mineralization, and ore-zone structures with an emphasis on the Supercrest zone: Chapter 14 in Gold in the Yellowknife greenstone belt, Northwest Territories: Results of the EXTEXH III Multidisciplinary Research Project (ed.) C.D. Anglin, H. Falck, D.F. Wright and E.J. Ambrose; Geological Association of Canada, Mineral Deposits Division, Special Publication No 3; 197-212.

Hughes, M.F. 2002. Arsenic toxicity and potential mechanism of action. *Toxicology Letters* **133**; 1-16.

International Centre for Diffraction Data (ICDD). 2003. Powder Diffraction File (PDF2). Release 2003. International Centre for Diffraction Data, Newtown Square, Pennsylvania, USA.

Indian and Northern Affairs Canada (INAC). 2007. [Online Source] Giant mine remediation plan. Report of the Giant mine remediation team-Department of Indian Affairs and Northern Development as submitted to the Mackenzie Valley Land and Water Board (MVLWB); 260pp. < http://www.mvlwb.ca/mv/Registry.aspx>. Date Accessed: June 20th, 2008.

Jain, C.K., and Ali, I. 2000. Arsenic: occurrence, toxicity and speciation techniques. *Water Resources* **34** (17); 4304-4312.

Jambor, J.L. 1992. New mineral names. *American Mineralogist*, **77**;1305-1309

Jamieson, H.E., Walker, S.R., Parsons, M.B., and Hall, G.E.M. Characterization of multiple secondary minerals in arsenic-rich gold mine tailings *(Presentation Abstract Goldschmit Conference- July 2008). Geochimica et Cosmochimica Acta*, **72**(12); A242

Keon, N.E., Swartz, C.H., Brabander, D.J., Harvey, C., and Hemond, H.F. 2001. Validation of an arsenic sequential extraction method for evaluating mobility in sediments. *Environmental Science and Technology* **35**; 2778-2784.

Kerr, D.E. 2006. Surficial geology and exploration geochemistry: Chapter 20 in Gold in the Yellowknife greenstone belt, Northwest Territories: Results of the EXTEXH III Multidisciplinary Research Project (ed.) C.D. Anglin, H. Falck, D.F. Wright and E.J. Ambrose; Geological Association of Canada, Mineral Deposits Division, Special Publication No 3; 301-324.

Knight, R.D. and Henderson, P.J. 2006. Smelter dust in humus around Royun-Noranda, Quebec. *Geochemistry: Exploration, Environment, Analysis*, **6**; 203-214.

Langmir, D. 1997. Aqueous Environmental Geochemistry. Prentice-Hall Inc. Upper Saddle River, New Jersey. 600pp.

Ljung, K., Selinus, O., Otabbong, E., and Berglund, M. 2006. Metal and Arsenic Distribution in Soil Particle Sizes Relevant to Soil Ingestion by Children. *Applied Geochemistry* **21**; 1613-1624.

Mackenzie Valley Land and Water Board (MVLWB). 2008. [Online Source] Giant mine remediation plan- City of Yellowknife Letter Re: Environmental Assessment Mar. 31-08. 33pp.<http://www.mvlwb.ca/mv/Registry.aspx>. Date Accessed: July 25th, 2008.

Malcolm, W. 1929. Gold fields of Nova Scotia. *Geological Survey of Canada Memoir*, **156**. 253 pp.

Malcolm, W. 1976. Gold fields of Nova Scotia. *Geological Survey of Canada Memoir*, **385**; 253 pp.

Manceau, A., Marcus, M.A., and Tamura, N. 2002. Quantitative speciation of heavy metals in soils and sediments by synchrotron X-Ray techniques. *In*: Applications of Synchrotron Radiation in Low-Temperature Geochemistry and Environmental

Science. P.A. Fenter, M.L. Rivers, N.C. Sturchio and S.R. Sutton, eds. *Reviews in Mineralogical Geochemsitry*, **49**; 341-428.

Matschullat, J. 2000. Arsenic in the geosphere-A review. *Science of the Total Environment*, **249**; 297-312.

Masschelyn, P.H., DeLaune, R.D. and Patrick, W.H. 1991. Effect of redox potential and pH on arsenic speciation and solubility in a contaminated soil. *Environmental Science and Technology*, **25**: 1414-1419.

Meunier, L., Walker, S.R., Koch, I., Jamieson, H.E., Parsons, M.B., and Reimer, K.J. 2008. Mineralogy and bioavailability of arsenic in tailings and soil from Nova Scotia gold mines (*Poster Abstract*). Metals in the Human Environment Strategic Network (*MITHE-SN*) Symposium, Gatineau Quebec January 28th-29th, 2008.

Meunier, L., Walker, S.R., Koch, I., Wragg, J., Parsons, M.B., Jamieson, H.E., and Reimer, K.J. *In progress*. Effects of soil composition and mineralogy on the bioaccessibility of arsenic from tailings and soil in the Nova Scotia Gold Mine Districts. To be submitted to *Environmental Sciences and Technology*.

Mihaljevič, M., Poňavič, M., Ettler, V. and Šebek, O. 2003. A comparison of sequential extraction techniques for determining arsenic fractionation in synthetic mineral mixtures. *Analytical and Bioanalytical Chemistry* **377**; 723-729.

Moir, I., Falck, H., Hauser, B., and Robb, M. 2006. The history of mining and its impact on the development of Yellowknife: Chapter 2 in Gold in the Yellowknife greenstone belt, Northwest Territories: Results of the EXTEXH III Multidisciplinary Research Project (ed.) C.D. Anglin, H. Falck, D.F. Wright and E.J. Ambrose; Geological Association of Canada, Mineral Deposits Division, Special Publication No 3;11-28.

More, M.A., and Pawson, H.E. 1978. Giant Yellowknife Mines Limited *In* Milling Practice in Canada (D.E. Pickett, ed). *Canadian Institute of Mining and Metallurgy, Special Volume* **16**; 102-108.

Morton, W.E., and Dunnette, D.A. 1994. Health effects of environmental As. In: As in the Environment *In*: Advances in Environmental Science and Technology **26**: Arsenic in the Environment, Part 1: Cycling and Characterization. Edited by: Nriagu, J.O. John Wiley and Sons, Inc., New York.

Nardin, E.W. 1910. Bromo-Cyaniding of Gold Ores *In*: More Recent Cyanide Practice (2nd ed.) Bain, H.F. Mining and Scientific Press, San Francisco, p. 226-231.

Nesbit, H.W., Muir, I.J. 1998. Oxidation states and speciation of secondary products on pyrite and arsenopyrite reacted with mine waste waters and air. *Mineralogy and Petrology*, **62**; 123-144.

Nordstrom, D.K. and Archer, D.G. 2003. Arsenic thermodynamic data and environmental geochemistry. *In*: Arsenic in Groundwater: Geochemistry and Occurrence. Stollenwerk, K.G. (ed). Kluwer, Boston; 1-25.

Parsons, M (personal comm.). 2007. Personal communication August 2007 regarding the location of previous soil sample at the North Brookfield Mine, from unpublished data.

Pienizt, R, Smol, J.P., and Lean, D.R.S. 1997. Physical and chemical limnology of 24 lakes located between Yellowknife and Contwoyto Lake, Northwest Territories (Canada). *Canadian Journal of Fisheries and Aquatic Sciences*, **54**; 347-358.

Pokrovski, G.S., Zakirov, I.V., Roux, J., Testemale, D., Hazemann, J.L., Bychkov, A.Y., and Golikova, G.V. 2002. Experimental study of arsenic speciation in vapor phase at 500°C: Implications for As transport and fractionation in low-density crustal fluids and volcanic gases. *Geochimica et Cosmochimica Acta*, **66**; 3453-3480

Ravel, B and Newville, M. 2005. ATHENA, ARTEMIS, HEPHAESTUS: data analysis for X-ray absorption spectroscopy using IREFFIT. *Journal of Synchrotron Radiation*, **12** (4); 537-541.

Reimann, C. and Garrett, R.G. 2005. Geochemical background-concept and reality. *Science of the Total Environment*, **350**; 12-27.

Richardson, G.M., Bright, D.A., and Dodd, M. 2006. Do current standards of practice in Canada measure what is relevant to human exposure at contaminated sites? II: oral bioaccessibility of contaminants in soil. *Human and Ecological Risk Assessment* **12**: 606-616.

Riveros, P.A., Dutrizac, J.E., and Spencer, P. 2001. Arsenic disposal practices in the metallurgical industry. *Canadian Metallurgical Quarterly*, **40**; 395-420.

RiskLogic Scientific Services Inc (Risklogic). 2002a. Determining natural (background) arsenic soil concentrations in Yellowknife, NWT and deriving site-specific human health-based remediation objectives for arsenic in the Yellowknife area. Report of Yellowknife Arsenic Soils Remediation Committee (YSARC) c/o Environment Canada, Yellowknife, April 2002; 21 pp.

RiskLogic Scientific Services Inc. 2002b. Assessment of ecological risks posed by arsenic contamination in Yellowknife, NWT. Report of Yellowknife Arsenic Soils Remediation Committee (YSARC) c/o Environment Canada, Yellowknife, April 2002; 25pp.

RiskLogic Scientific Services Inc. 2002c. Assessment of Human Health Risks Posed by Arsenic Contamination in Yellowknife, NWT. Report of Yellowknife Arsenic Soils Remediation Committee (YSARC) c/o Environment Canada, Yellowknife, April 2002; 50 pp.

Ritchie, J.N. 1901. Chlorination Plant at Brookfield. *Industrial Advocate*, **28**; 11-15.

Ruby M.V., Schoof, R., Brattin, W., Goldade, M., Post, S., Harnois, M., Mosby, D.E., Casteel, S.W., Berti, W., Carpenter, M., Edwards, D., Cragin, D., and Chappell, W. 1999. Advances in Evaluating the Oral Bioavailability of Inorganics in Soils for Use in Human Health Risk Assessment. *Environmental Science and Technology* **33**(21): 3697-3705.

Ryan, R.J. and Smith, P.K. 1998. A review of the mesothermal gold deposits of the Meguma Group, Nova Scotia, Canada. *Ore Geology Reviews* **13**; 153-183.

Sadiq, M. 1997. Arsenic chemistry in soils: an overview of thermodynamic predictions and field observations. *Water, Air, and Soil Pollution*, **93**; 117-136.

Sangster, A.L., 1990. Metallogeny of the Meguma Terrane, Nova Scotia, *In*: Mineral Deposit Studies in Nova Scotia (A.L. Sangster ed.). Geological Survey of Canada Paper **90-8**; 115-162.

Sangster, A.L. 1992. Light stable isotope evidence for a metamorphic origin for bedding-parallel, gold-bearing veins in Cambrian flysch, Meguma Group, Nova Scotia; In International Association on the Genesis of Ore Deposits, Eighth quadrennial symposium: *Exploration and Mining Geology* **1**; 69-79.

Sangster, A.L., and Smith, P.K. 2007. Metallogenic Summary, Meguma Gold Deposits, *In*: Mineral Deposits of Canada: A synthesis of Major Deposit Types, District Metallogeny, the Evolution of Geological Provinces and Exploration Methods (ed) W.D. Goodfellow; Geological Association of Canada Mineral Deposits Division Special Publication No 5; 723-732.

Sarkar, D., Datta, R., and Sharma, S. 2005. Fate and bioavailability of arsenic in organo-arsenical pesticide-applied soils. Part-I: incubation study. *Chemosphere*, **60**; 188-195.

Savage, K.S., Bird, D.K., and Ashley, R.P. 2000. Legacy of the California gold rush: environmental geochemistry of arsenic in the southern mother lode gold district. *International Geology Review*, **42**; 385-415.

Schenk, P.E. 1997. Sequence stratigraphy and provenance on Gondwana's margin: The Meguma Zone (Cambrian to Devonian) of Nova Scotia, Canada. *Geological Society of America Bulletin*, **109**; 295-409.

Scott, M.J., and Morgan, J.J. 1995. Reactions at oxide surfaces. 1. Oxidation of As(III) by synthetic birnessite. *Environmental Science and Technology*, **29**; 1898-1905.

Siddorn, J.P., Cruden, A.R., Hauser, R.L., Armstrong, J.P., and Kirkham, G. 2006. The Giant-Con deposits: Preliminary integrated structural and mineralization history. Chapter 15 in Gold in the Yellowknife greenstone belt, Northwest Territories: Results of the EXTEXH III Multidisciplinary Research Project (ed.) C.D. Anglin, H. Falck, D.F. Wright and E.J. Ambrose; Geological Association of Canada, Mineral Deposits Division, Special Publication No 3; 213-231.

Smith, P.K., Parsons, M.B., and Goodwin, T.A. 2005. Field trip FT-B5: Geology, and environmental geochemistry of lode gold deposits in Nova Scotia. Halifax, 2005, GAC/MAC/CSPG/CSSS Joint Annual Meeting, Halifax, Nova Scotia. Atlantic Geoscience Society Field Guide B5. 114p.

Smedley, P.L., and Kinniburgh, D.G. 2002. A review of the source, behaviour and distribution of arsenic in natural waters. *Applied Geochemistry* 17; 517-568.

SRK Consulting Engineers and Scientists (SRK). 2005. Giant mine-surface water chemistry *In*: Supporting document B6- Giant mine remediation plan (Indian and Northern Affairs Canada-2007). 40pp.

Strumm, W., and Morgan J.J. 1996. Aquatic Chemistry. John Wiley and Sons Inc., New York, USA. 1022pp.

Tait, R.J.C. 1961. Recent progress in milling and gold extraction at Giant Yellowknife Gold Mines Limited. *Canadian Institute of Mining Metallurgy*, Transactions. **64;** 204-216.

United States Environmental Protection Agency (US EPA). 2001. [Online Source] National Primary Drinking Water Regulations; Arsenic and Clarifications to Compliance and New Source Contaminants Monitoring. <http://www.epa.gov/fedrgstr/EPA-WATER/2001/January/Day-22/w1668.htm >. Date Accessed: July 27th, 2008.

Valberg, P.A., Beck, B.D., Bowers, T.S., Keating, J.L., Bergstrom, P.D., and Boardman, P.D. 1997. Issues in Setting Health-Based Cleanup Levels for Arsenic in Soil. *Regulatory Toxicology and Pharmacology* **26:** 219-229.

Van Herreweghe, S., Swennen, R., Vandecasteele, C and Cappuyns, V. 2003. Solid phase speciation of arsenic by sequential extraction in standard reference materials and industrially contaminated soil samples. *Environmental Pollution*, **122**(3); 323-342.

Vink, B.W. 1996. Stability relations of antimony and arsenic compounds in the light of revised and extended Eh-pH diagrams. *Chemical Geology*, **130**; 21-30.

Walker, S.R., Jamieson, H.E., Lanzirotti, A., and Andrade, C.F. 2005. Determining arsenic speciation in iron oxides derived from a gold-roasting operation: Application of synchrotron micro-XRD and micro-XANES at the grain scale. *Canadian Mineralogist* **43;** 1205-1224.

Walker, S.R. 2006. The Solid-Phase Speciation of Arsenic in Roasted and Weathered Sulphides at the Giant Gold Mine, Yellowknife, NWT: Application of Synchrotron microXANES and microXRD at the Grain Scale. PhD Thesis, Queen's University, Kingston, Ontario, Canada, September 2006; 185 pp.

Walker, S.R., Meunier, L., Jamieson, H.E., Parsons, M.B., Kosh, I., and Reimer, K.J. 2008. Mineralogy and bioaccessibility of arsenic in mine tailings and soil (*Presentation*

Abstract). Geological Association of Canada and the Mineralogical Association of Canada (GAC-MAC) Annual Meeting, Quebec City Quebec May, 2008; 180.

World Health Organization (WHO). 2001. Arsenic and arsenic compounds. Environmental Health Criteria 224, 2nd Edition, 1217-1232.

Wilson, E.B. 1897. The Chlorination Process. John Wiley and Sons, Inc., New York. 125 pp.

Yan-Chu, H. 1994. Chapter 2: Arsenic Distribution in Soils *In*: Advances in Environmental Science and Technology **v. 26**: Arsenic in the Environment, Part 1: Cycling and Characterization. Edited by: Nriagu, J.O. John Wiley and Sons, Inc., New York; 17-50.

Yang, L., and Donahoe, R.J. 2007. The form, distribution and mobility of arsenic in soils contaminated by arsenic trioxide, at sites in southeast USA. *Applied Geochemistry* **22;** 320-341.

Zobrist, J., Dowdle, P.R., Davis, J.A., Oremland, R.S., 2000. Mobilization of arsenite by dissimilatory reduction of adsorbed arsenate. *Environmental Science and Technology* **34,** 4747–4753.

Appendix A: Sample Location Photographs

The following photos are a sample of soil core samples taken from the Giant and North Brookfield mines. Remaining photographs from sample locations and cores can be found in the attached CD.

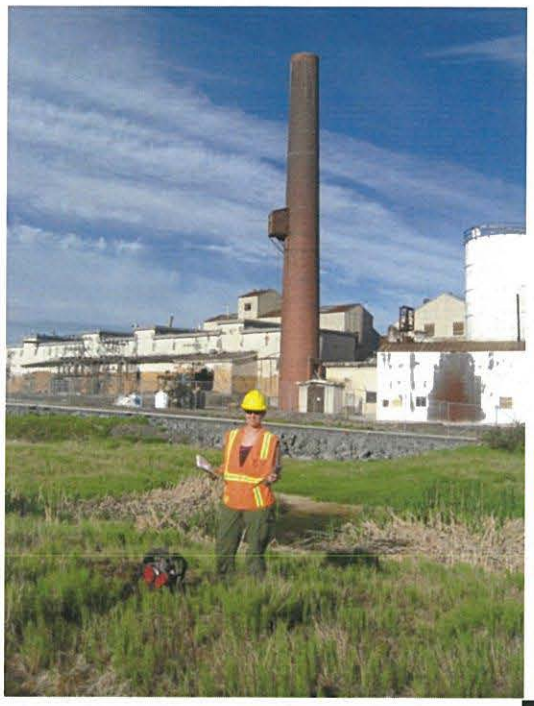

Figure A-1A: Location of soil core sample from adjacent to the roaster (Site 31) at the Giant mine, NT. Sample was taken from a marshy area, with standing water located 5m from the site.

Figure A-1B: Photograph of the Site 31 core at Giant after being split longitudinally, thawed and air-dried. Sample shows high organic content at the surface, followed by the presence of clay rich material at depth.

Figure A-2A: Location of soil core sample from close to the roaster (Site 231) at the North Brookfield mine, NS. Sample was taken from an area identified by M. Parsons (pers. com. 2007) as containing high As.

Figure A-2B: Photograph of the Site 31 core at Giant after being split longitudinally, thawed and air-dried. Sample shows high organic content at the surface, followed by the presence of clay rich material at depth.

Appendix B: Soil Descriptions

The following photos is an example of soil core descriptions from Site 31 at the Giant mine, NT. Remaining descriptions from Giant and North Brookfield can be found in the attached CD along with the method of soil description from the North American Soil Geochemical Landscape Project.

Table B-1: Sample of Giant mine soil descriptions from Site 31 close to the roaster

Location	Depth (cm)	Horizon	Depth (cm)	Samples (depth in cm)		Munsell Number and Colour			Grain Size	Roots	Reason for Separation
Site 31		E	0-3								
		Of	3-6 cm	YK-50	3-5	5 YR	3	/2	-	VF; A; O	OM decomposition
		OCt	6-9 cm	YK-244 YK-51	6-7 7-8	10 YR	6/ 2	5/ 2	sandy silt loam	-	Colour difference
	41	C1	9-20.5 cm	YK-52 YK-245 YK-246 YK-53	9-10 12-13 15-16 18.5-19.5	10 YR	6	/3	silty clay	M; T; W	Grain size change and colour difference
			20.5-24	YK-247 YK-54	22-23 24-25	10 YR	6	/2	silty clay	M; T; W	Same colour, GS and roots as previous C1
			24-26			7.5 YR	4	/1	silty clay loam	-	Darker gray colour, GS and roots same as previous C1

Table B-2: Sample of North Brookfield mine soil descriptions from Site 2 close to the historic roaster footings

Location	Depth (cm)	Horizons	Depth (cm)	Samples (depth in cm)		Munsell Number and Colour			Grain Size	Roots	Reason for Separation
Site 2		E	0-2								
		A	2-7.5	NB-129 NB-82	2-3 3-7	10YR	5	/3	-	Two roots (M-@ bottom of horizon)	Colour and OM content
	55	A Ct	7.5-14	NB-83 NB-200	7-10 11-13	10YR	5	/4	-	Three roots M/F; T; W	Colour and lack of OM. On average stones are larger than in the A horizon
		C1	14.5-50	NB-201 NB-202 NB-203 NB-84 NB-204 NB-205 NB-206 NB-85 NB-207	14.5-16.5 18.5-20.5 22-24 26-29 31-33 35-37 38.5-40 43-45 46.5-48.5	2.5 Y	6	/4	-	-	Colour change, lack of roots and stone percentages

Appendix C: List of Examined Sub-Samples and Analyses Performed

This includes a full list of samples examined during this thesis and the analytical techniques used.

Table C-1: Giant Mine Soil Core Sub-Samples

Sample Location	Sample Number	Thin Section	Bulk XANES	SSE	OC Analysis	ESEM	Sample Depth
Site 13	YK-300	X	X		X	X	2.3
	YK-301	X			X	X	5.3
Site 14	YK-302	X	X		X		1.8
	YK-303	X	X		X	X	5.1
Site 19	YK-126	X	X		X	X	0.8
	YK-231		X		X		2.8
	YK-127	X	X	X	X	X	5.1
	YK-233				X		14.3
	YK-235	X		X	X		25.9
	YK-27	X			X	X	28.1
	YK-28		X		X		32.6
Site 28	YK-115	X	X	X	X	X	2.4
	YK-236				X		5.9
	YK-116				X		13.5
	YK-238		X		X		24.1
	YK-45	X			X	X	25.9
	YK-46			X	X		30.0
	YK-239	X	X		X	X	33.5
	YK-47		X		X		38.2
Site 29	YK-114	X	X		X	X	2.4
	YK-48	X		X	X		8.1
	YK-240				X		12.5
	YK-26	X	X		X	X	16.3
	YK-49	X	X		X	X	23.0
	YK-241				X		22.5
	YK-242	X	X		X	X	28.3
	YK-243	X	X	X	X	X	32.6
Site 31	YK-50	X	X	X	X	X	1.7
	YK-244		X		X		6.0
	YK-51	X			X		7.7
	YK-52	X	X		X	X	11.1
	YK-245				X		16.2
	YK-53		X		X		27.3
	YK-54	X		X	X	X	37.6

Table C-2: Giant Mine Outcrop Soil Samples

Sample Location	Sample Number	Thin Section	Bulk XANES	SSE	OC Analysis	ESEM	Sample Depth
Site 40	YK-58	X	X		X	X	OSS
Site 41	YK-59	X	X	X	X	X	OSS
Site 43	YK-61	X	X	X	X	X	OSS
Site 45	YK-304	X	X		X	X	OSS
Site 42	YK-60	X			X	X	OSS

Table C-3: North Brookfield Soil Core Sub-Samples

Sample Location	Sample Number	Thin Section	SSE	OC Analysis	ESEM	Sample Depth
Site 2	NB-129		X	X		0.6
	NB-82	X			X	3.4
	NB-83	X				7.3
	NB-200			X		11.2
	NB-201		X	X		15.2
	NB-85	X	X	X		47.1
Site 4	NB-93		X	X		4.4
	NB-208	X				9.4
	NB-94			X		13.3
	NB-95	X	X	X		24.4
	NB-211			X		34.4
Site 8	NB-76			X		1.8
	NB-71			X		6.6
	NB-72		X	X		14.3
	NB-73			X		20.3
	NB-75	X	X	X		34.6

Appendix D: Giant Mine- Soil Chemistry on Unsieved Samples

Aqua Regia analyses on bulk unsieved soils from the Giant mine, NT were performed by the author at the Analytical Services Unit (ASU) at Queen's University. Included in this Appendix are the Mess-3 and SS-2 measured values and control limits for all ICP-AES analyses performed at ASU.

Table D-1: ICP AES Results for Unsieved Giant Soil Core and Outcrop Samples

Sample	YK-01	YK-02	YK-03	YK-04	YK-05*	YK-06	YK-120	YK-07*	YK-08	YK-09
Location	Site 2			Site 4			Site 6			
Sample Type	O	Oct	C	O	Oct	C1	O	Oct	Oct	C1
Compression Corrected Depth	1.4	9.2	22.1	3.1	14.3	45.6	1.7	8.3	20.3	37.7
Ag	<2.0	<2.0	<2.0	<2.0	<2.0	<2.0	<2.0	<2.0	<2.0	<2.0
Al	23400	29600	31000	15400	15650	26100	15100	26850	25900	21000
As	48.4	33.8	10	218	180	7.8	320	565	200	9
Au	<5	<5	<5	<5	<5	<5	<5	<5	<5	5.5
B	28.3	37.5	36.1	<20	21.6	22	<20	27.9	25.7	<20
Ba	185	254	280	71.1	101.4	223	113	209.5	241	157
Be	<4.0	<4.0	<4.0	<4.0	<4.0	<4.0	<4.0	<4.0	<4.0	<4.0
Ca	5540	5500	6270	24000	7200	5310	14000	11000	10400	5280
Cd	<1.0	<1.0	<1.0	<1.0	<1.0	<1.0	<1.0	<1.0	<1.0	<1.0
Co	12.5	15.5	17.1	<5.0	9.7	11.6	11.4	12.4	13.2	10.8
Cr	42.2	50.5	62.2	<20	29.9	49	34.7	47.3	45.1	41.9
Cu	28.2	28.5	30.6	50.6	10.35	32.4	34.9	32	27.1	19
Fe	28100	32900	39100	2880	18700	27300	21700	26550	25200	25100
K	5210	6700	7090	865	2820	4540	3180	4890	4570	3950
Mg	9230	11100	13600	2940	6065	9160	8680	9395	8790	8250
Mn	300	455	1199	154	348	283	354	355	612	263
Mo	<2.0	<2.0	<2.0	2.1	<2.0	<2.0	<2.0	<2.0	<2.0	<2.0
Na	489	632	751	134	269.5	461	251	375.5	397	400
Ni	28.6	32.6	36.5	7.3	14.95	29.6	26.9	27.5	25.4	21.9
P	607	597	568	501	516	407	729	541	496	424
Pb	10.3	<10	<10	<10	<10	<10	36.9	16.85	<10	<10
S	388	96.8	72.7	1520	278.5	171	1780	806.5	543	146
Sb	<10	<10	<10	65.2	<10	<10	18.3	19.6	<10	<10
Se	<10	<10	<10	<10	<10	<10	<10	<10	<10	<10
Si	<10	<10	<10	<10	<10	<10	<10	<10	<10	<10
Sn	<2.0	<2.0	<2.0	<2.0	<2.0	<2.0	<2.0	<2.0	<2.0	<2.0
Sr	49.9	65.2	59.5	58	35.95	45.7	34.6	58.35	61.8	38.2
Ti	916	1222	1243	64.9	740	971	431	862	884	995
Tl	<1.0	<1.0	<1.0	<1.0	<1.0	<1.0	<1.0	<1.0	<1.0	<1.0
U	<10	<10	<10	<10	<10	<10	<10	<10	<10	<10
V	55.1	62.7	71.7	13	37.9	53.9	45.1	58.05	54.9	49.7
Zn	64.3	70.1	73.8	70.8	38.75	55.9	73.8	64.95	54.8	51.9

Table D-1: ICP AES Results for Unsieved Giant Soil Core and Outcrop Samples *(cont.)*

Sample	YK-222	YK-223	YK-224	YK-10	YK-225	YK-226	YK-11	YK-227	YK-12	YK-13
Location	Site 11						Site 11 (cont.)			
Sample Type	O	O	O	O	O	O	O	O	Oct	C3
Compression Corrected Depth	3.1	7.0	10.9	15.6	21.5	26.6	31.3	35.6	39.1	42.2
Ag	<2.0	<2.0	<2.0	<2.0	<2.0	<2.0	<2.0	<2.0	<2.0	<2.0
Al	1860	1440	924	935	1500	2220	5700	5960	9050	15700
As	631	35	18.95	16.1	21.2	39.3	143	161	109	11.3
Au	-	-	-	<5	-	-	<5	-	<5	<5
B	<20	<20	<20	<20	<20	<20	<20	<20	<20	<20
Ba	87	38	38.3	30.9	60.1	70.6	82.4	115	86.6	92.7
Be	<4.0	<4.0	<4.0	<4.0	<4.0	<4.0	<4.0	<4.0	<4.0	<4.0
Ca	24800	37900	38950	23400	38400	36700	22700	44800	15500	5830
Cd	<1.0	<1.0	<1.0	<1.0	<1.0	<1.0	<1.0	<1.0	<1.0	<1.0
Co	<5.0	<5.0	<5.0	<5.0	<5.0	<5.0	<5.0	<5.0	<5.0	7
Cr	<20	<20	<20	<20	<20	<20	<20	<20	21.2	34.1
Cu	22	12	11	8.3	14.2	16.8	12.8	15.7	14.3	14.2
Fe	4070	1090	753	832	1420	2560	7090	7070	11900	16900
K	1100	699	622	472	402	382	580	502	1370	2540
Mg	2340	1770	1800	1390	1950	2100	2860	3250	4360	6240
Mn	244	296	154.5	24.2	76	69.9	59.6	37.5	94.1	160
Mo	<2.0	<2.0	<2.0	<2.0	<2.0	<2.0	<2.0	<2.0	<2.0	<2.0
Na	<75	<75	<75	<75	77.9	82.2	141	125	209	328
Ni	8	<5.0	<5.0	<5.0	<5.0	6.8	6.9	7	11	21.6
P	491	564	468	358	416	366	363	477	307	291
Pb	50	<10	<10	<10	<10	<10	<10	<10	<10	<10
S	1660	1680	1320	936	1210	1210	1200	1900	772	289
Sb	180	12	<10	<10	<10	<10	<10	<10	<10	<10
Se	<10	<10	<10	<10	<10	<10	<10	<10	<10	<10
Si	<10	<10	<10	<10	<10	<10	<10	<10	<10	<10
Sn	<2.0	<2.0	<2.0	<2.0	<2.0	<2.0	<2.0	<2.0	<2.0	<2.0
Sr	36	38	42.65	33	47.4	58.4	56.3	90.1	50.2	35.6
Ti	37	13	10.1	25.9	19.1	27.3	142	101	388	872
Tl	<1.0	<1.0	<1.0	<1.0	<1.0	<1.0	<1.0	<1.0	<1.0	<1.0
U	<10	<10	<10	<10	<10	<10	<10	<10	<10	<10
V	<10	<10	<10	<10	<10	<10	13.5	14.2	24.7	38.9
Zn	96	38	<15	<15	<15	<15	<15	<15	20	33.5

Table D-1: ICP AES Results for Unsieved Giant Soil Core and Outcrop Samples *(cont.)*

Sample	YK-124	YK-125	YK-14	YK-15	YK-300	YK-301	YK-302	YK303	YK-16	YK-17*
Location	Site 12				Site 13		Site 14			
Sample Type	O	O	O	Oct	O	O	O	O	O	O
Compression Corrected Depth	2.1	7.5	25.7	31.5	2.3	5.3	1.8	5.1	1.8	36.8
Ag	<2.0	<2.0	<2.0	<2.0	-	-	-	-	<2.0	<2.0
Al	3130	610	8440	15600	-	-	-	-	5970	12800
As	742	82.1	30.4	42.9	139	21.3	163	187	139	58.7
Au	<5	<5	<5	<5	-	-	-	-	<5	<5
B	<20	<20	<20	<20	-	-	-	-	<20	21.05
Ba	32	41.8	74.5	62.9	-	-	-	-	63.6	137.5
Be	<4.0	<4.0	<4.0	<4.0	-	-	-	-	<4.0	<4.0
Ca	34220	33600	20500	7790	-	-	-	-	23900	23650
Cd	<1.0	<1.0	<1.0	<1.0	-	-	-	-	2.9	<1.0
Co	11.3	<5.0	6.6	9.8	-	-	-	-	7.6	5.95
Cr	<20	<20	24.4	46.9	-	-	-	-	<20	25.4
Cu	107	18.3	29.3	20.3	-	-	-	-	35.9	43.75
Fe	15900	745	13200	23500	8310	1660	8620	16300	9840	11300
K	528	300	759	1470	-	-	-	-	1430	1975
Mg	5020	1420	5070	8610	5320	3480	4120	6410	4640	4670
Mn	474	303	301	256	-	-	-	-	356	329.5
Mo	<2.0	<2.0	<2.0	<2.0	-	-	-	-	<2.0	<2.0
Na	111	89.5	155	199	-	-	-	-	106	236
Ni	20.4	7.2	26	28.8	-	-	-	-	16.4	12.9
P	536	444	320	258	-	-	-	-	1330	675.5
Pb	49.6	<10	<10	<10	-	-	-	-	30.3	<10
S	2520	1390	1020	436	2500	2260	2280	1620	2250	1055
Sb	87.5	28	<10	<10	14.6	<10	13.7	33.5	18.6	<10
Se	<10	<10	<10	<10	-	-	-	-	<10	<10
Si	<10	<10	<10	<10	-	-	-	-	<10	<10
Sn	<2.0	<2.0	<2.0	<2.0	-	-	-	-	<2.0	<2.0
Sr	19.9	26.4	42	23.6	-	-	-	-	32.2	54.55
Ti	40.7	<10	296	567	117	20.8	82.9	297	159	386
Tl	<1.0	<1.0	<1.0	<1.0	-	-	-	-	<1.0	<1.0
U	<10	<10	<10	<10	-	-	-	-	<10	<10
V	10.6	<10	22.8	40	-	-	-	-	24.3	22.9
Zn	84.7	25	18.2	32.7	571	23.7	204	103	181	21.25

Table D-1: ICP AES Results for Unsieved Giant Soil Core and Outcrop Samples *(cont.)*

Sample	YK-128	YK-18	YK-19	YK-21	YK-20	YK-112	YK-113	YK-22	YK-23	YK-24*	YK-25
Location	Site 15			Site 16		Site 17					
Sample Type	O	O	O	Op	C1	Op	Oct	Oct	C1	C2	C3
Compression Corrected Depth	2.1	12.6	23.9	0.3	11.0	1.4	4.9	11.2	28.0	39.5	43.0
Ag	<2.0	<2.0	<2.0	<2.0	<2.0	<2.0	<2.0	<2.0	<2.0	<2.0	<2.0
Al	2520	9470	1950	17500	18100	16900	26300	32000	32700	10260	11600
As	72.3	297	10.4	117	21.8	328	383	500	240	75.4	82.4
Au	<5	<5	<5	<5	5.1	<5	9.12	19.3	7.6	<5	<5
B	<20	<20	<20	24.1	20	<20	<20	35.8	31.1	<20	<20
Ba	28.9	65.7	40.7	111	136	117	193	220	238	60.85	69.7
Be	<4.0	<4.0	<4.0	<4.0	<4.0	<4.0	<4.0	<4.0	<4.0	<4.0	<4.0
Ca	15300	12400	23400	6650	3780	9710	7830	7200	7190	7135	5100
Cd	<1.0	<1.0	<1.0	<1.0	<1.0	1.3	<1.0	<1.0	<1.0	<1.0	<1.0
Co	<5.0	8.5	<5.0	12.5	9.2	6.9	11.2	12.9	13.9	5.45	6.8
Cr	<20	236	<20	39.1	38.4	27.8	41.6	45	47.5	21.35	28
Cu	63.5	30.1	29.1	23.6	21.5	16.8	17.7	23.6	29.4	10.25	14.6
Fe	3710	15900	3540	22200	21100	16700	26300	30800	32400	12400	13800
K	1350	1000	184	4270	3860	2030	3790	5230	5490	1425	1710
Mg	2400	5420	1520	7820	6980	5090	8010	9350	10600	3905	4780
Mn	95.7	212	20.2	354	229	236	377	413	410	155.5	175
Mo	<2.0	<2.0	<2.0	<2.0	<2.0	<2.0	<2.0	<2.0	<2.0	<2.0	<2.0
Na	88.5	201	91	295	370	243	399	607	554	234	309
Ni	7.5	19.3	7.6	28.7	20.9	16.1	23.5	27	30.2	11	14.1
P	1200	430	469	620	497	309	277	249	558	425	512
Pb	85.5	<10	<10	<10	<10	<10	<10	<10	<10	<10	<10
S	2130	792	2470	608	380	399	237	174	80.3	52.95	37.1
Sb	<10	13.4	<10	11.1	<10	<10	<10	<10	<10	<10	<10
Se	<10	<10	<10	<10	<10	<10	<10	<10	<10	<10	<10
Si	<10	<10	<10	<10	<10	<10	<10	<10	<10	<10	<10
Sn	<2.0	<2.0	<2.0	<2.0	<2.0	<2.0	<2.0	<2.0	<2.0	<2.0	<2.0
Sr	28.1	38.2	65.3	35	32.6	31.1	56.7	70.1	72.5	21.45	16.5
Ti	42.8	444	44.8	787	814	533	671	1009	957	488	664
Tl	<1.0	<1.0	<1.0	<1.0	<1.0	<1.0	<1.0	<1.0	<1.0	<1.0	<1.0
U	<10	<10	20.7	<10	<10	<10	<10	<10	<10	<10	<10
V	10.9	28	<10	51.6	41.3	29.4	44.4	53.6	61.5	24.9	28.2
Zn	84.6	34.6	<15	60.2	45	151	43.7	49.2	60.7	20.15	25.6

Table D-1: ICP AES Results for Unsieved Giant Soil Core and Outcrop Samples *(cont.)*

Sample	YK-126	YK-231	YK-127*	YK-232	YK-233	YK-234	YK-27	YK-28	YK-235
Location	Site 19								
Sample Type	O	O	C2	C2	C2	C2	C2	C3	C3
Compression Corrected Depth	0.8	2.8	5.1	9.0	14.3	20.3	25.9	28.1	32.6
Ag	<2.0	<2.0	<2.0	<2.0	<2.0	<2.0	<2.0	<2.0	<2.0
Al	4560	11850	15400	16100	15700	15600	17600	17700	17900
As	161	258.3	322	230	246.5	147	107	46	82.7
Au	<5	-	<5	-	-	-	<5	<5	-
B	<20	<20	<20	<20	<20	<20	<20	<20	<20
Ba	81.3	91.3	105	103	104	97.2	105	85.8	82.4
Be	<4.0	<4.0	<4.0	<4.0	<4.0	<4.0	<4.0	<4.0	<4.0
Ca	39212	39600	8940	7700	6670	7780	8140	8690	5280
Cd	1.4	<1.0	<1.0	<1.0	<1.0	<1.0	<1.0	<1.0	<1.0
Co	6.1	7.9	8.7	9.2	9	8.9	10.7	12.3	14.5
Cr	<20	30.6	36.75	36.1	35.5	38	40.7	46.9	53.6
Cu	26.4	25.05	24.2	23.1	23.4	31.1	25	30.7	32.9
Fe	8350	16100	18800	18900	18900	19000	25100	29000	26700
K	1280	1115	1405	1010	955	995	1310	1080	1120
Mg	3320	5500	5915	6060	5900	6230	7630	9210	9150
Mn	222	254.5	249.5	257	279	272	285	315	350
Mo	<2.0	<2.0	<2.0	<2.0	<2.0	<2.0	<2.0	<2.0	<2.0
Na	109	211	340.5	292	285	341	264	334	365
Ni	12	17.7	18.95	19.1	19.9	19.2	21.9	25.6	31.2
P	1040	444.5	377	287	264	284	311	362	317
Pb	29.3	17.9	<10	<10	<10	<10	<10	<10	<10
S	2250	591.5	326	182	142	163	250	257	89.1
Sb	20.7	<10	<10	<10	<10	<10	<10	<10	<10
Se	<10	<10	<10	<10	<10	<10	<10	<10	<10
Si	<10	<10	<10	<10	<10	<10	<10	<10	<10
Sn	<2.0	<2.0	<2.0	<2.0	<2.0	<2.0	<2.0	<2.0	<2.0
Sr	39.2	18.75	20.4	18.1	16.5	17.8	17.6	18.4	15.2
Ti	132	344	665	550	454	602	657	1143	705
Tl	<1.0	<1.0	<1.0	<1.0	<1.0	<1.0	<1.0	<1.0	<1.0
U	<10	<10	<10	<10	<10	<10	<10	<10	<10
V	22.5	29.7	35.65	37.8	36.5	38.1	47.4	73.3	52
Zn	302	122.5	65.5	37.2	32.4	38.7	33.5	38	36.3

Table D-1: ICP AES Results for Unsieved Giant Soil Core and Outcrop Samples *(cont.)*

Sample	YK-117	YK-29	YK-30	YK-31	YK-123	YK-32*	YK-33	YK-34	YK-35	YK-36
Location	Site 21				Site 24				Site 25	
Sample Type	O	O	O	O	O	U	O	C1	O	Oct
Compression Corrected Depth	1.4	5.7	28.1	35.6	1.6	10.1	32.0	43.7	1.6	17.6
Ag	<2.0	<2.0	<2.0	<2.0	<2.0	<2.0	<2.0	<2.0	<2.0	<2.0
Al	2690	1240	4440	8560	6440	22200	4220	18000	893	3290
As	63	40.8	36.1	78.1	202	246	55.8	28.6	58.4	29.4
Au	<5	<5	<5	<5	<5	<5	<5	<5	<5	<5
B	<20	33.8	<20	<20	<20	23.85	<20	<20	24.9	<20
Ba	73.4	53.9	50	65.3	77.4	159	81.8	163	88.6	39.1
Be	<4.0	<4.0	<4.0	<4.0	<4.0	<4.0	<4.0	<4.0	<4.0	<4.0
Ca	39677	41900	28700	23000	26426	10900	22100	14800	28100	7390
Cd	<1.0	<1.0	<1.0	<1.0	<1.0	<1.0	<1.0	<1.0	<1.0	<1.0
Co	<5.0	<5.0	<5.0	5.8	8.4	8.85	<5.0	8.4	<5.0	<5.0
Cr	<20	<20	<20	30.2	<20	35.1	<20	31.6	<20	<20
Cu	26.4	21.1	87.3	112	35.9	14.35	12.5	19.4	10.5	6
Fe	5270	1150	5500	10900	12300	19150	4070	18300	1030	4130
K	823	599	349	556	1340	3535	500	2870	343	344
Mg	3430	2990	3240	4540	2720	6630	1580	6340	2770	1930
Mn	281	151	281	199	235	282.5	164	205	533	127
Mo	<2.0	<2.0	<2.0	<2.0	<2.0	<2.0	<2.0	<2.0	<2.0	<2.0
Na	95.5	90.4	117	183	148	354.5	219	393	<75	111
Ni	6.8	<5.0	11.4	15.7	15.5	18.5	6.5	18.4	<5.0	<5.0
P	620	602	417	542	900	552	464	520	516	271
Pb	12	<10	<10	<10	63.8	<10	<10	<10	<10	<10
S	1840	1700	1330	1390	2330	1110	1780	1110	1440	330
Sb	27.1	22.7	<10	<10	112	<10	<10	<10	50.4	<10
Se	<10	<10	<10	<10	<10	<10	<10	<10	<10	<10
Si	<10	<10	<10	<10	<10	<10	<10	<10	<10	<10
Sn	<2.0	<2.0	<2.0	<2.0	<2.0	<2.0	<2.0	<2.0	<2.0	<2.0
Sr	36.5	52.1	31	26.5	23.2	53.4	43.5	56.6	66.5	20
Ti	70.9	36.1	167	412	115	714	85	671	81.5	194
Tl	<1.0	<1.0	<1.0	<1.0	<1.0	<1.0	<1.0	<1.0	<1.0	<1.0
U	<10	<10	<10	<10	<10	<10	<10	<10	<10	<10
V	10.9	<10	15.1	27.8	17.4	37.35	15.9	37.8	<10	<10
Zn	131	64.7	47.6	44.9	66	44.05	<15	33	23.6	<15

Table D-1: ICP AES Results for Unsieved Giant Soil Core and Outcrop Samples *(cont)*

Sample	YK-37	YK-38*	YK-39	YK-40	YK-41	YK-121	YK-122*	YK-44	YK-42	YK-43
Location	Site 25 (cont.)		Site 26			Site 27				
Sample Type	C2	C2	O	C2	C2	O	O	Oct	C2	C2
Compression Corrected Depth	38.5	47.0	10.0	24.4	42.8	3.4	13.8	24.1	27.5	32.1
Ag	<2.0	<2.0	<2.0	<2.0	<2.0	<2.0	<2.0	<2.0	<2.0	<2.0
Al	4640	9750	1710	6050	7070	1870	2985	5450	7770	6780
As	26.1	23.85	49.1	144	42.7	211	72.8	157	161	140
Au	<5	<5	<5	<5	<5	<5	<5	<5	<5	<5
B	<20	<20	<20	<20	<20	<20	<20	<20	<20	<20
Ba	20.8	57.95	49.7	31.2	30.1	82.1	70.05	29.8	34.6	29.5
Be	<4.0	<4.0	<4.0	<4.0	<4.0	<4.0	<4.0	<4.0	<4.0	<4.0
Ca	1800	3460	22000	7000	2200	25373	26555	5300	2460	2010
Cd	<1.0	<1.0	<1.0	<1.0	<1.0	<1.0	<1.0	<1.0	<1.0	<1.0
Co	<5.0	7.75	<5.0	<5.0	<5.0	<5.0	<5.0	<5.0	<5.0	<5.0
Cr	<20	23.6	<20	<20	<20	<20	<20	<20	<20	<20
Cu	<5.0	9.05	15.7	15.8	<5.0	15	11.15	6.3	7.7	<5.0
Fe	7220	15800	1670	6440	7710	2510	3505	7350	11300	9930
K	484	1390	476	331	568	1160	602.5	563	643	617
Mg	2070	4055	1230	1940	2780	2720	2400	2220	2870	2660
Mn	173	434.5	802	57.2	112	679	208.5	72.2	128	94.6
Mo	<2.0	<2.0	<2.0	<2.0	<2.0	<2.0	<2.0	<2.0	<2.0	<2.0
Na	115	186	<75	95.9	131	<75	81.6	92	113	106
Ni	5.5	11.6	<5.0	5.4	7.1	8.7	<5.0	5.9	7.4	7.3
P	284	400	542	200	302	568	316.5	260	204	267
Pb	<10	<10	<10	<10	<10	14.2	<10	<10	<10	<10
S	50.1	71.9	1450	292	45.1	1710	1175	233	55.1	49
Sb	<10	<10	47.1	<10	<10	49.8	<10	<10	<10	<10
Se	<10	<10	<10	<10	<10	<10	<10	<10	<10	<10
Si	<10	<10	<10	<10	<10	<10	<10	<10	<10	<10
Sn	<2.0	<2.0	<2.0	<2.0	<2.0	<2.0	<2.0	<2.0	<2.0	<2.0
Sr	6.2	12.45	30.7	15.8	8.3	75	80.3	16.1	10.1	8.3
Ti	305	596	36.4	317	378	36.9	87.95	222	359	295
Tl	<1.0	<1.0	<1.0	<1.0	<1.0	<1.0	<1.0	<1.0	<1.0	<1.0
U	<10	<10	<10	<10	<10	<10	<10	<10	<10	<10
V	11.5	25.5	<10	13.6	15.3	<10	<10	14.6	27.6	22.8
Zn	<15	22.25	22.5	<15	<15	67.7	28	<15	15.1	<15

Table D-1: ICP AES Results for Unsieved Giant Soil Core and Outcrop Samples *(cont.)*

Sample	YK-115*	YK-236	YK-116	YK-237	YK-238	YK-45*	YK-46	YK-239	YK-47
Location	Site 28								
Sample Type	O	O	O	O	U	U	U	O	O
Compression Corrected Depth	2.4	5.9	13.5	19.4	24.1	25.9	30.0	33.5	38.2
Ag	<2.0	<2.0	<2.0	<2.0	<2.0	<2.0	<2.0	<2.0	<2.0
Al	6795	4070	4220	4710	13000	18250	20700	17200	8980
As	321	133	248	170	245	393	484	607	302
Au	<5	-	<5	-	-	<5	<5	-	<5
B	<20	<20	<20	<20	<20	23.25	25.4	<20	<20
Ba	115.5	91.9	87.3	92.7	125	139.5	158	183	132
Be	<4.0	<4.0	<4.0	<4.0	<4.0	<4.0	<4.0	<4.0	<4.0
Ca	27408	23700	22842	28800	20400	15100	13100	23550	26500
Cd	<1.0	<1.0	<1.0	<1.0	<1.0	<1.0	<1.0	<1.0	<1.0
Co	<5.0	<5.0	<5.0	<5.0	5.9	8.7	9.7	6.85	<5.0
Cr	<20	<20	<20	<20	<20	28.9	32.5	23.45	<20
Cu	22.15	22.6	16.1	19	19.2	17.75	21.5	30.45	21.9
Fe	8000	4810	4920	4540	12800	19050	21100	16100	8940
K	1165	772	761	597	2070	3165	3510	1920	1120
Mg	3925	3480	2820	3110	5350	6735	7210	5770	3750
Mn	251.5	153	205	143	166	218	226	143.5	76.4
Mo	3.25	10.6	5.9	4.2	<2.0	<2.0	<2.0	<2.0	<2.0
Na	135	<75	88.2	82.3	196	306.5	383	227.5	190
Ni	10.3	9.1	7.6	7.4	13.4	16.7	19.1	18.1	11.2
P	546.5	489	444	462	474	519	497	486	462
Pb	12.1	<10	<10	<10	<10	<10	<10	<10	<10
S	2170	2170	1860	2380	1590	972	709	1455	1920
Sb	47.85	24.4	33.4	20.4	<10	<10	<10	<10	<10
Se	<10	<10	<10	<10	<10	<10	<10	<10	<10
Si	<10	<10	<10	<10	<10	<10	<10	<10	<10
Sn	<2.0	<2.0	<2.0	<2.0	<2.0	<2.0	<2.0	<2.0	<2.0
Sr	59.4	61.3	49	65.4	65.8	66.45	68.9	75.55	78.3
Ti	165	122	102	90.6	331	706	759	308.5	387
Tl	<1.0	<1.0	<1.0	<1.0	<1.0	<1.0	<1.0	<1.0	<1.0
U	<10	<10	<10	<10	<10	<10	<10	20.4	<10
V	17.3	11	12.6	13.3	27.4	38.7	42.6	30.95	28.4
Zn	60.4	53.2	50.9	22.2	30.3	41.55	42.8	25.8	<15

Table D-1: ICP AES Results for Unsieved Giant Soil Core and Outcrop Samples *(cont.)*

Sample	YK-114	YK-48	YK-240	YK-26	YK-241	YK-49	YK-242	YK-243	YK-50	YK-244	YK-51
Location	Site 29								Site 31		
Sample Type	O	O	O	O	U	O	O	O	O	Oct	Oct
Compression Corrected Depth	2.4	8.1	12.5	16.3	23.0	22.5	28.3	32.6	1.7	6.0	7.7
Ag	<2.0	<2.0	<2.0	<2.0	<2.0	<2.0	<2.0	<2.0	<2.0	<2.0	<2.0
Al	10700	11700	13400	12500	16200	13900	17100	29700	7280	27100	24300
As	936	1495	1850	1434	762.5	876	1330	374	1423	333.5	327
Au	<5	<5	-	<5	-	<5	-	-	<5	-	5.9
B	<20	<20	<20	<20	<20	<20	<20	<20	21.6	<20	22.8
Ba	113	83.2	117	81.6	143	86.1	162	296	82	212	205
Be	<4.0	<4.0	<4.0	<4.0	<4.0	<4.0	<4.0	<4.0	<4.0	<4.0	<4.0
Ca	32210	16100	29600	16600	18100	7920	22000	8330	21600	12600	10000
Cd	<1.0	<1.0	1.1	1.6	<1.0	<1.0	<1.0	<1.0	<1.0	<1.0	<1.0
Co	9.7	10.6	10.7	13.6	12.1	12.2	11.3	18.2	6	13.6	13.4
Cr	<20	<20	<20	22.9	29.1	32	28.3	46.4	<20	44.2	41.7
Cu	80.5	68.7	103	107	118	53.9	117	45.1	34.5	30.6	27.9
Fe	14900	14500	14600	21600	19600	23900	19200	28000	10700	27400	26800
K	590	337	313	581	2210	1570	2330	4850	1020	5160	4480
Mg	4610	3950	4610	6600	7490	7580	7210	9820	6070	10500	9690
Mn	1130	1130	1150	565	575	450	457	427	272	439	437
Mo	2.8	3.6	3.3	<2.0	2.4	<2.0	2.4	<2.0	<2.0	<2.0	<2.0
Na	99.3	114	83.7	269	275	274	260	458	135	347	414
Ni	14.3	12.4	19.6	31.5	33.5	25.9	31.4	37.8	13.9	27	25.1
P	897	613	828	528	588	455	680	469	577	581	530
Pb	37.9	36	50.6	19.9	14	<10	44.7	<10	39.2	<10	<10
S	2970	1180	2080	1760	2160	648	2270	264	1390	454	269
Sb	101	118	136	92.3	25	28.9	129	<10	210	<10	<10
Se	<10	<10	<10	<10	<10	<10	<10	<10	<10	<10	<10
Si	<10	<10	<10	<10	<10	<10	<10	<10	<10	<10	<10
Sn	<2.0	<2.0	<2.0	<2.0	<2.0	<2.0	<2.0	<2.0	<2.0	<2.0	<2.0
Sr	44.5	30.6	47.6	32.5	39.2	21.3	45.1	76	107	97.6	74.9
Ti	142	188	119	659	424	633	346	834	169	771	824
Tl	<1.0	<1.0	<1.0	<1.0	<1.0	<1.0	<1.0	<1.0	<1.0	<1.0	<1.0
U	55.5	33.7	59	39.4	47.6	<10	49.2	<10	<10	<10	<10
V	22.6	21.8	22.8	60.5	38.1	50.9	36	54.4	16.9	51.5	50.2
Zn	134	129	135	90	89	67.1	94.9	53	73.7	52.5	51.4

Table D-1: ICP AES Results for Unsieved Giant Soil Core and Outcrop Samples
(cont.)

Sample	YK-52	YK-245	YK-246	YK-53	YK-54	YK-118	YK-119	YK-228	YK-55	YK-229	YK-56*
Location	Site 31 (cont.)					Site 32					
Sample Type	C1	C1	C1	C1	C1	O	O	O	O	O	O
Compression Corrected Depth	11.1	16.2	21.4	27.3	37.6	0.7	3.6	6.5	8.6	10.1	12.2
Ag	<2.0	<2.0	<2.0	<2.0	<2.0	<2.0	<2.0	<2.0	<2.0	<2.0	<2.0
Al	25100	22300	19350	21700	25700	4090	3640	2240	3080	6210	14600
As	270	227	201.5	209	158	1727	370	29.9	29.1	42	204
Au	<5	-	-	5.4	<5	<5	<5	-	<5	-	<5
B	29.1	<20	<20	27.2	30.6	21.6	<20	<20	<20	<20	<20
Ba	198	167	147.5	177	266	163	138	95.5	81.9	113	127.5
Be	<4.0	<4.0	<4.0	<4.0	<4.0	<4.0	<4.0	<4.0	<4.0	<4.0	<4.0
Ca	8040	4740	4420	5550	8990	33470	47196	38800	39700	48800	18050
Cd	<1.0	<1.0	<1.0	<1.0	<1.0	1.3	1	<1.0	<1.0	<1.0	<1.0
Co	12.9	12	11.05	11	15.2	5.7	<5.0	<5.0	<5.0	<5.0	9.55
Cr	43.1	41.9	36.9	39.2	42	<20	<20	<20	<20	<20	36.05
Cu	27	19.6	17	22.7	37.5	43.5	48.3	33	35.1	31.1	29.05
Fe	27200	26100	23500	23600	24100	8030	3760	2180	3180	6350	19250
K	4930	4900	4035	4180	4180	873	652	365	379	666	1530
Mg	9570	8820	7900	8330	8800	2760	2540	2380	2230	3370	6735
Mn	375	329	294	290	331	659	349	42.6	159	122	293.5
Mo	<2.0	<2.0	<2.0	<2.0	<2.0	<2.0	<2.0	<2.0	<2.0	<2.0	<2.0
Na	401	366	338	445	511	87.8	85.8	<75	89.8	97.3	251.5
Ni	24.9	25.4	22.65	23.2	30.8	14.9	9.9	7.9	9.5	10.4	21.55
P	526	458	441	437	435	1380	1210	590	514	610	448.5
Pb	<10	<10	<10	<10	<10	75.1	<10	<10	<10	<10	<10
S	181	46.9	45.8	85.3	352	1930	1440	1500	1130	1390	542
Sb	<10	<10	<10	<10	<10	126	33	34	23.3	20.3	<10
Se	<10	<10	<10	<10	<10	<10	<10	<10	<10	<10	<10
Si	<10	<10	<10	<10	<10	<10	<10	<10	<10	<10	<10
Sn	<2.0	<2.0	<2.0	<2.0	<2.0	<2.0	<2.0	<2.0	<2.0	<2.0	<2.0
Sr	67.7	44.3	38.7	48.3	75.4	25.5	32.9	36.5	33.3	41.7	24.05
Ti	893	874	715	928	922	28.7	37.8	36.9	76.3	125	470
Tl	<1.0	<1.0	<1.0	<1.0	<1.0	<1.0	<1.0	<1.0	<1.0	<1.0	<1.0
U	<10	<10	<10	<10	<10	<10	<10	<10	<10	<10	<10
V	52.6	47.5	42.55	46.8	50.5	12.8	11.8	10.9	11.5	17.9	40.35
Zn	53.6	49.9	43.3	47.4	48.9	138	44.6	<15	<15	<15	32.45

Table D-1: ICP AES Results for Unsieved Giant Soil Core and Outcrop Samples

Sample	YK-230	YK-57*	YK-58	YK-59	YK-60	YK-61	YK-304	YK-68*	YK-62	YK-64	YK-65
Location	Site 32 (cont.)		Site 40	Site 41	Site 42	Site 43	Site 45	Site 44	Site 47	Site 48	Site 49
Sample Type	Oct	Oct	O	O	O	O	O	O	O	O	C1
Compression Corrected Depth	15.8	18.7	OSS	OSS	OSS	OSS	OSS	OSS	OSS	OSS	OSS
Ag	<2.0	<2.0	<2.0	<2.0	<2.0	<2.0	-	<2.0	<2.0	<2.0	<2.0
Al	20300	23000	1720	12600	11100	7930	-	2180	21800	6080	25900
As	215	197	911	3280	666	1589	709	100	2067	2543	102
Au	-	<5	<5	<5	<5	<5	-	<5	<5	<5	<5
B	<20	25.15	<20	<20	<20	<20	-	25.2	<20	<20	27.6
Ba	142	159.5	70	181	148	526	-	75.55	72.9	464	210
Be	<4.0	<4.0	<4.0	<4.0	<4.0	<4.0	-	<4.0	<4.0	<4.0	<4.0
Ca	5650	6495	26500	11300	29100	15800	-	45500	2620	15600	8930
Cd	<1.0	<1.0	<1.0	<1.0	3.1	1.2	-	<1.0	<1.0	1.2	<1.0
Co	13.7	14	<5.0	22.8	13.2	53.8	-	<5.0	15.9	14.5	15.1
Cr	49.6	51.5	<20	38.2	35.9	<20	-	<20	33.8	<20	55.6
Cu	24.7	22.95	38.9	60.2	129	48.4	-	54.95	10.9	37	32.5
Fe	27000	29100	2890	19700	17100	12800	-	2540	35200	13400	31600
K	3300	4165	194	395	545	640	-	118.5	1180	676	5710
Mg	9410	9960	3160	4910	6740	3360	-	2815	8270	4240	12700
Mn	401	411.5	558	3360	1310	6700	8100	867	783	4960	438
Mo	<2.0	<2.0	5.5	12.2	<2.0	<2.0	1010	<2.0	<2.0	<2.0	<2.0
Na	357	450.5	<75	125	106	169	-	86.45	147	160	659
Ni	29.6	29.3	5.6	25.6	24.3	25.3	-	6	17	15.1	33.1
P	235	310	407	493	1470	686	-	528	626	741	468
Pb	<10	<10	37	96.7	65.3	43.8	-	<10	14.2	70.8	<10
S	112	121	1200	982	2050	1170	1600	1075	231	1270	119
Sb	<10	<10	216	506	48.5	131	52.9	<10	49.6	208	<10
Se	<10	<10	<10	<10	<10	<10		<10	<10	<10	<10
Si	<10	<10	<10	<10	<10	<10		<10	<10	<10	<10
Sn	<2.0	<2.0	<2.0	<2.0	<2.0	<2.0	-	<2.0	<2.0	<2.0	<2.0
Sr	23	29.65	33.3	16.2	35.2	34.8	-	46.6	18.5	28.9	36.7
Ti	732	1069	27.1	585	263	217	466	71.75	718	121	1194
Tl	<1.0	<1.0	<1.0	1.2	<1.0	4.1	-	<1.0	<1.0	2.9	<1.0
U	<10	<10	<10	<10	<10	<10	-	<10	<10	<10	<10
V	48.2	57.25	<10	40.1	33.4	21	-	<10	80	19.6	61.1
Zn	44.7	48.6	186	181	334	115	225	45.2	129	265	58.5

Table D-2: Mess-3 Standards

Sample	Mess-3(1)	Mess-3(1)	Mess-3(1)	Mess-3(1)	Mess-3(1)	Mess-3(1)	Mess-3(1)	Mess-3(1)
Ag	<2.0	<2.0	<2.0	<2.0	<2.0	<2.0	<2.0	<2.0
Al	18900	32900	22700	28700	26400	24300	22400	24200
As	15.4	16.6	16.8	16.8	16.6	16.1	17	15.6
Au	<5	-	<5	<5	<5	<5	-	-
B	30.4	62.8	41.8	61	28.5	<20	<20	<20
Ba	304	390	338	395	367	400	349	340
Be	<4.0	<4.0	<4.0	<4.0	<4.0	<4.0	<4.0	<4.0
Ca	12500	13300	12500	12800	12700	13200	13500	12700
Cd	<1.0	<1.0	<1.0	<1.0	<1.0	<1.0	<1.0	<1.0
Co	10.7	12.1	11.6	12.1	11.7	12	12	11.7
Cr	32	48.4	36.6	45.8	41	40.4	37	38.6
Cu	36	32.3	31.5	32.1	31.8	33.2	35	31.5
Fe	31500	36700	33300	34500	34800	35600	34100	33300
K	4970	7860	5830	6860	6580	6040	5750	6290
Mg	12900	14300	12800	13500	13000	13600	14000	12900
Mn	284	299	287	307	290	315	314	289
Mo	<2.0	<2.0	<2.0	2.1	<2.0	<2.0	<2.0	<2.0
Na	9900	11300	10700	10700	10500	11000	11600	10700
Ni	33.8	37.2	35.6	37	36.6	38	39	37.6
P	963	1040	1000	1060	993	997	948	915
Pb	14.9	16.5	16.3	16.1	15.8	15.9	16	16.3
S	1520	1610	1520	1650	1610	1620	1530	1490
Sb	<10	<10	<10	<10	<10	<10	<10	<10
Se	<10	<10	<10	<10	<10	<10	<10	<10
Si	<10	<10	<10	<10	<10	<10	<10	<10
Sn	<2.0	<2.0	<2.0	<2.0	<2.0	<2.0	<2.0	<2.0
Sr	57.6	71.3	63.5	70.1	63	65.5	64	61.5
Ti	14.8	79.4	24.3	95.9	12.6	33.4	37	10.1
Tl	<1.0	<1.0	<1.0	<1.0	<1.0	<1.0	<1.0	<1.0
U	<10	<10	<10	<10	<10	<10	<10	<10
V	78.4	122	87.5	115	97.8	91.4	81	86.8
Zn	123	135	129	132	127	126	133	126

Table D-3: SS-2 Standards

Sample	SS-2	SS-2	SS-2	SS-2	SS-2	SS-2	SS-2	SS-2
Ag	<2.0	<2.0	<2.0	<2.0	<2.0	<2.0	<2.0	<2.0
Al	17900	18100	17200	17900	18700	18800	17100	18200
As	76.1	49.2	52.5	74.3	80	80	63	76.7
Au	<5	-	<5	<5	<5	<5	-	-
B	20.8	22.7	20.6	25.6	28.4	<20	<20	<20
Ba	239	221	238	238	234	249	233	231
Be	<4.0	<4.0	<4.0	<4.0	<4.0	<4.0	<4.0	<4.0
Ca	1E+05	1E+05	1E+05	1E+05	1E+05	1E+05	####	1E+05
Cd	2.1	2.2	2.1	2.2	2.3	2.4	2	2
Co	14.1	13.3	13.4	14.5	14.3	15.3	14	14.6
Cr	43.5	43.6	42.8	44.9	43.8	46.2	41	42.9
Cu	190	194	200	197	199	208	183	184
Fe	25900	26500	24600	25700	26800	28400	26400	27600
K	5060	5140	4850	5040	5240	5380	4480	4620
Mg	13400	12500	11800	12000	12600	13100	12700	12400
Mn	565	534	561	532	537	562	544	534
Mo	2.3	2.2	<2.0	2.4	3.1	2.4	2	2.5
Na	727	740	723	816	712	708	648	640
Ni	53.2	54.6	53.4	54.5	53.5	58.3	55	55.3
P	754	445	499	741	701	728	545	696
Pb	116	110	114	108	115	124	122	120
S	2060	2070	1920	2150	2200	2330	2040	2030
Sb	<10	<10	<10	<10	<10	<10	<10	<10
Se	<10	<10	<10	<10	<10	<10	<10	<10
Si	<10	<10	<10	<10	<10	<10	<10	<10
Sn	2.8	2.9	<2.0	4.2	3.1	2.1	2	<2.0
Sr	238	205	220	211	214	224	212	211
Ti	1160	775	739	1460	1220	1120	1000	1120
Tl	<1.0	<1.0	<1.0	<1.0	<1.0	<1.0	<1.0	<1.0
U	<10	<10	<10	<10	<10	<10	<10	<10
V	49.4	48.5	46.3	50.6	49.7	47.5	46	47.6
Zn	467	469	468	474	480	452	468	468

Table D-4: Mess-3 and SS-2 Control Limits set by ASU, Queen's University

	LOW WARNING	HIGH WARNING	LOW WARNING	HIGH WARNING
Sample	Mess-3(1)	Mess-3(1)	SS-2	SS-2
Ag	<2.0	<2.0	-	-
Al	18800	30500	14900	20600
As	14	17	62.9	95.1
Au	-	-	-	-
B	N/A	N/A	N/A	N/A
Ba	313	427	214	272
Be	<4.0	<4.0	N/A	N/A
Ca	11900	15300	104000	137000
Cd	<1.0	<1.0	0.6	2.5
Co	11	14	12.5	16.3
Cr	31	50	39.1	52.2
Cu	30	37	169	214
Fe	32300	40700	23200	30500
K	4880	7880	4210	6310
Mg	12400	15200	11500	14400
Mn	283	324	477	625
Mo	<2.0	<2.0	1.5	3.7
Na	10400	12800	669	1010
Ni	35	41	51.1	58.8
P	949	1170	503	811
Pb	16	20	105	125
S	1550	1930	1930	2390
Sb	<10	<10	<10	<10
Se	<10	<10	<10	<10
Si	N/A	N/A	<10	<10
Sn	<2.0	<2.0	1.6	3.9
Sr	59	77	193	248
Ti	N/A	N/A	769	1480
Tl	<1.0	1	<1.0	<1.0
U	<10	<10	<10	<10
V	77	117	42.1	55.8
Zn	125	147	417	519

Appendix E: North Brookfield Mine- Soil Chemistry on Unsieved Samples

Aqua Regia analyses on bulk unsieved soils from the North Brookfield mine, NS were performed by the author at the Analytical Services Unit (ASU) at Queen's University.

Table E-1: ICP AES Results for Unsieved North Brookfield Soil Core Samples

Sample	NB-130	NB-86	NB-214	NB-87*	NB-215	NB-216	NB-88	NB-217	NB-218	NB-219
Location	Site 1									
Sample Type	A	A	Abt	B	B	BCt	C1	C1	C1	C1
Compression Corrected Depth	0.6	2.3	9.2	14.4	19.5	24.1	17.2	33.3	37.9	42.5
Ag	<2.0	<2.0	<2.0	<2.0	<2.0	<2.0	<2.0	<2.0	<2.0	<2.0
Al	26000	21100	27700	30900	30300	30300	28000	26450	28800	29300
As	388	343	154	67.15	40	23	49.9	21.75	5	39
Au	<5	<5	-	<5	-	-	<5	-	-	-
B	<20	<20	<20	<20	<20	<20	<20	<20	<20	<20
Ba	70.1	52.3	51	65.35	55	59	54.9	48.45	51	74
Be	<4.0	<4.0	<4.0	<4.0	<4.0	<4.0	<4.0	<4.0	<4.0	<4.0
Ca	865	475	291	212.5	183	164	148	151	161	156
Cd	<1.0	<1.0	<1.0	<1.0	<1.0	<1.0	<1.0	<1.0	<1.0	<1.0
Co	8.4	8	8	9.75	9	11	10.8	9.1	10	11
Cr	27.1	28.8	31	37.55	35	36	37.8	32.3	31	35
Cu	22.5	21.1	26	26.65	28	28	31.8	30.5	29	33
Fe	39400	35800	41400	46050	42800	42300	62900	39850	39900	42700
K	1510	850	1010	1470	1070	1460	1360	1175	1290	2180
Mg	4420	4010	5200	5770	5660	7280	8560	7750	8860	8130
Mn	1443	1270	1500	1490	1450	1710	2200	2105	2510	2361
Mo	<2.0	<2.0	<2.0	<2.0	<2.0	<2.0	<2.0	<2.0	<2.0	<2.0
Na	166	96	132	180.5	121	199	140	152	132	290
Ni	18.9	19	20	21.45	23	24	25.4	23.6	26	24
P	536	439	414	461.5	320	225	310	179.5	114	346
Pb	24.1	19.2	14	12.65	14	11	12	10.1	<10	13
S	416	298	238	208	181	147	160	102.05	39	85
Sb	<10	<10	<10	<10	<10	<10	<10	<10	<10	<10
Se	<10	<10	<10	<10	<10	<10	<10	<10	<10	<10
Si	<10	<10	<10	<10	<10	<10	<10	<10	<10	<10
Sn	<2.0	<2.0	<2.0	<2.0	<2.0	<2.0	<2.0	<2.0	<2.0	<2.0
Sr	12.3	7.5	5	8	<5.0	6	6.1	<5.0	<5.0	10
Ti	167	130	39	524	148	320	713	435.5	526	381
Tl	<1.0	<1.0	<1.0	<1.0	<1.0	<1.0	<1.0	<1.0	<1.0	<1.0
U	<10	<10	<10	<10	<10	<10	<10	<10	<10	<10
V	24.7	25.8	25	31.85	29	26	27.6	22.35	18	27
Zn	77.4	78.5	81	86.95	80	77	78.9	67	74	69

Table E-1: ICP AES Results for Unsieved North Brookfield Soil Core Samples (*cont.*)

Sample	NB-220	NB-89	NB-221	NB-129	NB-82*	NB-83	NB-200	NB-201	NB-202
Location	Site 1 (cont.)			Site 2					
Sample Type	C1	C1	C1	A	A	AC	AC	C1	C1
Compression Corrected Depth	46.0	47.1	50.0	0.6	3.4	7.3	11.2	15.2	19.6
Ag	<2.0	<2.0	<2.0	<2.0	<2.0	<2.0	<2.0	<2.0	<2.0
Al	28500	24600	25700	16100	16600	22400	22100	26100	28000
As	36	29.1	24	4303	3417	3676	1920	418	155
Au	-	<5	-	<5	<5	<5	-	-	-
B	<20	<20	<20	<20	<20	<20	<20	<20	<20
Ba	69	61.1	59	52.4	61.7	71.3	50	48	49
Be	<4.0	<4.0	<4.0	<4.0	<4.0	<4.0	<4.0	<4.0	<4.0
Ca	157	145	130	2010	1910	2040	1030	490	274
Cd	<1.0	<1.0	<1.0	<1.0	<1.0	<1.0	<1.0	<1.0	<1.0
Co	13	13.7	14	18.4	17.5	18.2	14	10	9
Cr	35	33.9	32	<20	20	28.1	27	33	35
Cu	40	33.8	31	31.5	35.5	40.6	37	37	38
Fe	45200	44800	39500	38400	38600	46900	39200	41100	51200
K	1750	1650	1870	1860	2440	2630	1550	1250	1110
Mg	8470	8320	8060	5320	5500	7560	6200	6930	7580
Mn	2060	1960	2540	1420	1040	1360	1250	1610	1760
Mo	<2.0	<2.0	<2.0	8.3	9.1	10.7	7	7	5
Na	120	139	149	105	118	147	124	113	95
Ni	25	22.5	21	24.5	24	29.9	33	28	30
P	378	325	306	639	603	721	402	319	274
Pb	17	14.3	13	36.1	34	35.4	21	14	13
S	151	131	109	429	388	542	335	279	121
Sb	<10	<10	<10	<10	<10	<10	<10	<10	<10
Se	<10	<10	<10	<10	<10	<10	<10	<10	<10
Si	<10	<10	<10	<10	<10	<10	<10	<10	<10
Sn	<2.0	<2.0	<2.0	<2.0	<2.0	<2.0	<2.0	<2.0	<2.0
Sr	8	7.6	7	18.3	18.4	19.7	12	8	6
Ti	589	737	936	70.3	272	314	131	259	269
Tl	<1.0	<1.0	<1.0	<1.0	<1.0	<1.0	<1.0	<1.0	1
U	<10	<10	<10	<10	<10	<10	<10	<10	<10
V	26	23.9	25	14.1	17.4	23.2	21	24	23
Zn	73	67.3	64	107	102	142	121	101	100

Table E-1: ICP AES Results for Unsieved North Brookfield Soil Core Samples *(cont.)*

Sample	NB-203	NB-84	NB-204	NB-205	NB-206	NB-85	NB-207	NB-90	NB-91	NB-92
Location	Site 2 (cont.)							Site 3		
Sample Type	C1	C1	C1	C1	C1	C1	C1	A-Ae	BCt	C1
Compression Corrected Depth	23.6	28.6	33.7	38.2	41.8	47.1	50.5	5.0	24.4	41.0
Ag	<2.0	<2.0	<2.0	<2.0	<2.0	<2.0	<2.0	<2.0	<2.0	<2.0
Al	27850	27700	29200	26800	26600	25700	27000	26200	29900	40500
As	86.3	48.7	38	35	38	34.8	36	80	74.1	97.4
Au	-	<5	-	-	-	<5	-	<5	<5	<5
B	<20	<20	<20	<20	<20	<20	<20	<20	<20	<20
Ba	53	62	59	54	54	55.8	54	72.9	41.6	64.9
Be	<4.0	<4.0	<4.0	<4.0	<4.0	<4.0	<4.0	<4.0	<4.0	<4.0
Ca	228	208	159	137	138	130	115	526	164	188
Cd	<1.0	<1.0	<1.0	<1.0	<1.0	<1.0	<1.0	<1.0	<1.0	<1.0
Co	9.55	11.5	11	11	10	9.6	11	7.7	9.1	18.8
Cr	34.05	35.3	36	35	35	33.3	34	27.6	29.7	40.8
Cu	39	32.3	31	28	30	29.1	30	13.7	13.7	32.5
Fe	43000	44600	58700	56400	41800	43200	42600	38200	44600	45400
K	1245	1530	1380	1230	1200	1480	1200	1300	930	1380
Mg	6975	7550	7400	7520	7410	7890	7570	3610	3420	7040
Mn	1900	2180	2110	2150	2260	1940	1930	1270	1030	1470
Mo	4.9	3.4	3	2	<2.0	<2.0	<2.0	<2.0	<2.0	<2.0
Na	110	148	148	105	132	140	127	128	109	135
Ni	27.85	28	30	28	28	25.4	27	14.3	14.4	38.7
P	298	314	276	250	249	272	239	344	214	208
Pb	14.6	14	13	12	12	13	13	19.8	10.6	14
S	137	166	155	141	130	127	118	378	195	181
Sb	<10	<10	<10	<10	<10	<10	<10	<10	<10	<10
Se	<10	<10	<10	<10	<10	<10	<10	<10	<10	<10
Si	<10	<10	<10	<10	<10	<10	<10	<10	<10	<10
Sn	<2.0	<2.0	<2.0	<2.0	<2.0	<2.0	<2.0	<2.0	<2.0	<2.0
Sr	5.4	6.8	6	<5.0	<5.0	5.7	<5.0	13.4	<5.0	6.1
Ti	485.5	705	559	545	569	766	378	563	418	494
Tl	<1.0	<1.0	<1.0	<1.0	<1.0	<1.0	<1.0	<1.0	<1.0	<1.0
U	<10	<10	<10	<10	<10	<10	<10	<10	<10	<10
V	25.7	26.9	28	28	26	25.1	24	34	35.6	34.9
Zn	88.9	79.1	77	75	71	68.9	70	53.1	40.4	66.9

Table E-1: ICP AES Results for Unsieved North Brookfield Soil Core Samples *(cont.)*

Sample	YK-131	NB-93	NB-208	NB-94	NB-209	NB-95*	NB-210	NB-211	NB-99	NB-100
Location	Site 4								Site 5	
Sample Type	O	O	B	B	BCt	BCt	C1	C1	Ap	Ap
Compression Corrected Depth	1.4	4.4	9.4	13.3	18.8	24.4	28.8	34.4	4.4	11.4
Ag	<2.0	<2.0	<2.0	<2.0	<2.0	<2.0	<2.0	<2.0	<2.0	<2.0
Al	2170	17100	27400	26000	31000	29450	27900	25900	24700	32400
As	8	45.8	41	35	30	27.2	19	18.55	28.2	41.1
Au	<5	-	-	<5	-	<5	-	-	<5	<5
B	<20	<20	<20	<20	<20	<20	<20	<20	<20	<20
Ba	41.7	55.9	33	38.6	46	53.25	42	44.9	65	78.7
Be	<4.0	<4.0	<4.0	<4.0	<4.0	<4.0	<4.0	<4.0	<4.0	<4.0
Ca	501	132	<100	119	103	130	101	<100	389	301
Cd	<1.0	<1.0	<1.0	<1.0	<1.0	<1.0	<1.0	<1.0	<1.0	<1.0
Co	<5.0	<5.0	6	6.7	8	7.65	8	8.4	8	11.5
Cr	<20	20.5	32	30.4	34	32.25	31	30.85	29.5	38.4
Cu	8.6	13.9	15	13.8	21	19.15	17	20.7	16.6	21.9
Fe	1810	29700	68700	48800	43200	39000	38300	38900	37000	49000
K	643	720	808	1040	897	1225	907	946	1240	1650
Mg	933	2470	5240	5420	6480	6325	6920	7780	4820	5820
Mn	62.3	617	1330	1230	1400	1330	1620	1805	1280	1540
Mo	<2.0	<2.0	<2.0	<2.0	<2.0	<2.0	<2.0	<2.0	<2.0	<2.0
Na	182	134	92	124	98	137.5	86	101.7	156	206
Ni	5.3	9.8	15	15	22	19.95	23	24.1	15.6	18.5
P	506	252	233	232	187	197.5	144	104.7	388	472
Pb	16.3	30.5	14	14.4	15	12	11	12.4	14.7	22.1
S	1230	240	266	341	225	294.5	188	112.5	312	361
Sb	<10	<10	<10	<10	<10	<10	<10	<10	<10	<10
Se	<10	<10	<10	<10	<10	<10	<10	<10	<10	<10
Si	<10	<10	<10	<10	<10	<10	<10	<10	<10	<10
Sn	<2.0	<2.0	<2.0	<2.0	<2.0	<2.0	<2.0	<2.0	<2.0	<2.0
Sr	18.1	<5.0	<5.0	<5.0	<5.0	5	<5.0	<5.0	8.3	8.7
Ti	18.4	196	303	483	174	598	494	462.5	307	660
Tl	<1.0	<1.0	<1.0	<1.0	<1.0	<1.0	<1.0	<1.0	<1.0	<1.0
U	<10	<10	<10	<10	<10	<10	<10	<10	<10	<10
V	<10	30.4	35	30.9	27	29.3	22	21.4	26.3	35.9
Zn	57.8	36.2	46	46.1	57	54.95	58	58.55	71.1	100

Table E-1: ICP AES Results for Unsieved North Brookfield Soil Core Samples *(cont.)*

Sample	NB-101*	NB-66-1	NB-96*	NB-97	NB-98	NB-76	NB-70	NB-71	NB-212	NB-72
Location	Site 5 (cont.)	Site 6	Site 7			Site 8				
Sample Type	BCt	C1/C2	A-Ae	B	BCt	O	O	Ae	B	B
Compression Corrected Depth	36.6	64.5	4.0	14.1	24.9	1.8	5.4	6.6	11.3	14.3
Ag	<2.0	<2.0	<2.0	<2.0	<2.0	<2.0	<2.0	<2.0	<2.0	<2.0
Al	25250	20600	12450	38000	39000	1020	3540	10500	20300	33700
As	28	29.3	114.5	127	88.9	1.9	3.2	19	27	36.2
Au	<5	<5	<5	<5	<5	<5	<5	<5	-	<5
B	<20	<20	<20	<20	<20	<20	<20	<20	<20	<20
Ba	56.3	42.7	45.35	49.8	69.1	13.7	28	18.1	31	50.1
Be	<4.0	<4.0	<4.0	<4.0	<4.0	<4.0	<4.0	<4.0	<4.0	<4.0
Ca	183	200	292	173	157	1310	321	169	123	186
Cd	<1.0	<1.0	<1.0	<1.0	<1.0	<1.0	<1.0	<1.0	<1.0	<1.0
Co	9.9	8.4	<5.0	9.5	12.7	<5.0	<5.0	<5.0	<5.0	9.5
Cr	31.1	30.8	<20	40.7	42.5	<20	<20	<20	26	42.4
Cu	20.3	20.3	11	23.5	35.5	6.6	6.2	9.3	13	20.1
Fe	41250	32600	20700	46700	47900	779	3910	21300	43500	61700
K	1285	1230	671.5	1200	1390	681	525	611	997	1200
Mg	6005	6060	1445	4980	8260	584	569	1530	3130	4820
Mn	1360	1270	530	1400	1830	78.9	159	557	772	1330
Mo	<2.0	<2.0	<2.0	<2.0	<2.0	<2.0	<2.0	<2.0	<2.0	<2.0
Na	138.5	123	81.8	147	141	152	124	97.6	104	123
Ni	16.95	19.3	6.7	20.1	31.7	<5.0	<5.0	5.7	10	21.7
P	278	134	221.5	358	239	575	347	172	237	406
Pb	11.2	<10	22.2	10.9	13	<10	40.9	17.5	18	22.4
S	239.5	63.5	180.5	268	176	1330	472	121	143	322
Sb	<10	<10	<10	<10	<10	<10	<10	<10	<10	<10
Se	<10	<10	<10	<10	<10	<10	<10	<10	<10	<10
Si	<10	<10	<10	<10	<10	<10	<10	<10	<10	<10
Sn	<2.0	<2.0	<2.0	<2.0	<2.0	<2.0	<2.0	<2.0	<2.0	<2.0
Sr	5.3	<5.0	5.9	5.9	<5.0	11	8.4	<5.0	<5.0	<5.0
Ti	582	650	192.5	578	847	16.7	154	268	178	364
Tl	<1.0	<1.0	<1.0	<1.0	<1.0	<1.0	<1.0	<1.0	<1.0	<1.0
U	<10	<10	<10	<10	<10	<10	<10	<10	<10	<10
V	28.85	21.9	24.8	32.6	33.6	<10	<10	31.3	37	36.5
Zn	60.3	60.4	20.45	53.1	71.5	27.9	24.2	23	37	73.8

Table E-1: ICP AES Results for Unsieved North Brookfield Soil Core Samples *(cont.)*

Sample	NB-73	NB-77*	NB-213	NB-74	NB-75	NB-78	NB-79	NB-80	NB-81	NB-106
Location	Site 8 (cont.)					Site 9				Site 10
Sample Type	BCt	BCt	C1	C1	C2	Ae	B	BCt	C1	B
Compression Corrected Depth	20.3	24.4	29.8	34.6	39.9	2.2	22.5	28.7	32.4	5.3
Ag	<2.0	<2.0	<2.0	<2.0	<2.0	<2.0	<2.0	<2.0	<2.0	<2.0
Al	28400	28950	26000	24600	26800	13200	15800	29600	36200	25200
As	26.5	28.15	28	29	36	82.8	43.9	51.9	50.5	49.6
Au	<5	<5	-	<5	<5	<5	<5	<5	<5	<5
B	<20	<20	<20	<20	<20	<20	<20	<20	<20	<20
Ba	48.5	63.65	59	70.2	86.3	48	16.1	42.5	51.5	83.9
Be	<4.0	<4.0	<4.0	<4.0	<4.0	<4.0	<4.0	<4.0	<4.0	<4.0
Ca	180	145.5	<100	127	146	253	109	137	166	413
Cd	<1.0	<1.0	<1.0	<1.0	<1.0	<1.0	<1.0	<1.0	<1.0	<1.0
Co	10.7	12.05	11	11.3	13.1	<5.0	<5.0	8.5	15.6	10.6
Cr	34	35.8	32	34.8	35.1	<20	<20	32.9	39.5	32
Cu	22.7	29.45	31	30.9	36	12.6	6.1	16.2	29.3	18.3
Fe	38100	39850	38700	37200	39200	23300	24300	39000	40900	41200
K	1240	1500	1480	1700	2240	1000	436	939	990	1380
Mg	5790	6840	7660	7060	7390	1680	864	4260	6330	5720
Mn	1320	1340	1330	1430	1410	301	520	900	1370	1790
Mo	<2.0	<2.0	<2.0	<2.0	<2.0	<2.0	<2.0	<2.0	<2.0	<2.0
Na	120	123	112	143	171	86	84.4	104	121	185
Ni	23.3	27.5	25	24.8	23.6	7.1	<5.0	18.3	34.1	19.7
P	288	232.5	201	220	367	262	117	189	200	603
Pb	14.8	15.4	13	14.2	18.4	24.3	<10	10.6	11.5	20.2
S	203	128	69	82.4	92.2	232	54.4	261	403	320
Sb	<10	<10	<10	<10	<10	<10	<10	<10	<10	<10
Se	<10	<10	<10	<10	<10	<10	<10	<10	<10	<10
Si	<10	<10	<10	<10	<10	<10	<10	<10	<10	<10
Sn	<2.0	<2.0	<2.0	<2.0	<2.0	<2.0	<2.0	<2.0	<2.0	<2.0
Sr	<5.0	<5.0	<5.0	<5.0	5.4	6	<5.0	<5.0	<5.0	10.3
Ti	497	564	584	564	844	130	163	91.2	398	322
Tl	<1.0	<1.0	<1.0	<1.0	<1.0	<1.0	<1.0	<1.0	<1.0	<1.0
U	<10	<10	<10	<10	<10	<10	<10	<10	<10	<10
V	25.8	26.85	27	20.6	29.8	27.6	34.8	32.2	30.2	27.9
Zn	77.7	80.65	68	71.1	77.5	21.7	<15	43.4	66.6	98.2

Table E-1: ICP AES Results for Unsieved North Brookfield Soil Core Samples *(cont.)*

Sample	NB-107	NB-108	NB-105	NB-102	NB-103	NB-109	NB-104	NB-110*	NB-111
Location	Site 10 (cont.)		Site 11					Site 12	
Sample Type	B	C1	A	ABt	B	B	BCt	A	B
Compression Corrected Depth	34.4	42.1	12.9	20.1	25.4	34.4	45.8	6.9	68.0
Ag	<2.0	<2.0	<2.0	<2.0	<2.0	<2.0	<2.0	<2.0	<2.0
Al	25300	24700	25200	28100	30200	26400	33100	27100	31000
As	23	25	39.1	30.1	26.6	25.6	30.9	45.55	25.3
Au	<5	<5	<5	<5	<5	<5	<5	<5	<5
B	<20	<20	<20	<20	<20	<20	<20	<20	<20
Ba	56.1	57.7	64.4	60.5	64.9	52.7	72.5	68.2	65.7
Be	<4.0	<4.0	<4.0	<4.0	<4.0	<4.0	<4.0	<4.0	<4.0
Ca	163	112	232	176	172	153	191	217	179
Cd	<1.0	<1.0	<1.0	<1.0	<1.0	<1.0	<1.0	<1.0	<1.0
Co	11	10.8	7.7	8.3	8.5	6.5	9.8	11.35	12.8
Cr	33.2	32.6	30.6	31.9	34.5	28.8	37	34.1	36
Cu	22.9	29.2	24.2	24.6	24.9	19.2	28.9	20.55	21.7
Fe	42100	43700	42100	40300	43400	40300	46100	42550	44200
K	1470	1660	1430	1190	1490	1100	1520	1485	1470
Mg	7400	8590	5190	5070	5490	3750	6020	5810	5940
Mn	2230	1930	1470	1290	1550	936	1480	2090	2270
Mo	<2.0	<2.0	<2.0	<2.0	<2.0	<2.0	<2.0	<2.0	<2.0
Na	161	172	189	119	164	131	165	190	182
Ni	21.8	21.2	20	25	24.4	15.5	28.9	20.05	22.5
P	273	253	395	365	343	384	368	555.5	424
Pb	10.5	12.4	17.2	15	12.6	15.8	14	16.25	12.4
S	150	105	265	164	145	192	151	302.5	320
Sb	<10	<10	<10	<10	<10	<10	<10	<10	<10
Se	<10	<10	<10	<10	<10	<10	<10	<10	<10
Si	<10	<10	<10	<10	<10	<10	<10	<10	<10
Sn	<2.0	<2.0	<2.0	<2.0	<2.0	<2.0	<2.0	<2.0	<2.0
Sr	6.8	6.4	7.1	5.5	6.3	5.1	6.8	7.95	7.1
Ti	892	742	670	565	641	445	636	590	627
Tl	<1.0	<1.0	<1.0	<1.0	<1.0	<1.0	<1.0	<1.0	<1.0
U	<10	<10	<10	<10	<10	<10	<10	<10	<10
V	25.2	24.8	27.4	27.4	28.1	29.2	30.8	29.55	28.8
Zn	70.8	66.5	71.6	80.7	77.1	63.1	87.8	77.7	102

Appendix F: Organic Carbon Results

Organic carbon analysis was performed at Dr. Paul Grogen's Lab at Queen's University

Table F-1: Organic Carbon Results [%] from the Giant Mine

Sample Number	Organic Carbon [%]	Sample Number	Organic Carbon [%]
YK-45	12.80	YK-235	3.494
YK-46	13.66	YK-236	38.43
YK-47	29.61	YK-238	22.37
YK-48	19.66	YK-238	22.37
YK-49	17.76	YK-239	19.42
YK-50	29.35	YK-240	28.97
YK-52	2.147	YK-241	17.76
YK-53	0.8175	YK-242	22.58
YK-54	3.612	YK-243	40.1
YK-58	38.45	YK-244	6.943
YK-59	23.51	YK-245	0.3104
YK-60	30.16	YK-245	0.3104
YK-61	30.24	YK-26	22.52
YK- 114	33.25	YK-27	0.5035
YK- 115	31.51	YK-28	2.711
YK- 116	36.66	YK-300	24.26
YK-126	37.1	YK-301	19.88
YK-127	4.97	YK-302	37.5
YK-231	8.923	YK-303	15.74
YK-233	2.296	YK-304	22.93

Table F-2: Organic Carbon Results [%] from the North Brookfield Mine

Sample Number	Organic Carbon [%]
NB-129	3.242
NB-200	1.666
NB-201	1.386
NB-85	0.4836
NB-93	11.13
NB-94	1.537
NB-95	1.5
NB-211	0.3523
NB-76	50.48
NB-71	3.888
NB-72	5.467
NB-73	2.996
NB-75	0.1389

Appendix G: Selected Sequential Selective Extraction (SSE) Results

The following table is an example of SSE results from three samples at the Giant mine, NT that was performed at ALS Chemex. Also included is a comparison between the NIST-2711 soil run at ALS and the same soil run by G.E.M. Hall at the GSC-Ottawa. Remaining leaches from Giant and the North Brookfield can be found in the attached CD.

Table G-1: Selected Sequential Selective Extraction Results from Giant

Site 19: YK-127	Ag ppm	Al ppm	As ppm	As %	Au ppm	B ppm	Ba ppm	Be ppm	Bi ppm
Adsorbed/exchangeable	<0.002	76	16.4	5.83	<0.05	<2	30.6	<0.05	<0.005
Organics	0.003	1000	98.1	34.87	<0.05	<2	22.7	0.08	0.03
Carbonates	<0.002	171	48.7	17.31	<0.05	<2	6.88	<0.05	<0.005
Amorphous Iron Oxides	0.023	3150	67	23.82	<0.05	<2	16.35	0.17	0.077
Crystalline Iron Oxides	0.004	1880	42.3	15.04	<0.05	2	7.46	0.08	0.064
Scorodite	<0.002	4930	6.9	2.45	<0.05	2	13.1	0.1	0.019
Sulphides	0.009	1410	0.8	0.28	<0.05	<2	4.28	<0.05	0.007
Residuals and Silicates	0.026	19850	1.1	0.39	<0.05	<2	311	1.22	0.028
Totals	**0.065**	**32467**	**281.3**	**100.00**	**0**	**4**	**412.37**	**1.65**	**0.225**
Site 19: YK-235									
Adsorbed/exchangeable	<0.002	41	2.3	2.13	<0.05	<2	39.2	<0.05	<0.005
Organics	0.002	1160	33.8	31.35	<0.05	<2	15.35	<0.05	0.021
Carbonates	<0.002	80	16.2	15.03	<0.05	<2	4.96	<0.05	<0.005
Amorphous Iron Oxides	0.022	3560	25.8	23.93	<0.05	<2	10.75	0.13	0.095
Crystalline Iron Oxides	0.007	1880	24.2	22.45	<0.05	2	4.84	0.07	0.051
Scorodite	<0.002	6100	5.1	4.73	<0.05	2	8.12	0.1	0.022
Sulphides	0.008	1060	<0.1	0.09	<0.05	<2	2.73	<0.05	0.005
Residuals and Silicates	0.014	20000	0.3	0.28	<0.05	<2	313	1.32	0.027
Totals	**0.053**	**33881**	**107.8**	**100.00**	**0**	**4**	**398.95**	**1.62**	**0.221**
Site 28: YK-115									
Adsorbed/exchangeable	0.007	85	40.8	4.73	<0.05	<2	32.8	<0.05	<0.005
Organics	0.019	1450	56.3	6.53	<0.05	<2	40.5	0.09	0.016
Carbonates	<0.002	550	28.9	3.35	<0.05	3	14.75	<0.05	<0.005
Amorphous Iron Oxides	0.11	982	45.7	5.30	<0.05	5	30.3	0.06	<0.005
Crystalline Iron Oxides	0.057	920	653	75.77	<0.05	4	7.74	<0.05	0.065
Scorodite	0.003	1840	27.1	3.14	<0.05	<2	6.99	0.06	0.021
Sulphides	0.035	530	8.1	0.94	0.14	<2	4.35	<0.05	0.006
Residuals and Silicates	0.016	6670	1.9	0.22	<0.05	3	59.6	0.2	0.013
Totals	**0.247**	**13027**	**861.8**	**100.00**	**0.14**	**15**	**197.03**	**0.41**	**0.121**

Table G-1: Selected Sequential Selective Extraction Results *(cont.)*

Site 19: YK-127	Br ppm	Ca ppm	Cd ppm	Ce ppm	Co ppm	Cr ppm	Cs ppm	Cu ppm	Dy ppm
Adsorbed/exchangeable	4	3440	0.01	0.09	<0.05	0.29	0.007	0.15	0.006
Organics	98	1110	0.07	4.06	0.5	2.45	0.047	3.92	0.202
Carbonates	2	50	0.01	0.086	0.09	0.96	0.007	0.17	<0.005
Amorphous Iron Oxides	<2	550	0.04	3.18	2.26	7.26	0.079	3.84	0.208
Crystalline Iron Oxides	<2	100	0.01	0.774	1.54	7.04	0.118	4.23	0.035
Scorodite	5	610	0.02	11.35	1.98	14.8	0.294	3.8	0.245
Sulphides	28	370	0.01	11.9	0.41	15.35	0.16	0.9	0.296
Residuals and Silicates	14	7680	0.07	6.61	2.07	21.4	0.849	3.45	0.706
Totals	**151**	**13910**	**0.24**	**38.05**	**8.85**	**69.55**	**1.561**	**20.46**	**1.698**
Site 19: YK-235									
Adsorbed/exchangeable	3	1860	<0.01	0.114	0.05	0.87	0.068	0.19	0.007
Organics	107	310	0.01	2.58	0.61	2.53	0.13	4.02	0.338
Carbonates	<2	20	<0.01	0.081	0.21	1.03	0.012	0.18	0.005
Amorphous Iron Oxides	<2	720	0.01	8.97	4.9	10.3	0.187	13.1	0.439
Crystalline Iron Oxides	<2	80	0.01	1.185	1.88	9.22	0.24	9.29	0.066
Scorodite	4	720	0.02	18.5	2.86	21.5	0.468	2.49	0.408
Sulphides	25	450	0.01	11.65	0.42	11.3	0.144	0.19	0.324
Residuals and Silicates	5	7200	0.06	2.49	1.92	26.6	0.726	1.17	0.525
Totals	**144**	**11360**	**0.12**	**45.57**	**12.85**	**83.35**	**1.975**	**30.63**	**2.112**
Site 28: YK-115									
Adsorbed/exchangeable	5	19350	0.04	0.06	0.05	0.44	0.005	0.18	<0.005
Organics	67	3710	0.15	7.23	1.13	1.89	0.023	5.17	0.382
Carbonates	3	2270	0.02	0.289	0.16	1.16	0.018	0.61	0.015
Amorphous Iron Oxides	<2	2560	0.08	0.684	1.64	1.63	0.04	0.42	0.036
Crystalline Iron Oxides	<2	310	0.01	1.605	0.69	<0.05	0.096	3.58	0.059
Scorodite	3	150	0.02	5.7	0.84	7.07	0.177	9.21	0.174
Sulphides	32	70	0.02	2.22	0.31	5	0.126	2.72	0.066
Residuals and Silicates	30	730	0.02	3.52	0.27	5.51	0.274	1.14	0.201
Totals	**140**	**29150**	**0.36**	**21.308**	**5.09**	**22.7**	**0.759**	**23.03**	**0.933**

Table G-1: Selected Sequential Selective Extraction Results *(cont.)*

Site 19: YK-127	Er ppm	Eu ppm	Fe ppm	Ga ppm	Gd ppm	Ge ppm	Hf ppm	Hg ppm	Ho ppm
Adsorbed/exchangeable	<0.005	0.008	34	<0.05	0.006	<0.1	<0.01	<0.1	<0.005
Organics	0.101	0.055	1180	0.67	0.286	<0.1	0.08	<0.1	0.039
Carbonates	<0.005	<0.005	70	<0.05	<0.005	<0.1	0.01	<0.1	<0.005
Amorphous Iron Oxides	0.099	0.041	3670	0.94	0.236	<0.1	0.01	<0.1	0.038
Crystalline Iron Oxides	0.018	0.013	3620	0.75	0.052	<0.1	0.01	<0.1	0.007
Scorodite	0.104	0.096	5660	2.24	0.598	<0.1	0.02	<0.1	0.039
Sulphides	0.125	0.089	1090	0.53	0.686	<0.1	0.04	<0.1	0.051
Residuals and Silicates	0.454	0.421	4560	10.7	0.781	<0.1	2.35	<0.1	0.15
Totals	**0.901**	**0.723**	**19884**	**15.83**	**2.645**	**0**	**2.52**	**0**	**0.324**
Site 19: YK-235									
Adsorbed/exchangeable	0.005	0.013	34	<0.05	0.015	<0.1	<0.01	<0.1	<0.005
Organics	0.197	0.102	1200	0.59	0.45	<0.1	0.11	<0.1	0.067
Carbonates	<0.005	<0.005	50	<0.05	0.005	<0.1	<0.01	<0.1	<0.005
Amorphous Iron Oxides	0.223	0.099	4310	1.09	0.572	<0.1	0.01	<0.1	0.081
Crystalline Iron Oxides	0.033	0.021	4050	0.8	0.091	<0.1	0.02	<0.1	0.012
Scorodite	0.169	0.154	9040	2.5	1.03	0.1	0.03	<0.1	0.065
Sulphides	0.142	0.102	1290	0.36	0.685	<0.1	0.07	<0.1	0.051
Residuals and Silicates	0.372	0.333	4690	11.35	0.452	0.1	3.08	<0.1	0.119
Totals	**1.141**	**0.824**	**24664**	**16.69**	**3.3**	**0.2**	**3.32**	**0**	**0.395**
Site 28: YK-115									
Adsorbed/exchangeable	<0.005	0.014	38	<0.05	0.006	<0.1	<0.01	<0.1	<0.005
Organics	0.204	0.134	1270	0.85	0.647	<0.1	0.14	<0.1	0.074
Carbonates	0.01	0.007	623	0.19	0.026	<0.1	0.06	<0.1	<0.005
Amorphous Iron Oxides	0.02	0.014	1290	0.1	0.043	<0.1	<0.01	<0.1	0.007
Crystalline Iron Oxides	0.032	0.019	1890	0.14	0.109	<0.1	0.01	0.1	0.011
Scorodite	0.087	0.063	2120	1.12	0.344	<0.1	0.04	0.1	0.032
Sulphides	0.026	0.023	479	0.34	0.13	<0.1	0.05	<0.1	0.011
Residuals and Silicates	0.137	0.081	853	1.95	0.23	<0.1	0.72	<0.1	0.041
Totals	**0.516**	**0.355**	**8563**	**4.69**	**1.535**	**0**	**1.02**	**0.2**	**0.176**

Table G-1: Selected Sequential Selective Extraction Results *(cont.)*

Site 19: YK-127	I ppm	In ppm	K ppm	La ppm	Li ppm	Lu ppm	Mg ppm	Mn ppm	Mo ppm
Adsorbed/exchangeable	0.1	<0.005	39	0.033	0.13	<0.005	209	2	0.01
Organics	0.3	<0.005	92	1.475	0.82	0.012	136	25.1	0.04
Carbonates	<0.1	<0.005	18	0.022	0.18	<0.005	23	8.3	<0.01
Amorphous Iron Oxides	0.1	<0.005	117	0.996	3.83	0.009	1080	39.2	<0.01
Crystalline Iron Oxides	0.1	<0.005	121	0.343	5.14	<0.005	1060	24.7	0.06
Scorodite	<0.1	0.005	314	5.74	8.17	0.011	2130	52	0.04
Sulphides	1.1	<0.005	160	5.85	2.22	0.012	402	16.6	0.21
Residuals and Silicates	0.3	0.015	17050	3.31	9.9	0.08	2030	131.5	0.05
Totals	**2**	**0.02**	**17911**	**17.769**	**30.39**	**0.124**	**7070**	**299.4**	**0.41**
Site 19: YK-235									
Adsorbed/exchangable	0.1	<0.005	21	0.058	0.3	<0.005	159	3.6	0.01
Organics	0.4	<0.005	197	2.43	1.49	0.023	218	14.8	0.04
Carbonates	0.1	<0.005	15	0.035	0.23	<0.005	20	10.9	<0.01
Amorphous Iron Oxides	0.3	<0.005	120	3.23	12.95	0.022	1340	74.4	0.01
Crystalline Iron Oxides	0.1	<0.005	142	0.591	7.58	<0.005	1070	27.7	0.12
Scorodite	<0.1	0.005	276	9.36	11.7	0.016	3680	91.7	0.05
Sulphides	0.6	<0.005	110	5.84	1.5	0.015	483	23	0.13
Residuals and Silicates	0.2	0.017	17750	1.145	5.39	0.073	1690	128	0.05
Totals	**1.8**	**0.022**	**18631**	**22.689**	**41.14**	**0.149**	**8660**	**374.1**	**0.41**
Site 28: YK-115									
Adsorbed/exchangeable	<0.1	<0.005	398	0.043	0.15	<0.005	2810	9	0.35
Organics	1.1	<0.005	91	4.36	0.46	0.028	671	68.8	1.99
Carbonates	0.2	<0.005	79	0.197	0.27	<0.005	95	37.1	0.04
Amorphous Iron Oxides	1.2	<0.005	79	0.55	1.01	<0.005	257	61.7	0.02
Crystalline Iron Oxides	0.9	<0.005	182	0.999	2.89	<0.005	473	15.2	0.22
Scorodite	0.5	<0.005	289	2.77	2.22	0.009	594	12.1	0.17
Sulphides	3.5	<0.005	150	1.04	0.87	<0.005	142	4.3	1.22
Residuals and Silicates	0.3	<0.005	3110	1.665	3.33	0.027	355	16.3	0.17
Totals	**7.7**	**0**	**4378**	**11.624**	**11.2**	**0.064**	**5397**	**224.5**	**4.18**

Table G-1: Selected Sequential Selective Extraction Results *(cont.)*

Site 19: YK-127	Na ppm	Nb ppm	Nd ppm	Ni ppm	P ppm	Pb ppm	Pr ppm	Rb ppm	Re ppm
Adsorbed/exchangeable	<10	0.01	0.025	<0.05	9	0.1	0.005	0.21	<0.001
Organics	<10	0.15	1.485	1.1	<5	1.2	0.431	0.8	<0.001
Carbonates	6300	0.01	0.025	0.11	1550	<0.1	0.008	0.12	<0.001
Amorphous Iron Oxides	120	0.03	0.967	5.45	432	3.4	0.242	1.49	<0.001
Crystalline Iron Oxides	90	0.38	0.308	4.18	130	0.8	0.078	1.57	<0.001
Scorodite	190	0.07	4.81	5.66	64	0.6	1.355	3.89	0.001
Sulphides	50	0.7	5.06	6.6	18	0.5	1.38	1.79	<0.001
Residuals and Silicates	21300	3.22	3.12	5.03	80	12.7	0.812	49.9	0.001
Totals	**28050**	**4.57**	**15.8**	**28.13**	**2283**	**19.3**	**4.311**	**59.77**	**0.002**
Site 19: YK-235									
Adsorbed/exchangeable	30	0.01	0.058	0.06	<5	<0.1	0.014	0.48	<0.001
Organics	<10	0.14	2.45	1.33	<5	0.5	0.632	1.69	<0.001
Carbonates	2760	0.01	0.023	0.13	391	<0.1	0.03	0.13	<0.001
Amorphous Iron Oxides	80	0.04	2.94	9.55	441	3	0.752	1.83	<0.001
Crystalline Iron Oxides	80	0.51	0.534	5.74	130	0.7	0.167	1.88	<0.001
Scorodite	180	0.15	7.95	9.55	55	0.8	2.22	3.16	<0.001
Sulphides	40	0.32	5.02	4.88	12	0.4	1.395	1.14	<0.001
Residuals and Silicates	21700	3.16	1.315	4.8	64	12.5	0.318	31.3	0.001
Totals	**24870**	**4.34**	**20.29**	**36.04**	**1093**	**17.9**	**5.528**	**41.61**	**0.001**
Site 28: YK-115									
Adsorbed/exchangeable	90	0.01	0.036	0.06	32	0.2	0.015	0.21	<0.001
Organics	<10	0.12	3.78	1.88	<5	6.5	1.07	0.54	<0.001
Carbonates	50400	0.07	0.145	0.31	19150	0.4	0.044	0.41	<0.001
Amorphous Iron Oxides	3740	<0.01	0.215	3.4	1770	5.8	0.066	0.73	<0.001
Crystalline Iron Oxides	260	0.03	0.617	3.63	290	3.2	0.173	1.84	<0.001
Scorodite	80	0.01	2.54	4.88	173	1	0.721	2.5	<0.001
Sulphides	30	0.29	0.888	12.25	45	0.4	0.272	1.63	<0.001
Residuals and Silicates	2160	1.1	1.31	1.21	39	3.1	0.383	11.3	<0.001
Totals	**56760**	**1.63**	**9.531**	**27.62**	**21499**	**20.6**	**2.744**	**19.16**	**0**

Table G-1: Selected Sequential Selective Extraction Results *(cont.)*

Site 19: YK-127	Sb ppm	Se ppm	Sm ppm	Sn ppm	Sr ppm	Ta ppm	Tb ppm	Te ppm	Th ppm
Adsorbed/ exchangeable	0.209	<0.5	0.006	<0.05	5.09	<0.01	<0.005	<0.05	0.01
Organics	1.225	<0.5	0.297	0.11	2.22	0.01	0.043	<0.05	1.12
Carbonates	0.287	<0.5	<0.005	<0.05	0.34	<0.01	<0.005	<0.05	0.03
Amorphous Iron Oxides	0.19	<0.5	0.219	<0.05	1.4	<0.01	0.037	<0.05	0.01
Crystalline Iron Oxides	0.282	<0.5	0.054	0.09	0.68	<0.01	0.007	<0.05	0.05
Scorodite	2.84	0.5	0.788	0.4	4.48	<0.01	0.067	0.05	0.98
Sulphides	0.38	<0.5	0.896	0.16	1.76	<0.01	0.074	<0.05	3.07
Residuals and Silicates	0.764	<0.5	0.714	0.99	116	0.49	0.129	<0.05	1.86
Totals	**6.177**	**0.5**	**2.974**	**1.75**	**131.97**	**0.5**	**0.357**	**0.05**	**7.13**
Site 19: YK-235									
Adsorbed/exchangeable	0.091	<0.5	0.014	<0.05	2.92	<0.01	<0.005	<0.05	0.01
Organics	0.239	<0.5	0.506	0.11	2.24	0.01	0.068	<0.05	1.45
Carbonates	0.096	<0.5	<0.005	<0.05	0.2	<0.01	<0.005	<0.05	0.04
Amorphous Iron Oxides	0.065	<0.5	0.6	<0.05	1.65	0.01	0.087	<0.05	0.01
Crystalline Iron Oxides	0.13	<0.5	0.086	0.13	0.57	<0.01	0.013	<0.05	0.05
Scorodite	0.889	0.6	1.35	0.28	4.2	<0.01	0.114	0.05	3.23
Sulphides	0.098	<0.5	0.847	0.13	1.77	0.01	0.084	<0.05	3.21
Residuals and Silicates	0.412	<0.5	0.393	1.05	109	0.43	0.087	<0.05	0.85
Totals	**2.02**	**0.6**	**3.796**	**1.7**	**122.55**	**0.46**	**0.453**	**0.05**	**8.85**
Site 28: YK-115									
Adsorbed/exchangeable	0.79	<0.5	0.012	<0.05	36.5	<0.01	<0.005	<0.05	0.01
Organics	4.9	<0.5	0.666	0.07	21.2	<0.01	0.087	<0.05	1.59
Carbonates	1.325	<0.5	0.022	<0.05	7.02	<0.01	<0.005	<0.05	0.26
Amorphous Iron Oxides	0.442	<0.5	0.033	<0.05	7.63	<0.01	0.006	<0.05	0.03
Crystalline Iron Oxides	2.38	<0.5	0.097	<0.05	1.61	<0.01	0.013	<0.05	0.04
Scorodite	34.1	0.5	0.448	0.19	3.62	<0.01	0.041	<0.05	0.46
Sulphides	14.95	0.8	0.153	0.16	1.92	<0.01	0.016	<0.05	0.81
Residuals and Silicates	4.65	<0.5	0.245	0.29	26.8	0.1	0.036	<0.05	0.89
Totals	**63.537**	**1.3**	**1.676**	**0.71**	**106.3**	**0.1**	**0.199**	**0**	**4.09**

Table G-1: Selected Sequential Selective Extraction Results
(cont.)

Site 19: YK-127	Ti ppm	Tl ppm	Tm ppm	U ppm	W ppm	Y ppm	Yb ppm	Zn ppm	Zr ppm
Adsorbed/ exchangeable	3	<0.005	<0.005	0.006	0.09	0.015	<0.005	<0.2	0.06
Organics	58	0.006	0.015	0.22	0.04	0.98	0.09	3.2	2.27
Carbonates	9	<0.005	<0.005	0.012	<0.01	0.013	<0.005	2.9	0.16
Amorphous Iron Oxides	21	0.013	0.012	0.064	<0.01	1.015	0.072	13.9	0.1
Crystalline Iron Oxides	32	0.013	<0.005	0.026	0.1	0.144	0.03	10.4	0.22
Scorodite	250	0.032	0.013	0.242	0.1	1.01	0.071	12.2	0.27
Sulphides	163	0.013	0.013	0.287	0.16	1.15	0.077	2.9	1.19
Residuals and Silicates	1385	0.353	0.069	0.657	0.43	3.97	0.488	10.8	63
Totals	**1921**	**0.43**	**0.122**	**1.514**	**0.92**	**8.297**	**0.828**	**56.3**	**67.27**
Site 19: YK-235									
Adsorbed/exchangeable	4	0.006	<0.005	0.012	0.08	0.044	<0.005	<0.2	<0.05
Organics	69	0.014	0.024	0.224	0.03	1.81	0.147	1.5	3.57
Carbonates	4	<0.005	<0.005	0.019	<0.01	0.02	<0.005	0.2	0.09
Amorphous Iron Oxides	45	0.019	0.027	0.087	<0.01	2.17	0.16	9.4	0.08
Crystalline Iron Oxides	58	0.021	0.005	0.043	0.11	0.259	0.027	7.3	0.83
Scorodite	330	0.027	0.02	0.39	0.13	1.625	0.117	15.8	0.38
Sulphides	242	0.007	0.017	0.295	0.08	1.275	0.104	2.5	2.26
Residuals and Silicates	1260	0.328	0.062	0.716	0.38	2.99	0.438	9.9	84.8
Totals	**2012**	**0.422**	**0.155**	**1.786**	**0.81**	**10.193**	**0.993**	**46.6**	**92.01**
Site 28: YK-115									
Adsorbed/exchangeable	3	<0.005	<0.005	0.02	0.01	0.021	<0.005	2.3	0.1
Organics	28	0.006	0.026	4.05	0.07	2.28	0.172	44.5	4.93
Carbonates	51	<0.005	<0.005	0.627	0.01	0.083	0.007	1.2	1.63
Amorphous Iron Oxides	4	0.009	<0.005	0.192	<0.01	0.301	0.012	10.6	<0.05
Crystalline Iron Oxides	6	0.016	<0.005	0.176	0.02	0.363	0.025	5.8	0.19
Scorodite	58	0.014	0.011	0.817	0.02	0.626	0.066	4.5	0.32
Sulphides	92	0.009	<0.005	0.16	0.29	0.266	0.025	2.4	1.27
Residuals and Silicates	286	0.072	0.022	0.218	0.17	1.15	0.149	3.6	20.7
Totals	**528**	**0.126**	**0.059**	**6.26**	**0.59**	**5.09**	**0.456**	**74.9**	**29.14**

Table G-2: Comparison of NIST-2711 Standard from ALS Chemex (WRYE) and GSC Ottawa (PARSON)

	As	Ca	Fe	Mn	Sb	Ti
WRYE: NIST-2711	ppm	ppm	ppm	ppm	ppm	ppm
Adsorbed/ exchangable	13.8	8990	36	16.2	0.584	3
Organics	31.4	2480	1410	65	2.15	101
Carbonates	14.6	4150	221	148	1.56	7
Amorphous Iron Oxides	27.2	2410	2800	151	0.242	8
Crystalline Iron Oxides	21	160	3900	33.6	0.748	12
Scorodite	7.9	430	11200	65.7	5.72	381
Sulphides	3.7	290	2010	16.6	3.24	222
Residuals and Silicates	1.7	4170	3870	105	2.79	1700
Totals	**121.3**	**23080**	**25447**	**601.1**	**17.034**	**2434**
PARSONS: NIST-2711 (1)						
Adsorbed/ exchangable	11.77	10926	< 1	18.7	0.616	< 0.4
Organics	-	-	-	-	-	-
Carbonates	21.9	6499	9	102.2	1.72	< 1
Amorphous Iron Oxides	31.5	2149	3030	254.9	0.247	5.1
Crystalline Iron Oxides	16.1	209	7105	52.0	0.67	8
Scorodite	9.0	531	12588	68.1	8.33	439
Sulphides	3.9	291	1521	14.9	2.65	224.9
Residuals and Silicates	0.2	6207	3897	98.8	3.60	1761
Totals	**94.4**	**26813**	**27353**	**610**	**17.83**	**2439**
PARSONS: NIST-2711(2)						
Adsorbed/ exchangable	11.89	10854	< 1	18.9	0.619	< 0.4
Organics						
Carbonates	22.19	6693	9	105.7	1.67	< 1
Amorphous Iron Oxides	31.24	2148	3008	255.9	0.251	5.2
Crystalline Iron Oxides	16.14	209	6620	52.1	0.65	7
Scorodite	8.95	509	12276	66.6	7.86	416
Sulphides	3.91	307	1578	15.8	2.52	239.0
Residuals and Silicates	< 0.2	6060	3871	98.6	3.72	1734
Totals	**94.21**	**26780**	**27049**	**614**	**17.29**	**2403**

Table G-3: Duplicate SSE Sample						
YK-Site 19 Duplicate (1)	As ppm	Ca ppm	Fe ppm	Mn ppm	Sb ppm	Ti ppm
Adsorbed/ exchangable	16.4	3440	34	2	0.209	3
Organics	98.1	1110	1180	25.1	1.225	58
Carbonates	48.7	50	70	8.3	0.287	9
Amorphous Iron Oxides	67	550	3670	39.2	0.19	21
Crystalline Iron Oxides	42.3	100	3620	24.7	0.282	32
Scorodite	6.9	610	5660	52	2.84	250
Sulphides	0.8	370	1090	16.6	0.38	163
Residuals and Silicates	1.1	7680	4560	131.5	0.764	1385
Totals	**281.3**	**13910**	**19884**	**299.4**	**6.177**	**1921**
YK-Site 19 Duplicate (2)						
Adsorbed/ exchangable	17.3	3480	41	2.3	0.212	5
Organics	96.1	1130	1160	24	1.29	58
Carbonates	47.2	50	98	7.5	0.288	8
Amorphous Iron Oxides	68.3	540	3380	37	0.194	17
Crystalline Iron Oxides	51.7	110	4010	28.3	0.355	32
Scorodite	7.8	600	5590	51	3.91	243
Sulphides	1.3	420	1350	19.3	0.569	184
Residuals and Silicates	1	6730	4640	124.5	0.833	1420
Totals	**290.7**	**13060**	**20269**	**293.9**	**7.651**	**1967**

Table G-4: Percent Standard Deviation in SSE Results		
	NIST-2711 Montana Soil	Duplicate Sample
As	17.7	9.0
Ca	10.5	3.7
Fe	4.7	8.5
Mn	1.2	6.2
Sb	2.2	9.9
Ti	0.4	8.9

Appendix H: Sequential Selective Extraction (SSE) Plots for Manganese and Titanium at Giant and North Brookfield Mines

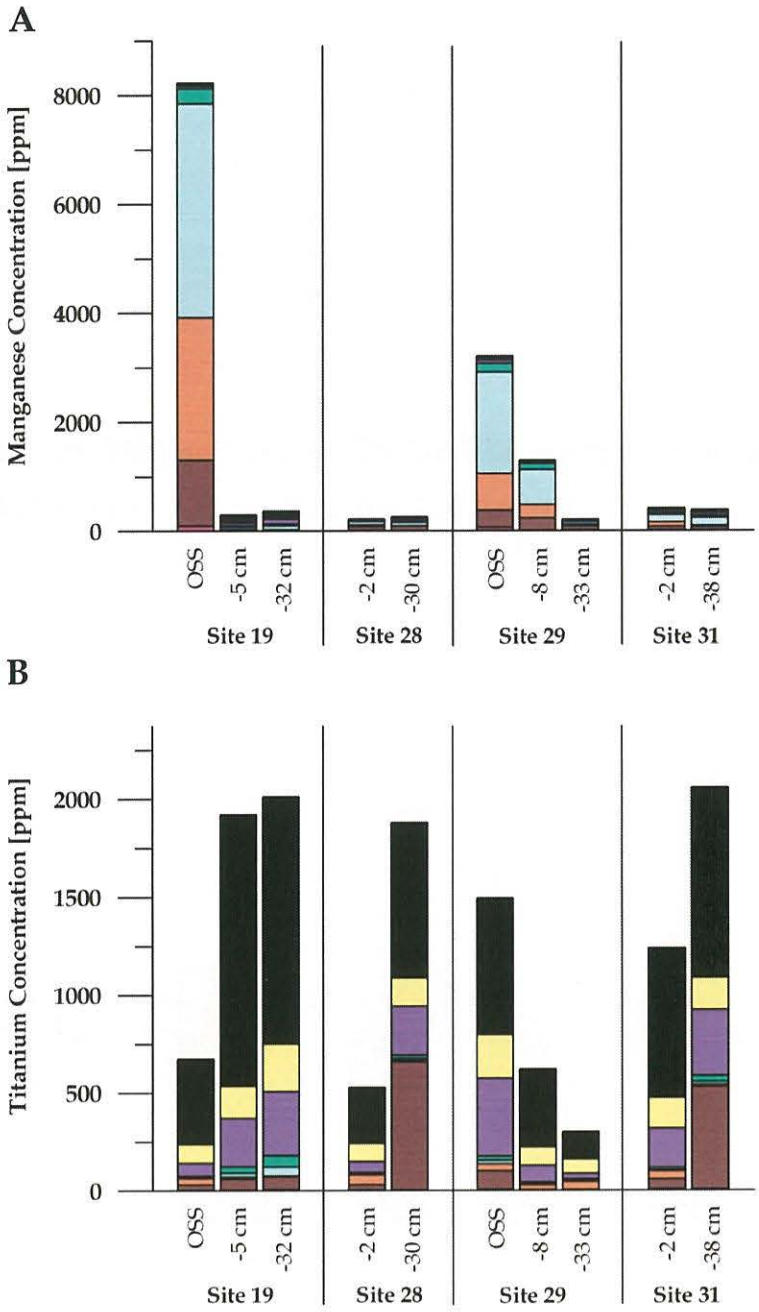

Figure H- 1: Sequential selective extraction results for manganese (Mn) and titanium (Ti) at the Giant Mine. Samples are organized by location and depth in the soil profile.

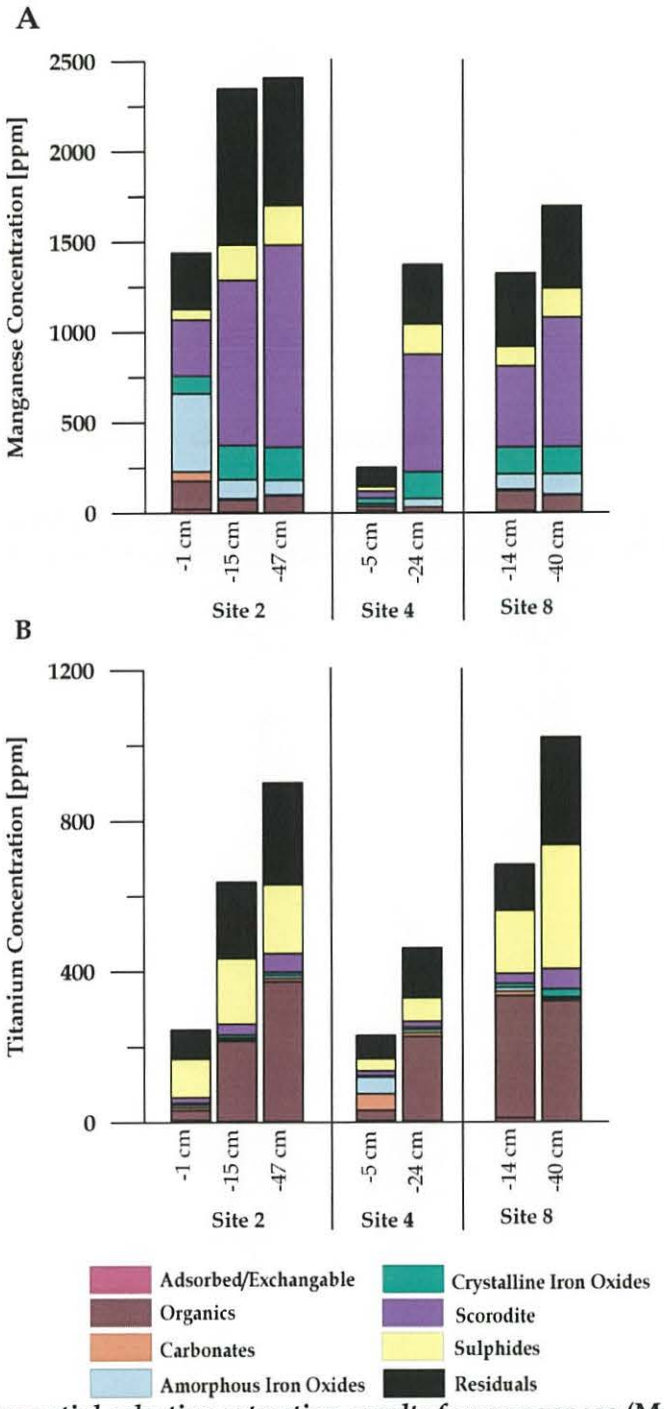

Figure H- 2: Sequential selective extraction results for manganese (Mn) and titanium (Ti) at the North Brookfield Mine. Samples are organized by location and depth in the soil profile.

Appendix I: Conventional X-Ray Diffraction Results

Conventional X-ray diffraction was performed on three samples using the Phillips PW3020/00 X'Pert MPD/MRD Rontgen Diffractometer System at Queen's University

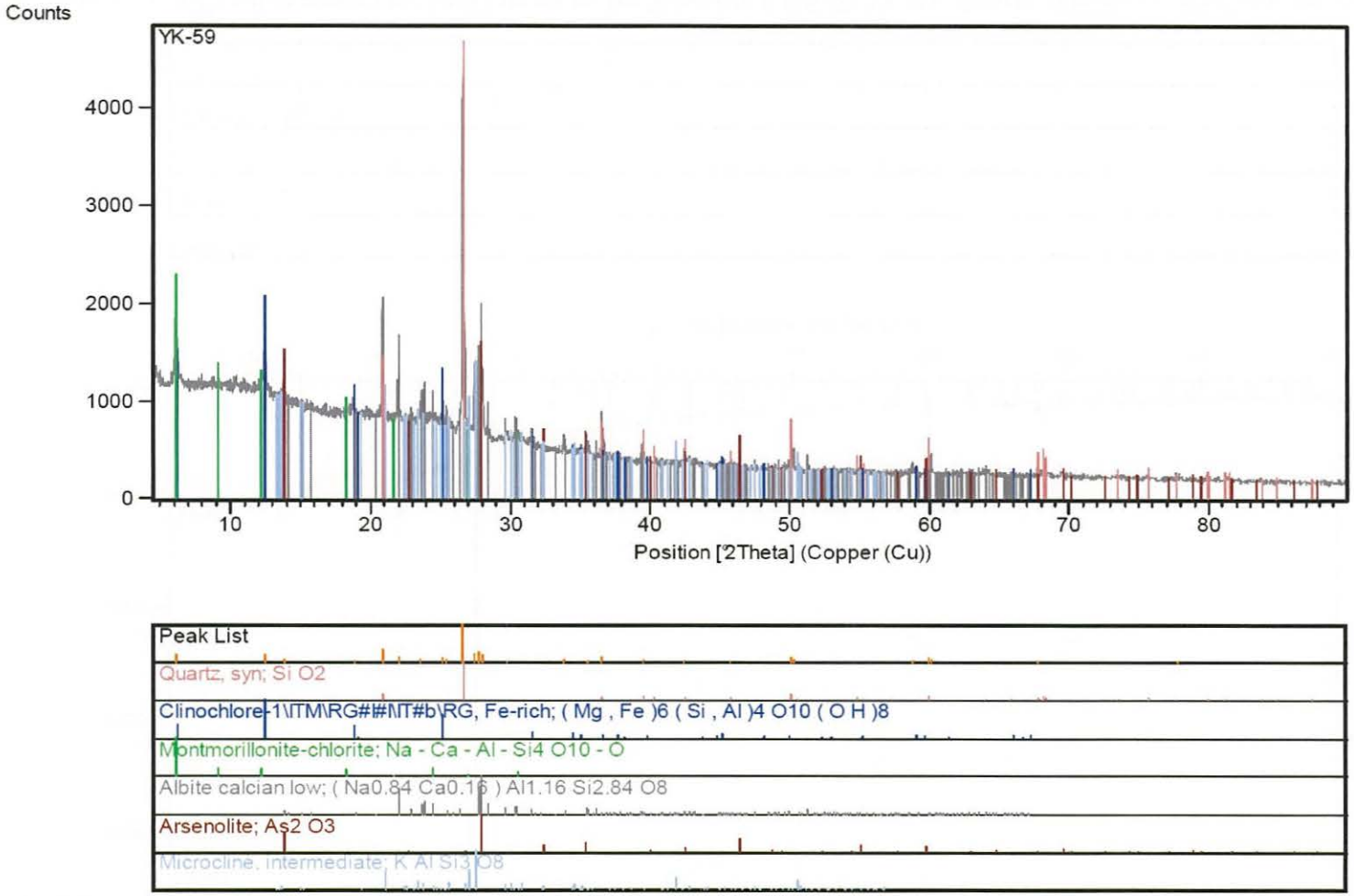

Figure I-1: Bulk X-ray diffraction pattern for OSS sample by the Fault (OSS-41: YK-59). Quartz, clinochlore, montmorillonite-chlorite, albite, arsenolite and microcline were identified.

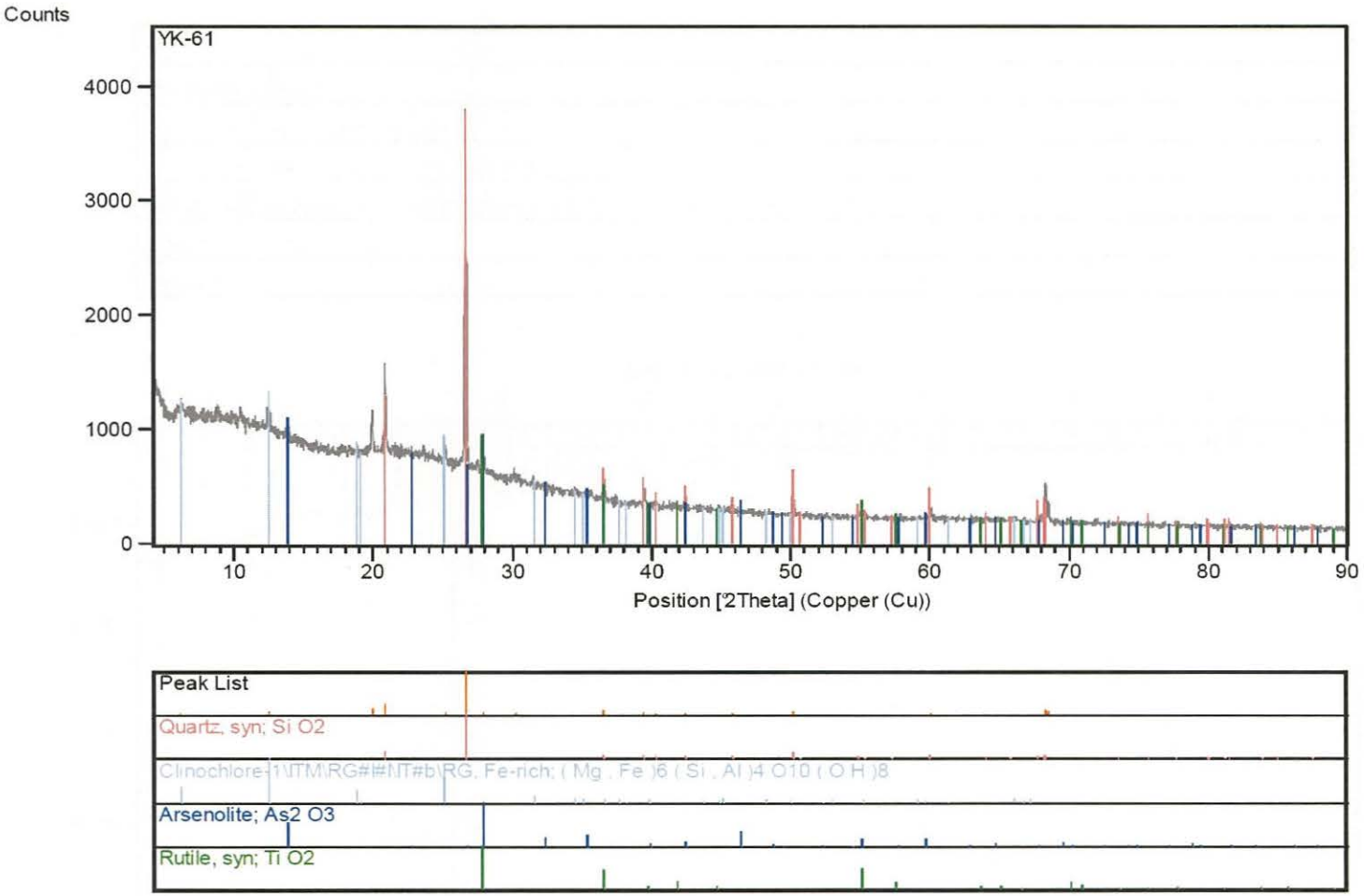

Figure I-2: Bulk X-ray diffraction pattern for OSS sample by the Townsite (OSS 43: YK-61). Quartz, clinochlore, arsenolite and rutile were identified.

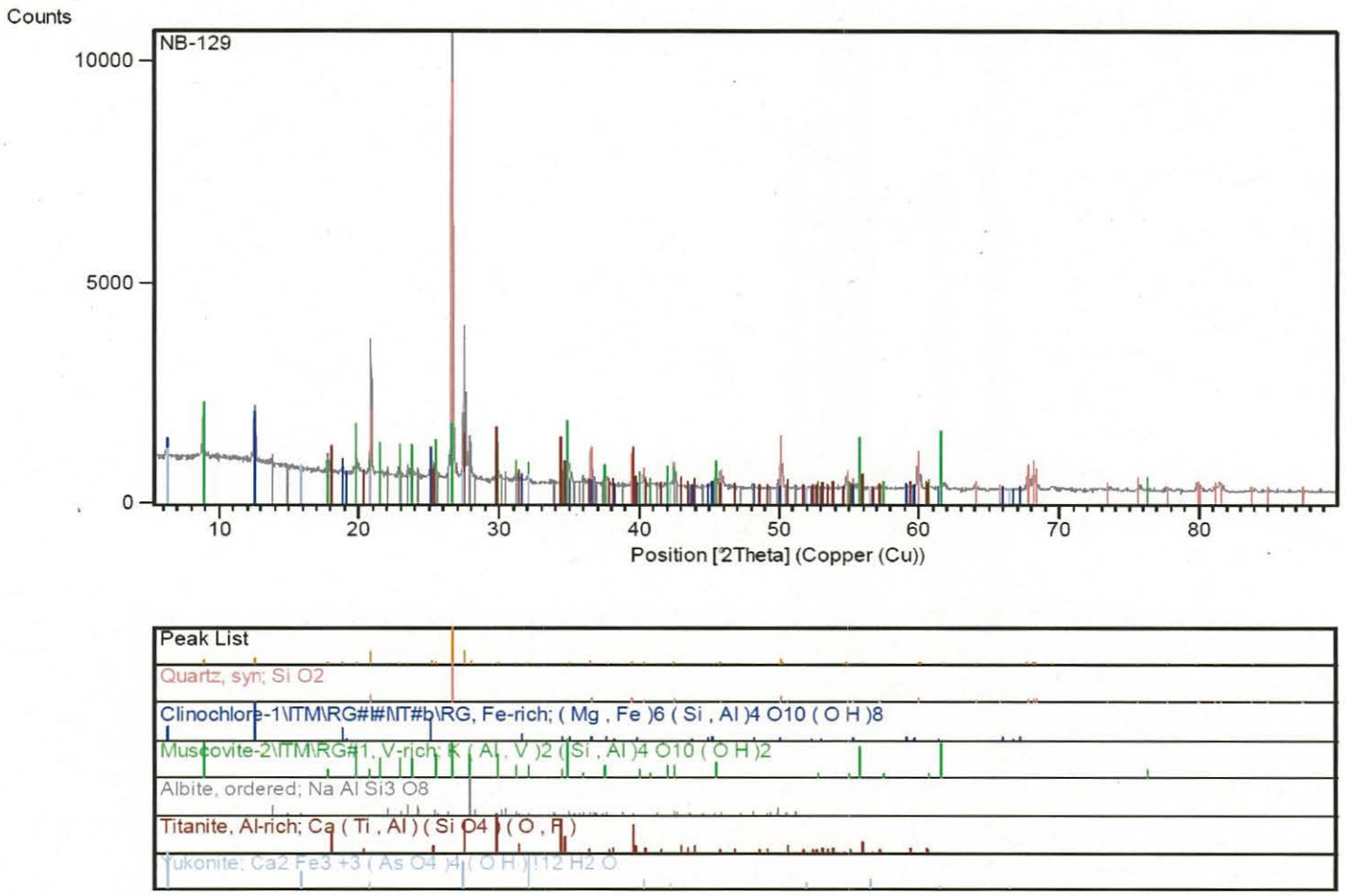

Figure I-3: Bulk X-ray diffraction pattern for a surface soil adjacent to the roaster at North Brookfield (Site 2: YK-129). Quartz, clinochlore, muscovite, albite, and titanite were identified. The yukonike lines were kept in the pattern to show that it overlaps with other mineral forms and may therefore be present in the soils.

Appendix J: Petrography, Synchrotron Analyses, and ESEM Photomicrographs by Sample Location

The following is a sample of petrographic, synchrotron and ESEM analyses from sub-samples taken closest to the roaster at Giant and North Brookfield mines. Remaining sub-sample mineralogical information can be found in the attached CD.

YK-50:T1

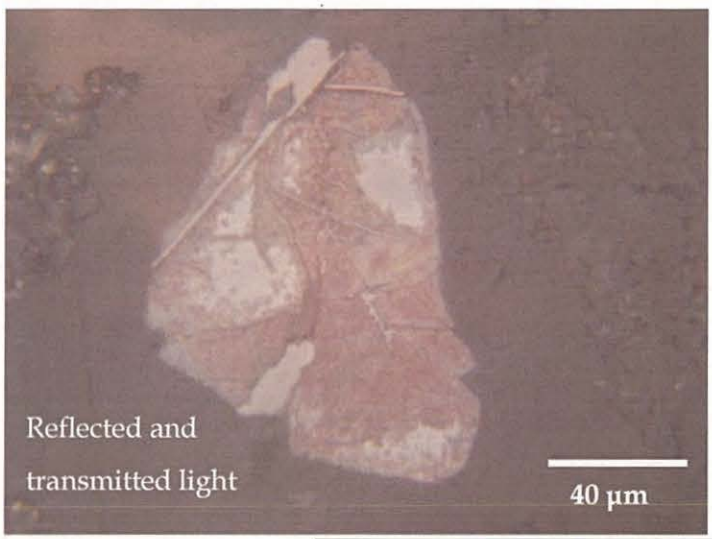

µXRD T1:
- hematite
- -muscovite
- Clinochlore

False Colour µXRF Map
Green= Ti
Blue= Fe
Red=As

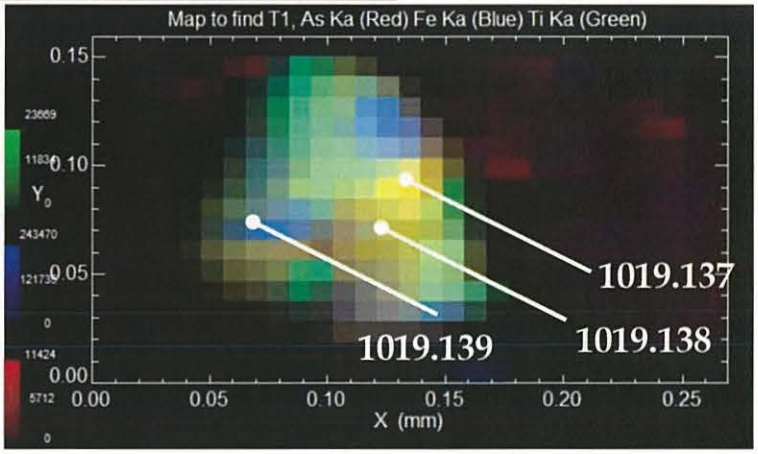

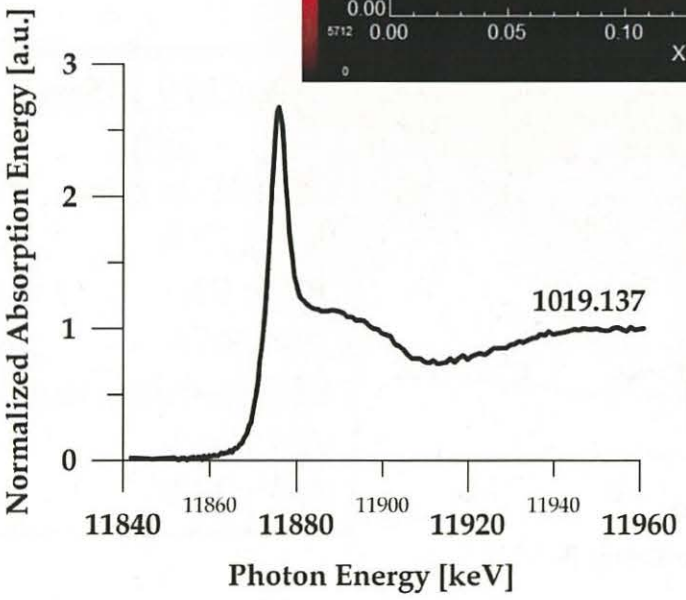

Nsls1019.137
As^{5+}: 92%
As^{3+}: 8%
As^{-1}: 0%

YK-50: T7

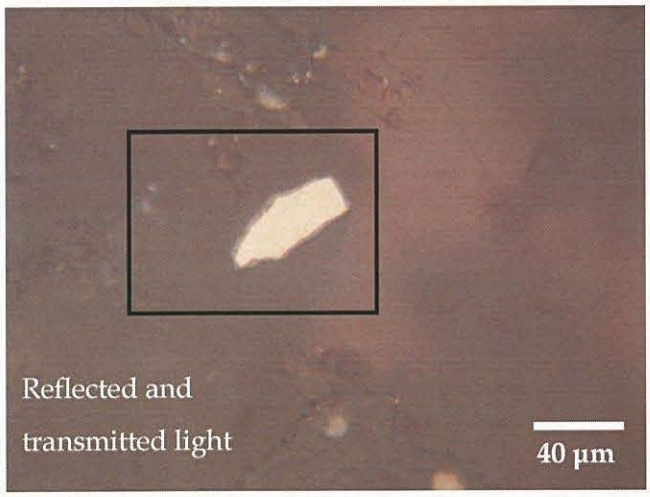

xrdYK50-
T7.135

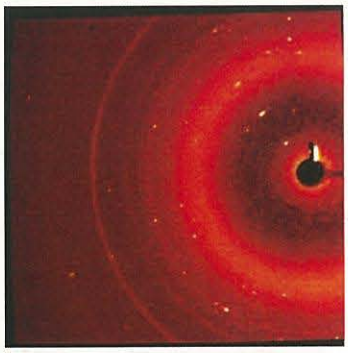

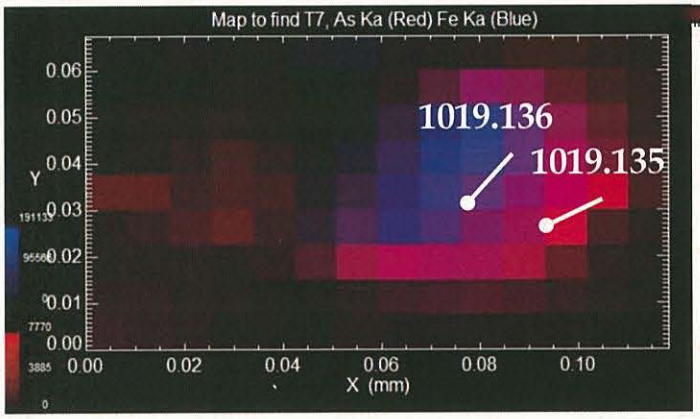

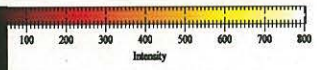

False Colour µXRF Map
Blue= Fe
Red=As

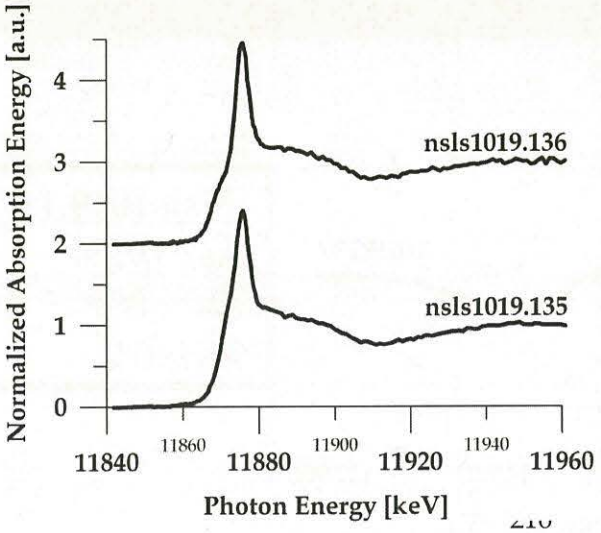

Nsls1019.135and. 136

Sulphide core:
As^{5+}: 75%
As^{3+}: 0%
As^{-1}: 25%

Maghemite rim:
As^{5+}: 66%
As^{3+}: 34%

YK-50: T7

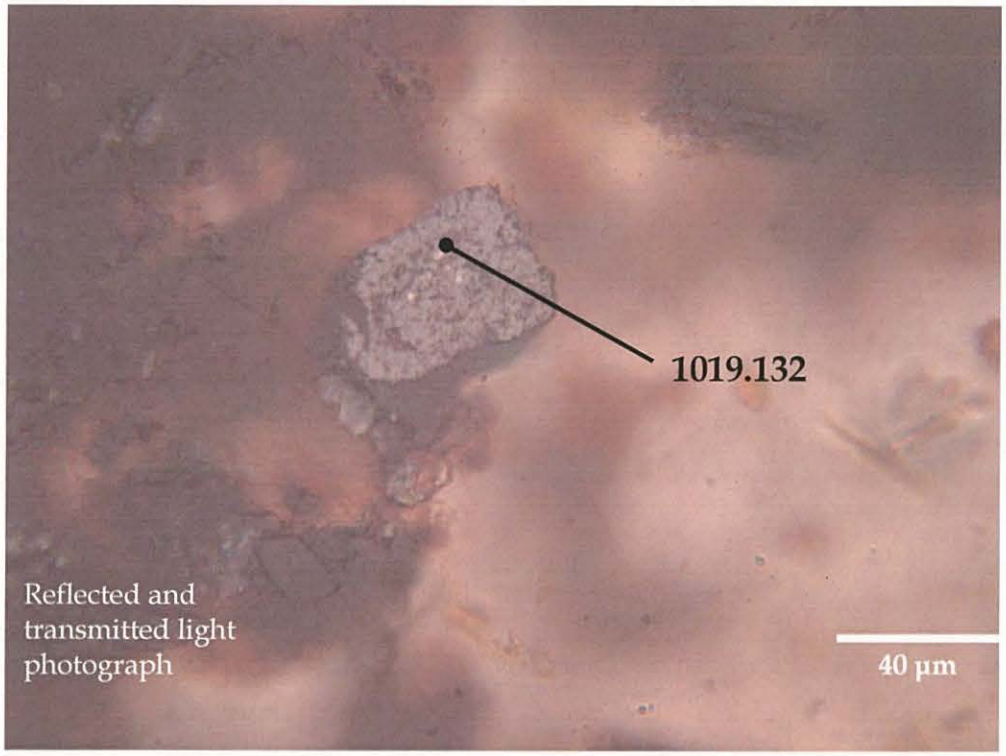

xrdYK50-T9.132
- maghemite

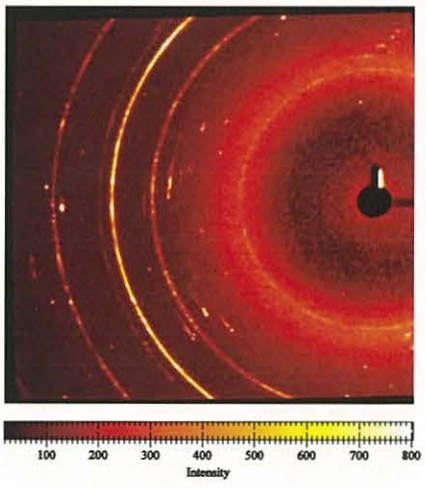

YK-50:T11

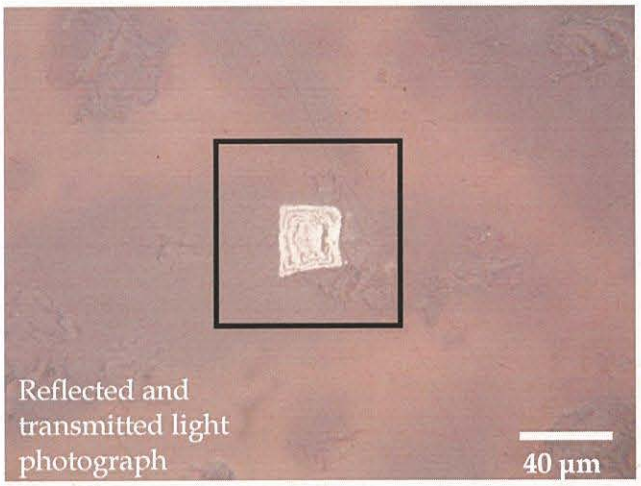

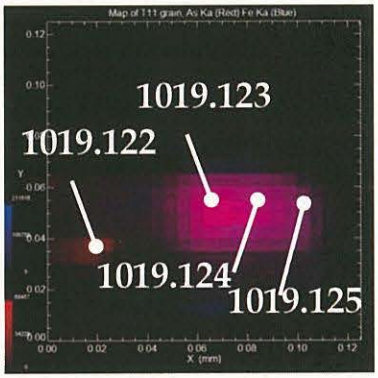

False Colour µXRF Map
Blue= Fe
Red=As

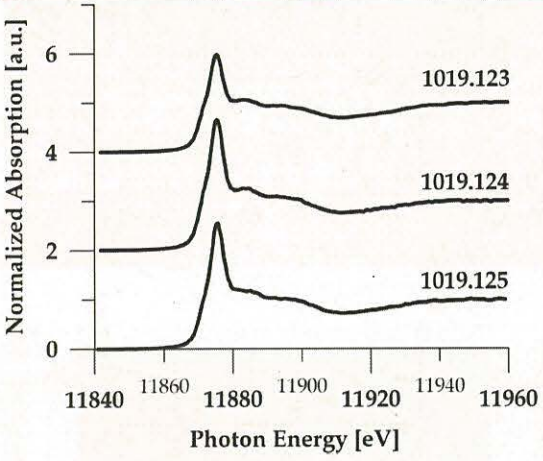

Nsls1019.123-.125
Concentric roaster oxide composed of maghemite
As^{5+}: 74%
As^{3+}: 26%
As^{-1}: 0%

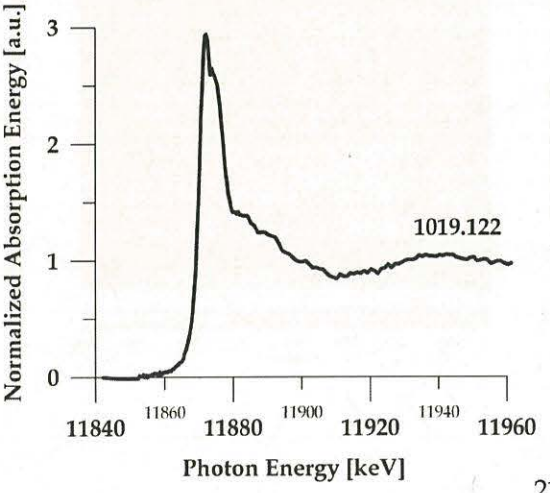

Nsls1019.122
Diffuse high As, no Fe (no XRD)
- Mostly As^{3+}

YK-50:T14

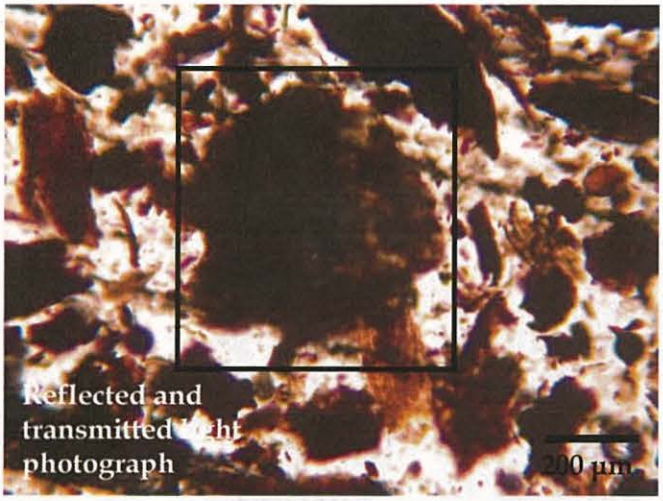

xrdYK50-14.118
- arsenolite

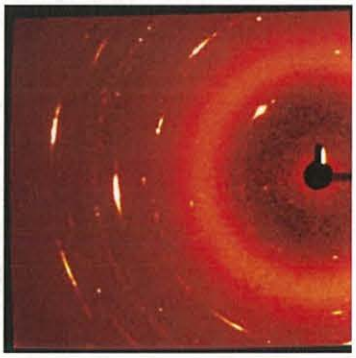

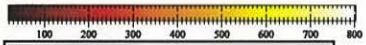

False Colour µXRF Map
Blue= Fe
Red=As

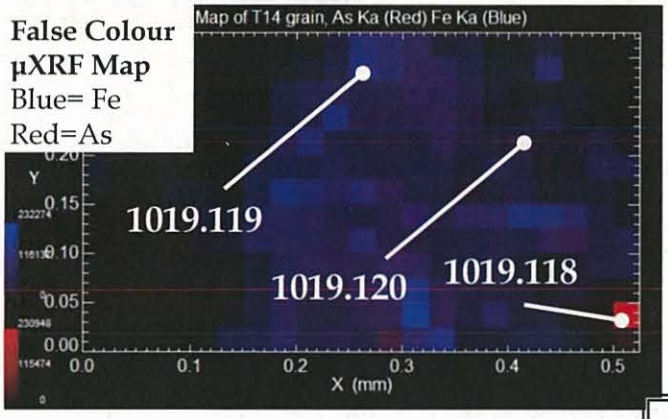

µXRD .119:
- maghemite
- muscovite
- clinochlore

µXRD .120:
- clinochlore

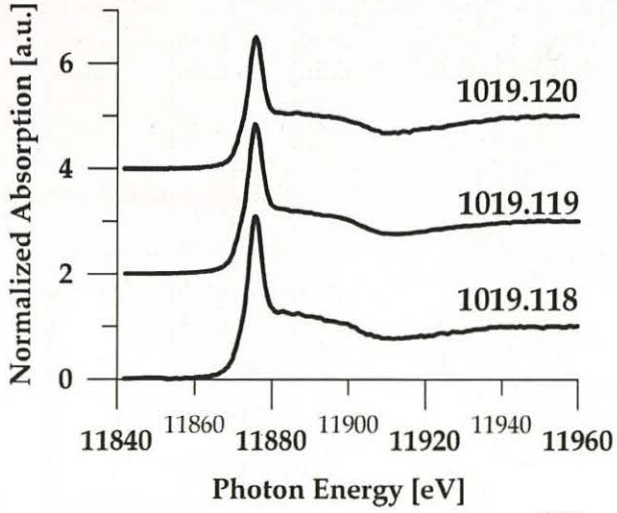

Nsls1019.118-.120

Arsenolite:
As^{5+}: 10%
As^{3+}: 90%
As^{-1}: 0%

Mag/mus/clin mix:
As^{5+}: 38%
As^{3+}: 38%
As^{-1}: 26%

Clinochlore only:
As^{5+}: 83%
As^{3+}: 17%
As^{-1}: 0%

YK-50:T20

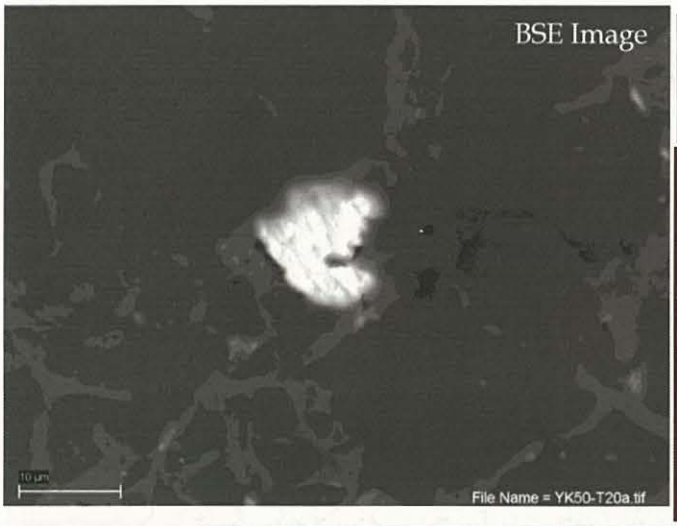

xrdYK50-20.006
- arsenolite

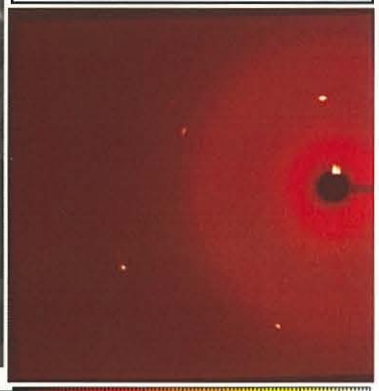

False Colour µXRF Map
Blue= Fe
Red=As

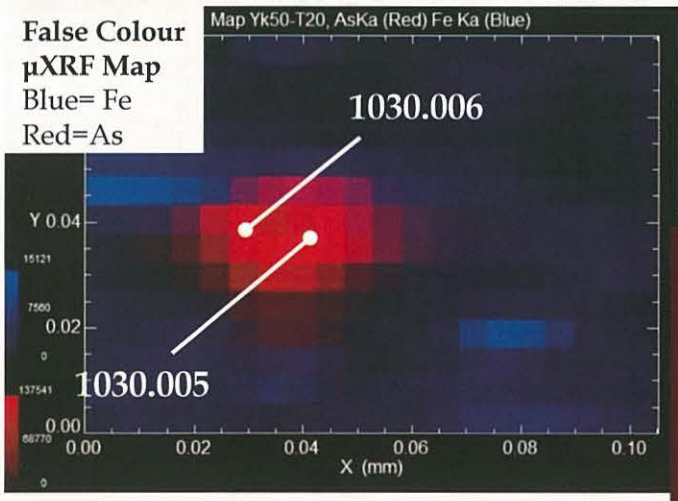

xrdYK50-20.005
- arsenolite

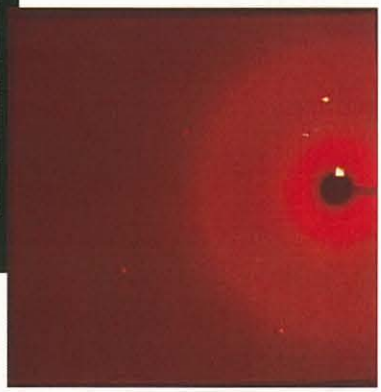

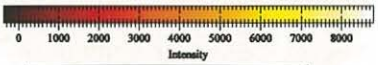

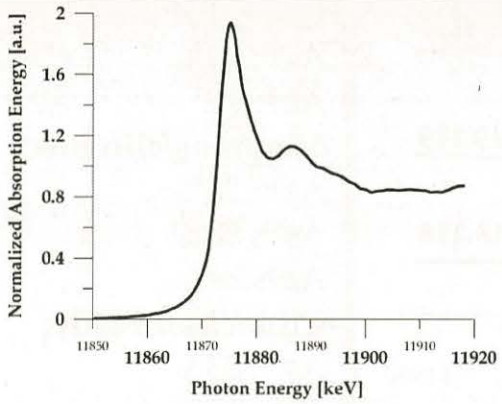

Nsls1030.006
Arsenolite:
As^{5+}: 0%
As^{3+}: 100%
As^{-1}: 0%

YK-50:T21

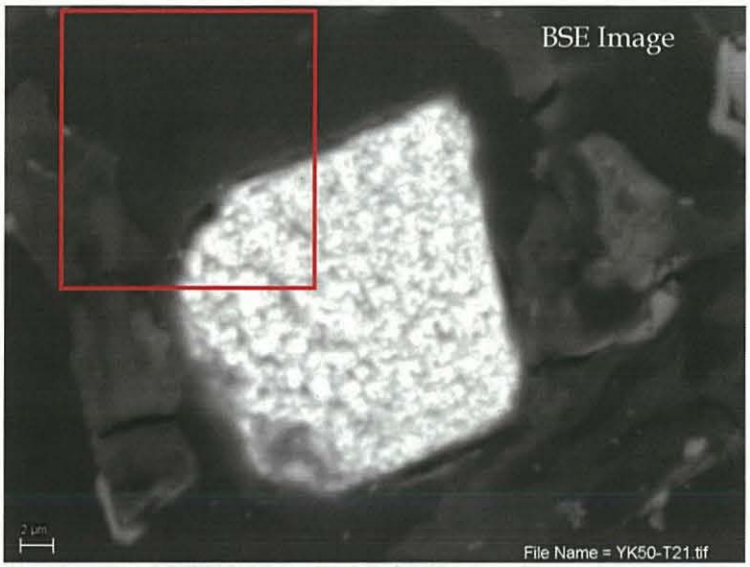

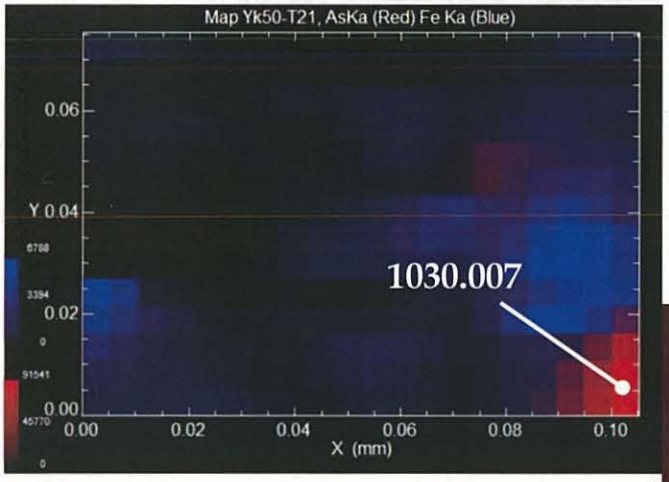

False Colour µXRF Map
Blue= Fe
Red=As

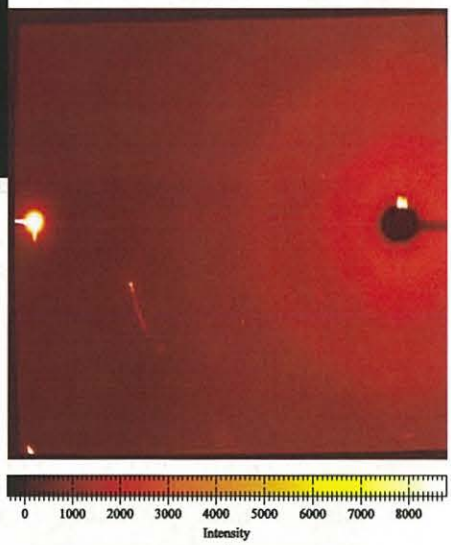

xrdYK50-21.006
- arsenolite

YK-50:T23

xrdYK50-23.008
- arsenolite

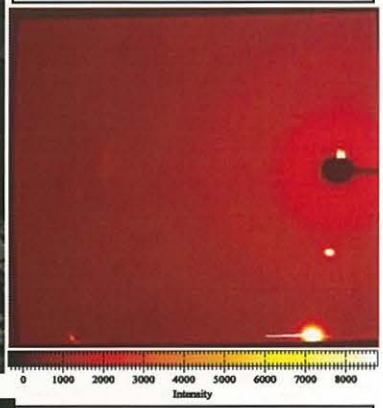

False Colour µXRF Map
Blue= Fe
Red=As

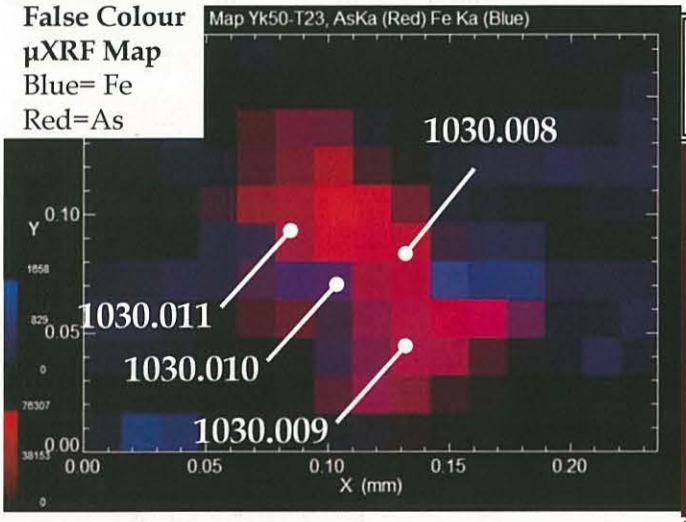

xrdYK50-23.009
- arsenolite

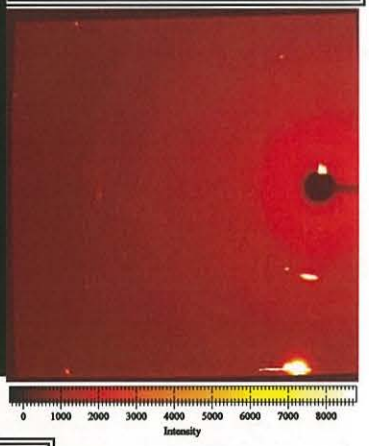

xrdYK50-23.010
- arsenolite

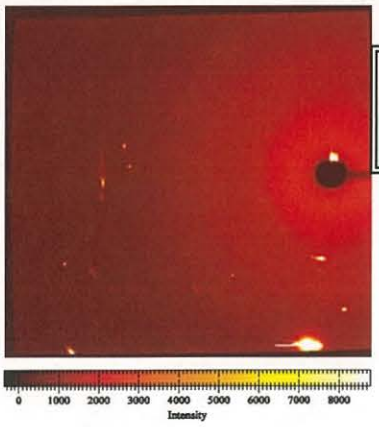

YK-50:T24

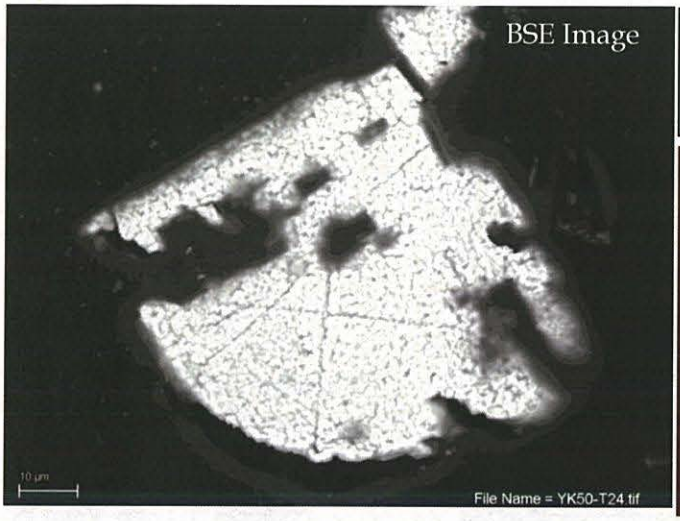

xrdYK50-24.012
- arsenolite

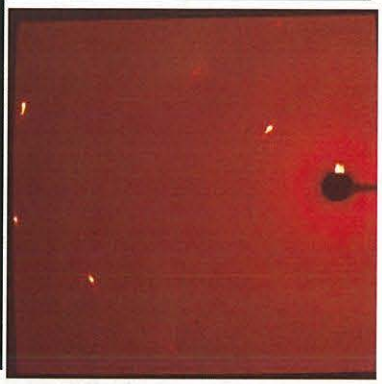

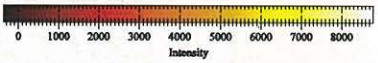

False Colour µXRF Map
Blue= Fe
Red=As

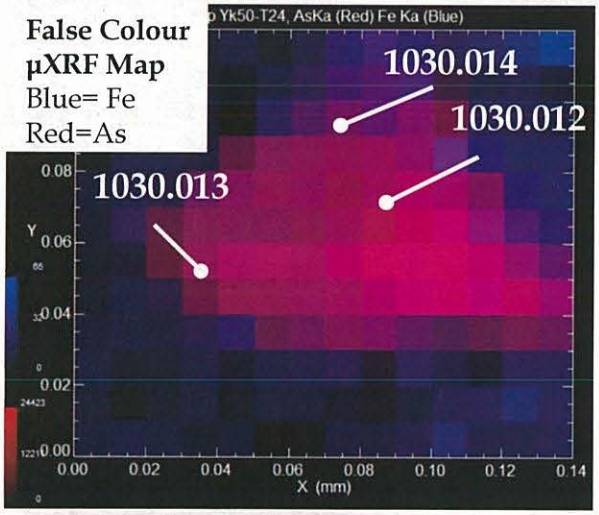

xrdYK50-24.013
- arsenolite

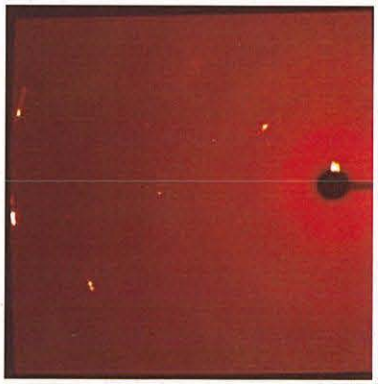

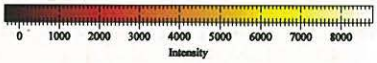

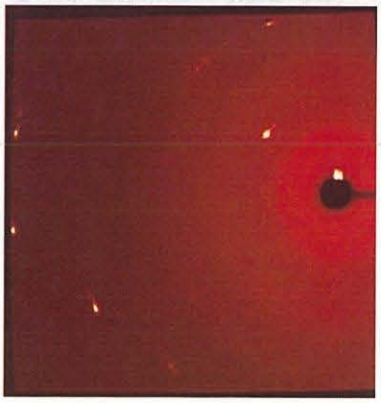

xrdYK50-24.014
- arsenolite

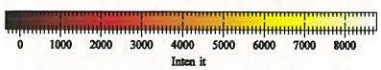

YK-50:T26

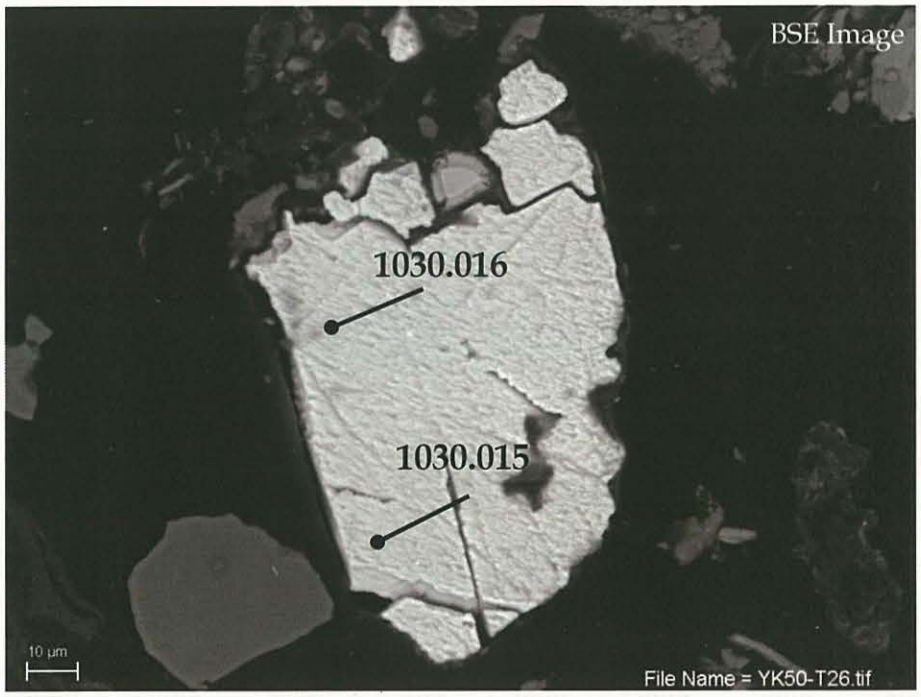

xrdYK50-26.015
- arsenolite
Nsls1030.016
As^{3+} only

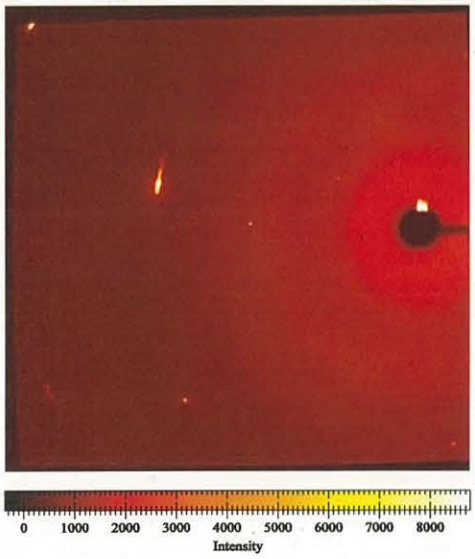

xrdYK50-26.016
- arsenolite

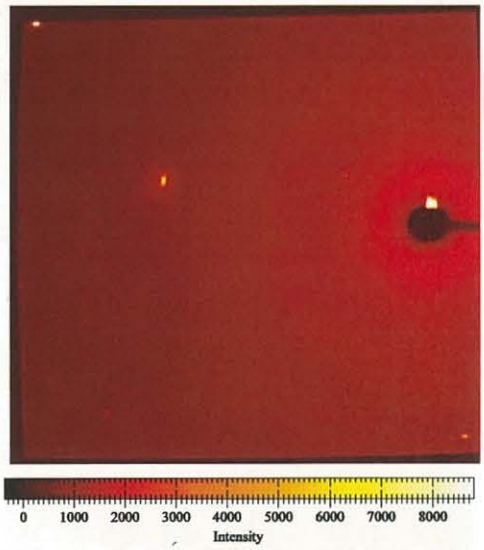

YK-50:T27

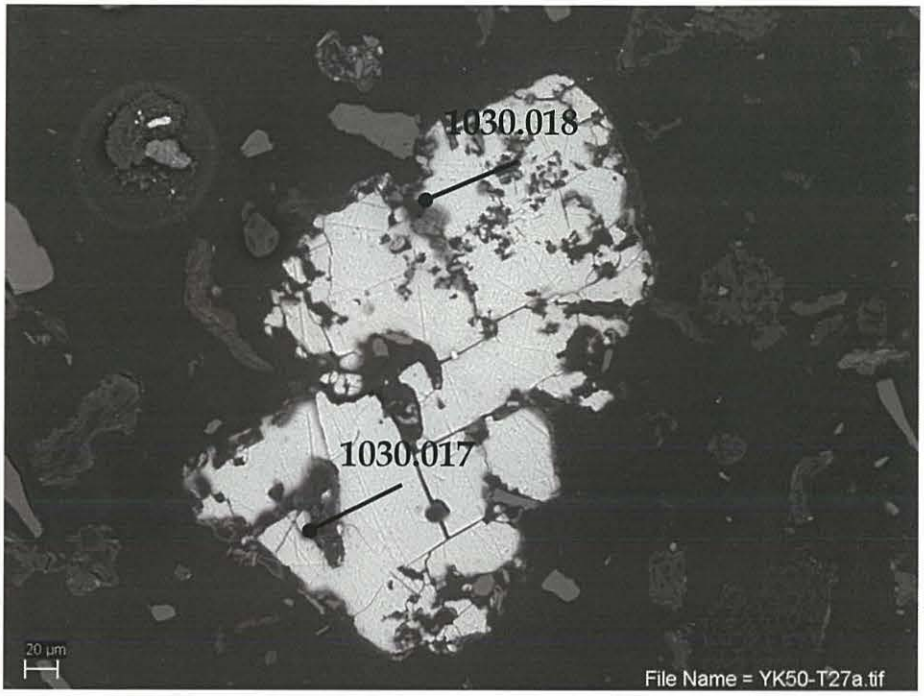

xrdYK50-26.017
- arsenolite

xrdYK50-26.018
- arsenolite